UNIVERSITY OF CALIFORNIA, SAN DIEGO

The pattern recognition receptor toll-like receptor 3 regulates skin barrier homeostasis

A dissertation submitted in partial satisfaction of the
requirements for the degree Doctor of Philosophy

in

Biomedical Sciences

by

Andrew W. Borkowski

Committee in charge:

Professor Richard Gallo, Chair
Professor Michael Karin
Professor Victor Nizet
Professor Eyal Raz
Professor Benjamin Yu

2014

The Dissertation of Andrew William Borkowski is approved, and it is acceptable in quality and form for publication on microfilm and electronically:

Chair

University of California, San Diego

2014

TABLE OF CONTENTS

LIST OF FIGURES

LIST OF TABLES

ACKNOWLEDGEMENTS

Chapter 1, in part, is a reprint of the material as it appears in The Journal of Investigative Dermatology 2013 (with edits for style). A. W. Borkowski, K. Park, Y. Uchida, R. L. Gallo. Activation of TLR3 in keratinocytes increases expression of genes involved in formation of the epidermis, lipid accumulation and epidermal organelles. *J Invest Dermatol.* 2013, 133(8): 2031-40. The dissertation author was the primary investigator and author of this paper.

Chapter 2, in full, is currently being prepared for publication. A. W. Borkowski, I. Kuo, J. J. Bernard, T.Yoshida, M. R. Williams, N. Hung, B. D. Yu, L. A. Beck, and R. L. Gallo. The dissertation author was the primary investigator and author of this paper.

Chapter 3, in full, is unpublished data. A. W. Borkowski, R. L. Gallo. The dissertation author was the primary investigator and author of this material.

Chapter 4, in full, is unpublished data. A. W. Borkowski, D. J. Coleman, A. K. Indra, R. L. Gallo. The dissertation author was the primary investigator and author of this material.

Appendix A, in full, is a reprint of the material as it appears in The Journal of Investigative Dermatology 2011. A. W. Borkowski, R. L. Gallo. The coordinated response of the physical and antimicrobial peptide barriers of the skin. *J Invest Dermatol.* 2011, 131(2): 285-287. The dissertation author was the primary investigator and author of this paper.

Appendix B, in full, is a reprint of material that is submitted for publication and will appear in The Journal of Investigative Dermatology 2014. A. W. Borkowski, R. L. Gallo. The dissertation author was the primary investigator and author of this paper.

VITA

2005	Bachelor of Science, Massachusetts Institute of Technology, Cambridge, MA
2005-2006	Research Technician, Altana Pharma AG, Konstanz, Germany
2006-2008	Research Technician, Whitehead Institute, Cambridge, MA
2014	Doctor of Philosophy, University of California, San Diego

PUBLICATIONS

Borkowski AW, Gallo RL. UVB Radiation Illuminates the Role of TLR3 in the Epidermis. *J Invest Dermatol.* 2014 May 1. Doi:10.1038/jid.2014.167. [Epub ahead of print]

Jackson WS, Krost C, Borkowski AW, Kaczmarczyk L. Translation of the Prion Protein mRNA Is Robust in Astrocytes but Does Not Amplify during Reactive Astrocytosis in the Mouse Brain. *PLoS One.* 2014 Apr 21;9(4):e95958. doi: 10.1371/journal.pone.0095958. eCollection 2014.

Jackson WS, Borkowski AW, Watson NE, King OD, Faas H, Jasanoff A, Lindquist S. Profoundly different prion diseases in knock-in mice carrying single PrP codon substitutions associated with human diseases. *Proc Natl Acad Sci U S A.* 2013, 110(36): 14759-64.

Park K, Elias PM, Hupe M, Borkowski AW, Gallo RL, Shin K, Lee Y, Holleran WM, Uchida Y. Resveratrol stimulates sphingosine-1-phosphate signaling of cathelicidin production. *J Invest Dermatol.* 2013, 133(8): 1942-49.

Borkowski AW, Park K, Uchida Y, Gallo RL. Activation of TLR3 in keratinocytes increases expression of genes involved in formation of the epidermis, lipid accumulation and epidermal organelles. *J Invest Dermatol.* 2013, 133(8): 2031-40.

van Sorge NM, Beasley FC, Gusarov I, Gonzalez DJ, von Köckritz-Blickwede M, Anik S, Borkowski AW, Dorrestein PC, Nudler E, Nizet V. Methicillin-resistant Staphylococcus aureus bacterial nitric oxide synthase affects antibiotic sensitivity and skin abscess development. *J Biol Chem.* 2013, 288(9): 6417-26.

Park K, Elias PM, Shin KO, Lee YM, Hupe M, Borkowski AW, Gallo RL, Saba J, Holleran WM, Uchida Y. (2013) A novel role of a lipid species, sphingosine-1-phosphate, in epithelial innate immunity. *Mol Cell Biol.* 2013, 33(4): 752-62.

Kuo IH, Carpenter-Mendini A, Yoshida T, McGirt LY, Ivanov AI, Barnes KC, Gallo RL, Borkowski AW, Yamasaki K, Leung DY, Georas SN, De Benedetto A, Beck LA. Activation of epidermal toll-like receptor 2 enhances tight junction function – Implications for atopic dermatitis and skin barrier repair. *J Invest Dermatol.* 2013, 133(4): 988-98.

Bernard JJ, Cowing-Zitron C, Nakatsuji T, Muehleisen B, Moto J, Borkowski AW, Martinez L, Greidinger EL, Yu BD, Gallo RL. Ultraviolet radiation damages self noncoding RNA and is detected by TLR3. *Nature Medicine* 2012, 18: 1286-90.

Borkowski AW, Gallo RL. The coordinated response of the physical and antimicrobial peptide barriers of the skin. Commentary. *J Invest Dermatol*. 2011, 131(2): 285-287.

Yamasaki K, Kanada K, Macleod DT, Borkowski AW, Morizane S, Nakatsuji T, Cogen AL, Gallo RL. TLR2 expression is increased in rosacea and stimulates enhanced serine protease production by keratinocytes. *J Invest Dermatol*. 2011, *131*(3): 688-697.

Faas H, Jackson WS, Borkowski AW, Wang X, Ma J, Lindquist S, Jasanoff A. Context-dependent perturbation of neural systems in transgenic mice expressing a cytosolic prion protein. *Neuroimage* 2010, 49(3): 2607-2617

Jackson WS, Borkowski AW, Faas H, Steele AD, King OD, Watson N, Jasanoff A, Lindquist S. Spontaneous generation of prion infectivity in fatal familial insomnia knockin mice. *Neuron* 2009, 63(4): 438-450.

Steele AD, Hutter G, Jackson WS, Heppner FL, Borkowski AW, King OD, Raymond GJ, Aguzzi A, Lindquist S. Heat shock factor 1 regulates lifespan as distinct from disease onset in prion disease. *Proc Natl Acad Sci USA* 2008, 105(36): 13626-13631.

Steele AD, King OD, Jackson WS, Hetz CA, Borkowski AW, Thielen P, Wollmann R, Lindquist S. Diminishing apoptosis by deletion of Bas or overexpression of Bcl-2 does not protect against infectious prion toxicity in vivo. *J Neurosci* 2007, 27(47): 13022-13027.

Steele AD, Hetz C, Yi CH, Jackson WS, Borkowski AW, Yuan J, Wollmann RH, Lindquist S. Prion pathogenesis is independent of caspase-12. *Prion* 2007, 4: 243-247.

ABSTRACT OF THE DISSERTATION

The pattern recognition receptor toll-like receptor 3 regulates skin barrier homeostasis

by

Andrew W. Borkowski

Doctor of Philosophy in Biomedical Sciences

University of California, San Diego, 2014

Professor Richard Gallo, Chair

Ultraviolet (UV) injury to the skin, and the subsequent release of non-coding double-stranded RNA (dsRNA) from necrotic keratinocytes, is an endogenous activator of Toll-like receptor 3 (TLR3). Because changes in keratinocyte growth and differentiation follow injury, we hypothesized that TLR3 might trigger some elements of the barrier repair program in keratinocytes and contribute to skin barrier repair. dsRNA was observed to induce TLR3-dependent increases in human keratinocyte mRNA abundance for ABCA12 (ATP-binding cassette, sub-family A, member 12), glucocerebrosidase, acid sphingomyelinase, and

transglutaminase 1. Additionally tight junction gene expression and function is increased in keratinocytes treated with dsRNA. We also observe that treatment with dsRNA resulted in increases in sphingomyelin and increased epidermal lipid staining by oil-red O as well as TLR3-dependent increases in lamellar bodies and keratohyalin granules. Finally we demonstrate that *Tlr3*$^{-/-}$ mice display a delay in skin barrier repair following UVB damage. These data suggest that TLR3 participates in the program of skin barrier repair.

Scavenger receptors can facilitate entry of dsRNA into airway epithelial cells. For this reason we hypothesized that scavenger receptors on keratinocytes could also facilitate entry of dsRNA into keratinocytes. We observe that scavenger receptor ligands block Poly (I:C) induced inflammatory responses in keratinocytes but surprisingly, can stimulate increases in ABCA12, GBA, and SMPD1 mRNA. Additionally, *Msr1*$^{-/-}$ mice display a skin barrier repair defect. These findings demonstrate an important role for scavenger receptors in skin barrier repair.

UVB damage to the skin can lead to the activation of interleukin-1 receptor (IL-1R) which mediates carcinogenesis and can inhibit hair growth. Herein we show that *Il1r*$^{-/-}$ mice develop dermal hair cysts after chronic UVB exposure and that their skin contains significantly fewer macrophages. We also demonstrate that IL-1R signaling is required for barrier disruption after UVB exposure in mice, though does not significantly contribute to the upregulation of Poly (I:C)-induced skin barrier repair genes. These observations show that IL-1R signaling contributes to homeostasis in skin following UVB exposure. Taken together these studies broaden our understanding of cellular mechanisms that respond to UVB-damage in the skin.

INTRODUCTION

Skin serves as an indispensible protective barrier against the environment. It functions to protect the body from various environmental assaults including pathogenic microbes, ultraviolet radiation, and mechanical injury as well as functioning to prevent water loss. The protective properties of the skin reside in the outermost layer of the epidermis known as the stratum corneum or cornified envelope [1]. The cornified envelope of the epidermis is made up of terminally differentiated, flattened, anucleate corneocytes attached to one another by corneodesmosomes and surrounded by a hydrophobic lipid matrix [2], [3]. This specialized lipid layer is made up of roughly equimolar ratio of ceramides, cholesterol, and free fatty acid with very little phospholipid content [3], [4]. The unique architecture of the stratum corneum allows for minimal water loss as the hydrophobic lipid layers prevent the egress of bodily fluids. The lipid bilayer also hinders the ingress of microbes as it contains numerous antimicrobial molecules including antimicrobial peptides [5]–[7] and antimicrobial lipids [8], [9]. The antimicrobial and permeability barriers of the skin are very closely linked and disruption of the skin barrier stimulates components of both barriers [7], [10]–[12]. In addition to producing antimicrobial compounds, the skin is home to numerous commensal bacteria [13]–[15], that also produce antibiotics that prevent growth of pathogenic organisms [16]. Additionally, secretions from sebaceous glands contain antimicrobial fatty acids [17], [18].

Maintaining proper barrier function in the skin is highly regulated process and dependent upon proper differentiation of basal keratinocytes. The skin is a very dynamic organ with a majority of the cells known as keratinocytes constantly differentiating into corneocytes, which make up the cornified envelope. Once basal keratinocytes begin differentiating, they take about 14 days to become terminally differentiated corneocytes, which then spend another 14 days in the stratum corneum before being shed in a process known as desquamation.

Injury or infection to the skin often results in skin barrier disruption and this barrier must be quickly replenished. This is accomplished by the rapid trafficking of a specialized organelle known as a lamellar body [19], [20], present in the granular layer of the epidermis to the stratum corneum, where it deposits the specialized lipids that make up the stratum corneum [21]. Following this response, upregulation in ceramide [22], [23], cholesterol [24], [25], and free fatty acid [26], [27] synthesis takes place in order to generate lamellar membrane lipids which are depleted during skin barrier repair. Deficiencies in components important for lipid trafficking and metabolism are seen in a number of dermatological conditions. Patients with harlequin ichthyosis or lamellar ichthyosis type 2, which present with dramatic cutaneous phenotypes, lack ATP-binding cassette, sub-family A, member 12 (ABCA12) [28], [29], a lipid transporter that loads epidermal lipids into lamellar bodies [30]–[32]. Deficiencies in enzymes that metabolize precursors of ceramides also lead to diseases with dermatological symptoms, including Gaucher's disease in patients that lack glucocerebrosidase (GBA) [33] and Niemann-Pick Disease in patients that lack acid sphingomyelinase (SMPD1) [34], [35]. As these genes are important for skin barrier repair, their activity is increased following skin barrier disruption [36], [37].

The mechanisms that regulate barrier repair have been shown to be dependent on a calcium gradient that exists in the epidermis [38], [39]. The concentration of calcium is low in the basal and spinous layers but is very high in the granular layer of the epidermis [40]. When skin barrier disruption occurs, water loss through the skin disturbs the calcium concentration gradient and stimulates process of barrier repair [38].

In this thesis we show evidence that toll-like receptor 3 (TLR3) activation, independent of calcium dependent mechanisms, can stimulate skin barrier repair [11]. TLR3 is a toll-like receptor (TLR) that can recognize dsRNA [41]. TLRs are a class of pattern recognition receptors (PRRs) that recognize specific structural components or nucleic acids of microbes known as microbe associated molecular patterns [42]. They have also been shown to recognize specific

endogenous danger signals that can result from cell death also termed danger associated molecular patterns (DAMPs) [43]–[45]. TLR3 has canonically been described as a viral recognition receptor [46] and deficiencies in this receptor or different components of its signaling pathway often result in viral encephalitis [47]–[49]. In the last decade however, TLR3 has been observed to recognize endogenous sources of RNA. TLR3 has since been shown to recognize mRNA [50] as well as the RNA from necrotic cells [50]–[52].

In recent years members in our lab have shown that inflammation in the skin resulting from mechanical or UVB injury is dependent on TLR3 activation by endogenous RNA [52], [53]. It has also been observed that TLR3 is important for wound healing [54], [55]. Herein, we propose that cell damage resulting from ultraviolet B radiation (UVB) exposure causes TLR3 activation and show that this leads to increases in skin barrier repair gene expression, epidermal lipids, epidermal organelles, and promotes a skin barrier repair program. Previous studies have shown that UVB damage to the skin results in skin barrier disruption [56], [57] though we propose for the first time that TLR3 contributes to mechanisms of repair independent of or in addition to mechanisms based on calcium gradient sensing. Herein we show that *Tlr3*$^{-/-}$ mice display skin barrier repair defects after UVB exposure compared to WT mice.

Because extracellular RNA must be first trafficked to the endosome in order to activate TLR3 [58], it must first be taken up by an extracellular receptor. A number of recent studies have demonstrated that Poly (I:C), a dsRNA mimetic, can be taken into the cell by scavenger receptors [59]–[61]. It has also recently been shown that MARCO, a scavenger receptor present on keratinocytes enhances uptake of herpes simplex virus 1 [62]. Herein we show that treatment of keratinocytes with various scavenger receptor ligands increases transcripts of skin barrier repair genes and additionally, mice deficient in macrophage scavenger receptor 1 (*Msr1*) display a skin barrier repair defect. Scavenger receptor recognition of extracellular RNA may represent another

pathway stimulating skin barrier repair, independent of TLR3 or calcium dependent repair pathways.

As acute inflammation in the skin was shown to be regulated by TLR3, we wanted to investigate the TLR3-dependent effects of chronic UVB exposure on the skin. Chronic UVB exposure is associated with skin cancer [63] and cutaneous carcinogenesis is mediated by a number of inflammatory factors including interleukin-1 receptor (IL-1R) [64], [65]. IL-1R plays important roles in responding to cellular damage and infection in the host [66] and can be activated following UVB exposure [67]. Herein we show that our model of UVB-induced carcinogenesis failed to produce tumors though did produce dermal hair cysts in *Il1r*$^{-/-}$ mice. A number of past studies have shown that IL-1R signaling inhibits hair growth [68], [69] and that IL-1R signaling may be defective in patients with alopecia areata [70], [71], a disease characterized by hair loss on the scalp and other parts of the body [72]. Findings from this study reinforce previous data that IL-1R may act as a negative regulator of hair growth and thus could be a target of future therapeutics for hair loss.

In summary the studies of this dissertation were designed to show that pattern recognition receptors present in the skin can stimulate pathways that help maintain homeostasis of the barrier. Herein we show that TLR3 represents an important receptor in the skin that recognizes cellular damage and responds by initiating components of the skin barrier repair. These changes are independent of calcium gradient sensing and represent a novel pathway that stimulates skin barrier repair. While we have shown evidence that scavenger receptors play a role in skin barrier repair, more research must be done to confirm this mechanism and the specific pathways that are activated following ligand binding. It is likely that yet undiscovered receptors and pathways play a part in skin barrier repair. Although we did not see changes in skin barrier repair genes with TLR2 ligands, it has been demonstrated that TLR2 activation by bacterial ligands promotes aspects of the skin barrier and that *Tlr2*$^{-/-}$ mice display a skin barrier repair defect [73], [74]. It

can be assumed that additional pattern recognition receptors play a role in epidermal homeostasis though have yet to be discovered. Future research will undoubtedly uncover additional sensors of epidermal damage that are important for skin barrier repair and shed light on this underexposed field of research.

References

[1] P. M. Elias, “The skin barrier as an innate immune element.,” *Semin. Immunopathol.*, vol. 29, pp. 3–14, 2007.

[2] E. Candi, R. Schmidt, and G. Melino, “The cornified envelope: a model of cell death in the skin.,” *Nat. Rev. Mol. Cell Biol.*, vol. 6, no. 4, pp. 328–40, Apr. 2005.

[3] K. R. Feingold and P. M. Elias, “Role of lipids in the formation and maintenance of the cutaneous permeability barrier.,” *Biochim. Biophys. Acta*, vol. 1841, pp. 280–294, 2013.

[4] W. M. Holleran, M. Q. Man, W. N. Gao, G. K. Menon, P. M. Elias, and K. R. Feingold, “Sphingolipids are required for mammalian epidermal barrier function. Inhibition of sphingolipid synthesis delays barrier recovery after acute perturbation.,” *J. Clin. Invest.*, vol. 88, pp. 1338–1345, 1991.

[5] Y. Lai and R. L. Gallo, “AMPed up immunity: how antimicrobial peptides have multiple roles in immune defense,” *Trends in Immunology*, vol. 30. pp. 131–141, 2009.

[6] M. H. Braff, M. Zaiou, J. Fierer, V. Nizet, and R. L. Gallo, “Keratinocyte production of cathelicidin provides direct activity against bacterial skin pathogens.,” *Infect. Immun.*, vol. 73, pp. 6771–6781, 2005.

[7] M. H. Braff, A. Di Nardo, and R. L. Gallo, “Keratinocytes store the antimicrobial peptide cathelicidin in lamellar bodies.,” *J. Invest. Dermatol.*, vol. 124, pp. 394–400, 2005.

[8] D. J. Bibel, S. J. Miller, B. E. Brown, B. B. Pandey, P. M. Elias, H. R. Shinefield, and R. Aly, “Antimicrobial activity of stratum corneum lipids from normal and essential fatty acid-deficient mice.,” *J. Invest. Dermatol.*, vol. 92, pp. 632–638, 1989.

[9] S. J. Miller, R. Aly, H. R. Shinefeld, and P. M. Elias, “In vitro and in vivo antistaphylococcal activity of human stratum corneum lipids.,” *Arch. Dermatol.*, vol. 124, pp. 209–215, 1988.

[10] K. M. Aberg, M.-Q. Man, R. L. Gallo, T. Ganz, D. Crumrine, B. E. Brown, E.-H. Choi, D.-K. Kim, J. M. Schröder, K. R. Feingold, and P. M. Elias, “Co-regulation and interdependence of the mammalian epidermal permeability and antimicrobial barriers.,” *J. Invest. Dermatol.*, vol. 128, pp. 917–925, 2008.

[11] A. W. Borkowski, K. Park, Y. Uchida, and R. L. Gallo, “Activation of TLR3 in keratinocytes increases expression of genes involved in formation of the epidermis, lipid accumulation, and epidermal organelles.,” *J. Invest. Dermatol.*, vol. 133, no. 8, pp. 2031–40, Aug. 2013.

[12] K. M. Aberg, K. A. Radek, E.-H. Choi, D.-K. Kim, M. Demerjian, M. Hupe, J. Kerbleski, R. L. Gallo, T. Ganz, T. Mauro, K. R. Feingold, and P. M. Elias, “Psychological stress

downregulates epidermal antimicrobial peptide expression and increases severity of cutaneous infections in mice.," *J. Clin. Invest.*, vol. 117, pp. 3339–3349, 2007.

[13] E. A. Grice, H. H. Kong, S. Conlan, C. B. Deming, J. Davis, A. C. Young, G. G. Bouffard, R. W. Blakesley, P. R. Murray, E. D. Green, M. L. Turner, and J. A. Segre, "Topographical and temporal diversity of the human skin microbiome.," *Science*, vol. 324, pp. 1190–1192, 2009.

[14] The Human Microbiome Project Consortium, "Structure, function and diversity of the healthy human microbiome.," *Nature*, vol. 486, pp. 207–14, 2012.

[15] K. A. Capone, S. E. Dowd, G. N. Stamatas, and J. Nikolovski, "Diversity of the human skin microbiome early in life.," *J. Invest. Dermatol.*, vol. 131, pp. 2026–2032, 2011.

[16] A. L. Cogen, K. Yamasaki, K. M. Sanchez, R. A. Dorschner, Y. Lai, D. T. MacLeod, J. W. Torpey, M. Otto, V. Nizet, J. E. Kim, and R. L. Gallo, "Selective antimicrobial action is provided by phenol-soluble modulins derived from Staphylococcus epidermidis, a normal resident of the skin.," *J. Invest. Dermatol.*, vol. 130, pp. 192–200, 2010.

[17] T. Nakatsuji, M. C. Kao, L. Zhang, C. C. Zouboulis, R. L. Gallo, and C.-M. Huang, "Sebum free fatty acids enhance the innate immune defense of human sebocytes by upregulating beta-defensin-2 expression.," *J. Invest. Dermatol.*, vol. 130, pp. 985–994, 2010.

[18] C. C. Zouboulis, H. Seltmann, H. Neitzel, and C. E. Orfanos, "Establishment and characterization of an immortalized human sebaceous gland cell line (SZ95).," *J. Invest. Dermatol.*, vol. 113, pp. 1011–1020, 1999.

[19] P. M. Elias, C. Cullander, T. Mauro, U. Rassner, L. Kömüves, B. E. Brown, and G. K. Menon, "The secretory granular cell: the outermost granular cell as a specialized secretory cell.," *J. Investig. Dermatol. Symp. Proc.*, vol. 3, pp. 87–100, 1998.

[20] E. Peter M., M. Fartasch, D. Crumrine, M. Behne, Y. Uchida, and W. M. Holleran, "Origin of the Corneocyte Lipid Envelope (CLE): Observations in Harlequin Ichthyosis and Cultured Human Keratinocytes," *J. Invest. Dermatol.*, vol. 115, no. 4, pp. 765–769, Oct. 2000.

[21] G. K. Menon, K. R. Feingold, and P. M. Elias, "Lamellar body secretory response to barrier disruption.," *J. Invest. Dermatol.*, vol. 98, no. 3, pp. 279–289, 1992.

[22] W. M. Holleran, K. R. Feingold, M. Q. Man, W. N. Gao, J. M. Lee, and P. M. Elias, "Regulation of epidermal sphingolipid synthesis by permeability barrier function.," *J. Lipid Res.*, vol. 32, no. 7, pp. 1151–8, Jul. 1991.

[23] W. M. Holleran, W. N. Gao, K. R. Feingold, and P. M. Elias, "Localization of epidermal sphingolipid synthesis and serine palmitoyl transferase activity: alterations imposed by permeability barrier requirements.," *Arch. Dermatol. Res.*, vol. 287, no. 3–4, pp. 254–8, Jan. 1995.

[24] K. R. Feingold, M. Q. Man, G. K. Menon, S. S. Cho, B. E. Brown, and P. M. Elias, “Cholesterol synthesis is required for cutaneous barrier function in mice.,” *J. Clin. Invest.*, vol. 86, pp. 1738–1745, 1990.

[25] G. Menon, K. Feingold, and A. Moser, “De novo sterologenesis in the skin. II. Regulation by cutaneous barrier requirements.,” *J. Lipid Res.*, vol. 26, no. 5, pp. 418–427, 1985.

[26] M. Mao-Qiang, P. M. Elias, and K. R. Feingold, “Fatty acids are required for epidermal permeability barrier function.,” *J. Clin. Invest.*, vol. 92, no. 2, pp. 791–8, Aug. 1993.

[27] K. Ottey and L. Wood, “Cutaneous permeability barrier disruption increases fatty acid synthetic enzyme activity in the epidermis of hairless mice.,” *J. Invest. Dermatol.*, vol. 104, no. 3, pp. 401–404, 1995.

[28] M. Akiyama, Y. Sugiyama-Nakagiri, K. Sakai, J. R. McMillan, M. Goto, K. Arita, Y. Tsuji-Abe, N. Tabata, K. Matsuoka, R. Sasaki, D. Sawamura, and H. Shimizu, “Mutations in lipid transporter ABCA12 in harlequin ichthyosis and functional recovery by corrective gene transfer,” *J. Clin. Invest.*, vol. 115, no. 7, pp. 2–9, 2005.

[29] C. Lefévre, S. Audebert, F. Jobard, B. Bouadjar, H. Lakhdar, O. Boughdene-Stambouli, C. Blanchet-Bardon, R. Heilig, M. Foglio, J. Weissenbach, M. Lathrop, J.-F. Prud’homme, and J. Fischer, “Mutations in the transporter ABCA12 are associated with lamellar ichthyosis type 2.,” *Hum. Mol. Genet.*, vol. 12, no. 18, pp. 2369–78, Sep. 2003.

[30] M. Akiyama, “The roles of ABCA12 in keratinocyte differentiation and lipid barrier formation in the epidermis.,” *Dermatoendocrinol.*, vol. 3, pp. 107–112, 2011.

[31] T. Yanagi, M. Akiyama, H. Nishihara, J. Ishikawa, K. Sakai, Y. Miyamura, A. Naoe, T. Kitahara, S. Tanaka, and H. Shimizu, “Self-improvement of keratinocyte differentiation defects during skin maturation in ABCA12-deficient harlequin ichthyosis model mice.,” *Am. J. Pathol.*, vol. 177, pp. 106–118, 2010.

[32] Y. Zuo, D. Z. Zhuang, R. Han, G. Isaac, J. J. Tobin, M. McKee, R. Welti, J. L. Brissette, M. L. Fitzgerald, and M. W. Freeman, “ABCA12 maintains the epidermal lipid permeability barrier by facilitating formation of ceramide linoleic esters.,” *J. Biol. Chem.*, vol. 283, pp. 36624–36635, 2008.

[33] G. A. Grabowski, “Phenotype, diagnosis, and treatment of Gaucher’s disease,” *The Lancet*, vol. 372. pp. 1263–1271, 2008.

[34] E. H. Schuchman, “Acid sphingomyelinase, cell membranes and human disease: Lessons from Niemann-Pick disease,” *FEBS Letters*, vol. 584. pp. 1895–1900, 2010.

[35] K. Horinouchi, S. Erlich, D. P. Perl, K. Ferlinz, C. L. Bisgaier, K. Sandhoff, R. J. Desnick, C. L. Stewart, and E. H. Schuchman, “Acid sphingomyelinase deficient mice: a model of types A and B Niemann-Pick disease.,” *Nat. Genet.*, vol. 10, pp. 288–293, 1995.

[36] W. M. Holleran, Y. Takagi, G. K. Menon, S. M. Jackson, J. M. Lee, K. R. Feingold, and P. M. Elias, “Permeability barrier requirements regulate epidermal beta-glucocerebrosidase.,” *J. Lipid Res.*, vol. 35, no. 5, pp. 905–12, May 1994.

[37] J. M. Jensen, S. Schütze, M. Förl, M. Krönke, and E. Proksch, “Roles for tumor necrosis factor receptor p55 and sphingomyelinase in repairing the cutaneous permeability barrier.,” *J. Clin. Invest.*, vol. 104, no. 12, pp. 1761–70, Dec. 1999.

[38] S. H. Lee, P. M. Elias, E. Proksch, G. K. Menon, M. Mao-Quiang, and K. R. Feingold, “Calcium and potassium are important regulators of barrier homeostasis in murine epidermis.,” *J. Clin. Invest.*, vol. 89, no. 2, pp. 530–8, Feb. 1992.

[39] K. R. Feingold and M. Denda, “Regulation of permeability barrier homeostasis.,” *Clin. Dermatol.*, vol. 30, no. 3, pp. 263–8, 2012.

[40] P. Elias, S. Ahn, B. Brown, D. Crumrine, and K. R. Feingold, “Origin of the epidermal calcium gradient: regulation by barrier status and role of active vs passive mechanisms.,” *J. Invest. Dermatol.*, vol. 119, no. 6, pp. 1269–74, Dec. 2002.

[41] L. Liu, I. Botos, Y. Wang, J. N. Leonard, J. Shiloach, D. M. Segal, and D. R. Davies, “Structural basis of toll-like receptor 3 signaling with double-stranded RNA.,” *Science*, vol. 320, no. 5874, pp. 379–81, Apr. 2008.

[42] T. Kawai and S. Akira, “Toll-like receptor and RIG-I-like receptor signaling.,” *Ann. N. Y. Acad. Sci.*, vol. 1143, pp. 1–20, Nov. 2008.

[43] C.-J. Chen, H. Kono, D. Golenbock, G. Reed, S. Akira, and K. L. Rock, “Identification of a key pathway required for the sterile inflammatory response triggered by dying cells.,” *Nat. Med.*, vol. 13, pp. 851–856, 2007.

[44] D. L. Rosin and M. D. Okusa, “Dangers within: DAMP responses to damage and cell death in kidney disease.,” *J. Am. Soc. Nephrol.*, vol. 22, no. 3, pp. 416–25, Mar. 2011.

[45] A. Kaczmarek, P. Vandenabeele, and D. V Krysko, “Necroptosis: the release of damage-associated molecular patterns and its physiological relevance.,” *Immunity*, vol. 38, no. 2, pp. 209–23, Feb. 2013.

[46] F. Dunlevy, N. McElvaney, and C. Greene, “TLR3 Sensing of Viral Infection,” *Open Infect. Dis. J.*, vol. 4, pp. 1–10, 2010.

[47] S.-Y. Zhang, E. Jouanguy, S. Ugolini, A. Smahi, G. Elain, P. Romero, D. Segal, V. Sancho-Shimizu, L. Lorenzo, A. Puel, C. Picard, A. Chapgier, S. Plancoulaine, M. Titeux, C. Cognet, H. von Bernuth, C.-L. Ku, A. Casrouge, X.-X. Zhang, L. Barreiro, J. Leonard, C. Hamilton, P. Lebon, B. Héron, L. Vallée, L. Quintana-Murci, A. Hovnanian, F. Rozenberg, E. Vivier, F. Geissmann, M. Tardieu, L. Abel, and J.-L. Casanova, “TLR3 deficiency in patients with herpes simplex encephalitis.,” *Science*, vol. 317, no. 5844, pp. 1522–7, Sep. 2007.

[48] A. Casrouge, S.-Y. Zhang, C. Eidenschenk, E. Jouanguy, A. Puel, K. Yang, A. Alcais, C. Picard, N. Mahfoufi, N. Nicolas, L. Lorenzo, S. Plancoulaine, B. Sénéchal, F. Geissmann, K. Tabeta, K. Hoebe, X. Du, R. L. Miller, B. Héron, C. Mignot, T. B. de Villemeur, P. Lebon, O. Dulac, F. Rozenberg, B. Beutler, M. Tardieu, L. Abel, and J.-L. Casanova, "Herpes simplex virus encephalitis in human UNC-93B deficiency.," *Science*, vol. 314, no. 5797, pp. 308–12, Oct. 2006.

[49] V. Sancho-Shimizu, R. Perez de Diego, L. Lorenzo, R. Halwani, A. Alangari, E. Israelsson, S. Fabrega, A. Cardon, J. Maluenda, M. Tatematsu, F. Mahvelati, M. Herman, M. Ciancanelli, Y. Guo, Z. AlSum, N. Alhamis, A. S. Al-Makadma, A. Ghadiri, S. Boucherit, S. Plancoulaine, C. Picard, F. Rozenberg, M. Tardieu, P. Lebon, E. Jouanguy, N. Rezaei, T. Seya, M. Matsumoto, D. Chaussabel, A. Puel, S.-Y. Zhang, L. Abel, S. Al-Muhsen, and J.-L. Casanova, "Herpes simplex encephalitis in children with autosomal recessive and dominant TRIF deficiency," *J. Clin. Invest.*, vol. 121, no. 12, pp. 4890–4902, 2011.

[50] K. Karikó, H. Ni, J. Capodici, M. Lamphier, and D. Weissman, "mRNA is an endogenous ligand for Toll-like receptor 3.," *J. Biol. Chem.*, vol. 279, no. 13, pp. 12542–50, Mar. 2004.

[51] K. A. Cavassani, M. Ishii, H. Wen, M. A. Schaller, P. M. Lincoln, N. W. Lukacs, C. M. Hogaboam, and S. L. Kunkel, "TLR3 is an endogenous sensor of tissue necrosis during acute inflammatory events.," *J. Exp. Med.*, vol. 205, no. 11, pp. 2609–21, Oct. 2008.

[52] Y. Lai, A. Di Nardo, T. Nakatsuji, A. Leichtle, Y. Yang, A. L. Cogen, Z.-R. Wu, L. V Hooper, R. R. Schmidt, S. von Aulock, K. a Radek, C.-M. Huang, A. F. Ryan, and R. L. Gallo, "Commensal bacteria regulate Toll-like receptor 3-dependent inflammation after skin injury.," *Nat. Med.*, vol. 15, no. 12, pp. 1377–82, Dec. 2009.

[53] J. J. Bernard, C. Cowing-Zitron, T. Nakatsuji, B. Muehleisen, J. Muto, A. W. Borkowski, L. Martinez, E. L. Greidinger, B. D. Yu, and R. L. Gallo, "Ultraviolet radiation damages self noncoding RNA and is detected by TLR3.," *Nat. Med.*, vol. 18, no. 8, pp. 1286–90, Aug. 2012.

[54] Q. Lin, D. Fang, J. Fang, X. Ren, X. Yang, F. Wen, and S. B. Su, "Impaired wound healing with defective expression of chemokines and recruitment of myeloid cells in TLR3-deficient mice.," *J. Immunol.*, vol. 186, no. 6, pp. 3710–7, Mar. 2011.

[55] Q. Lin, L. Wang, Y. Lin, X. Liu, X. Ren, S. Wen, X. Du, T. Lu, S. Y. Su, X. Yang, W. Huang, S. Zhou, F. Wen, and S. B. Su, "Toll-like receptor 3 ligand polyinosinic:polycytidylic acid promotes wound healing in human and murine skin.," *J. Invest. Dermatol.*, vol. 132, no. 8, pp. 2085–92, Aug. 2012.

[56] A. Haratake, Y. Uchida, and M. Schmuth, "UVB-induced alterations in permeability barrier function: roles for epidermal hyperproliferation and thymocyte-mediated response," *J. Invest. Dermatol.*, vol. 108, no. 5, pp. 769–775, 1997.

[57] W. M. Holleran, Y. Uchida, L. Halkier-Sorensen, a Haratake, M. Hara, J. H. Epstein, and P. M. Elias, “Structural and biochemical basis for the UVB-induced alterations in epidermal barrier function.,” *Photodermatol. Photoimmunol. Photomed.*, vol. 13, no. 4, pp. 117–28, Aug. 1997.

[58] M. Matsumoto, H. Oshiumi, and T. Seya, “Antiviral responses induced by the TLR3 pathway.,” *Rev. Med. Virol.*, vol. 21, p. 2011, 2011.

[59] G. V Limmon, M. Arredouani, K. L. McCann, R. a Corn Minor, L. Kobzik, and F. Imani, “Scavenger receptor class-A is a novel cell surface receptor for double-stranded RNA.,” *FASEB J.*, vol. 22, pp. 159–67, 2008.

[60] S. J. DeWitte-Orr, S. E. Collins, C. M. T. Bauer, D. M. Bowdish, and K. L. Mossman, “An accessory to the ‘Trinity’: SR-As are essential pathogen sensors of extracellular dsRNA, mediating entry and leading to subsequent type I IFN responses,” *PLoS Pathog.*, vol. 6, no. 3, pp. 1–15, 2010.

[61] A. Dieudonné, D. Torres, S. Blanchard, S. Taront, P. Jeannin, Y. Delneste, M. Pichavant, F. Trottein, and P. Gosset, “Scavenger receptors in human airway epithelial cells: Role in response to double-stranded RNA,” *PLoS One*, vol. 7, no. 8, pp. 1–13, 2012.

[62] D. T. MacLeod, T. Nakatsuji, K. Yamasaki, L. Kobzik, and R. L. Gallo, “HSV-1 exploits the innate immune scavenger receptor MARCO to enhance epithelial adsorption and infection.,” *Nat. Commun.*, vol. 4, p. 1963, 2013.

[63] R. Lucas, T. McMichael, W. Smith, and B. Armstrong, “Solar ultraviolet radiation: global burden of disease from solar ultraviolet radiation,” in *Environmental Burden of Disease Series, No. 13*, no. 13, A. Prüss-Üstün, H. Zeeb, C. Mathers, and M. Repacholi, Eds. Geneva: WHO Document Production Services, 2006, p. 87 pp.

[64] C. Cataisson, R. Salcedo, S. Hakim, B. A. Moffitt, L. Wright, M. Yi, R. Stephens, R.-M. Dai, L. Lyakh, D. Schenten, H. S. Yuspa, and G. Trinchieri, “IL-1R-MyD88 signaling in keratinocyte transformation and carcinogenesis.,” *J. Exp. Med.*, vol. 209, no. 9, pp. 1689–702, Aug. 2012.

[65] K. Loser, J. Apelt, M. Voskort, M. Mohaupt, S. Balkow, T. Schwarz, S. Grabbe, and S. Beissert, “IL-10 controls ultraviolet-induced carcinogenesis in mice.,” *J. Immunol.*, vol. 179, no. 1, pp. 365–71, Jul. 2007.

[66] J. E. Sims and D. E. Smith, “The IL-1 family: regulators of immunity.,” *Nat. Rev. Immunol.*, vol. 10, pp. 89–102, 2010.

[67] L. Feldmeyer, M. Keller, G. Niklaus, D. Hohl, S. Werner, and H.-D. Beer, “The inflammasome mediates UVB-induced activation and secretion of interleukin-1beta by keratinocytes.,” *Curr. Biol.*, vol. 17, no. 13, pp. 1140–5, Jul. 2007.

[68] R. Hoffmann, W. Eicheler, E. Wenzel, and R. Happle, “Interleukin-1beta-induced inhibition of hair growth in vitro is mediated by cyclic AMP.,” *J. Invest. Dermatol.*, vol. 108, pp. 40–42, 1997.

[69] C. S. Harmon and T. D. Nevins, “IL-1 alpha inhibits human hair follicle growth and hair fiber production in whole-organ cultures.,” *Lymphokine Cytokine Res.*, vol. 12, pp. 197–203, 1993.

[70] J. K. Tarlow, F. E. Clay, M. J. Cork, A. I. Blakemore, A. J. McDonagh, A. G. Messenger, and G. W. Duff, “Severity of alopecia areata is associated with a polymorphism in the interleukin-1 receptor antagonist gene.,” *J. Invest. Dermatol.*, vol. 103, pp. 387–390, 1994.

[71] R. Hoffmann, E. Wenzel, A. Huth, P. van der Steen, M. Schäufele, H. P. Henninger, and R. Happle, “Cytokine mRNA levels in Alopecia areata before and after treatment with the contact allergen diphenylcyclopropenone.,” *J. Invest. Dermatol.*, vol. 103, no. 4, pp. 530–3, Oct. 1994.

[72] A. J. Papadopoulos, R. A. Schwartz, and C. K. Janniger, “Alopecia areata. Pathogenesis, diagnosis, and therapy.,” *Am. J. Clin. Dermatol.*, vol. 1, no. 2, pp. 101–5.

[73] T. Yuki, H. Yoshida, Y. Akazawa, A. Komiya, Y. Sugiyama, and S. Inoue, “Activation of TLR2 enhances tight junction barrier in epidermal keratinocytes.,” *J. Immunol.*, vol. 187, no. 6, pp. 3230–7, Sep. 2011.

[74] I.-H. Kuo, A. Carpenter-Mendini, T. Yoshida, L. Y. McGirt, A. I. Ivanov, K. C. Barnes, R. L. Gallo, A. W. Borkowski, K. Yamasaki, D. Y. Leung, S. N. Georas, A. De Benedetto, and L. a Beck, “Activation of epidermal toll-like receptor 2 enhances tight junction function: implications for atopic dermatitis and skin barrier repair.,” *J. Invest. Dermatol.*, vol. 133, no. 4, pp. 988–98, Apr. 2013.

CHAPTER 1:

Activation of TLR3 in keratinocytes increases expression of genes involved in formation of the epidermis, lipid accumulation and epidermal organelles

Abstract

Injury to the skin, and the subsequent release of non-coding double-stranded RNA from necrotic keratinocytes, has been identified as an endogenous activator of Toll-like receptor 3 (TLR3). Since changes in keratinocyte growth and differentiation follow injury, we hypothesized that TLR3 might trigger some elements of the barrier repair program in keratinocytes. Double-stranded RNA was observed to induce TLR3-dependent increases in human keratinocyte mRNA abundance for ABCA12 (ATP-binding cassette, sub-family A, member 12), glucocerebrosidase, acid sphingomyelinase, and transglutaminase 1. Additionally, treatment with double-stranded RNA resulted in increases in sphingomyelin and morphologic changes including increased epidermal lipid staining by oil-red O and TLR3-dependent increases in lamellar bodies and keratohyalin granules. These observations show that double-stranded RNA can stimulate some events in keratinocytes that are important for skin barrier repair and maintenance.

Introduction

Rapid recovery of epidermal barrier function following injury prevents water loss and opportunistic infection by infiltrating microbes. Barrier repair after injury involves trafficking of lamellar bodies (LB) to the SC, where they secrete their contents [1], and activation of several other genes, including the ATP-binding cassette sub-family A, member 12 (ABCA12), an essential lipid transporter in the epidermis responsible for harlequin ichthyosis [2] and lamellar ichthyosis type 2 [3], and lipid metabolism enzymes, glucocerebrosidase (GBA) [4] and acid sphingomyelinase (SMPD1) [5]. Cholesterol [6], free fatty acid [7], [8], and ceramide synthesis all also increase following skin barrier disruption [9], [10] and are essential for barrier repair. The mechanisms that regulate the complex events that comprise barrier repair are incompletely defined, though a calcium gradient in the epidermis plays an important role [11], [12]. In the present study we sought to test the hypothesis that double-stranded RNA, recently discovered to be an endogenous product produced by epidermal injury following trauma or excess UVB exposure [13], [14], might serve as a trigger for expression of genes important to the epidermal barrier repair process.

dsRNA recognition can occur by several mechanisms including binding to Toll-like receptor 3 (TLR3). TLR3 signaling has largely been described as a recognition and response system to combat viral infections [15], [16]. Patients who have mutations in TLR3[17], UNC-93B, an ER membrane protein important for its trafficking to the endosome [18], or TIR-domain-containing adapter-inducing interferon-β (TRIF), a key adaptor signaling molecule for TLR3 signaling [19], are more susceptible to herpes simplex virus encephalitis. Thus, the importance of TLR3 in sensing viruses is not disputed, though more recently it has been shown to have an expanded role in a number of epithelial tissues. For example, inflammatory cytokines are induced by RNA released during necrosis in the gut [20] or damage to the skin [13], [14]. Additionally, recent publications have also demonstrated that TLR3 is important for wound

healing, as *Tlr3*$^{-/-}$ mice have a slightly delayed wound healing phenotype [21], while Polyinosinic acid:Polycytidylic acid (Poly (I:C)), a double-stranded RNA (dsRNA) analog and ligand for TLR3, can promote wound healing in mice [22].

These recent findings suggest that TLR3 may have multiple functions in the skin and may signal the start of barrier repair processes in addition to its role in viral defense. We show herein that TLR3 activation increased expression of genes critical to barrier formation, increased the appearance of epidermal lipids, and increased LB and keratohyalin granules (KHG), important elements of the epithelial barrier repair response. These findings therefore identify TLR3 as a potential regulator of epidermal regeneration following injury.

Methods

Cell Culture and Stimuli. NHEK were obtained from Cascade Biologics/Invitrogen. (catalog number: C-001-5C, Portland, OR), and grown in serum-free EpiLife cell culture media (Cascade Biologics/Invitrogen) containing 0.06 mM Ca^{2+} and 1 × EpiLife Defined Growth Supplement (EDGS, Cascade Biologics/Invitrogen) at 37 °C under standard tissue culture conditions. All cultures were maintained for up to eight passages in this media with the addition of 100 U ml^{-1} penicillin, 100 μg ml^{-1} streptomycin, and 250 ng ml^{-1} amphotericin B. Cells at 60-80% confluence were treated with Bafilomycin A1 (5 nM; Sigma), poly(I:C) (1 μg ml^{-1}; Invivogen), IL-6 (10 ng ml^{-1}; R&D Systems), or tumor necrosis factor-α (50 ng ml^{-1}; Chemicon, Temecula, CA) in 12-well flat bottom plates (Corning Incorporated Life Sciences, Lowell, MA) for up to 24 hours. After cell stimulation, RNA was extracted using TRIzol reagent (Invitrogen, Carlsbad, CA). RNA was stored at -80°C. For visualization or analysis of lipids, cells were switched to advanced stage differentiation media (DMEM:F-12 (2:1), 10% FBS(Invitrogen),400 ng ml^{-1} hydrocortisone (Sigma), 10 ug ml^{-1} human recombinant insulin (Sigma), and freshly made

50 ug ml^{-1} ascorbic acid (Sigma)) for 24 to 72 hours during stimulation. Media was changed every other day and freshly prepared and filter sterilized Vitamin C was added.

Quantitative real-time PCR. Total RNA was extracted from cultured keratinocytes using TRIzol® Reagent (Invitrogen, Carlsbad, CA) and 1 ug RNA was reverse-transcribed using iScript™ cDNA Synthesis Kit (Bio-Rad, Hercules, CA). Pre-developed Taqman® Gene Expression Assays (Applied Biosystems, Foster City, CA) were used to evaluate mRNA transcript levels of ABCA12, GBA, SMPD1, TGM1,TNF, IL-6, KRT1, KRT14, IVL, FLG, LOR, and TLR3. GAPDH mRNA transcript levels were evaluated using a VIC-CATCCATGACAACTTTGGTA-MGB probe with primers 5' CTTAGCACCCCTGGCCAAG-3' and 5'-TGGTCATGAGTCCTTCCACG-3'. All analyses were performed in triplicate and representative of three to five independent cell stimulation experiments that were analyzed in an ABI Prism 7000 Sequence Detection System. Fold induction relative to GAPDH was calculated using the $\Delta\Delta C_t$ method. Results were considered to be significant if $P < 0.05$.

Gene expression profiling. Labeling of cDNA and hybridization to Agilent Unrestricted AMADID Release GE 4x44K 60mer (G4845A) was performed at UCSD's Biomedical Genomics (BIOGEM) Core. Gene expression analysis was performed following multiple loess normalization of the raw data. Significantly changes in gene expression were identified using Significance of Microarrays (SAM) 4.0 with the following filters: 1. False Discovery Rate of 0.01% and 2. Average fold change of ≥ 2. Hierarchical clustering and heat map generation were performed using Genespring GX software (Agilent). Gene ontology and pathway term enrichment was performed using DAVID. P-values represent a modified Fisher's exact test (EASE = 1) n = 3. [23], [24].

Lipid Analysis. Cer, GlcCer, SM, and Chol were obtained from Avanti Polar Lipids Inc. (Alabaster, AL), Sigma (St. Louis, MO), and Matreya (Pleasant Gap, PA). Total lipids were extracted from NHEKs and separated into individual lipid species by high performance thin layer chromatography. Individual lipid content was determined by scanning densitometry [25].

Ultrastructural Analysis. 3-D skin constructs were immersed in modified Karnovsky's fixative (2.5% glutaraldehyde and 2% paraformaldehyde in 0.15 M sodium cacodylate buffer, pH 7.4) for at least 4 hours, post fixed in 1% osmium tetroxide in 0.15 M cacodylate buffer for 1 hour and stained en bloc in 3% uranyl acetate for 1 hour. Samples were dehydrated in ethanol, embedded in Durcupan epoxy resin (Sigma-Aldrich), sectioned at 50 to 60 nm on a Leica UCT ultramicrotome, and picked up on Formvar and carbon-coated copper grids. Sections were stained with 3% uranyl acetate for 5 minutes and Sato's lead stain for 1 minute. Grids were viewed using a JEOL 1200EX II (JEOL, Peabody, MA) transmission electron microscope and photographed using a Gatan digital camera (Gatan, Pleasanton, CA), or viewed using a Tecnai G^2 Spirit BioTWIN transmission electron microscope equipped with an Eagle 4k HS digital camera (FEI, Hilsboro, OR). Pictures taken at 2000X represent 73 μm^2. Approximately 50 pictures were taken of control and Poly (I:C)-treated samples and LB and KHG were counted.

Three-dimensional skin constructs. Three-dimensional skin constructs were purchased from Mattek Corporation and maintained by differentiating Epiderm-201^{TM} Under-developed skin model in EPI-201 differentiation medium (EPI-100-DM) (MatTek Corporation, Ashland, MA) for 72 h at an air-liquid interface during Poly (I:C) stimulation. 3-D constructs made from NHEK treated with siRNA were grown on a collagen fibroblast matrix as previously published [26]. Skin constructs were grown for 6 days after lifting to air/liquid interface, then treated with 1 ug/ml Poly (I:C) and supplemented with 50 ug/ml Vitamin C for 3 additional days.

siRNA constructs. TLR3 and control siRNA were purchased from Dharmacon (Chicago, IL). One nanomole of each siRNA was electroporated into 3 x 10^6 keratinocytes using Amaxa nucleofection reagents (VPD-1002) (Lonza AG, Walkersville, MD).

Non-targeting Pool ON-TARGETplus SMARTpool

1. 5'- UGGUUUACAUGUCGACUAA -3'
2. 5'- UGGUUUACAUGUUGUGUGA -3'
3. 5'- UGGUUUACAUGUUUUCUGA -3'
4. 5 – UGGUUUACAUGUUUUCCUA -3'

TLR3 ON-TARGETplus SMARTpool:

1. 5'- UCACGCAAUUGGAAGAUUA -3'
2. 5'- AGACCAAUCUCUCAAAUUU -3'
3. 5'- CAGCAUCUGUCUUUAAUAA -3'
4. 5'- GAACUAAAGAUCAUCGAUU -3'

Oil Red O staining. Following stimulation, cells were washed once with cold PBS and fixed in 4% paraformaldehyde (Sigma) in PBS for at least 10 minutes at 4°C. Tissue samples were embedded in OCT and frozen prior to being sectioned (10 µm). Cells/tissues were then rinsed with 60% isopropanol. Oil Red O working solution was then applied to cells/tissues for 15 minutes. Samples were again rinsed with 60% isopropanol and followed by another rinse with PBS. Samples were counterstained with hematoxylin solution (Sigma) and mounted using Permount (Fisher). Images were obtained using an Olympus BX51 microscope equipped with Olympus UplanFL objective lenses (40X/0.75). All images were taken at room temperature. Images were acquired with an Olympus DP71 camera using DP Controller 3.3.1.292 and DP Manager Version 3,3,1,222 software by Olympus Corporation.

Lipid Quantification using Oil Red O. Following stimulation, cells were washed once with cold PBS and fixed in 4% paraformaldehyde (Sigma) in PBS for at least 10 minutes at 4°C. Cells/tissues were then rinsed first with PBS, then with 60% isopropanol. Oil Red O working solution was then applied to cells for 2h. Cells were then washed exhaustively with water. 1 ml of 100% isopropanol was added for 30s then removed and absorbance @ 510 nm was measured. Absorbance values were normalized to total protein and fold change was determined after Poly (I:C) treatment.

Results

Gene expression profiling of lipid metabolism and lipid transporter pathways. To identify gene expression pathways in addition to the known inflammatory response associated with TLR3 activation of keratinocytes, we examined the transcriptome of NHEK 24 hours after exposure to the dsRNA Poly(I:C). In response to Poly (I:C), a total of 5542 differentially regulated genes changed by at least 2-fold (2773 upregulated and 2769 downregulated; SAM: triplicate; FDR < 0.01%; delta value = 1.397) (Table 1.1). These genes were further analyzed using the Database for Annotation, Visualization and Integrated Discovery (DAVID) [23], [24]. This analysis suggested Poly(I:C) affected a number of pathways involved in lipid metabolism and transport. Specifically, changes were observed in the expression of genes in glycosphingolipid biosynthesis, ABC transporters, sphingolipid metabolism, and other lipid biosynthesis/metabolism and inflammatory pathways (Figure 1.1a). Several specific genes identified by this approach are known to play a role in maintaining or forming the skin barrier, such as: ABCA12 (3.74-fold), GBA (2.02-fold), SMPD1 (2.04-fold), TGM1 (2.40-fold), as well as tumor necrosis factor (TNF) (5.31-fold), interleukin 6 (IL-6) (27.31- fold), and TLR3 (14.58-fold). Involucrin (IVL), loricrin (LOR), keratin 1 (KRT1), keratin 14 (KRT14) and filaggrin

(FLG), markers of epidermal differentiation, were not changed significantly (Figure 1.1b). The results of the microarray showed that genes involved in synthesis of ceramides (UGCG, SPTLC1, SPTLC2), free fatty acids (ACACA and FASN) and cholesterol (FDFT1, HMCCR, and HMGSC1) were not significantly altered other than acetyl CoA carboxylase (ACACA) (0.33-fold).

Poly (I:C) enhances transcript abundance of genes involved in skin barrier formation. To validate the results of the gene expression profile of Poly (I:C)-treated NHEK, we measured a number of genes by real time PCR. mRNA of ABCA12, GBA, SMPD1, and TGM1 were significantly upregulated following treatment with Poly (I:C) (Figure 1.2a, Table 1.2). As expected, traditional inflammatory markers TNF, IL-6, and TLR3 were also upregulated (Figure 1.2b, Table 1.2). Consistent with microarray data, this treatment did not induce expression of involucrin (IVL), keratin 1 (KRT1), loricrin (LOR), filaggrin (FLG), or keratin 14 (KRT14) (Figure 1.2c, Table 1.2). Interestingly, Poly (I:C) treatment significantly induced expression of mRNA for ceramide synthesis enzymes, including serine palmitoyltransferase (SPTLC1 and SPTLC2) and glucosylceramide synthase (UGCG) (Figure 1.1b, Table 1.2). Ligands for TLR2,-7, -8, and -9 did not significantly alter expression of these barrier repair genes (Figure 1.3). A dose-dependent increase in the mRNA levels of ABCA12, GBA, SMPD1, TNF, and IL-6 was observed following treatment with Poly (I:C), with maximal expression seen after treatment with 0.5 to 1 μg/ml Poly (I:C) (Figure 1.2d). Increases in transcript abundance for ABCA12, GBA AND SMPD1 were not seen until 24 hours after treatment, while TNF expression increased more rapidly and was maximal at 1hr (Figure 1.2e). However, the latter effect on gene expression was not due to induction of these cytokines as treatment of NHEK with TNF or IL-6 had no significant effect on the induction of ABCA12, GBA, or SMPD1 mRNA levels (Figure 1.2e).

Lipoteichoic acid blocks Poly (I:C) induced increases in gene expression. Previous studies by Lai *et al.* showed that activation of TLR2 with lipoteichoic acid (LTA), a major component of the cell wall of gram-positive bacteria, can block Poly (I:C)-induced increases in the inflammatory cytokines TNF and IL-6 [13]. In order to determine whether this same type of regulation affects Poly(I:C)-induced skin barrier repair genes, we treated NHEK with the TLR2 ligands Malp2, Pam3CSK4, and LTA prior to treatment with Poly (I:C). We observed that 10 µg/ml pretreatments with LTA blocked Poly(I:C) induced increases in ABCA12, GBA, TNF, and TLR3 (Figure 1.4). Treatments with Malp2 and Pam3CSK4 had no significant effect on Poly(I:C)-induced skin barrier repair gene increases.

TLR3 activation is required for dsRNA-induced changes in gene expression. To determine if the increases in ABCA12, GBA, SMPD1, and TGM1 mRNA after Poly (I:C) treatment were dependent on TLR3 activation, we used siRNA to knockdown TLR3 in NHEK. When TLR3 was significantly decreased in keratinocytes, Poly (I:C) failed to induce a significant increase in mRNA for the barrier repair genes ABCA12, GBA, SMPD1, TGM1 and TNF (Figure 1.5a). Since TLR3 signaling is dependent on proper acidification and maturation of endosomes [27], we used Bafilomycin A1 (BafA1), a specific inhibitor of the V-type ATPase required for acidification of endosomes and lysosomes, to inhibit TLR3 signaling. BafA1 blocked Poly (I:C)-induced increases in ABCA12, GBA, and SMPD1 mRNA as well as increases in mRNA of the inflammatory cytokines TNF and IL-6 (Figure 1.5b). Similar effects on gene expression were seen when TRIF, a key signaling molecule downstream of TLR3, was knocked down (Figure 1.6). Unlike silencing of TLR3 or TRIF, knocking down MAVS, a key signaling molecule for RIG-I-like receptors that recognizes cytosolic dsRNA, had no significant effect on Poly (I:C)-induced expression of ABCA12, GBA, SMPD1, TGM1 (Figure 1.7). Although TLR3 activation

was important for Poly (I:C)-induced increases in UGCG mRNA, alterations in mRNA for several lipid synthesis genes was largely independent of TLR3 (Figure 1.5c).

Activation of TLR3 alters epidermal lipid content. To determine whether increases in ABCA12, GBA, and SMPD1 transcripts were paralleled by changes in epidermal lipid composition, we first stained for the presence of lipid in NHEK grown in differentiating conditions. A large increase in oil red O-staining bodies was seen when NHEK were exposed to Poly (I:C) for 72 hours (Figure 1.8a). A significantly higher expression of ABCA12 and GBA was also seen upon Poly (I:C) treatment under these conditions (Figure 1.9). Lipids were then quantified by measuring the amount of oil red O dye that was retained after staining and normalizing this to total protein. Poly (I:C) treatment induced significant increases in lipids stained by oil red O at days 1, 2 and 3 (Figure 1.8b). Next, 3-dimensional skin constructs were exposed to Poly (I:C) to determine the response of stratified and differentiated keratinocytes, that model the epidermis but are not influenced by the presence of resident or recruited leukocytes that would be present in vivo. In these 3-D skin constructs, the stratum corneum (SC) of Poly (I:C)-treated samples stained more strongly for oil red O compared to control samples (Figure 1.8c).

To measure the response of specific lipid components produced by cultured keratinocytes, total lipids were isolated from NHEK after Poly (I:C) treatment and resolved using high performance thin layer chromatography. Sphingomyelin was significantly increased following Poly (I:C) treatment and this increase was blocked following siRNA silencing of TLR3 (Figure 1.8d). Glucosylceramide levels were significantly decreased after Poly (I:C) treatment although this change was independent of TLR3 (Figure 1.8e). Ceramides increased following Poly (I:C) treatment, though this increase was not abolished by knock-down of TLR3 (Figure

1.8f). Cholesterol levels were not significantly altered after Poly (I:C) treatment in either control or TLR3 knockdown keratinocytes (Figure 1.8g).

TLR3 activation increases the quantity of lamellar bodies and keratohyalin granules in the epidermis. Since we observed increases in the staining of lipids following exposure to dsRNA, we next sought to determine if other morphological changes in keratinocytes could be observed by electron microscopy. To assess this, we quantitated the number of lamellar bodies (LB) and keratohyalin granules (KHG) in the upper stratum granulosum in 3-D epidermal skin constructs. Skin constructs treated with Poly (I:C) had significantly more LB (Figure 1.10a) and KHG (Figure 1.10b). The observed increases in LB and KHG were dependent on TLR3, as skin constructs generated from TLR3-knockdown NHEK failed to exhibit significant increases in LB and KHG when exposed to Poly (I:C) (Figure 1.10c).

Discussion

TLR activation is classically considered to result in pro-inflammatory responses. In this study, we demonstrate that TLR3 activation of keratinocytes also leads to changes in expression of some genes in keratinocytes that are associated with epidermal structure. An increase in transcript abundance of ABCA12, GBA, SMPD1, and TGM1 occurred in a TLR3-dependent manner. This response was followed by increases in epidermal lipid accumulation as well as increases in the abundance of LB and KHG in epidermal equivalents. These observations are consistent with recent observations that dsRNA is released by damaged cells and can serve as a damage-associated molecular pattern (DAMP). Thus, we now show that skin epithelial cells initiate some of the events associated with barrier repair after recognition of dsRNA.

The protective properties of the skin barrier reside in the SC and are heavily dependent on the lipid-rich lamellar membranes surrounding differentiated keratinocytes [9], [28], [29].

Previous studies have characterized the barrier repair response, delineating the increase in epidermal lipid synthesis and metabolism in the skin [6], [9], [30], [31] and secretion of LB following barrier disruption [1]. Because our current observations show TLR3 activation is accompanied by increases in mRNA encoding genes involved in epidermal formation, accumulation of epidermal lipids, and formation of epidermal organelles, we provide evidence that TLR3 may be a previously unknown mechanism by which keratinocytes detect epidermal injury and initiate some of the steps involved in formation of a functional skin barrier. However, since mice lacking TLR3 appear to develop normally, this recognition system is not critical to normal development. Furthermore, although many Poly (I:C) induced changes in lipid composition and quantity were observed, not all of these changes were TLR3 dependent. It is important to keep in mind that we did not observe a global upregulation in lipid or differentiation markers. In contrast, we observed that dsRNA can induce TLR3-dependent changes only in specific elements involved in the process of repair. How these responses combine into the complete barrier repair program remain to be determined.

A number of receptors are known to recognize and respond to dsRNA [32], making it important to determine whether TLR3 activation was required for the gene expression changes seen in response to dsRNA. Using both RNA silencing and pharmacological inhibition, we demonstrated that increases in skin barrier genes in response to Poly (I:C) were dependent on TLR3. Since the Poly (I:C)-induced changes in mRNA of these barrier genes were almost completely abrogated when TLR3 activation was silenced, our data suggest that TLR3 activation is required for the observed changes. These data do not rule out the contribution of cytoplasmic sensors of dsRNA that exist in the cell, including RIG-I, MDA5, PKR, and NLRP3, although the failure of MAVS knockdown to partially inhibit the Poly (I:C) response argues against a role for cytoplasmic RNA recognition. Thus, the relevance of these sensors in keratinocytes is yet to be clearly defined.

As changes in gene expression are not seen until 24 hours after Poly (I:C) treatment, it is possible that the change in transcription of ABCA12, GBA, SMPD1 and TGM1 is not a direct downstream transcriptional event of TLR3 activation, but rather an autocrine or paracrine effect dependent on synthesis of intermediate genes. TNF and IL-6 are produced following TLR3 activation and have been shown to improve the skin barrier [5], [33]. Therefore, we also examined the direct effects of these cytokines on induction of the barrier genes of interest. Since no changes in gene expression of ABCA12, GBA, or SMPD1 were observed with TNF or IL-6 treatment of keratinocytes under conditions similar to those where Poly (I:C) did induce these cytokines, it is unlikely that these cytokines acting alone are responsible for the observed effects. Future work will seek to better understand the factors responsible for transcriptional regulation of ABCA12, GBA, SMPD1, and TGM1 by TLR3, with specific interest in determining if these genes represent an immediate canonical response to TLR3 or are activated in response to stimulation of intermediate factors that may function in an autocrine manner.

Poly (I:C) recognition by TLR3 in keratinocytes appears to be functionally relevant. Sphingolipids, such as ceramides and its precursors sphingomyelin and glucosylceramide, are essential for the formation and maintenance of the skin barrier [9], [30]. Poly (I:C)-treated keratinocytes displayed a rapid appearance of lipid-containing vesicles and an increase in ceramides. More intense lipid staining in the stratum corneum was also observed in 3-D skin constructs treated with Poly (I:C). Additionally, sphingomyelin levels were increased by Poly (I:C) treatment in a TLR3-dependent manner. In contrast, levels of glucosylceramides decreased following Poly (I:C) treatment, but not in a TLR3-dependent manner. These observations confirmed the importance of TLR3 activation in perturbing epidermal lipid levels but suggest other pathways influenced by the addition of Poly(I:C) also contribute to the response of some lipids. It remains to be determined whether Poly (I:C) treatment of NHEK can stimulate *de* novo lipid synthesis. As our mRNA data of a number of lipid metabolism genes show that dsRNA can

alter these transcripts, it is possible that the enzyme activity could also be altered, but this remains to be explored. As ORO-positive vesicles most likely contain a mix of nonpolar lipids, we do not believe that the TLR3-dependent increases in sphingomyelin are being detected in those experiments, rather other lipid species that have yet to be identified. Future studies will hopefully elucidate whether *de novo* lipid synthesis is occurring and which additional lipid species are increased in a TLR3-dependent manner.

To further investigate functional changes in keratinocytes following Poly (I:C) treatment, we examined ultrastructural changes in keratinocytes within 3-D skin constructs. Treatment of keratinocytes with Poly (I:C) yielded a higher amount of both LB and KHG in the granular layer of the epidermis. Although LB have been found to be depleted in the granular layer following barrier disruption due to their rapid trafficking and secretion of barrier components [1], they are rapidly regenerated to aid in future barrier repair as well as proper differentiation and barrier formation. We speculate that TLR3 activation by endogenous dsRNA could be an initiation event that leads to downstream effects of epidermal lipid production, trafficking, and metabolism. Increases in KHG also provide further evidence that Poly (I:C) treatment could promote barrier formation or repair as KHG also contain essential barrier components of the stratum corneum including profilaggrin and LOR. Though we do not see increases in transcripts of FLG and LOR after Poly (I:C) treatment, the increased presence of KHG provides evidence suggesting that dsRNA can influence barrier formation.

We believe that this work identifies a key recognition event that could trigger some elements of skin barrier formation during the process of repair. How this recognition event is propagated after TLR3 activation remains to be determined. These results however, could be utilized in the treatment of certain dermatological diseases such as atopic dermatitis (AD). For years it has been known that AD patients have significantly decreased ceramide levels in the stratum corneum [34], [35]. Although some recent studies have shown AD to be associated with

FLG mutations [36], a number of reports cite and characterize cases of AD that are independent of *FLG* mutations [37] and demonstrate that AD patients have abnormal ceramide profiles and lamellar lipid organization [38], [39]. From our research, it could be speculated that this deficiency of ceramides in the stratum corneum of AD patients could be treated by pharmacological activation of pathways downstream of TLR3, thus leading to increases in ceramides. Of course, many unwanted inflammatory side effects may result from TLR3 activation, so it will be important to determine specifically which pathways downstream of TLR3 are involved in the increase of epidermal lipids. By examining these downstream pathways, we may also discover more about the regulatory events involved in ceramide biosynthesis and metabolism that could be affected in AD patients. Future studies will involve identifying and characterizing these downstream pathways of TLR3 activation relevant to barrier repair.

Acknowledgements

We thank J Sprague, G Hardiman, and R Sasik at the UCSD Biomedical Genomics laboratory for assisting in microarray analysis. We thank Y Jones and T Meerloo at the UCSD EM Core for processing samples and helpful discussion and Dr. Marilyn Farquhar for helpful discussion of EM images.

This work was supported by US National Institutes of Health (NIH) grants R01-AR052728, NIH R01-AI052453 and R01 AI0833358 to R.L.G., the UCSD Training in Immunology Grant 5T32AI060536-05 and UCSD Dermatologist Investigator Training Program Grant 1T32AR062496-01 supporting A.W.B.

Chapter 1, in part, is a reprint of the material as it appears in The Journal of Investigative Dermatology 2013 (with edits for style). A. W. Borkowski, K. Park, Y. Uchida, R. L. Gallo. Activation of TLR3 in keratinocytes increases expression of genes involved in formation of the

epidermis, lipid accumulation and epidermal organelles. *J Invest Dermatol*. 2013, 133(8): 2031-40. The dissertation author was the primary investigator and author of this paper.

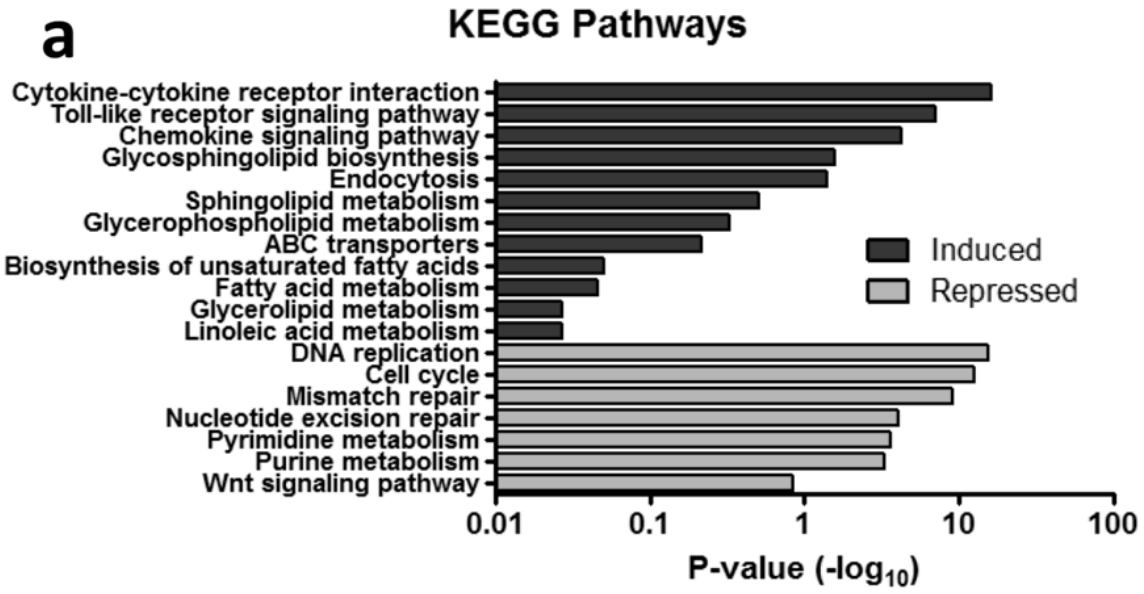

b

Gene	Control			+ 1 µg/ml Poly (I:C)		
IL-6	0.95	0.92	1.13	16.45	21.09	35.75
TLR3	0.96	1.00	1.04	13.14	14.80	15.80
TNF	1.05	0.88	1.07	4.79	5.43	5.70
ABCA12	0.88	1.03	1.09	3.03	3.46	4.73
TGM1	1.07	1.02	0.91	2.31	2.50	2.38
SMPD1	1.02	0.91	1.07	1.93	1.98	2.23
GBA	0.98	0.97	1.05	1.95	1.97	2.16
MAVS	1.04	0.97	1.00	1.82	1.63	1.63
HMGCS1	0.91	1.06	1.03	1.22	1.65	1.93
LOR	1.26	0.84	0.90	2.28	1.37	0.95
SPTLC1	0.98	1.04	0.99	1.17	1.20	1.19
HMGCR	0.96	1.03	1.01	0.93	1.05	1.13
KRT14	1.08	1.00	0.93	1.07	1.08	0.91
FDFT1	1.04	0.93	1.03	0.85	0.80	0.89
FLG	0.92	0.99	1.10	0.90	0.79	0.82
SPTLC2	1.00	1.03	0.97	0.77	0.82	0.84
FASN	1.04	0.96	1.00	0.75	0.60	0.66
UGCG	0.95	1.02	1.03	0.58	0.72	0.71
IVL	0.92	1.07	1.01	0.48	0.65	0.66
KRT1	1.03	1.07	0.90	0.48	0.70	0.37
ACACA	0.89	1.06	1.05	0.30	0.34	0.35

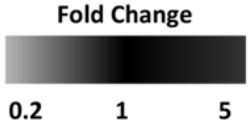

Figure 1.1: Gene expression profiling of NHEK identifies upregulation of genes involved in lipid biosynthesis, metabolism, and transporter pathways following treatment with dsRNA. (a) Significantly changed genes analyzed using DAVID to identify significant pathways (EASE = 1.0). (b) Genes involved in barrier formation with a significant change as identified by SAM.

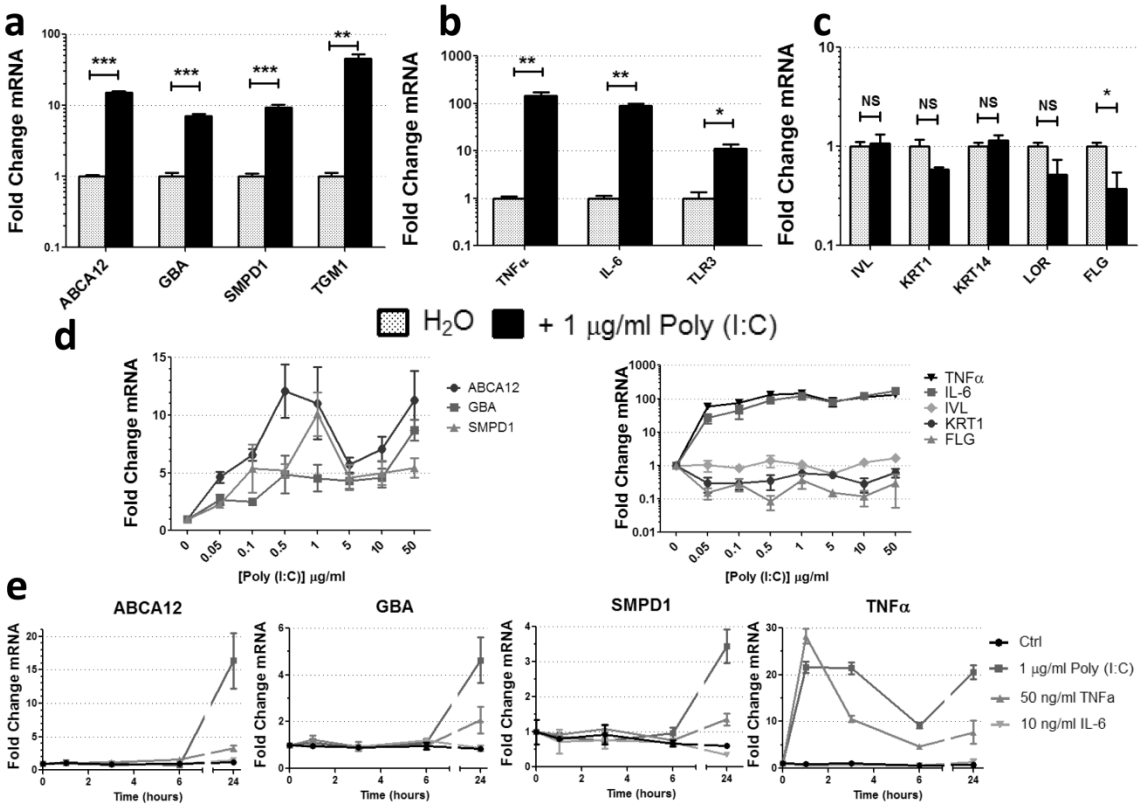

Figure 1.2: Poly (I:C) enhances transcript abundance of genes involved in skin barrier formation. Normal human epidermal keratinocytes were cultured in the presence of 1 μg/ml Poly (I:C) for 24 h. Real-time PCR was used to quantify mRNA levels and fold change values are calculated relative and normalized to GAPDH expression for a number of (a) barrier genes, (b) inflammatory cytokines, and (c) keratinocyte differentiation markers. (d) NHEK were cultured with various doses of Poly (I:C) for 24 h. (e) NHEK were incubated with 1 μg/ml Poly (I:C), 50 ng/ml TNF, or 10 ng/ml IL-6 for 0, 1, 3, 6, or 24 h. Data are mean ± SEM, n = 3, and are representative of at least three independent experiments. **P* < 0.05. Two tailed T-test.

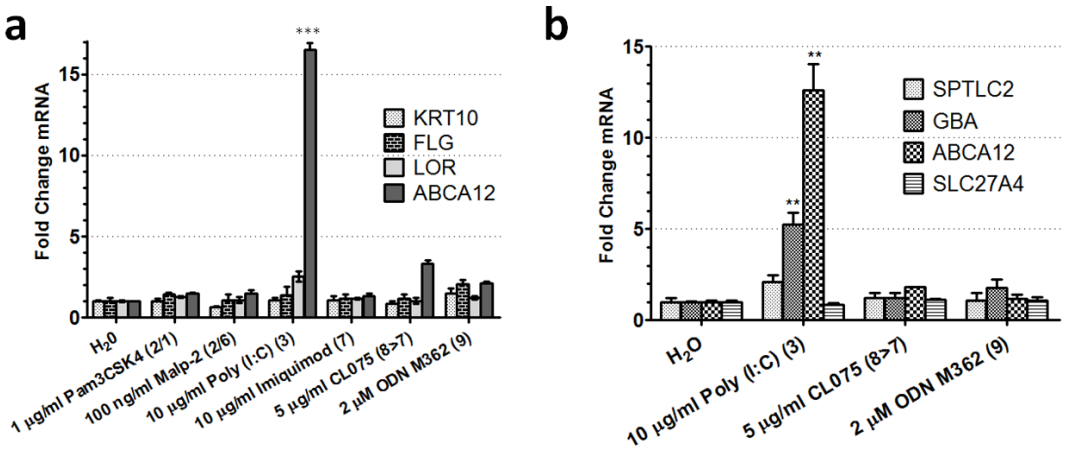

Figure 1.3: TLR3 ligand induces barrier repair genes. (a and b) NHEK were treated with 1 µg/ml Pam3CSK, 100 ng/ml Malp-2, 10 µg/ml Poly (I:C), 10 µg/ml Imiquimod, 5 µg/ml CL075, or 2 µM ODN M362 for 24 h. Real-time PCR was used to quantify mRNA levels and fold change values were calculated relative to and normalized to GAPDH expression. Data are mean ± SEM, n=3, and representative of at least three independent experiments. $^{**}P < 0.01$. $^{***}P < 0.001$ Two-tailed T-test.

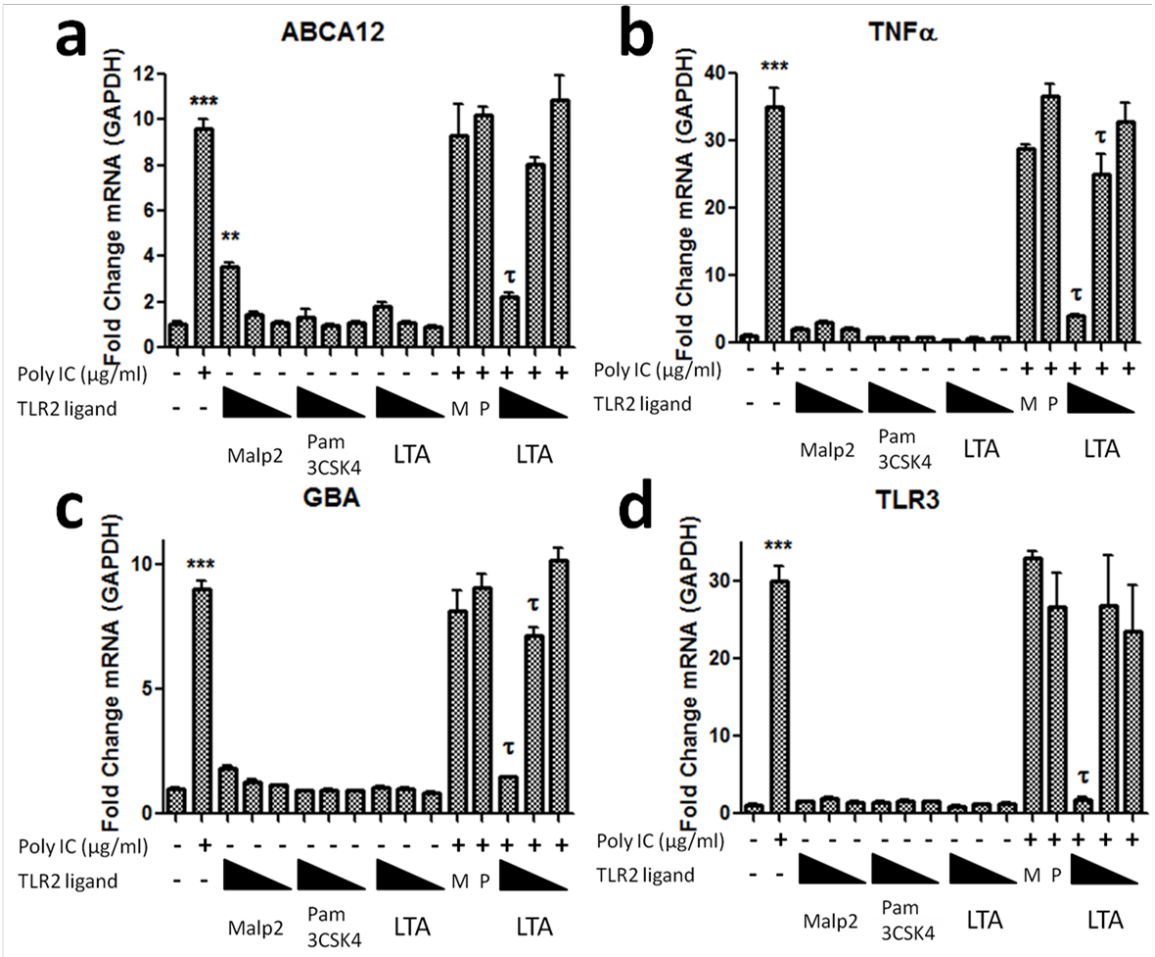

Figure 1.4: Lipoteichoic acid blocks Poly (I:C) induced increases in gene expression. NHEK were cultured in the presence of either Malp2 (10, 100, or 1000 ng/ml), Pam3CSK4 (0.1, 1, or 10 µg/ml), or LTA (0.1, 1, or 10 µg/ml) for 30 minutes prior to 0 or 1 µg/ml Poly (I:C) for 24 hours. Highest concentrations of Malp2 and Pam3CSK4 were used in combination with Poly (I:C). Real-time PCR was used to quantify mRNA levels and fold change values are calculated relative and normalized to GAPDH. ** = $P < 0.01$; ** * = $P < 0.001$ compared to water control. τ = $P <$ 0.01 compared to 1 µg/ml Poly (I:C). One-way ANOVA. Error bars represent SEM. n = 3.

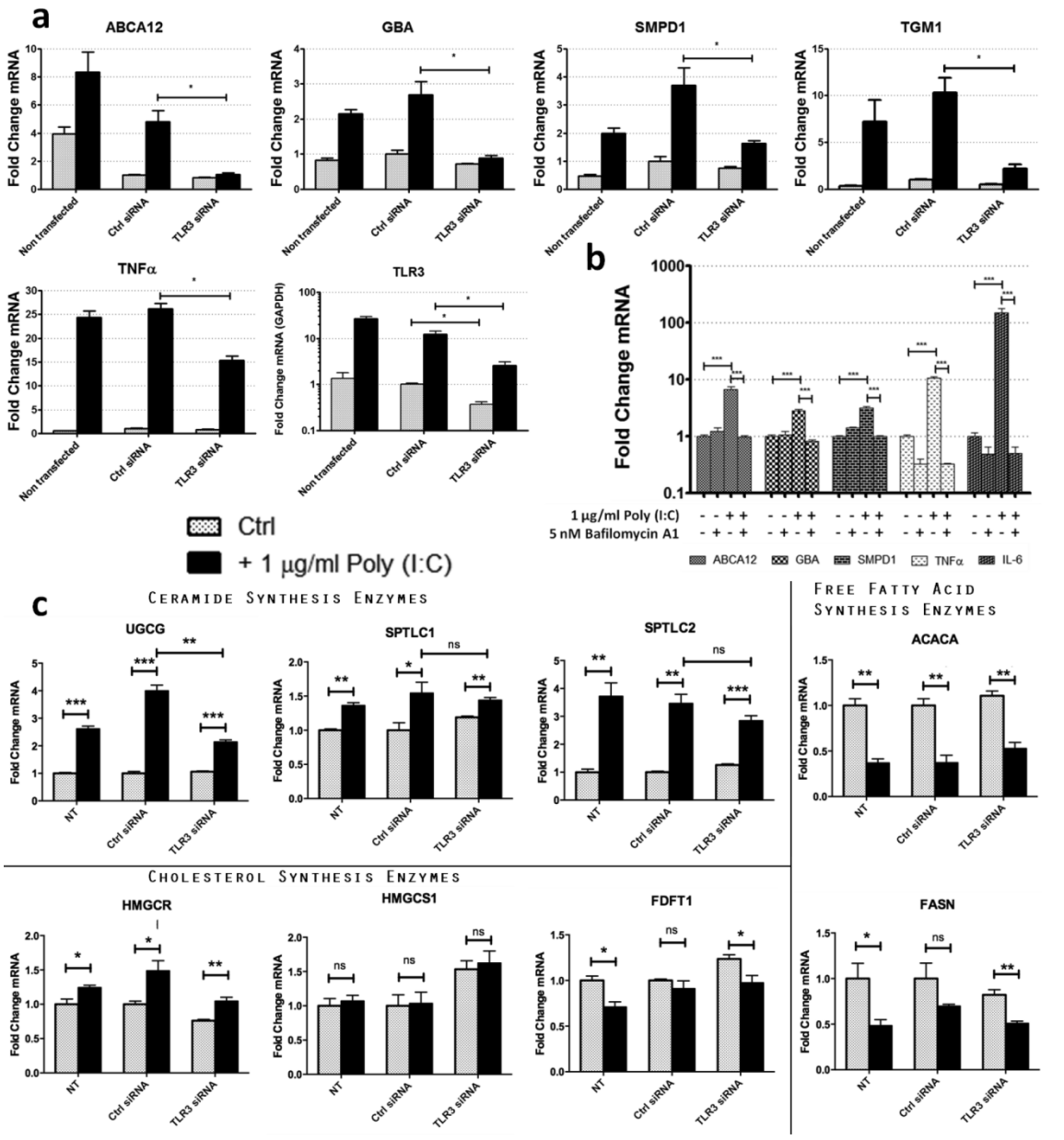

Figure 1.5: TLR3 activation is required for dsRNA-induced changes in gene expression. (a) TLR3 was silenced in NHEK for 48 h before treatment with 1 µg/ml Poly (I:C) for 24 h. Real-time PCR was used to quantify mRNA levels and fold change values are calculated relative and normalized to GAPDH expression. **P* < 0.05. Two tailed T-test. (b) NHEK were treated with 5 nM Bafilomycin A1 for 1 h prior to treatment with 1 µg/ml Poly (I:C) for 24 h. ****P* < 0.001. One-way ANOVA. **(c)** TLR3 was silenced in NHEK for 48 h before treatment with 1 µg/ml Poly (I:C) for 24 h. Real-time PCR was used to quantify mRNA levels and fold change values are calculated relative to and normalized to GAPDH expression. **P* < 0.05. Two tailed T-test. Data are mean ±SEM, n = 3, and are representative of at least three independent experiments.

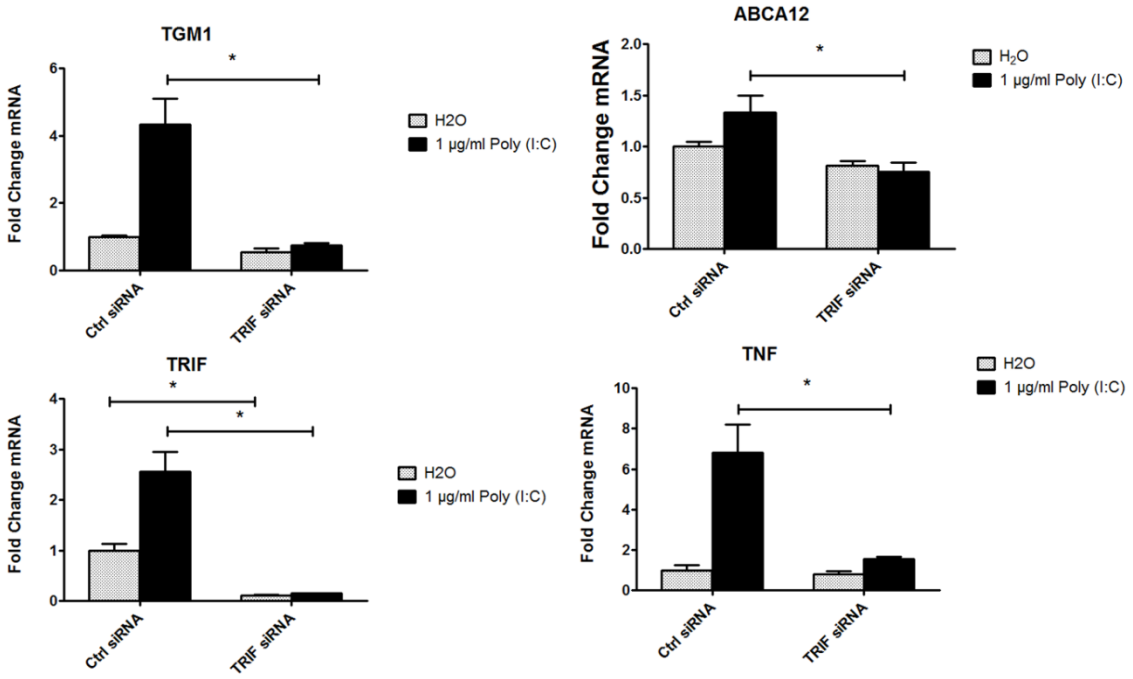

Figure 1.6: TRIF is required for dsRNA-induced changes in skin barrier repair gene expression. TRIF was silenced in NHEK for 48 h before treatment with 1 µg/ml Poly (I:C) for 24 h. Real-time PCR was used to quantify mRNA levels and fold change values are calculated relative to and normalized to GAPDH expression.*$P < 0.05$. Two tailed T-test. Data are mean ± SEM, n = 3.

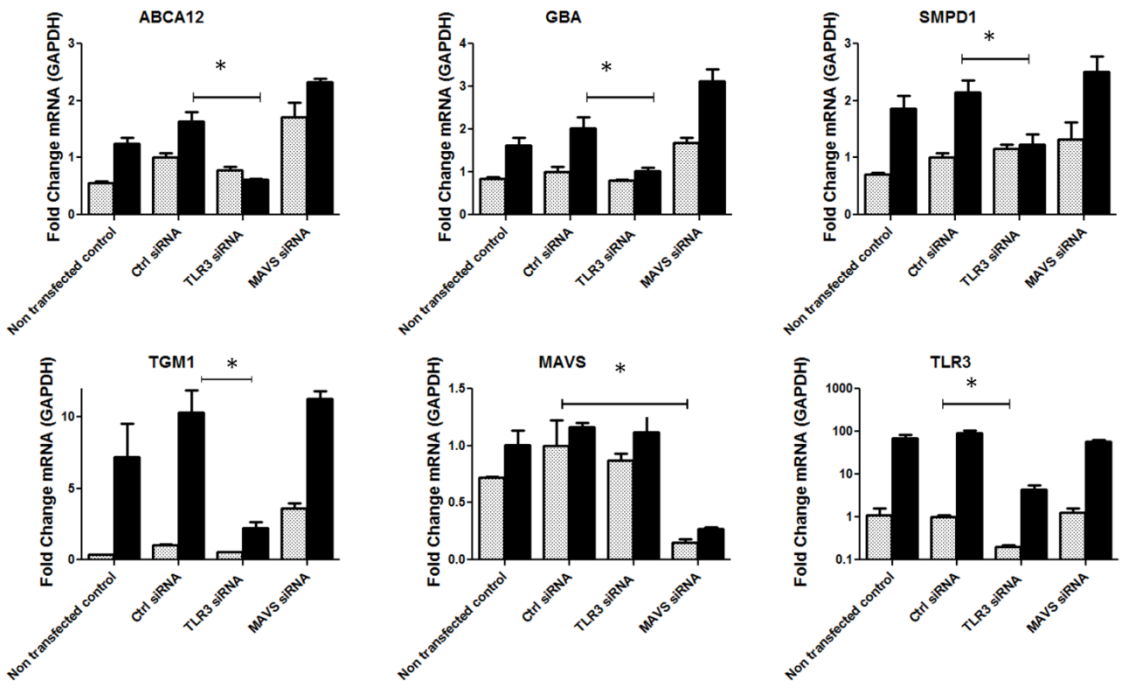

Figure 1.7: MAVS is not required for dsRNA-induced changes in skin barrier repair gene expression. MAVS was silenced in NHEK for 48 h before treatment with 1 µg/ml Poly (I:C) for 24 h. Real-time PCR was used to quantify mRNA levels and fold change values are calculated relative to and normalized to GAPDH expression. *$P < 0.05$. Two tailed T-test. Data are mean ± SEM, n = 3.

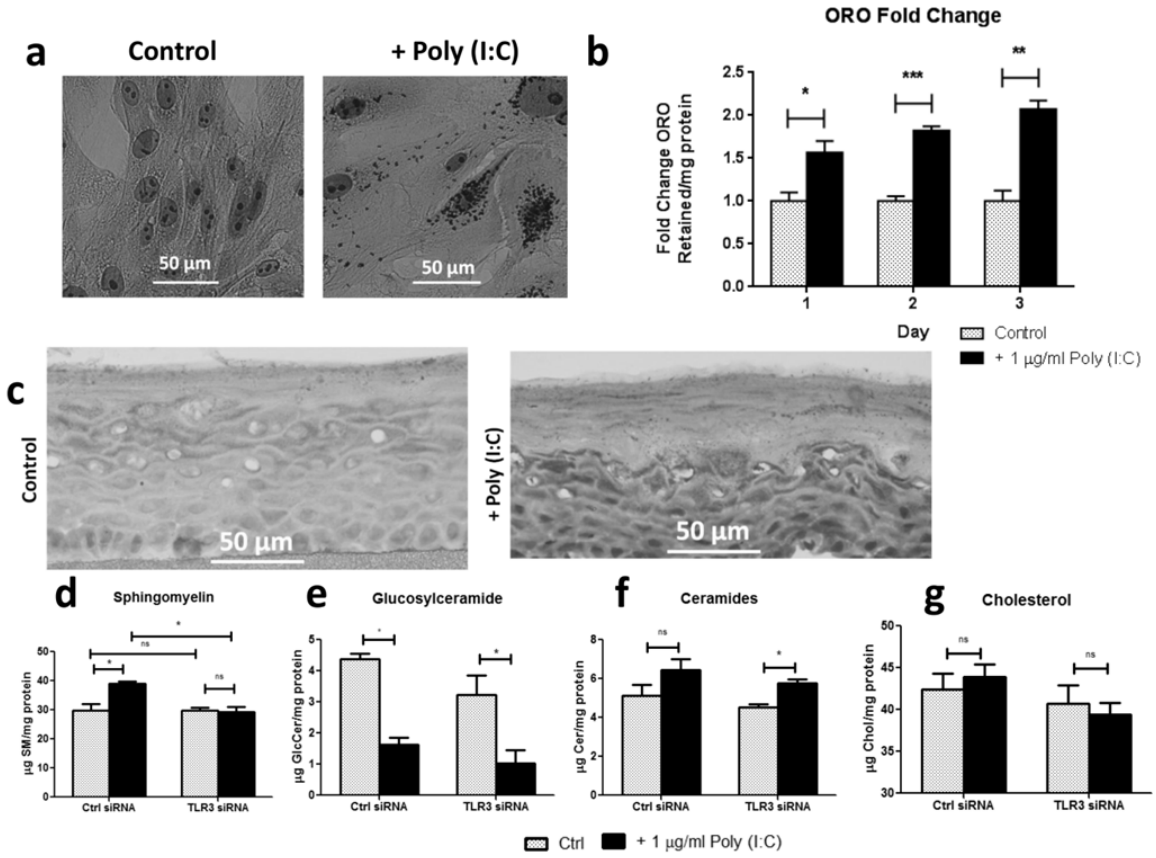

Figure 1.8: Activation of TLR3 alters epidermal lipid content. (a) NHEK were treated for 72 h with 10 µg/ml Poly (I:C), stained with Oil Red O and counterstained with Hematoxylin. Scale bar = 50 µm. (b) NHEK were treated with 1 µg/ml Poly (I:C) for 1, 2, or 3 days, then stained with Oil Red O. (c) 3-D tissue constructs were treated with 1 µg/ml Poly (I:C) for 72 h. Samples were stained with Oil Red O and counterstained with Hematoxylin. Scale bar = 50 µm. (d-g) NHEK were treated with 1 µg/ml Poly (I:C) for 24 h following siRNA knockdown of TLR3. (d) Sphingomyelin, (e) glucosylceramide (f) ceramides, and (g) cholesterol were quantified using HPTLC relative to total protein. $*P < 0.05$. Two-tailed T-test. Data are mean ±SEM, n =3, and are representative of at least three independent experiments.

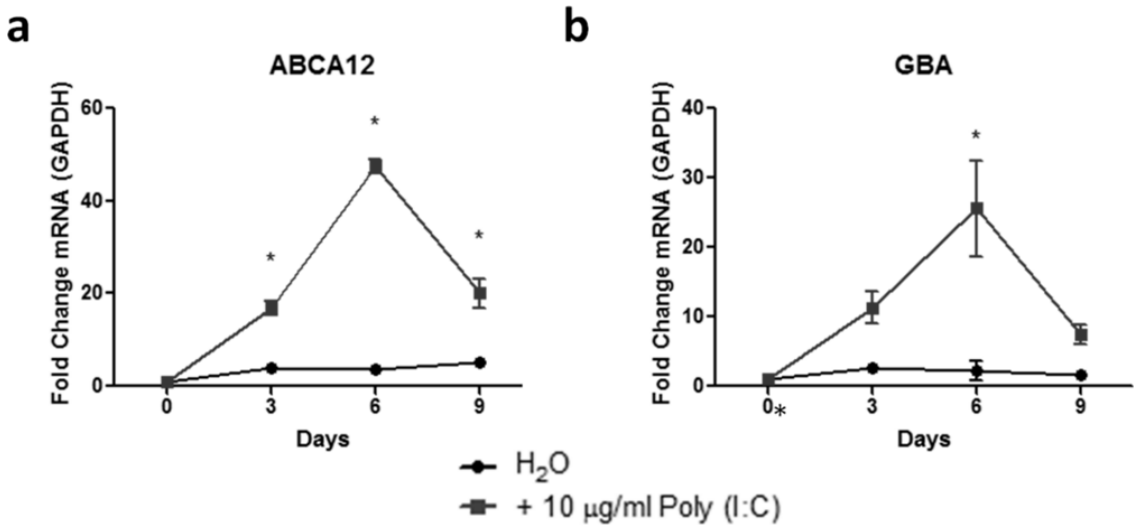

Figure 1.9: TLR3 ligand induces barrier repair genes independent of differentiation. (a and b) NHEK were treated with 1 µg/ml Poly (I:C) in advanced stage differentiation media for 0, 3, 6 and 9 d. Real-time PCR was used to quantify mRNA levels and fold change values are calculated relative and normalized to GAPDH expression. Data are mean ± SEM, n = 3, and representative of at least three independent experiments. *$P < 0.001$ Two-way ANOVA.

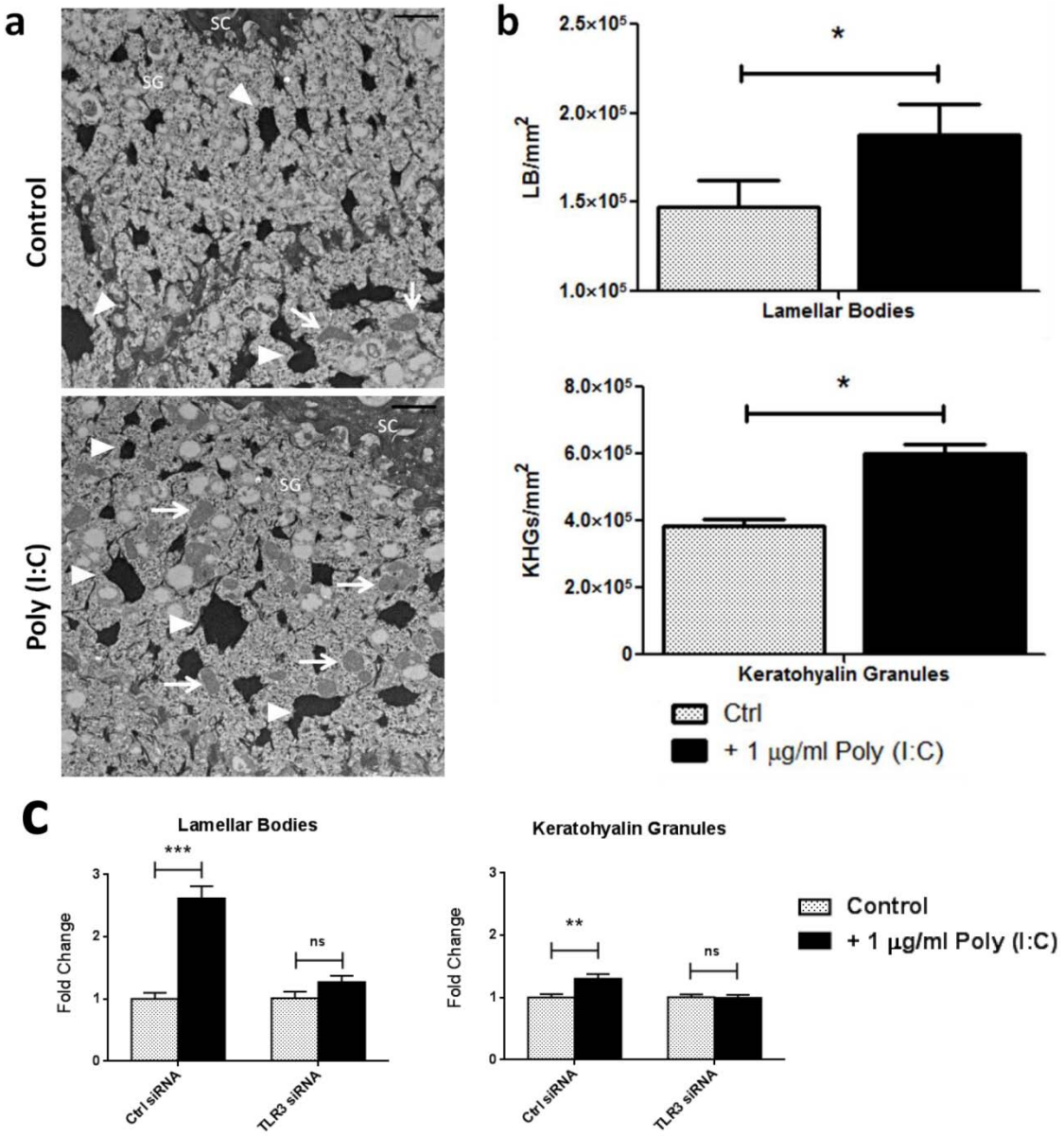

Figure 1.10: TLR3 activation increases the quantity of LB and KHG in the epidermis. (a) Transmission electron microscopy of 3-D skin construct treated with 1 µg/ml Poly IC for 72 h. Arrow = LB. Arrowhead= KHG. Scale bar = 1 µm. SC = stratum corneum. SG = stratum granulosum. (b) Quantification of LB and KHG. *P < 0.05; One-tailed T-test. Control (n = 54), 1 µg/ml Poly (I:C) (n = 47). Data are mean ± SEM. (c) Quantification of LB and KHG in TLR3 knockdown NHEK. *P < 0.05, **P < 0.01, ***P < 0.001. One tailed T-Test. Control siRNA Control (n=54), Control siRNA + 1 µg/ml Poly (I:C) (n = 51), TLR3 siRNA Control (n = 55), TLR3 siRNA + 1 µg/ml Poly (I:C) (n = 54). Data are mean ± SEM.

Table 1.1: Gene expression profiling identifies over 5000 genes regulated by Poly (I:C) treatment at 24 hours. 5542 significantly changed genes (>2-fold) after treatment of NHEK with 1 μg/ml Poly (I:C) for 24 h. Analysis was performed using SAM 4.0 (FDR < 0.01%, n =3, Δ = 1.397).

Poly (I:C) upregulated genes (1-332 of 2773)

Gene Name	Fold Change	Gene Name	Fold Change	Gene Name	Fold Change	Gene Name	Fold Change
SEPT4	2.267	ADAMTS6	4.127	ARL5B	2.282	BAMBI	4.295
A_24_P196019	2.076	ADAMTS6	5.367	ARMCX1	2.244	BATF	2.113
A_24_P247074	2.724	ADAMTS9	3.145	ARNTL2	6.339	BATF2	28.898
A_24_P255874	2.434	ADAP1	2.171	ARPM1	2.823	BATF3	3.148
A_24_P273245	2.326	ADAP2	2.048	ARPM1	2.735	BAZ1A	2.737
A_24_P349547	8.026	ADAR	4.398	ARPM1	2.673	BAZ1A	2.688
A_24_P358305	2.001	ADAT2	3.386	ARPM1	2.814	BAZ1A	2.876
A_24_P691826	7.223	ADC	2.039	ARPM1	2.692	BAZ1A	2.834
A_24_P7750	2.466	ADCY4	9.424	ARPM1	2.694	BAZ1A	2.648
A_24_P84608	2.436	ADCY7	2.647	ARPM1	2.728	BAZ1A	2.638
A_32_P101860	8.535	ADM2	2.318	ARPM1	2.701	BAZ1A	2.642
A_32_P144220	2.398	ADORA2A	3.129	ARPM1	2.600	BAZ1A	2.648
A_32_P214340	3.259	ADPRH	2.757	ARPM1	2.743	BAZ1A	2.677
A_32_P75661	2.685	ADPRHL2	2.479	ARSA	2.115	BAZ1A	2.693
A_32_P88905	5.598	AGPAT3	2.214	ASAH2	2.065	BAZ2B	2.027
A_33_P3219454	2.811	AGXT2L2	2.192	ASAP2	2.385	BAZ2B	2.017
A_33_P3221980	2.288	AIDA	2.327	ASPRV1	2.100	BAZ2B	2.021
A_33_P3227731	2.264	AIM2	52.001	ATF3	16.662	BCAP29	2.255
A_33_P3231005	3.271	AK090649	2.201	ATF3	11.906	BCL2L13	2.679
A_33_P3233953	2.216	AK124325	2.479	ATF3	41.415	BCL2L13	2.779
A_33_P3235831	2.080	AK316198	6.016	ATF4	2.119	BCL2L13	2.803
A_33_P3239102	3.092	AKIRIN1	2.477	ATF5	2.288	BCL2L13	2.698
A_33_P3263274	3.111	AKIRIN1	2.156	ATF5	2.440	BCL2L13	2.777
A_33_P3265205	2.420	AKIRIN2	2.001	ATF5	2.478	BCL2L13	2.707
A_33_P3278152	2.077	AKT3	2.138	ATF5	2.391	BCL2L13	2.806
A_33_P3278303	3.971	ALOX15B	5.237	ATF5	2.386	BCL2L13	2.181
A_33_P3291871	3.376	AMBRA1	2.106	ATF5	2.371	BCL2L13	2.714
A_33_P3295077	2.189	AMOTL2	2.945	ATF5	2.371	BCL2L13	2.832
A_33_P3298980	4.946	AMPD3	5.921	ATF5	2.315	BCL2L13	2.850
A_33_P3303430	2.423	ANGPTL4	3.136	ATF5	2.385	BCL2L14	2.272
A_33_P3306327	2.054	ANKFY1	2.096	ATF5	2.287	BCL2L14	2.691
A_33_P3314073	2.232	ANKIB1	3.068	ATG3	2.038	BCL2L14	2.676
A_33_P3315074	4.361	ANKK1	2.469	ATL1	3.369	BCL2L14	2.393
A_33_P3319502	12.340	ANKLE2	2.322	ATL3	2.590	BCL2L14	2.410
A_33_P3319785	2.753	ANKLE2	2.197	ATL3	2.529	BCL2L14	2.427
A_33_P3327140	2.899	ANKLE2	2.194	ATL3	2.564	BCL2L14	2.448
A_33_P3329740	2.230	ANKLE2	2.228	ATL3	2.512	BCL2L14	2.579
A_33_P3340424	2.182	ANKLE2	2.302	ATL3	2.502	BCL2L14	2.473
A_33_P3341509	2.097	ANKLE2	2.253	ATL3	2.436	BCL2L14	2.582
A_33_P3347387	2.529	ANKLE2	2.231	ATL3	2.478	BCL3	2.547
A_33_P3349384	2.507	ANKLE2	2.383	ATL3	2.436	BHLHE40	2.141
A_33_P3349597	4.758	ANKLE2	3.155	ATL3	2.576	BID	2.018
A_33_P3351999	2.068	ANKLE2	2.330	ATL3	2.605	BIK	2.488
A_33_P3352085	5.492	ANKLE2	2.244	ATP2B4	2.649	BIRC2	2.743
A_33_P3362239	4.067	ANKMY1	3.075	ATP9A	2.587	BIRC3	50.121
A_33_P3368895	2.207	ANKRD37	2.290	ATXN1	4.233	BLZF1	4.748
A_33_P3380236	4.090	ANO9	2.277	ATXN7L1	2.286	BLZF1	4.174
A_33_P3400292	4.325	ANPEP	3.922	ATXN8	3.077	BLZF1	3.638
A_33_P3403851	10.355	ANTXR2	3.818	AX721280	2.307	BMP2	6.240
A_33_P3411384	2.330	ANTXR2	3.374	AZI2	2.204	BPGM	4.829
A_33_P3673310	5.048	ANTXR2	4.177	AZI2	2.025	BSPRY	5.126
A4GALT	2.683	ANXA2	2.191	B2M	11.355	BST2	18.749
ABCA1	2.741	ANXA8L2	2.799	B2M	11.027	BST2	13.440
ABCA1	2.201	APOBEC3A	24.341	B2M	10.492	BTC	7.601
ABCA12	3.741	APOBEC3B	4.815	B2M	11.131	BTG1	4.971
ABCD1	3.636	APOBEC3F	4.048	B2M	10.889	BTN2A1	5.394
ABHD3	2.048	APOBEC3G	18.313	B2M	10.454	BTN2A1	3.995
ABI1	2.416	APOL1	7.584	B2M	11.134	BTN2A2	5.498
ABI3BP	3.995	APOL2	6.192	B2M	10.446	BTN2A3	2.511
ABI3BP	2.126	APOL3	4.099	B2M	10.950	BTN3A1	4.674
ABL2	2.741	APOL4	8.751	B2M	11.528	BTN3A1	3.119
ABL2	2.241	APOL6	6.945	B3GALNT1	2.433	BTN3A2	4.222
ABL2	2.208	APOL6	3.295	B3GALT4	5.827	C10orf10	2.088
ABLIM3	2.004	APOL6	2.494	B3GNT2	6.683	C10orf118	2.041
ABR	2.103	AQP9	2.071	B3GNT3	2.262	C10orf47	2.170
ABTB2	2.740	AQP9	2.303	B3GNT7	2.713	C10orf78	2.460
ACADVL	2.136	AQP9	2.117	B3GNT8	2.475	C11orf17	2.021
ACBD5	2.685	AQP9	2.263	B3GNT8	2.536	C11orf52	5.634
ACE2	12.825	AQP9	2.066	B3GNT8	2.517	C12orf35	2.076
ACHE	2.031	AQP9	2.190	B3GNT8	2.527	C12orf70	7.043
ACOT1	2.085	AQP9	2.232	B3GNT8	2.547	C13orf31	2.128
ACOT4	2.521	AQP9	2.139	B3GNT8	2.544	C14orf73	3.248
ACOXL	3.038	AQP9	2.122	B3GNT8	2.491	C15orf39	2.337
ACP2	2.593	AQP9	2.210	B3GNT8	2.562	C15orf48	502.136
ACP2	3.173	ARFRP1	2.822	B3GNT8	2.551	C16orf67	2.619
ACSL5	2.257	ARFRP1	2.454	B3GNT8	2.643	C16orf7	2.568
ACVRL1	7.917	ARHGAP17	2.283	B4GALT1	3.293	C16orf87	2.204
ADAM10	2.264	ARHGAP27	5.042	B4GALT5	7.027	C17orf28	3.144
ADAM19	3.873	ARHGEF15	2.639	BACH1	2.909	C17orf48	2.064
ADAM8	8.012	ARID3B	2.870	BAG1	2.678	C17orf67	4.718
ADAMTS1	2.794	ARID5A	3.514	BAG1	2.670	C17orf67	4.659
ADAMTS1	2.800	ARID5A	2.058	BAG1	2.664	C17orf96	24.069
ADAMTS4	7.336	ARL14	2.221	BAK1	3.559	C19orf10	2.054

Table 1.1: continued

Poly (I:C) upregulated genes (333-664 of 2773)

Gene Name	Fold Change	Gene Name	Fold Change	Gene Name	Fold Change	Gene Name	Fold Change
C19orf12	2.937	CANT1	2.614	CD40	8.909	CLSTN3	2.140
C19orf28	3.839	CANT1	2.850	CD40	8.556	CLTB	3.223
C19orf66	2.738	CAP1	2.096	CD47	3.389	CMIP	2.409
C1GALT1C1	2.625	CAP1	2.268	CD58	2.921	CMPK2	140.473
C1orf106	6.496	CAPG	2.371	CD58	3.220	CMTM3	2.026
C1orf106	6.703	CAPG	2.590	CD63	2.010	CNKSR1	2.404
C1orf106	6.541	CAPN3	2.433	CD68	12.529	CNP	3.725
C1orf106	6.603	CARD11	3.229	CD70	6.303	COG3	2.028
C1orf106	6.531	CARD16	2.877	CD74	2.028	COG5	2.200
C1orf106	6.329	CARD17	3.336	CD82	2.509	COL17A1	2.628
C1orf106	6.737	CARD6	4.460	CD83	2.965	COL22A1	2.632
C1orf106	6.427	CARD6	4.412	CDCP1	2.194	COL5A3	4.190
C1orf106	6.449	CARD8	2.427	CDCP1	2.220	COL9A2	2.470
C1orf106	6.400	CASP1	2.793	CDCP1	2.173	COQ10B	2.491
C1orf38	9.024	CASP10	4.199	CDCP1	2.144	COQ10B	2.555
C1orf54	4.389	CASP2	2.367	CDCP1	2.141	COQ10B	2.492
C1orf55	2.080	CASP4	2.680	CDCP1	2.071	COQ10B	2.472
C1orf68	3.627	CASP5	2.615	CDCP1	2.242	COQ10B	2.421
C1orf74	6.461	CASP7	3.401	CDCP1	2.074	COQ10B	2.460
C1orf74	6.632	CASP8	2.102	CDCP1	2.482	COQ10B	2.479
C1orf74	6.668	CAST	2.974	CDCP1	2.256	COQ10B	2.425
C1orf74	6.690	CASZ1	2.097	CDCP1	2.055	COQ10B	2.245
C1orf74	6.661	CBLN3	2.945	CDGAP	2.598	COQ10B	2.641
C1orf74	6.579	CBR3	4.621	CDH2	2.240	COQ10B	2.450
C1orf74	6.536	CCDC109B	3.086	CDH3	2.501	CORO6	4.074
C1orf74	6.390	CCDC149	2.066	CDK5R1	4.317	CORO7	2.753
C1orf74	6.445	CCDC64B	6.420	CDKL5	2.848	COX7A1	2.069
C1orf74	6.855	CCDC71	2.148	CDKN1A	2.408	CPAMD8	20.178
C1orf81	3.811	CCDC80	2.230	CDKN2A	2.954	CPEB2	5.350
C1QTNF1	4.191	CCDC88C	2.077	CDKN2A	3.289	CPEB4	3.304
C1R	23.423	CCDC9	3.446	CDKN2D	6.161	CPT1B	4.276
C1R	13.309	CCIN	2.545	CDSN	11.964	CRB3	6.300
C1RL	3.283	CCL2	2.488	CDYL2	2.208	CRCT1	2.171
C1S	16.502	CCL2	2.434	CEACAM1	7.912	CREB3	2.332
C1S	6.043	CCL2	2.431	CEACAM1	22.601	CRLF3	2.151
C20orf134	2.534	CCL2	2.303	CEACAM3	4.172	CRYAB	8.268
C21orf91	2.056	CCL2	2.421	CEACAM3	4.023	CSAG1	6.618
C3	3.273	CCL2	2.293	CFB	53.542	CSAG2	5.962
C3	4.903	CCL2	2.384	CFH	2.759	CSF1	2.521
C3orf21	2.465	CCL2	2.345	CFH	2.301	CSF2	9.979
C3orf32	3.812	CCL2	2.412	CFH	3.166	CSF3	4.995
C3orf38	2.869	CCL2	2.430	CFHR3	2.666	CSGALNACT2	2.081
C3orf39	2.569	CCL20	10.187	CFHR3	2.587	CSRNP1	7.073
C3orf52	2.433	CCL28	2.281	CFHR3	2.566	CSRNP1	4.583
C3orf67	2.714	CCL3	86.620	CFHR3	2.509	CSRNP2	2.612
C4orf33	3.187	CCL3L3	12.986	CFHR3	2.546	CTHRC1	3.374
C4orf34	2.763	CCL3L3	10.186	CFHR3	2.604	CTHRC1	3.131
C4orf34	2.692	CCL4	57.111	CFHR3	2.459	CTHRC1	3.299
C4orf34	2.642	CCL4	62.464	CFHR3	2.502	CTHRC1	3.150
C4orf34	2.610	CCL4L1	7.787	CFHR3	2.569	CTHRC1	3.268
C4orf34	2.688	CCL5	97.333	CFHR3	2.298	CTHRC1	3.094
C4orf34	2.652	CCND3	2.413	CFLAR	11.661	CTHRC1	3.373
C4orf34	2.580	CCNL1	2.264	CFLAR	21.420	CTHRC1	3.311
C4orf34	2.753	CCNL1	2.066	CH25H	3.548	CTHRC1	3.497
C4orf34	2.627	CCNYL1	3.468	CHGA	3.802	CTHRC1	3.276
C4orf34	2.612	CCRL1	8.529	CHIC2	2.310	CTNNA1	2.020
C4orf7	6.378	CCRN4L	3.416	CHIC2	2.193	CTSC	4.460
C5orf15	2.533	CD164	2.559	CHIC2	2.238	CTSC	10.931
C5orf15	2.734	CD164	2.102	CHIC2	2.270	CTSO	2.779
C5orf39	2.687	CD200	16.675	CHIC2	2.222	CTSS	6.046
C5orf41	3.386	CD200	16.247	CHIC2	2.281	CTSZ	8.787
C6orf150	3.790	CD200	16.581	CHIC2	2.364	CX3CL1	5.374
C6orf47	2.026	CD200	15.672	CHIC2	2.376	CXCL1	6.730
C6orf47	2.133	CD200	16.001	CHIC2	2.296	CXCL1	7.308
C6orf47	2.010	CD200	16.106	CHIC2	2.366	CXCL10	307.243
C6orf47	2.015	CD200	16.061	CHMP4B	3.409	CXCL10	40.821
C6orf47	2.059	CD200	4.796	CHMP4C	2.157	CXCL11	229.637
C6orf47	2.038	CD200	16.208	CHMP5	2.213	CXCL16	4.952
C6orf62	2.058	CD200	16.400	CHST2	2.706	CXCL16	4.574
C8orf47	7.396	CD200	15.814	CIB2	2.697	CXCL2	5.864
C8orf60	2.108	CD274	4.995	CILP2	2.073	CXCL2	9.228
C9orf21	2.428	CD274	8.630	CIR1	2.169	CXCL3	10.005
C9orf91	2.023	CD276	2.144	CITED2	3.002	CXCL6	3.158
CA8	2.432	CD38	20.915	CKAP4	2.352	CXCL9	56.790
CAB39	4.712	CD40	8.907	CKB	9.987	CXCR3	2.915
CAB39	3.461	CD40	8.981	CLCF1	4.450	CXorf38	3.209
CALCOCO2	2.089	CD40	9.042	CLDN14	71.772	CXorf40B	2.201
CALM1	2.381	CD40	9.032	CLDN23	8.485	CXorf40B	2.232
CALM3	2.922	CD40	8.680	CLDN4	11.020	CXorf49B	2.055
CALR	2.160	CD40	8.526	CLDN7	12.166	CXorf65	4.938
CAMK2D	2.515	CD40	8.771	CLIC4	3.246	CYB5R2	4.532
CAMK2D	2.938	CD40	8.902	CLIC4	2.428	CYB5R2	4.526
CAND1	2.160	CD40	9.167	CLIP1	2.222	CYP27B1	2.808

Table 1.1: continued

Poly (I:C) upregulated genes (665-996 of 2773)

Gene Name	Fold Change	Gene Name	Fold Change	Gene Name	Fold Change	Gene Name	Fold Change
CYP2J2	5.688	DUSP1	7.202	ENST00000376536	2.009	FAM63B	2.075
CYP2J2	5.646	DUSP1	7.209	ENST00000376793	17.213	FAM65A	2.139
CYP2J2	5.733	DUSP1	7.415	ENST00000377043	2.702	FAM71F1	4.263
CYP2J2	5.506	DUSP1	7.338	ENST00000378947	2.024	FAM83E	4.227
CYP2J2	5.668	DUSP1	7.274	ENST00000379253	2.637	FAM84B	2.377
CYP2J2	5.584	DUSP1	7.283	ENST00000381056	2.069	FAM98B	2.308
CYP2J2	5.603	DUSP1	7.058	ENST00000381081	2.272	FAS	3.088
CYP2J2	5.660	DUSP1	7.156	ENST00000381747	2.888	FAS	2.882
CYP2J2	5.894	DUSP1	7.060	ENST00000391418	2.422	FAS	3.025
CYP2J2	5.602	DUSP1	7.187	ENST00000394035	2.015	FAS	2.794
CYR61	2.111	DUSP10	5.507	ENST00000394157	2.237	FAS	2.847
CYTH1	2.834	DUSP11	2.286	ENST00000394253	4.065	FAS	2.870
CYTH1	3.019	DUSP11	2.598	ENST00000395861	2.509	FAS	2.897
CYTH4	3.310	DUSP8	2.072	ENST00000396446	2.439	FAS	3.377
DAB2IP	3.218	DYNLT1	2.908	ENST00000397559	2.066	FAS	2.938
DAB2IP	2.474	DYNLT3	2.157	ENST00000397571	5.998	FAS	2.909
DAB2IP	2.555	EBI3	15.700	ENST00000398769	3.336	FAS	2.872
DAB2IP	2.596	EBI3	15.060	ENST00000398782	2.578	FAS	2.950
DAB2IP	2.500	EBI3	16.336	ENST00000399288	2.118	FBXO10	2.029
DAB2IP	2.457	EBI3	15.553	ENST00000399561	2.016	FBXO11	2.050
DAB2IP	2.542	EBI3	15.089	ENST00000399573	4.841	FBXO6	10.957
DAB2IP	2.380	EBI3	14.528	ENST00000400702	6.497	FBXO7	2.088
DAB2IP	2.555	EBI3	14.499	ENST00000401931	2.500	FEM1B	2.377
DAB2IP	2.454	EBI3	15.398	ENST00000402522	5.811	FERMT1	4.835
DAB2IP	2.482	EBI3	14.731	ENST00000405395	3.449	FERMT1	4.098
DAPP1	3.279	EBI3	15.812	ENST00000409590	2.917	FERMT2	2.372
DBNDD2	2.918	ECE1	2.901	ENST00000410015	2.100	FERMT2	2.416
DCAF10	2.636	ECE1	2.107	ENST00000412305	2.946	FGD2	2.059
DCBLD2	2.053	EDN1	5.867	ENST00000412305	3.651	FGD6	2.128
DCP_22_0	10.654	EDN1	5.839	ENST00000420470	2.350	FGF2	15.117
DCP_22_0	10.961	EDN1	5.934	ENST00000434012	2.572	FGF2	17.765
DCP_22_2	10.245	EDN1	5.721	ENST00000439554	4.025	FGF5	2.360
DCP_22_2	10.113	EDN1	6.126	ENST00000452379	2.215	FICD	2.576
DCP_22_4	9.566	EDN1	6.016	ENTPD6	2.073	FKBP1A	2.030
DCP_22_4	9.582	EDN1	6.056	EPB41L4A	6.281	FKBP1B	3.781
DCP_22_6	8.280	EDN1	6.100	EPB41L4A	3.772	FLCN	2.154
DCP_22_6	8.346	EDN1	6.059	EPHA2	3.755	FLJ10357	2.498
DCP_22_7	5.444	EDN1	6.039	EPSTI1	17.308	FLJ11235	2.682
DCP_22_7	5.579	EDN1	5.984	EPSTI1	16.028	FLJ32255	2.386
DCP1A	3.282	EFNA1	4.209	EPSTI1	17.073	FLJ32810	2.148
DCP1A	4.399	EFNA1	4.165	EPSTI1	17.795	FLJ36031	2.119
DCUN1D3	2.187	EFNA1	4.206	EPSTI1	17.849	FLJ45949	3.926
DDAH2	2.005	EFNA1	4.330	EPSTI1	16.901	FLOT1	2.277
DDIT3	2.145	EFNA1	4.152	EPSTI1	17.675	FLT3LG	2.370
DDX58	39.995	EFNA1	4.275	EPSTI1	17.232	FMNL3	2.227
DDX58	18.527	EFNA1	4.224	EPSTI1	17.168	FMR1	2.307
DDX60	8.357	EFNA1	4.035	EPSTI1	17.320	FMR1	2.213
DDX60L	13.467	EFNA1	4.317	ERO1L	2.721	FNDC3A	2.446
DECR1	2.003	EFNA1	4.249	ERO1L	2.734	FNDC3B	3.018
DEFB1	6.162	EFTUD1	2.805	ERO1L	2.590	FOSL1	2.240
DEFB103A	2.088	EGFLAM	2.269	ERO1L	2.651	FOXI2	3.215
DEFB4	4.175	EGOT	6.482	ERO1L	2.661	FOXN2	3.735
DENND2C	2.571	EHD1	2.660	ERO1L	2.530	FOXN2	3.976
DENND3	2.614	EHD4	3.446	ERO1L	2.524	FOXO3	2.401
DENND3	4.556	EHF	2.096	ERO1L	2.649	FOXO3	2.222
DENND5A	2.278	EIF2AK2	4.546	ERO1L	2.514	FOXO3	2.260
DGKG	2.081	EIF2AK2	4.512	ERO1L	2.647	FOXP1	2.907
DGKQ	2.415	ELF1	3.313	ESM1	6.949	FRK	2.383
DHRS1	2.041	ELF1	3.616	ETV7	16.706	FTSJD2	2.382
DHX58	27.916	ELF3	4.199	EXOC3L	2.267	FUT2	5.108
DISC1	3.059	ELF4	3.078	EXOC6	3.621	FUT3	9.417
DKFZp686L14188	2.103	ELMO2	2.539	EXOC8	2.040	FUT4	2.252
DKFZp686O1327	3.168	ELOVL7	5.284	F8A1	2.006	FUT6	3.532
DKFZp761E198	2.099	EMILIN2	4.004	F8A1	2.023	FUT8	2.727
DLST	2.094	ENST00000258869	13.076	F8A2	2.011	FXYD5	2.133
DMD	3.079	ENST00000294737	2.253	FA2H	6.496	FYB	2.017
DMD	2.043	ENST00000307896	2.184	FABP6	2.502	FYTTD1	2.176
DNAJA1	2.340	ENST00000308076	5.345	FAM114A1	2.303	FZD4	4.358
DNAJA4	3.639	ENST00000315194	2.195	FAM122C	3.063	G0S2	10.828
DNAJB6	2.262	ENST00000322839	2.692	FAM125A	2.918	GAB2	4.601
DNAJB6	2.213	ENST00000326295	2.016	FAM126B	2.556	GABPB1	2.201
DNAJB9	2.348	ENST00000331393	2.946	FAM126B	2.455	GADD45A	2.385
DNAJC1	2.676	ENST00000334003	3.108	FAM160A1	2.500	GAL	2.413
DNTTIP1	2.382	ENST00000344275	2.752	FAM167B	2.657	GANC	3.087
DOPEY1	2.395	ENST00000356370	2.131	FAM174B	2.928	GATA3	2.190
DPH3B	2.004	ENST00000359635	10.434	FAM177A1	3.194	GATA6	2.302
DPP4	2.563	ENST00000368204	2.500	FAM18B2	2.034	GBA	2.027
DRAP1	2.105	ENST00000369159	8.235	FAM25A	2.744	GBAP	2.041
DSC2	5.140	ENST00000372154	2.162	FAM38A	2.392	GBP1	23.720
DSCAM	3.077	ENST00000373236	3.262	FAM46A	10.299	GBP2	3.025
DTNA	2.640	ENST00000373495	2.378	FAM46A	8.106	GBP3	5.056
DTX3L	6.072	ENST00000373544	2.336	FAM46C	3.817	GBP4	45.244
DUOXA1	2.864	ENST00000374976	3.029	FAM63A	5.614	GBP5	16.628

Table 1.1: continued

Poly (I:C) upregulated genes (997-1328 of 2773)

Gene Name	Fold Change	Gene Name	Fold Change	Gene Name	Fold Change	Gene Name	Fold Change
GCA	17.965	HIST1H2AC	3.494	HSPA1A	2.223	IL1B	7.356
GCH1	8.266	HIST1H2AC	2.161	HSPA1A	2.221	IL1B	7.135
GCH1	7.159	HIST1H2AD	6.172	HSPA1A	2.180	IL1B	7.217
GDF5	2.005	HIST1H2AE	2.121	HSPA1A	2.270	IL1B	7.276
GFPT1	2.319	HIST1H2BD	2.025	HSPA1A	2.179	IL1B	7.113
GFRA1	2.166	HIST2H2AA4	10.726	HSPA1A	2.100	IL1B	6.915
GJB4	3.756	HIST2H2AB	3.465	HSPA1B	2.226	IL1B	6.743
GJB4	2.801	HIST2H2BE	4.704	HSPC159	2.444	IL1B	7.248
GJD3	7.416	HIVEP1	2.221	HSPG2	2.762	IL1F5	2.178
GJD3	2.002	HIVEP2	2.284	HUWE1	2.018	IL1F9	59.025
GLIPR2	2.762	HLA-A	9.442	HUWE1	2.541	IL1R2	14.080
GLIPR2	3.952	HLA-A	10.182	HYAL3	2.096	IL1RN	26.839
GLRX	2.466	HLA-A	9.545	ICA1	2.106	IL1RN	6.465
GMIP	2.855	HLA-A	10.013	ICA1	2.176	IL22RA1	4.473
GMPR	26.141	HLA-A	10.020	ICAM1	44.717	IL23A	3.650
GNA15	2.260	HLA-A	9.958	ICAM1	45.720	IL24	4.456
GNAI2	2.069	HLA-A	9.952	ICAM1	44.410	IL24	3.060
GNB4	2.259	HLA-A	10.325	ICAM1	45.561	IL28A	21.648
GNG5	2.194	HLA-A	9.612	ICAM1	45.131	IL28B	10.170
GOLT1A	2.716	HLA-A	10.122	ICAM1	42.673	IL28RA	3.204
GPBP1	2.423	HLA-A	9.886	ICAM1	41.209	IL29	8.364
GPD2	4.236	HLA-B	27.224	ICAM1	42.422	IL2RG	4.937
GPD2	2.749	HLA-B	23.837	ICAM1	42.585	IL2RG	11.024
GPR109A	8.500	HLA-C	28.485	ICAM1	44.648	IL32	5.501
GPR109B	33.012	HLA-C	15.110	ICAM2	6.808	IL32	4.641
GPR119	2.937	HLA-DOB	2.399	IER2	2.989	IL4I1	19.095
GPR143	4.636	HLA-E	7.655	IER5	2.693	IL6	27.307
GPR160	2.594	HLA-F	16.058	IFFO1	3.359	IL6	27.871
GPR180	2.868	HLA-F	24.805	IFI16	2.758	IL6	26.167
GPR37L1	3.758	HLA-G	15.096	IFI27	14.723	IL6	24.582
GPRC5A	3.436	HLA-J	16.742	IFI30	8.268	IL6	25.810
GPRC5B	6.176	HLA-J	16.930	IFI35	11.868	IL6	27.651
GRAMD1C	2.480	HLA-J	16.305	IFI44	17.935	IL6	27.161
GRAMD3	2.570	HLA-J	15.669	IFI44L	38.362	IL6	24.429
GRB10	7.811	HLA-J	15.070	IFI6	26.789	IL6	26.545
GRB10	7.908	HLA-J	16.579	IFIH1	24.984	IL6	26.392
GRB10	7.799	HLA-J	15.756	IFIT1	39.507	IL7	2.575
GRB10	7.818	HLA-J	15.118	IFIT1L	2.526	IL7R	10.085
GRB10	7.965	HLA-J	16.044	IFIT2	528.393	IL8	39.670
GRB10	7.807	HLA-J	16.384	IFIT2	105.528	IMPA1	3.407
GRB10	7.941	HMHA1	2.404	IFIT3	67.971	INA	2.291
GRB10	7.580	HMOX1	3.281	IFIT5	4.724	INADL	2.373
GRB10	7.747	HMOX1	3.398	IFITM1	23.517	INHBA	11.136
GRB10	6.020	HMOX1	3.239	IFITM1	11.469	INHBA	10.843
GRB10	7.969	HMOX1	3.205	IFITM2	5.826	INHBA	11.450
GRB7	2.562	HMOX1	3.198	IFITM3	6.770	INHBA	10.976
GRHL3	2.126	HMOX1	3.303	IFITM4P	7.158	INHBA	10.443
GRINA	2.366	HMOX1	3.308	IFNB1	12.661	INHBA	10.832
GRN	3.136	HMOX1	3.470	IFNGR1	2.340	INHBA	10.276
GSDMB	5.675	HMOX1	3.499	IFNGR2	2.430	INHBA	10.169
GSDMD	2.163	HMOX1	3.463	IFNK	3.142	INHBA	10.410
GTF2B	2.134	HNRNPUL2	3.526	IFT172	2.716	INHBA	10.639
GTPBP1	2.991	HPSE	2.949	IGFBP4	2.077	INO80D	2.543
GTPBP2	2.379	HRASLS2	43.895	IGFBP6	37.377	INSIG2	2.693
GTPBP2	2.430	HRASLS2	58.119	IGFBP7	2.272	INSIG2	2.023
H1F0	2.992	HRASLS2	53.219	IGFL1	20.734	IQSEC2	2.273
HAPLN3	3.750	HRASLS2	56.954	IGSF8	2.182	IRAK2	6.406
HBEGF	6.267	HRASLS2	54.554	IKBKE	2.104	IRF1	8.634
HCFC2	2.533	HRASLS2	60.270	IKZF2	10.063	IRF5	4.558
hCG_1994695	4.637	HRASLS2	56.020	IKZF2	2.643	IRF6	5.605
hCG_1995004	10.597	HRASLS2	55.054	IL11	2.715	IRF7	17.598
HCG4	3.354	HRASLS2	54.282	IL13RA2	2.486	IRF9	3.131
HCP5	7.784	HRASLS2	55.861	IL15	9.233	IRX3	2.085
HDGFL1	2.209	HRASLS5	2.520	IL15RA	2.872	ISG15	88.028
HDX	5.264	HS3ST1	2.213	IL15RA	3.395	ISG20	30.339
HEJ1	2.290	HS3ST1	2.200	IL15RA	6.454	ITGA5	3.850
HERC5	10.713	HS3ST1	2.213	IL17C	5.115	ITGB8	2.321
HERC5	11.159	HS3ST1	2.305	IL17RA	2.275	ITIH4	3.321
HERC5	10.887	HS3ST1	2.130	IL18BP	2.876	ITM2B	2.013
HERC5	10.667	HS3ST1	2.110	IL18R1	2.319	ITM2B	2.602
HERC5	10.460	HS3ST1	2.124	IL18RAP	2.275	ITPKC	3.499
HERC5	10.359	HS3ST1	2.146	IL1A	3.925	ITPR3	2.006
HERC5	10.474	HS3ST1	2.149	IL1A	4.001	JAK2	11.328
HERC5	10.605	HS3ST1	2.317	IL1A	3.786	JAK3	2.187
HERC5	10.658	HSCB	2.018	IL1A	3.705	JARID2	2.309
HERC5	11.074	HSD11B1	5.962	IL1A	3.798	JHDM1D	5.690
HERC6	6.847	HSD3B7	5.535	IL1A	3.763	JHDM1D	2.583
HERC6	10.409	HSH2D	3.551	IL1A	3.841	JUN	2.395
HES4	12.070	HSH2D	21.466	IL1A	3.802	JUNB	3.231
HEXDC	2.023	HSPA1A	2.274	IL1A	3.808	KAT2B	2.029
HHIP	5.371	HSPA1A	2.203	IL1A	3.728	KCND3	2.240
HHIPL1	2.359	HSPA1A	2.209	IL1B	7.389	KCNG1	2.880
HIP1R	2.283	HSPA1A	2.222	IL1B	7.083	KCNK1	3.532

Table 1.1: continued

Poly (I:C) upregulated genes (1329-1660 of 2773)

Gene Name	Fold Change	Gene Name	Fold Change	Gene Name	Fold Change	Gene Name	Fold Change
KCNS3	3.377	KRT8P12	2.347	LOC100134229	2.685	MAFF	2.658
KCNS3	3.406	KYNU	9.320	LOC100134237	3.780	MAFF	2.642
KCNS3	3.328	L3MBTL4	2.322	LOC115110	3.254	MAL2	3.242
KCNS3	3.293	L3MBTL4	2.936	LOC151438	11.512	MAP3K10	2.601
KCNS3	3.511	LACTB	4.356	LOC152225	4.344	MAP3K13	2.566
KCNS3	3.403	LAMA2	4.330	LOC153546	2.031	MAP3K7IP3	2.312
KCNS3	3.341	LAMA3	7.808	LOC153684	2.321	MAP3K7IP3	2.629
KCNS3	3.323	LAMB3	5.062	LOC200830	11.105	MAP3K8	3.227
KCNS3	3.429	LAMC2	10.160	LOC283352	2.088	MAPK8IP2	2.315
KCNS3	3.493	LAMC2	6.477	LOC284475	3.039	MAPKSP1	2.320
KCTD21	2.283	LAMP3	38.799	LOC284757	2.590	MAPKSP1	2.277
KDM6A	2.094	LANCL3	3.088	LOC339192	2.788	MAPKSP1	2.310
KIAA0226	4.713	LAP3	7.549	LOC339988	6.234	MAPKSP1	2.313
KIAA0355	2.003	LARP6	2.091	LOC349114	2.006	MAPKSP1	2.353
KIAA0415	2.023	LARP6	2.079	LOC387763	17.937	MAPKSP1	2.399
KIAA0649	2.530	LARP6	2.044	LOC388588	2.093	MAPKSP1	2.323
KIAA0913	2.118	LARP6	2.073	LOC388692	2.921	MAPKSP1	2.295
KIAA1033	2.631	LARP6	2.015	LOC399744	2.085	MAPKSP1	2.296
KIAA1033	2.690	LARP6	2.117	LOC400043	3.754	MAPKSP1	2.435
KIAA1539	2.405	LARP6	2.035	LOC402036	2.154	MAPRE1	2.360
KIAA1804	2.549	LAYN	24.878	LOC643008	2.616	MARCKSL1	5.501
KIAA1949	3.110	LCE3D	3.376	LOC644173	2.100	MAST4	5.037
KIF13B	2.238	LCMT1	2.177	LOC644189	2.996	MATN2	2.515
KIF13B	3.167	LCMT1	2.233	LOC645431	6.424	MDK	4.838
KIRREL3	2.862	LCMT1	2.098	LOC645634	4.024	MDM4	2.077
KIRREL3	2.920	LCMT1	2.102	LOC645676	2.633	MDM4	2.048
KIRREL3	2.881	LCMT1	2.121	LOC645676	2.107	MDM4	2.088
KIRREL3	2.877	LCMT1	2.081	LOC646626	2.087	MDM4	2.073
KIRREL3	2.831	LCMT1	2.120	LOC646999	13.571	MDM4	2.121
KIRREL3	2.625	LCMT1	2.102	LOC648987	2.828	MDM4	2.049
KIRREL3	2.794	LCMT1	2.248	LOC654433	2.152	MDM4	2.021
KIRREL3	2.909	LCMT1	2.120	LOC728769	2.239	MDM4	2.086
KIRREL3	2.962	LCN2	3.850	LOC728875	2.446	MED18	2.059
KIRREL3	2.691	LDLR	2.075	LOC728875	2.435	MEI1	2.965
KISS1	2.322	LEMD1	6.344	LOC729770	2.390	MEIS3P1	2.515
KLF10	2.357	LGALS3	2.357	LOC730375	2.146	MESDC1	2.057
KLF4	4.209	LGALS3BP	4.666	LOC731275	2.102	METRNL	3.975
KLF6	2.542	LGALS8	3.575	LOX	6.206	MFSD8	2.587
KLF6	5.269	LGALS9	3.565	LOX	6.073	MFSD9	2.131
KLF7	4.796	LGALS9C	2.401	LOX	6.620	MGAT2	2.387
KLF8	2.081	LGI2	2.180	LOX	6.560	MGC4859	2.765
KLF9	2.309	LGMN	7.940	LOX	6.971	MICB	3.177
KLHDC7B	36.565	LIF	3.008	LOX	6.393	MICB	2.653
KLHDC7B	16.738	LIN52	3.268	LOX	6.499	MIER1	2.234
KLHL21	2.772	LIPA	2.238	LOX	5.974	MIR155HG	9.721
KLHL28	2.353	LLGL2	2.038	LOX	6.561	MKL1	2.040
KLHL36	2.268	LLGL2	2.045	LOX	6.157	MKNK1	2.542
KLK1	2.058	LMBR1L	2.232	LPAR2	2.396	MKRN1	2.083
KLK10	4.739	LMO2	21.774	LPAR6	2.063	MLKL	7.628
KLK11	5.077	LMO2	21.597	LRCH4	2.407	MLLT6	2.661
KLK11	4.937	LMO2	22.108	LRG1	2.127	MMD	2.498
KLK11	4.734	LMO2	21.232	LRP10	2.532	MMP1	2.619
KLK11	4.766	LMO2	20.993	LRRC3	2.948	MMP1	2.535
KLK11	4.912	LMO2	20.930	LSR	3.301	MMP1	2.524
KLK11	5.043	LMO2	21.663	LTB	7.353	MMP1	2.469
KLK11	4.836	LMO2	21.170	LY6E	4.069	MMP1	2.488
KLK11	4.640	LMO2	22.586	LY75	2.611	MMP1	2.391
KLK11	4.753	LMO2	22.622	LYN	4.568	MMP1	2.391
KLK11	5.022	LMO4	2.813	LYN	4.550	MMP1	2.427
KLRAQ1	2.102	LMO4	2.487	LYN	4.356	MMP1	2.509
KLRAQ1	2.329	LNPEP	3.073	LYN	4.353	MMP1	2.604
KPNA7	4.444	LOC100128460	2.497	LYN	4.314	MMP10	17.398
KPNA7	2.956	LOC100128562	2.909	LYN	4.398	MMP12	6.080
KRT19	3.801	LOC100128737	2.229	LYN	4.519	MMP13	15.588
KRT34	9.695	LOC100128994	3.920	LYN	4.478	MMP19	2.219
KRT34	9.234	LOC100128994	3.871	LYN	4.642	MMP25	2.546
KRT34	9.469	LOC100129085	2.151	LYN	4.379	MMP9	45.643
KRT34	9.499	LOC100129138	2.119	LYPD3	2.908	MMP9	45.112
KRT34	9.279	LOC100129931	2.011	LYPD3	3.032	MMP9	45.548
KRT34	9.572	LOC100129958	2.674	LYPD5	5.885	MMP9	45.544
KRT34	9.542	LOC100130331	3.405	LYPD6	3.451	MMP9	46.141
KRT34	9.348	LOC100130433	2.396	LYPD6	4.693	MMP9	46.635
KRT34	9.749	LOC100130935	4.383	LYSMD2	3.849	MMP9	45.983
KRT34	9.818	LOC100131046	2.172	MAFB	5.932	MMP9	41.219
KRT6A	3.351	LOC100131733	32.750	MAFB	5.655	MMP9	45.602
KRT6B	23.317	LOC100131864	2.061	MAFF	2.844	MMP9	46.680
KRT6C	4.136	LOC100132614	3.989	MAFF	2.699	MOBKL1B	2.205
KRT7	2.635	LOC100132831	2.894	MAFF	2.677	MOBKL2C	3.016
KRT75	2.146	LOC100133019	4.851	MAFF	2.712	MOBKL3	2.078
KRT78	4.309	LOC100133086	2.789	MAFF	2.721	MOV10	3.404
KRT8	2.517	LOC100133153	16.024	MAFF	2.861	MOV10	2.476
KRT8	2.049	LOC100133161	2.378	MAFF	2.838	MPDU1	2.229
KRT83	3.062	LOC100133331	2.338	MAFF	2.838	MPZL1	2.246

Table 1.1: continued

Poly (I:C) upregulated genes (1661-1992 of 2773)

Gene Name	Fold Change	Gene Name	Fold Change	Gene Name	Fold Change	Gene Name	Fold Change
MPZL2	2.312	NFKBIA	8.210	PAFAH1B1	2.135	PLA2G16	8.786
MR1	3.454	NFKBIA	8.085	PAFAH1B1	2.136	PLA2G16	8.984
MR1	2.962	NFKBIA	8.160	PANX1	2.208	PLA2G16	8.453
MRGPRG	2.888	NFKBIA	7.811	PAOX	3.318	PLA2G16	8.362
MRGPRX3	7.795	NFKBIE	2.693	PAOX	2.371	PLA2G4C	3.006
MRGPRX4	3.985	NFKBIZ	4.493	PAOX	4.673	PLA2G4D	2.219
MTHFR	2.014	NHLRC4	2.506	PAPD4	3.453	PLAT	6.244
MTHFR	2.044	NINJ1	4.619	PAPLN	3.048	PLAT	5.872
MTHFR	2.012	NIPA1	2.364	PAPPA	2.363	PLAT	6.151
MTHFR	2.062	NIPSNAP3A	2.215	PARD6B	2.722	PLAT	6.068
MTHFR	2.026	NKAIN4	4.139	PARP10	6.373	PLAT	6.164
MTMR11	3.498	NKAIN4	2.430	PARP12	5.003	PLAT	6.252
MTMR7	2.603	NKX3-1	2.885	PARP12	4.851	PLAT	6.051
MTMR9L	8.125	NLRC5	9.873	PARP12	5.128	PLAT	6.099
MTMR9L	2.325	NLRC5	2.216	PARP12	5.057	PLAT	6.244
MTSS1	9.654	NMI	10.648	PARP12	4.638	PLAT	6.053
MTSS1	3.713	NMI	10.660	PARP12	4.936	PLAU	8.254
MUC1	10.767	NMI	10.878	PARP12	5.005	PLAU	8.426
MVP	2.051	NMI	10.896	PARP12	4.734	PLAU	8.362
MX1	28.135	NMI	10.332	PARP12	5.016	PLAU	8.328
MX2	86.316	NMI	10.357	PARP12	4.977	PLAU	8.267
MXD1	4.907	NMI	10.180	PARP14	11.012	PLAU	8.140
MXD1	3.859	NMI	10.760	PARP3	2.299	PLAU	8.016
MYADM	2.224	NMI	11.105	PARP8	5.158	PLAU	8.027
MYCN	3.266	NMI	10.998	PARP8	5.142	PLAU	7.584
MYD88	8.176	NOD1	2.283	PARP8	5.070	PLAU	8.709
MYH3	2.224	NOD2	9.734	PARP8	5.218	PLAU	5.268
MYL12A	2.812	NOS2	2.004	PARP8	5.130	PLAUR	25.750
MYL12B	2.555	NPEPPS	2.062	PARP8	5.151	PLCB4	2.050
MYO1E	2.255	NPNT	4.132	PARP8	5.128	PLCG2	2.035
MYO1G	2.058	NPR1	6.981	PARP8	5.096	PLCG2	2.016
MYO5C	4.044	NR4A3	4.392	PARP8	5.377	PLD5	2.580
MYO6	2.228	NR5A2	2.898	PARP8	5.110	PLEKHA4	9.906
MYO9B	2.657	NRBP1	2.194	PARP9	10.195	PLEKHA7	11.411
N4BP1	3.311	NRCAM	4.088	PATL1	2.311	PLEKHF1	2.370
N4BP2L2	2.154	NRCAM	2.009	PATL2	2.059	PLEKHG5	3.032
NACC2	2.648	NRIP1	4.309	PBX4	6.253	PLEKHN1	3.297
NACC2	2.752	NRIP1	3.610	PCDH1	2.248	PLOD2	2.451
NACC2	2.800	NRK	2.415	PCGF5	6.567	PLSCR1	7.900
NACC2	2.642	NRSN2	2.026	PCGF5	3.755	PLSCR4	2.492
NACC2	2.630	NT5C2	2.679	PCSK6	2.402	PLXNA3	2.409
NACC2	2.641	NT5C2	2.569	PCSK6	2.286	PMAIP1	15.007
NACC2	2.676	NT5C3	15.982	PCTK3	2.189	PML	3.272
NACC2	2.621	NT5C3	16.398	PCYT1A	2.456	PML	6.158
NACC2	2.598	NT5E	3.654	PDCD1LG2	3.512	PML	6.679
NACC2	2.870	NT5E	3.395	PDCD1LG2	3.407	PNLIPRP3	25.170
NAGK	2.690	NTNG2	3.278	PDE4DIP	2.180	PNPLA8	2.022
NAGS	2.168	NTRK2	2.242	PDE4DIP	2.228	PNPT1	5.658
NAMPT	2.019	NUAK2	2.957	PDGFB	4.469	PNPT1	3.456
NANOS3	3.429	NUB1	4.465	PDGFRL	14.843	POF1B	2.423
NAPA	3.015	NUMB	2.210	PDLIM4	2.358	POM121L12	2.286
NAT1	2.084	NUPR1	4.069	PDLIM7	2.648	PPIC	2.775
NAT8L	2.470	OAS1	17.863	PDLIM7	4.640	PPM1J	5.472
NAV3	2.447	OAS2	10.426	PDLIM7	3.084	PPM1K	8.816
NAV3	7.027	OAS2	12.163	PDP1	4.476	PPP1R15A	2.491
NCCRP1	7.551	OAS2	2.448	PDPN	2.789	PPP1R3F	2.097
NCF2	9.061	OAS3	4.053	PDZD2	6.394	PPP3CC	3.487
NCOA7	5.144	OAS3	8.782	PDZK1IP1	6.513	PPPDE2	2.444
NCRNA00118	2.277	OASL	120.656	PELI1	2.991	PRAP1	2.025
NDFIP1	2.399	OCLN	5.769	PEX26	2.409	PRDM1	5.780
NDFIP1	2.020	OCLN	3.886	PGAM4	2.022	PRDM1	5.079
NDUFA9	2.090	ODF3B	6.678	PGM2L1	2.541	PRDM8	5.708
NECAP1	2.101	OGFR	3.702	PGM3	2.899	PRELID1	2.310
NECAP2	2.345	OLR1	2.723	PHACTR4	2.890	PRELID1	2.865
NEURL3	84.744	OPTN	2.363	PHF11	4.156	PRIC285	9.740
NFAT5	2.059	OR2A9P	2.008	PHF15	2.315	PRIC285	2.416
NFE2L3	3.901	OR2A9P	2.012	PHF15	2.268	PRICKLE4	2.467
NFKB2	3.193	OR7E13P	2.092	PHLDA2	4.312	PRKCD	2.525
NFKB2	3.076	OR7E156P	2.244	PI3	2.552	PRKCD	2.538
NFKB2	3.084	OR7E24	2.079	PI4K2B	2.208	PRKCD	2.450
NFKB2	3.172	OSMR	4.331	PION	5.175	PRKCD	2.600
NFKB2	3.065	OTUD4	2.584	PIP4K2C	2.282	PRKCD	2.444
NFKB2	3.182	OVOL1	8.017	PIWIL4	2.460	PRKCD	2.452
NFKB2	3.148	OXTR	2.575	PKIB	2.961	PRKCD	2.441
NFKB2	3.074	P2RX4	3.079	PKP1	5.423	PRKCD	2.465
NFKB2	3.089	P4HA2	4.739	PKP1	5.087	PRKCD	2.396
NFKB2	2.927	P4HA2	3.903	PLA2G10	2.622	PRKCD	2.468
NFKBIA	8.038	PAFAH1B1	2.190	PLA2G16	8.741	PRKD2	3.615
NFKBIA	8.048	PAFAH1B1	2.077	PLA2G16	8.709	PRLR	2.577
NFKBIA	8.363	PAFAH1B1	2.139	PLA2G16	8.681	PRR15	2.220
NFKBIA	8.257	PAFAH1B1	2.077	PLA2G16	8.780	PRSS8	2.467
NFKBIA	7.790	PAFAH1B1	2.110	PLA2G16	8.561	PSEN1	2.864
NFKBIA	8.052	PAFAH1B1	2.103	PLA2G16	8.804	PSEN1	3.009

Table 1.1: continued

Poly (I:C) upregulated genes (1993-2324 of 2773)

Gene Name	Fold Change	Gene Name	Fold Change	Gene Name	Fold Change	Gene Name	Fold Change
PSEN1	2.863	RAP2C	2.658	RNF144B	2.562	SC4MOL	2.023
PSEN1	2.924	RAP2C	2.856	RNF146	2.056	SC4MOL	2.040
PSEN1	2.990	RAPGEF3	2.061	RNF149	3.510	SC4MOL	2.099
PSEN1	2.822	RAPGEF5	2.122	RNF149	3.348	SC4MOL	2.047
PSEN1	2.927	RAPH1	3.642	RNF149	3.366	SC4MOL	2.054
PSEN1	3.060	RAPH1	2.445	RNF149	3.450	SC4MOL	2.177
PSEN1	3.003	RARRES1	4.870	RNF149	3.458	SCAMP1	2.248
PSEN1	2.992	RARRES3	6.513	RNF149	3.318	SCARB2	4.095
PSEN2	2.165	RASD1	2.432	RNF149	3.403	SCARNA17	2.872
PSEN2	2.211	RASD1	2.506	RNF149	3.523	SCARNA9	3.089
PSEN2	2.106	RASD1	2.403	RNF149	3.294	SCARNA9L	2.008
PSEN2	2.083	RASD1	2.472	RNF149	3.489	SCLT1	2.127
PSEN2	2.098	RASD1	2.515	RNF19B	7.780	SCNN1D	2.077
PSEN2	2.112	RASD1	2.453	RNF207	2.431	SCO2	2.788
PSEN2	2.062	RASD1	2.502	RNF208	2.255	SCYL2	2.048
PSEN2	2.072	RASD1	2.464	RNF213	4.360	SCYL3	2.116
PSEN2	2.217	RASD1	2.612	RNF213	11.042	SDC4	7.155
PSEN2	2.069	RASD1	2.572	RNF217	2.216	SDCBP	2.016
PSMA4	2.437	RASGRP3	14.311	RNF38	2.150	SDCBP2	7.970
PSMA6	2.648	RASGRP3	2.122	RNF38	2.325	SEC14L1	2.008
PSMB10	5.190	RASL10A	3.414	RNF43	2.140	SEC24A	2.137
PSMB8	3.486	RASSF10	2.739	ROBO3	3.270	SEC24A	2.796
PSMB9	11.394	RASSF10	2.869	ROBO4	6.269	SECISBP2L	2.059
PSME1	2.325	RBCK1	2.176	RP2	3.043	SECTM1	45.365
PSME2	3.291	RBCK1	2.412	RPS6KA3	3.532	SEMA3A	5.306
PSME4	2.650	RBM11	3.872	RPS6KC1	4.337	SEMA3C	3.142
PSME4	3.782	RBM20	4.279	RPS6KC1	4.250	SEMA7A	6.569
PTAFR	4.001	RBM43	3.103	RPS6KC1	4.214	SEMA7A	6.598
PTGER2	3.367	RBM47	2.048	RPS6KC1	3.994	SEMA7A	6.540
PTGIR	2.622	RBMS1	2.106	RPS6KC1	4.043	SEMA7A	6.540
PTGS2	2.677	RBMS1	2.013	RPS6KC1	4.233	SEMA7A	6.594
PTGS2	2.610	RBMS2	2.299	RPS6KC1	4.065	SEMA7A	6.374
PTGS2	2.542	RCAN3	2.251	RPS6KC1	4.345	SEMA7A	6.251
PTGS2	2.704	REC8	2.473	RPS6KC1	4.215	SEMA7A	6.584
PTGS2	2.629	RELA	2.826	RPS6KC1	4.187	SEMA7A	6.658
PTGS2	2.776	RELA	2.830	RRAD	10.327	SEMA7A	6.575
PTGS2	2.644	RELA	2.914	RRAGC	2.149	SERPINA1	2.920
PTGS2	2.781	RELA	2.873	RRBP1	2.873	SERPINA3	4.158
PTGS2	2.782	RELA	2.843	RSAD2	226.319	SERPINA3	8.946
PTGS2	2.841	RELA	2.912	RSPH3	2.978	SERPINA3	7.347
PTK2B	2.931	RELA	2.811	RTCD1	2.482	SERPINB1	34.696
PTK6	2.461	RELA	3.097	RTKN	2.075	SERPINB2	11.256
PTN	5.401	RELA	3.001	RTN3	2.080	SERPINB8	3.199
PTPN12	2.835	RELA	2.441	RTP4	39.184	SERPINB9	6.220
PTPRA	2.063	RELA	3.043	RUNX3	4.133	SERPING1	5.627
PTPRB	2.595	RELB	2.833	RUNX3	10.071	SERPING1	4.977
PTPRC	2.026	RET	7.619	RWDD2A	2.170	SERPING1	4.842
PTPRK	4.263	RET	11.861	S100A8	2.111	SERPINI1	2.480
PTPRK	3.125	RFX5	2.319	S100A9	3.438	SFN	3.935
PTPRK	4.411	RFX5	3.195	S1PR3	2.606	SFT2D2	2.975
PTTG1IP	2.125	RGS20	2.894	SAA1	4.922	SGPP2	18.197
PTTG1IP	2.099	RHBDF2	2.819	SAA2	9.448	SGPP2	7.858
PTTG1IP	2.118	RHBDL2	3.118	SAA2	2.226	SH2B3	2.183
PTTG1IP	2.062	RHBDL2	2.721	SAA4	2.880	SH2D2A	2.386
PTTG1IP	2.032	RHBDL2	3.253	SAA4	2.738	SH3D20	2.829
PTTG1IP	2.015	RHCG	4.977	SAA4	2.640	SH3GLB1	2.603
PTTG1IP	2.107	RHEBL1	3.776	SAA4	2.394	SH3KBP1	4.750
PTTG1IP	2.382	RHOB	2.825	SAA4	2.773	SH3KBP1	6.527
PTTG1IP	2.073	RHOB	3.345	SAA4	2.674	SH3PXD2A	2.568
PVRL2	3.118	RHOC	2.310	SAA4	2.777	SHISA2	6.760
PVRL2	3.772	RHPN1	2.248	SAA4	2.879	SIDT1	5.581
PVRL3	2.815	RHPN2	2.697	SAA4	2.779	SIGIRR	4.565
PVRL4	2.157	RICTOR	3.291	SAA4	2.590	SIGLEC16	3.464
QPCT	2.419	RILP	3.685	SALL4	5.161	SIRT7	2.498
QPCT	2.368	RIPK1	2.321	SAMD4A	3.102	SIRT7	2.282
RAB11FIP1	2.625	RIPK2	8.352	SAMD4A	2.796	SLAMF7	4.898
RAB24	7.733	RIPK3	2.787	SAMD8	2.472	SLC11A2	2.194
RAB25	3.355	RIPK3	6.850	SAMD9	18.306	SLC12A7	2.922
RAB2B	2.265	RIPK4	3.056	SAMD9L	57.571	SLC13A5	2.347
RAB2B	2.014	RNASEK	2.098	SAMD9L	99.832	SLC15A3	16.923
RAB31	2.015	RND3	2.985	SAMHD1	6.045	SLC15A4	2.122
RAB35	2.154	RND3	2.950	SAMHD1	3.653	SLC16A3	3.121
RAB3IP	2.434	RND3	3.056	SAP30BP	2.143	SLC16A4	2.808
RAB42	4.159	RND3	3.171	SAR1A	3.410	SLC17A5	2.247
RAB43	2.245	RND3	3.114	SAR1A	2.116	SLC18A3	2.906
RAB43	3.066	RND3	3.038	SAT1	3.274	SLC22A4	2.245
RAB5A	2.279	RND3	2.957	SAT1	3.404	SLC24A6	2.162
RAB8B	2.228	RND3	3.098	SBF1	2.020	SLC25A28	5.124
RABAC1	2.171	RND3	3.188	SBNO2	2.149	SLC25A30	2.629
RABGGTA	2.176	RND3	3.014	SBSN	2.098	SLC25A37	3.315
RAD51L3	4.027	RNF111	2.065	SC4MOL	2.030	SLC25A37	2.091
RALA	3.231	RNF114	3.302	SC4MOL	2.001	SLC26A11	2.154
RALGPS2	2.306	RNF122	10.840	SC4MOL	2.067	SLC28A3	4.738

Table 1.1: continued

Poly (I:C) upregulated genes (2325-2656 of 2773)

Gene Name	Fold Change	Gene Name	Fold Change	Gene Name	Fold Change	Gene Name	Fold Change
SLC2A6	3.358	STAT1	11.376	TLR2	4.614	TNFSF10	33.684
SLC2A6	2.179	STAT1	11.342	TLR2	4.531	TNFSF10	32.911
SLC30A4	2.142	STAT1	11.224	TLR2	4.712	TNFSF10	33.432
SLC31A2	2.451	STAT1	11.328	TLR2	4.549	TNFSF10	32.940
SLC35D2	2.145	STAT1	11.004	TLR2	4.808	TNFSF10	32.941
SLC37A1	3.069	STAT1	11.853	TLR2	4.601	TNFSF10	31.559
SLC41A2	6.735	STAT1	10.840	TLR2	4.679	TNFSF10	33.386
SLC44A4	4.105	STAT2	3.738	TLR2	4.514	TNFSF10	32.780
SLC4A8	2.429	STAT5A	6.528	TLR3	14.582	TNFSF10	31.067
SLC7A2	49.164	STAT6	2.746	TM2D3	2.031	TNFSF13	3.758
SLC9A7	2.593	STBD1	3.112	TM4SF1	2.486	TNFSF13B	29.604
SLC9A7	2.022	STOML1	3.258	TMBIM6	2.418	TNFSF15	2.065
SLCO4A1	7.987	STX11	3.386	TMC4	2.728	TNIP1	7.491
SLFN11	2.227	STX12	2.019	TMC6	3.537	TNIP2	3.060
SLFN12	2.877	STX7	2.192	TMC6	3.538	TNNC2	7.421
SLFN12	2.734	STYK1	4.805	TMC6	3.644	TNRC6C	2.918
SLFN12	2.723	SULF1	2.578	TMC6	3.457	TNS1	3.184
SLFN12	2.668	SUSD3	31.530	TMC6	3.539	TOR1AIP1	2.770
SLFN12	2.666	SUZ12P	2.026	TMC6	3.450	TOR1AIP1	2.508
SLFN12	2.858	SYNGR2	3.300	TMC6	3.401	TOR1B	2.575
SLFN12	2.809	SYNGR2	3.030	TMC6	3.372	TP53BP2	3.946
SLFN12	2.758	SYNPO	2.379	TMC6	3.489	TP53INP2	2.016
SLFN12	2.612	SYNPO	2.160	TMC6	3.520	TPM4	2.037
SLFN12	2.781	SYNPO2	2.553	TMC8	3.246	TPPP	2.058
SLFN5	2.138	SYS1	2.220	TMCC3	8.563	TRADD	3.500
SMARCA5	2.171	SYTL4	2.837	TMCO4	2.129	TRAF1	23.935
SMG7	2.039	TACSTD2	2.545	TMED5	2.135	TRAF4	2.068
SMPD1	2.047	TAGAP	2.975	TMED5	2.226	TRAF6	2.618
SMURF1	2.830	TAGLN	2.012	TMED7-TICAM2	2.082	TRAFD1	2.464
SNAPC3	2.024	TAP1	14.802	TMEFF1	3.225	TRANK1	6.563
SNRK	2.013	TAP2	3.912	TMEM102	2.384	TREX1	6.775
SNX3	2.130	TAPBP	2.607	TMEM106A	4.536	TRIB1	2.850
SNX6	2.406	TAPBP	3.571	TMEM106A	3.756	TRIM14	4.022
SNX6	2.372	TAPBP	2.411	TMEM110	3.937	TRIM14	3.469
SOAT1	2.415	TAPBPL	4.406	TMEM125	2.987	TRIM14	3.638
SOCS1	7.594	TBC1D3G	2.185	TMEM140	5.841	TRIM14	3.870
SOCS2	4.668	TBX19	2.354	TMEM167B	2.508	TRIM21	4.281
SOCS3	2.184	TBX3	4.015	TMEM170A	2.239	TRIM22	7.366
SOD2	52.923	TBX3	3.918	TMEM170A	2.228	TRIM25	2.185
SOX13	2.226	tcag7.1196	2.043	TMEM170A	2.211	TRIM26	3.094
SOX9	2.972	tcag7.907	2.367	TMEM170A	2.230	TRIM34	2.302
SP100	7.405	TCF15	2.759	TMEM170A	2.317	TRIM34	2.466
SP100	5.112	TCIRG1	2.900	TMEM170A	2.238	TRIM35	2.579
SP110	11.984	TCN2	3.396	TMEM170A	2.281	TRIM36	2.328
SP110	11.582	TCP11L1	2.838	TMEM170A	2.265	TRIM36	2.210
SP110	11.523	TCP11L1	2.096	TMEM170A	2.364	TRIM36	2.159
SP110	12.050	TDRD7	12.625	TMEM170A	2.305	TRIM36	2.160
SP110	11.549	TDRD7	12.950	TMEM171	7.363	TRIM36	2.221
SP110	11.413	TDRD7	12.418	TMEM173	3.081	TRIM36	2.191
SP110	11.563	TDRD7	12.859	TMEM185A	2.171	TRIM36	2.331
SP110	11.890	TDRD7	12.563	TMEM188	2.017	TRIM36	2.271
SP110	11.335	TDRD7	12.468	TMEM189	2.163	TRIM36	2.283
SP110	11.693	TDRD7	12.371	TMEM2	3.884	TRIM36	2.128
SP140	2.785	TDRD7	12.275	TMEM2	4.337	TRIM38	2.976
SP140L	2.222	TDRD7	12.206	TMEM201	2.340	TRIM5	3.167
SP6	2.165	TDRD7	12.955	TMEM217	8.075	TRIM56	2.781
SP8	33.720	TEP1	4.203	TMEM229B	5.417	TRIM69	2.686
SPAG9	3.006	TFPI2	2.645	TMEM27	38.188	TRIOBP	2.125
SPAG9	2.268	TGFA	3.891	TMEM30B	2.579	TRIP4	2.094
SPATS2L	2.920	TGFA	2.637	TMEM40	2.474	TRPC6	2.481
SPHK1	3.694	TGM1	2.397	TMEM40	2.080	TRPM4	2.599
SPINK6	5.613	THSD1	3.187	TMEM62	8.506	TRPV2	2.327
SPOCD1	2.808	TICAM1	5.006	TMEM63A	2.083	TSPAN14	2.474
SPOCK1	12.512	TICAM1	2.789	TMEM87A	2.309	TSPAN31	2.116
SPPL2A	2.632	TIMP2	2.963	TMEM87B	2.776	TTC9C	2.651
SPRY2	3.371	TINF2	4.998	TMEM88	2.610	TUBA3D	2.153
SPSB1	2.447	TLE4	2.276	TMEM92	8.659	TUBB2A	3.711
SPSB1	4.433	TLE4	4.258	TMOD2	2.621	TYMP	3.653
SPTAN1	2.232	TLK2	3.314	TMX1	2.514	UBA7	8.200
SPTBN1	2.179	TLK2	2.958	TNC	2.342	UBC	2.737
SPTBN5	4.966	TLK2	2.177	TNF	5.308	UBC	2.323
SQRDL	9.477	TLR1	4.145	TNFAIP2	55.229	UBC	2.368
SRGAP2	2.542	TLR1	4.181	TNFAIP3	12.026	UBD	29.511
SSTR2	4.314	TLR1	4.215	TNFAIP6	11.906	UBE2H	3.980
ST14	3.399	TLR1	4.299	TNFAIP8	5.173	UBE2L6	8.296
ST8SIA4	3.046	TLR1	4.478	TNFAIP8	5.040	UBFD1	2.489
STAP2	2.313	TLR1	4.360	TNFRSF10A	2.852	UBQLN1	2.215
STARD3NL	2.353	TLR1	4.318	TNFRSF14	2.751	UBQLN2	2.450
STARD4	3.318	TLR1	4.015	TNFRSF25	2.109	UBQLN2	2.566
STARD5	4.415	TLR1	4.203	TNFRSF8	2.011	UBQLN2	2.597
STAT1	11.331	TLR1	3.900	TNFRSF9	4.000	UBQLN2	2.611
STAT1	11.668	TLR2	4.824	TNFSF10	26.890	UBQLN2	2.667
STAT1	11.341	TLR2	4.425	TNFSF10	32.887	UBQLN2	2.449

Table 1.1: continued

Poly (I:C) upregulated genes (2657-2773 of 2773)

Gene Name	Fold Change	Gene Name	Fold Change	Gene Name	Fold Change	Gene Name	Fold Change
UBQLN2	2.556	ZFAND2A	3.256				
UBQLN2	2.504	ZFAND3	2.265				
UBQLN2	2.522	ZFP36	4.582				
UBQLN2	2.608	ZFYVE26	3.970				
UBXN2A	2.055	ZG16B	3.129				
UCA1	12.239	ZMIZ1	2.421				
UHRF1BP1	3.304	ZMIZ2	2.276				
ULBP2	4.692	ZMYND15	5.384				
UNC93B1	5.794	ZNF101	2.086				
UNC93B1	5.318	ZNF114	2.446				
UNC93B1	4.537	ZNF165	2.471				
URG4	2.221	ZNF224	2.030				
USP11	2.347	ZNF226	3.093				
USP12	2.030	ZNF267	3.387				
USP15	3.078	ZNF296	2.502				
USP15	2.107	ZNF350	2.143				
USP18	52.444	ZNF385C	3.012				
USP25	2.537	ZNF44	2.393				
USP31	2.704	ZNF460	2.657				
USP41	16.214	ZNF469	2.158				
USP43	3.882	ZNF562	2.226				
VAMP5	2.692	ZNF600	2.002				
VAMP8	2.042	ZNF613	2.081				
VEGFC	5.301	ZNF655	2.137				
VEZT	2.610	ZNF707	2.661				
VEZT	2.307	ZNF710	2.305				
VLDLR	2.209	ZNFX1	8.272				
VRK2	2.105	ZNFX1	3.506				
VSIG10L	2.758	ZNFX1	2.941				
VSIG10L	2.596	ZNRF2	2.005				
VSIG10L	2.459	ZP4	16.570				
VSIG10L	2.599	ZPLD1	4.962				
VSIG10L	2.431	ZSCAN12L1	2.103				
VSIG10L	2.536	ZSWIM3	2.433				
VSIG10L	2.572						
VSIG10L	2.680						
VSIG10L	2.577						
VSIG10L	2.269						
VTI1A	2.422						
VTI1A	2.329						
VTI1A	2.411						
VTI1A	2.379						
VTI1A	2.281						
VTI1A	2.343						
VTI1A	2.413						
VTI1A	2.378						
VTI1A	2.380						
VTI1A	2.389						
WARS	14.700						
WDR45	2.428						
WDR45	11.876						
WDR47	2.136						
WDR55	2.046						
WFDC2	22.721						
WFDC2	26.473						
WFDC3	3.457						
WHAMM	2.143						
WNT7A	2.370						
WNT7B	2.590						
WNT7B	2.478						
WNT7B	2.473						
WSB1	2.073						
WTAP	2.451						
WTAP	3.124						
XAF1	11.154						
XAF1	13.150						
XIAP	2.360						
XKR8	2.147						
XRN1	4.175						
YEATS2	2.583						
YPEL5	2.237						
ZBP1	4.648						
ZBP1	17.051						
ZBTB32	24.520						
ZBTB42	4.611						
ZBTB43	3.107						
ZBTB43	3.148						
ZC3H12C	4.138						
ZC3H7B	4.180						
ZC3HAV1	12.599						
ZC3HAV1	2.118						
ZCCHC2	2.341						
ZDHHC13	2.365						

Table 1.1: continued

Poly (I:C) downregulated genes (1-332 of 2769)

Gene Name	Fold Change	Gene Name	Fold Change	Gene Name	Fold Change	Gene Name	Fold Change
MARCH4	0.431	ADI1	0.473	APLN	0.404	B3GNT1	0.459
SEPT11	0.447	ADNP	0.440	APLN	0.401	B9D1	0.368
A_24_P135391	0.401	ADORA2B	0.037	APLN	0.418	B9D1	0.303
A_24_P135501	0.435	AFARP1	0.447	APLN	0.392	B9D2	0.496
A_24_P153324	0.375	AGAP1	0.361	APLN	0.357	BAIAP2	0.470
A_24_P161914	0.341	AGAP1	0.355	APLN	0.496	BAP1	0.462
A_24_P194962	0.455	AGAP1	0.394	APLN	0.385	BAX	0.464
A_24_P195724	0.384	AGAP1	0.392	APOE	0.493	BAX	0.470
A_24_P204144	0.495	AGAP1	0.374	APOO	0.315	BAX	0.473
A_24_P221485	0.411	AGAP1	0.387	APPL2	0.391	BAX	0.472
A_24_P24142	0.373	AGAP1	0.382	APPL2	0.373	BAX	0.470
A_24_P272548	0.472	AGAP1	0.396	APPL2	0.360	BAX	0.496
A_24_P316074	0.394	AGAP1	0.417	APPL2	0.378	BAX	0.497
A_24_P349636	0.375	AGBL5	0.366	APPL2	0.374	BAX	0.494
A_24_P383330	0.398	AGPAT5	0.163	APPL2	0.390	BAX	0.491
A_24_P409402	0.395	AGPS	0.380	APPL2	0.348	BAX	0.489
A_24_P41149	0.421	AHCY	0.413	APPL2	0.339	BCAT1	0.116
A_24_P418536	0.447	AHNAK2	0.476	APPL2	0.388	BCAT2	0.470
A_24_P42014	0.493	AHNAK2	0.470	APPL2	0.416	BCCIP	0.488
A_24_P603890	0.476	AIF1L	0.347	AQR	0.414	BCKDHB	0.479
A_24_P76358	0.333	AIG1	0.376	AREG	0.462	BCKDHB	0.414
A_24_P84808	0.370	AK027667	0.407	AREG	0.460	BCL11B	0.288
A_24_P93452	0.374	AK056005	0.458	ARG2	0.451	BCL2L10	0.464
A_32_P151782	0.404	AK130930	0.456	ARHGAP11A	0.433	BCL2L12	0.494
A_32_P514599	0.440	AK3L1	0.426	ARHGAP11A	0.367	BCL7A	0.382
A_32_P52153	0.322	AKAP1	0.492	ARHGAP11B	0.432	BDH1	0.319
A_32_P57702	0.267	AKR1B10	0.108	ARHGAP22	0.413	BDKRB1	0.358
A_33_P3218559	0.394	AKR1B10	0.149	ARHGAP4	0.407	BDKRB2	0.284
A_33_P3230073	0.384	AKR1B15	0.174	ARHGDIB	0.184	BEND3	0.335
A_33_P3242923	0.204	AKR1C1	0.341	ARHGEF10	0.429	BEND6	0.444
A_33_P3263157	0.356	AKR1C1	0.293	ARHGEF19	0.498	BEX1	0.203
A_33_P3270966	0.495	AKR1C3	0.285	ARHGEF4	0.348	BEX2	0.381
A_33_P3293734	0.314	AKR1C4	0.435	ARL3	0.380	BFSP1	0.418
A_33_P3296230	0.382	AKR7A2	0.336	ARL4D	0.340	BFSP1	0.418
A_33_P3317431	0.354	AKR7A2	0.328	ARMC9	0.431	BFSP1	0.416
A_33_P3324552	0.410	AKR7A2	0.331	ARMC9	0.432	BFSP1	0.386
A_33_P3329991	0.438	AKR7A2	0.329	ARRDC4	0.411	BFSP1	0.391
A_33_P3337931	0.451	AKR7A2	0.346	ARTN	0.385	BFSP1	0.399
A_33_P3359984	0.359	AKR7A2	0.322	ASAM	0.347	BFSP1	0.398
A_33_P3381429	0.406	AKR7A2	0.318	ASB1	0.406	BFSP1	0.404
A_33_P3390873	0.374	AKR7A2	0.340	ASB13	0.447	BFSP1	0.430
A_33_P3391803	0.384	AKR7A2	0.339	ASF1B	0.267	BFSP1	0.428
A_33_P3406702	0.357	AKR7A2	0.336	ASF1B	0.269	BICD2	0.349
A_33_P3412716	0.498	AKR7A3	0.420	ASF1B	0.265	BIRC5	0.056
A_33_P3416414	0.426	AKR7L	0.463	ASF1B	0.268	BIRC5	0.056
AADAT	0.401	ALDH18A1	0.491	ASF1B	0.242	BIRC5	0.054
AARSD1	0.494	ALDH1L1	0.419	ASF1B	0.262	BIRC5	0.056
AARSD1	0.489	ALDH3A1	0.365	ASF1B	0.266	BIRC5	0.053
AARSD1	0.495	ALDH3A1	0.284	ASF1B	0.265	BIRC5	0.053
AARSD1	0.495	ALDH3A2	0.230	ASF1B	0.266	BIRC5	0.055
ABCB6	0.212	ALDH3A2	0.345	ASF1B	0.287	BIRC5	0.058
ABCE1	0.406	ALDH4A1	0.287	ASPM	0.276	BIRC5	0.058
ABCE1	0.395	ALDH4A1	0.424	ASPM	0.316	BIRC5	0.056
ABHD14A	0.494	ALDH7A1	0.233	ATAD2	0.304	BLM	0.123
ABHD2	0.472	ALDH7A1	0.185	ATAD5	0.441	BNIP2	0.476
ABHD6	0.388	ALDH7A1	0.298	ATIC	0.421	BNIPL	0.364
ABI2	0.455	ALG10B	0.450	ATL2	0.498	BPHL	0.483
ABLIM1	0.473	ALG3	0.481	ATP1A1	0.465	BRCA1	0.139
ACAA2	0.430	ALKBH2	0.423	ATP5G1	0.373	BRCA1	0.141
ACACA	0.330	ALS2CR4	0.347	ATP6V1C1	0.381	BRCA1	0.144
ACADSB	0.335	ALS2CR4	0.156	ATP6V1E2	0.327	BRCA1	0.136
ACAT1	0.471	AMPD2	0.480	ATP9B	0.487	BRCA1	0.137
ACAT2	0.495	AMZ2	0.373	ATP9B	0.484	BRCA1	0.143
ACBD6	0.473	ANKH	0.364	ATP9B	0.480	BRCA1	0.154
ACCN2	0.131	ANKH	0.458	ATP9B	0.500	BRCA1	0.153
ACN9	0.312	ANKRD16	0.402	ATP9B	0.492	BRCA1	0.150
ACO1	0.090	ANKRD2	0.379	ATP9B	0.492	BRCA1	0.147
ACOX1	0.384	ANKRD32	0.421	ATRN	0.415	BTBD11	0.394
ACSF2	0.449	ANKRD32	0.434	ATXN10	0.461	BTBD16	0.169
ACSL1	0.495	ANKRD35	0.399	AURKA	0.237	BUB1	0.150
ACSL1	0.480	ANKS6	0.161	AURKAPS1	0.344	BUB1B	0.086
ACSL1	0.496	ANLN	0.235	AURKB	0.218	BX095413	0.432
ACSL1	0.491	ANP32A	0.393	AUTS2	0.401	BYSL	0.464
ACSL1	0.488	ANP32B	0.436	AUTS2	0.407	BZW2	0.479
ACSL1	0.499	ANTXR1	0.405	AUTS2	0.392	BZW2	0.407
ACSL1	0.490	AOX1	0.230	AUTS2	0.394	C10orf114	0.472
ACTR3B	0.350	AOX1	0.346	AUTS2	0.402	C10orf2	0.422
ACTR3B	0.458	AP3M2	0.451	AUTS2	0.416	C11orf41	0.483
ACY1	0.360	APEX1	0.362	AUTS2	0.424	C11orf46	0.460
ADA	0.374	APITD1	0.332	AUTS2	0.417	C11orf51	0.481
ADARB1	0.250	APLN	0.346	AUTS2	0.419	C11orf70	0.482
ADAT2	0.358	APLN	0.405	AUTS2	0.424	C11orf70	0.496
ADI1	0.438	APLN	0.428	AZI1	0.364	C11orf82	0.112

Table 1.1: continued

Poly (I:C) downregulated genes (333-664 of 2769)

Gene Name	Fold Change	Gene Name	Fold Change	Gene Name	Fold Change	Gene Name	Fold Change
C12orf24	0.201	C9orf116	0.443	CCNA2	0.102	CENPH	0.345
C12orf32	0.494	C9orf122	0.483	CCNA2	0.103	CENPJ	0.225
C12orf48	0.217	C9orf125	0.462	CCNA2	0.095	CENPK	0.256
C13orf15	0.173	CA10	0.240	CCNA2	0.099	CENPM	0.236
C14orf126	0.476	CA12	0.197	CCNA2	0.099	CENPM	0.154
C14orf143	0.456	CA2	0.404	CCNB1	0.107	CENPN	0.235
C14orf145	0.236	CABC1	0.403	CCNB1	0.112	CENPN	0.360
C14orf167	0.493	CABLES1	0.300	CCNB1	0.118	CENPO	0.369
C14orf2	0.484	CALML5	0.424	CCNB1	0.114	CENPO	0.447
C14orf33	0.427	CARD18	0.246	CCNB1	0.114	CENPP	0.182
C14orf80	0.402	CARHSP1	0.479	CCNB1	0.108	CENPP	0.404
C14orf80	0.343	CARS2	0.283	CCNB1	0.106	CENPQ	0.436
C15orf23	0.271	CASC5	0.134	CCNB1	0.110	CENPQ	0.424
C16orf35	0.408	CASC5	0.147	CCNB1	0.123	CENPQ	0.409
C16orf45	0.426	CASC5	0.123	CCNB1	0.141	CENPQ	0.430
C16orf48	0.365	CASC5	0.133	CCNB1	0.108	CENPQ	0.438
C16orf5	0.355	CASC5	0.135	CCNB1IP1	0.451	CENPQ	0.441
C16orf53	0.366	CASC5	0.135	CCNB2	0.099	CENPQ	0.426
C16orf59	0.157	CASC5	0.157	CCND2	0.441	CENPQ	0.447
C16orf63	0.340	CASC5	0.129	CCNE2	0.238	CENPQ	0.441
C16orf75	0.151	CASC5	0.123	CD109	0.442	CENPQ	0.439
C16orf93	0.386	CASC5	0.143	CD24	0.485	CEP250	0.385
C17orf61	0.459	CASK	0.361	CDC2	0.080	CEP250	0.492
C17orf79	0.426	CAT	0.476	CDC2	0.082	CEP55	0.069
C17orf89	0.306	CAT	0.431	CDC2	0.083	CEP55	0.065
C17orf89	0.277	CAT	0.447	CDC2	0.081	CEP55	0.069
C17orf97	0.467	CAT	0.445	CDC2	0.086	CEP55	0.072
C18orf55	0.145	CAT	0.446	CDC2	0.081	CEP55	0.064
C18orf56	0.372	CAT	0.442	CDC2	0.081	CEP55	0.065
C19orf48	0.207	CAT	0.464	CDC2	0.084	CEP55	0.066
C19orf51	0.430	CAT	0.478	CDC2	0.087	CEP55	0.069
C1orf112	0.269	CAT	0.450	CDC2	0.087	CEP55	0.143
C1orf112	0.253	CAT	0.427	CDC20	0.117	CEP55	0.074
C1orf112	0.268	CAV1	0.459	CDC25A	0.396	CEP55	0.072
C1orf112	0.257	CAV1	0.458	CDC25C	0.220	CEP78	0.335
C1orf112	0.275	CAV1	0.475	CDC45L	0.094	CERK	0.315
C1orf112	0.286	CAV1	0.476	CDC6	0.395	CHAF1A	0.345
C1orf112	0.262	CAV1	0.471	CDC7	0.211	CHAF1A	0.313
C1orf112	0.255	CAV1	0.490	CDCA2	0.094	CHAF1B	0.418
C1orf112	0.266	CAV1	0.485	CDCA3	0.203	CHAF1B	0.382
C1orf112	0.269	CAV1	0.490	CDCA5	0.072	CHAF1B	0.398
C1orf133	0.331	CAV1	0.484	CDCA5	0.071	CHAF1B	0.402
C1orf135	0.196	CBR4	0.412	CDCA5	0.070	CHAF1B	0.384
C1orf163	0.419	CBX2	0.253	CDCA5	0.070	CHAF1B	0.382
C1orf21	0.373	CBX5	0.186	CDCA5	0.068	CHAF1B	0.381
C1orf21	0.396	CC2D2A	0.293	CDCA5	0.069	CHAF1B	0.424
C1orf21	0.363	CC2D2A	0.335	CDCA5	0.075	CHAF1B	0.425
C1orf21	0.362	CC2D2A	0.402	CDCA5	0.071	CHAF1B	0.415
C1orf21	0.396	CCBL1	0.462	CDCA5	0.072	CHCHD10	0.404
C1orf21	0.356	CCDC104	0.424	CDCA5	0.073	CHCHD8	0.465
C1orf21	0.435	CCDC104	0.481	CDCA7	0.085	CHKA	0.396
C1orf21	0.370	CCDC106	0.486	CDCA7	0.479	CHML	0.381
C1orf21	0.421	CCDC111	0.464	CDCA7L	0.271	CHTF18	0.207
C1orf21	0.421	CCDC138	0.413	CDCA8	0.065	CIT	0.180
C1orf53	0.492	CCDC147	0.203	CDK4	0.187	CKAP2	0.378
C1orf96	0.308	CCDC18	0.424	CDKN1C	0.430	CKAP2L	0.129
C1orf96	0.481	CCDC3	0.213	CDKN2C	0.371	CKS1B	0.287
C1QBP	0.479	CCDC34	0.091	CDKN3	0.174	CKS1B	0.333
C20orf108	0.291	CCDC41	0.406	CDKN3	0.112	CLCA2	0.208
C20orf27	0.340	CCDC72	0.461	CDT1	0.232	CLEC2D	0.448
C20orf27	0.417	CCDC74B	0.123	CEBPA	0.436	CLMN	0.391
C20orf72	0.453	CCDC74B	0.412	CENPA	0.145	CLN8	0.361
C21orf45	0.311	CCDC75	0.295	CENPE	0.462	CLNS1A	0.486
C22orf29	0.388	CCDC75	0.331	CENPE	0.459	CLSPN	0.419
C2CD2	0.291	CCDC8	0.470	CENPE	0.443	CMTM4	0.421
C2orf7	0.452	CCDC86	0.477	CENPE	0.458	CMTM7	0.314
C3orf26	0.315	CCDC99	0.456	CENPE	0.472	CNTN1	0.481
C3orf47	0.498	CCDC99	0.424	CENPE	0.449	COL13A1	0.355
C4orf21	0.346	CCDC99	0.400	CENPE	0.469	COL13A1	0.359
C5	0.442	CCDC99	0.427	CENPE	0.464	COL13A1	0.367
C5orf26	0.382	CCDC99	0.434	CENPE	0.465	COL13A1	0.327
C5orf34	0.489	CCDC99	0.443	CENPE	0.475	COL13A1	0.395
C6orf125	0.428	CCDC99	0.417	CENPF	0.276	COL13A1	0.372
C6orf154	0.448	CCDC99	0.454	CENPF	0.047	COL13A1	0.381
C6orf167	0.335	CCDC99	0.438	CENPH	0.334	COL13A1	0.400
C6orf167	0.243	CCDC99	0.421	CENPH	0.332	COL13A1	0.387
C6orf173	0.182	CCDC99	0.447	CENPH	0.306	COL13A1	0.372
C6orf26	0.406	CCK	0.214	CENPH	0.316	COL1A2	0.391
C7orf44	0.466	CCNA2	0.098	CENPH	0.324	COL1A2	0.387
C7orf50	0.439	CCNA2	0.107	CENPH	0.319	COL1A2	0.388
C7orf68	0.382	CCNA2	0.106	CENPH	0.315	COL1A2	0.457
C8orf55	0.497	CCNA2	0.102	CENPH	0.327	COL1A2	0.397
C9orf116	0.423	CCNA2	0.099	CENPH	0.331	COL1A2	0.397

Table 1.1: continued

Poly (I:C) downregulated genes (665-996 of 2769)

Gene Name	Fold Change	Gene Name	Fold Change	Gene Name	Fold Change	Gene Name	Fold Change
COL1A2	0.463	DLGAP5	0.092	EEF1G	0.425	EXO1	0.165
COL1A2	0.469	DLK2	0.165	EEF2K	0.226	EXO1	0.161
COL1A2	0.470	DLX1	0.444	EFCAB1	0.305	EXO1	0.150
COL1A2	0.473	DNAH10	0.422	EFEMP1	0.338	EXO1	0.142
COL8A1	0.360	DNAH9	0.497	EFS	0.343	EXO1	0.155
COMMD8	0.454	DNAJC21	0.437	EGLN3	0.447	EXO1	0.141
COQ2	0.498	DNAJC9	0.500	EHD3	0.458	EXO1	0.158
COQ3	0.461	DNAJC9	0.471	EIF3E	0.425	EXO1	0.173
COQ3	0.487	DNAJC9	0.466	EIF3F	0.373	EXO1	0.188
COQ3	0.497	DNAJC9	0.481	EIF3L	0.354	EXOSC2	0.309
COQ3	0.457	DNAJC9	0.492	EIF4B	0.371	EXOSC2	0.367
COQ3	0.456	DNAJC9	0.488	EIF4B	0.280	EXOSC5	0.431
COQ3	0.452	DNAJC9	0.484	EIF4EBP1	0.495	EXOSC7	0.428
COQ3	0.471	DNAJC9	0.491	EIF4EBP2	0.371	EXOSC8	0.460
COQ3	0.498	DNAJC9	0.474	ELL2	0.313	EXPH5	0.180
COX11	0.387	DNAJC9	0.495	ELMOD2	0.255	EZH2	0.352
CP110	0.425	DOCK9	0.429	ELOVL6	0.231	F12	0.395
CPA4	0.152	DOCK9	0.474	EML1	0.480	F2R	0.145
CPD	0.366	DONSON	0.441	EMP2	0.422	FADS1	0.485
CPOX	0.437	DPH5	0.399	EMP2	0.408	FAH	0.396
CPS1	0.443	DPYSL4	0.372	EMP2	0.405	FAM101B	0.084
CR596214	0.288	DSCC1	0.194	EMP2	0.412	FAM102A	0.499
CR615245	0.379	DSCC1	0.182	EMP2	0.400	FAM108C1	0.415
CR617556	0.392	DSCC1	0.167	EMP2	0.276	FAM111B	0.203
CRABP2	0.435	DSCC1	0.183	EMP2	0.440	FAM117B	0.381
CRIP2	0.459	DSCC1	0.185	EMP2	0.417	FAM122B	0.414
CRNDE	0.329	DSCC1	0.199	EMP2	0.408	FAM127C	0.456
CSE1L	0.354	DSCC1	0.182	EMP2	0.433	FAM161A	0.449
CSE1L	0.304	DSCC1	0.180	EMP2	0.437	FAM161A	0.393
CSRP2	0.473	DSCC1	0.202	EMX2OS	0.304	FAM162A	0.457
CTDSPL	0.384	DSCC1	0.202	ENDOG	0.496	FAM167A	0.280
CTH	0.365	DSN1	0.418	ENOSF1	0.238	FAM168B	0.429
CTNNAL1	0.142	DST	0.285	ENST00000253461	0.477	FAM171A1	0.395
CTNNAL1	0.128	DST	0.303	ENST00000293743	0.157	FAM172A	0.271
CTNNBIP1	0.343	DTL	0.095	ENST00000328897	0.450	FAM173B	0.164
CTPS	0.477	DTL	0.110	ENST00000358739	0.436	FAM183A	0.499
CTSB	0.387	DTL	0.103	ENST00000360201	0.346	FAM198B	0.128
CTSF	0.468	DTL	0.100	ENST00000369242	0.466	FAM20B	0.449
CTSL2	0.296	DTL	0.095	ENST00000370958	0.354	FAM27A	0.362
CXCL14	0.016	DTL	0.099	ENST00000372591	0.475	FAM27A	0.497
CXCR7	0.358	DTL	0.096	ENST00000375052	0.421	FAM49A	0.435
CXorf57	0.344	DTL	0.103	ENST00000375280	0.369	FAM50B	0.431
CYB5B	0.414	DTL	0.120	ENST00000377803	0.204	FAM54A	0.197
CYB5D1	0.402	DTL	0.109	ENST00000379640	0.305	FAM64A	0.237
CYCS	0.279	DTWD1	0.454	ENST00000382966	0.353	FAM69A	0.480
CYHR1	0.418	DTWD1	0.479	ENST00000389758	0.343	FAM72D	0.458
CYP1A1	0.364	DTYMK	0.232	ENST00000398981	0.347	FAM82A1	0.447
CYP1B1	0.144	DUSP6	0.226	ENST00000409468	0.368	FAM83D	0.061
CYP1B1	0.279	DUT	0.275	ENST00000409736	0.436	FAM86A	0.446
CYP2U1	0.481	DUT	0.296	ENST00000416025	0.272	FAM86A	0.398
CYYR1	0.448	DVL2	0.498	ENST00000431042	0.424	FAM86A	0.475
D2HGDH	0.343	DYNC2H1	0.341	ENST00000438607	0.414	FAM86B2	0.416
D4S234E	0.309	DYNLRB2	0.491	ENST00000447029	0.331	FAM86B2	0.402
DAAM1	0.445	DZIP1	0.443	ENST00000447432	0.486	FAM86B2	0.406
DAPL1	0.280	E2F1	0.250	ENST00000457435	0.383	FAM92A1	0.355
DBF4	0.356	E2F1	0.262	ENST00000458238	0.154	FAM92A3	0.486
DBT	0.425	E2F1	0.265	ENST00000458619	0.477	FANCA	0.258
DCAF13	0.434	E2F1	0.314	ENTPD3	0.164	FANCA	0.236
DCAF16	0.456	E2F1	0.244	EPAS1	0.260	FANCA	0.264
DCAKD	0.494	E2F1	0.248	EPB41L1	0.357	FANCA	0.230
DCLRE1B	0.411	E2F1	0.254	EPB41L4B	0.406	FANCA	0.253
DDB2	0.365	E2F1	0.259	EPHX2	0.265	FANCA	0.468
DDB2	0.318	E2F1	0.250	EPN3	0.100	FANCA	0.247
DDX10	0.460	E2F1	0.276	EPO	0.394	FANCA	0.236
DDX11	0.482	E2F2	0.252	ERCC6L	0.150	FANCA	0.247
DEK	0.412	E2F7	0.267	ERF	0.482	FANCA	0.275
DENND2A	0.252	E2F8	0.399	ERI3	0.459	FANCA	0.380
DENND5B	0.458	EARS2	0.371	ESCO2	0.215	FANCA	0.234
DEPDC1	0.066	EBNA1BP2	0.354	ESCO2	0.152	FANCC	0.474
DEPDC1B	0.160	EBNA1BP2	0.353	ESPL1	0.373	FANCD2	0.317
DHFR	0.141	EBNA1BP2	0.355	ESYT2	0.408	FANCD2	0.296
DHFRL1	0.438	EBNA1BP2	0.359	ETF1	0.498	FANCE	0.365
DHODH	0.390	EBNA1BP2	0.369	ETFB	0.482	FANCG	0.249
DHRS13	0.463	EBNA1BP2	0.374	ETFB	0.485	FANCI	0.238
DIAPH3	0.198	EBNA1BP2	0.357	ETFB	0.480	FANCM	0.320
DIAPH3	0.239	EBNA1BP2	0.364	ETFB	0.497	FANK1	0.328
DICER1	0.469	EBNA1BP2	0.374	ETFB	0.486	FANK1	0.335
DIS3L	0.399	EBNA1BP2	0.363	ETFB	0.489	FANK1	0.372
DIXDC1	0.483	ECE2	0.352	ETFB	0.496	FANK1	0.335
DKC1	0.305	ECH1	0.481	ETV1	0.411	FANK1	0.331
DKFZP564C152	0.350	EEF1A1	0.470	ETV4	0.424	FANK1	0.382
DLEU1	0.302	EEF1B2	0.368	EVL	0.448	FANK1	0.374
DLEU2L	0.487	EEF1E1	0.431	EXO1	0.158	FANK1	0.344

Table 1.1: continued

Poly (I:C) downregulated genes (997-1328 of 2769)

Gene Name	Fold Change	Gene Name	Fold Change	Gene Name	Fold Change	Gene Name	Fold Change
FANK1	0.332	GINS4	0.135	HACL1	0.470	HMBS	0.334
FANK1	0.437	GJB2	0.267	HACL1	0.471	HMBS	0.335
FANK1	0.350	GJB2	0.263	HACL1	0.455	HMGB1L1	0.287
FAR1	0.496	GJB2	0.263	HACL1	0.460	HMGB2	0.090
FARSB	0.395	GJB2	0.264	HACL1	0.461	HMGB3	0.384
FBL	0.404	GJB2	0.261	HACL1	0.462	HMGB3	0.413
FBLN1	0.374	GJB2	0.256	HACL1	0.474	HMGB3L1	0.423
FBN2	0.391	GJB2	0.255	HADH	0.201	HMGN2	0.234
FBXL18	0.481	GJB2	0.259	HAT1	0.338	HMGN2	0.264
FBXO5	0.266	GJB2	0.258	HAUS5	0.287	HMGN2	0.248
FEN1	0.222	GJB2	0.272	HAUS6	0.321	HMMR	0.071
FGD3	0.395	GLRX5	0.464	HAUS7	0.490	HNRNPA0	0.321
FGFBP1	0.308	GLT8D2	0.488	HAUS8	0.403	HNRNPA1	0.331
FGFR1	0.477	GLT8D4	0.472	HAUS8	0.459	HNRNPA1	0.483
FGFR2	0.166	GM2A	0.450	HEATR1	0.422	HNRNPA1L2	0.360
FGFR2	0.339	GMNN	0.250	HEATR1	0.386	HNRNPA1L2	0.379
FGFR3	0.168	GMPR2	0.448	HEATR1	0.400	HNRNPA1L2	0.370
FH	0.394	GNG11	0.441	HEATR1	0.403	HNRNPA1L2	0.371
FHOD3	0.083	GNG11	0.440	HEATR1	0.385	HNRNPA1L2	0.498
FIGN	0.499	GNG11	0.433	HEATR1	0.388	HNRNPAB	0.450
FIGNL1	0.370	GNG11	0.451	HEATR1	0.397	HNRNPD	0.426
FJX1	0.361	GNG11	0.440	HEATR1	0.407	HNRPDL	0.278
FLJ13744	0.342	GNG11	0.435	HEATR1	0.416	HOMER2	0.447
FLJ32065	0.376	GNG11	0.427	HEATR1	0.403	HOPX	0.436
FLJ44342	0.446	GNG11	0.458	HEATR7B1	0.380	HOXA3	0.471
FLJ46906	0.417	GNG11	0.453	HEBP1	0.397	HOXA7	0.361
FLJ90757	0.454	GNG11	0.439	HEBP1	0.417	HOXA9	0.468
FOXA2	0.294	GNG12	0.460	HEBP1	0.437	HOXC13	0.362
FOXK1	0.499	GNL1	0.292	HEBP1	0.411	HP1BP3	0.454
FOXM1	0.161	GNL3L	0.469	HEBP1	0.412	HPDL	0.395
FOXQ1	0.396	GNPDA1	0.450	HEBP1	0.447	HPRT1	0.492
FOXRED2	0.375	GPAM	0.258	HEBP1	0.451	HPRT1	0.495
FREQ	0.499	GPC1	0.243	HEBP1	0.423	HR	0.329
FST	0.118	GPC6	0.300	HEBP1	0.426	HRASLS	0.436
FST	0.121	GPN3	0.436	HEBP1	0.420	HS3ST2	0.277
FST	0.124	GPNMB	0.409	HELLS	0.366	HS3ST2	0.260
FST	0.119	GPR110	0.241	HELLS	0.386	HS3ST2	0.263
FST	0.123	GPR115	0.499	HELZ	0.485	HS3ST2	0.256
FST	0.124	GPR125	0.301	HES2	0.423	HS3ST2	0.258
FST	0.124	GPR155	0.375	HIBADH	0.458	HS3ST2	0.261
FST	0.118	GPR155	0.471	HIRIP3	0.493	HS3ST2	0.261
FST	0.122	GPR56	0.421	HIRIP3	0.400	HS3ST2	0.260
FST	0.125	GPSM2	0.253	HIST1H1A	0.058	HS3ST2	0.262
FTL	0.282	GPT2	0.449	HIST1H1B	0.047	HS3ST2	0.277
FTL	0.269	GPX2	0.240	HIST1H1C	0.468	HS3ST3B1	0.277
FXN	0.471	GPX3	0.467	HIST1H1D	0.143	HS6ST1	0.498
FZD1	0.214	GRB14	0.352	HIST1H1E	0.203	HS6ST2	0.489
FZD10	0.375	GSG2	0.393	HIST1H2AI	0.173	HSD17B1	0.482
FZD2	0.204	GSR	0.388	HIST1H2AJ	0.473	HSD17B2	0.323
FZD3	0.489	GSR	0.486	HIST1H2AL	0.270	HSD17B2	0.312
FZD7	0.333	GSTA4	0.248	HIST1H2AM	0.279	HSD17B2	0.298
GALNT11	0.426	GSTA4	0.260	HIST1H2BE	0.401	HSD17B2	0.299
GALNT2	0.301	GSTA4	0.235	HIST1H2BF	0.349	HSD17B2	0.315
GALNTL4	0.417	GSTA4	0.249	HIST1H3A	0.345	HSD17B2	0.285
GAMT	0.306	GSTA4	0.221	HIST1H3B	0.111	HSD17B2	0.307
GAS1	0.386	GSTA4	0.251	HIST1H3D	0.339	HSD17B2	0.303
GBE1	0.488	GSTA4	0.231	HIST1H3E	0.285	HSD17B2	0.324
GBE1	0.474	GSTA4	0.228	HIST1H3F	0.211	HSD17B2	0.292
GBE1	0.474	GSTA4	0.238	HIST1H3H	0.211	HSDL2	0.497
GBE1	0.492	GSTA4	0.228	HIST1H3J	0.309	HSF2	0.486
GBE1	0.496	GSTA4	0.326	HIST1H4A	0.200	HSPA12A	0.214
GCAT	0.324	GSTM3	0.489	HIST1H4B	0.099	HSPA14	0.401
GCLC	0.321	GSTM3	0.472	HIST1H4C	0.116	HSPB3	0.321
GCSH	0.240	GSTM3	0.489	HIST1H4D	0.141	HSPD1	0.421
GDF11	0.475	GSTM3	0.487	HIST1H4E	0.130	HSPE1	0.361
GDF15	0.153	GSTM3	0.480	HIST1H4J	0.300	HTR7	0.481
GEMIN4	0.394	GSTM3	0.466	HIST1H4K	0.353	HTRA1	0.191
GEMIN5	0.442	GSTM3	0.497	HIST1H4K	0.441	IARS	0.411
GEMIN6	0.475	GSTM3	0.490	HIST1H4L	0.448	IARS	0.420
GGA2	0.396	GSTO2	0.413	HIST1H4L	0.111	ICAM5	0.475
GGCT	0.430	GTF2I	0.491	HIST2H3A	0.076	ICAM5	0.494
GHR	0.304	GTSE1	0.172	HJURP	0.047	ICAM5	0.477
GINS1	0.341	GYG2	0.475	HKDC1	0.257	ICAM5	0.498
GINS2	0.135	H19	0.301	HLCS	0.409	ICMT	0.447
GINS2	0.135	H2AFV	0.362	HLTF	0.380	IER5L	0.418
GINS2	0.136	H2AFX	0.303	HMBS	0.332	IFFO2	0.419
GINS2	0.133	H2AFZ	0.214	HMBS	0.332	IFRD2	0.331
GINS2	0.144	H3F3A	0.450	HMBS	0.315	IFT80	0.488
GINS2	0.145	H3F3A	0.387	HMBS	0.318	IFT81	0.436
GINS2	0.136	H3F3A	0.361	HMBS	0.323	IFT88	0.432
GINS2	0.138	HACL1	0.474	HMBS	0.319	IGF1R	0.398
GINS2	0.142	HACL1	0.459	HMBS	0.324	IGFBP5	0.455
GINS2	0.142	HACL1	0.452	HMBS	0.327	IGFL3	0.297

Table 1.1: continued

Poly (I:C) downregulated genes (1329-1660 of 2769)

Gene Name	Fold Change	Gene Name	Fold Change	Gene Name	Fold Change	Gene Name	Fold Change
IKBIP	0.353	KIAA0101	0.103	LDOC1	0.481	LOXL2	0.434
IKBIP	0.379	KIAA0101	0.109	LDOC1L	0.473	LOXL2	0.461
IL18	0.287	KIAA0101	0.106	LETM2	0.354	LPHN3	0.467
IL18	0.295	KIAA0101	0.101	LFNG	0.164	LPHN3	0.479
IL18	0.282	KIAA0101	0.104	LGALS7	0.299	LPXN	0.415
IL18	0.294	KIAA0101	0.107	LGR4	0.326	LRDD	0.480
IL18	0.286	KIAA0101	0.101	LGTN	0.467	LRIG1	0.317
IL18	0.292	KIAA0101	0.101	LGTN	0.494	LRIG1	0.312
IL18	0.310	KIAA0101	0.109	LGTN	0.496	LRIG1	0.323
IL18	0.300	KIAA0114	0.112	LGTN	0.478	LRIG1	0.308
IL18	0.291	KIAA0586	0.485	LGTN	0.481	LRIG1	0.331
IL18	0.304	KIAA0586	0.500	LGTN	0.497	LRIG1	0.323
IL1RAP	0.402	KIAA0586	0.483	LGTN	0.478	LRIG1	0.343
ILF3	0.328	KIAA0586	0.490	LGTN	0.492	LRIG1	0.319
ILF3	0.497	KIAA0586	0.496	LHPP	0.487	LRIG1	0.336
IMPA2	0.376	KIAA1324	0.474	LIG1	0.221	LRIG1	0.362
IMPA2	0.302	KIAA1430	0.441	LIMCH1	0.417	LRP4	0.175
IMPDH1	0.463	KIAA1549	0.223	LIN54	0.466	LRPPRC	0.332
IMPDH2	0.270	KIAA1712	0.481	LIN9	0.415	LRRC20	0.298
INCENP	0.322	KIAA1797	0.399	LMCD1	0.198	LSM3	0.472
INCENP	0.363	KIF11	0.144	LMNB1	0.133	LSM4	0.499
INCENP	0.340	KIF14	0.077	LMNB2	0.324	LSM5	0.349
INCENP	0.365	KIF15	0.183	LOC100128184	0.377	LY6D	0.467
INCENP	0.326	KIF18A	0.197	LOC100128372	0.335	LYAR	0.478
INCENP	0.327	KIF20A	0.133	LOC100128881	0.367	LZTFL1	0.379
INCENP	0.340	KIF20A	0.142	LOC100129550	0.109	MAD2L1	0.089
INCENP	0.328	KIF20A	0.135	LOC100130506	0.314	MAF	0.487
INCENP	0.326	KIF20A	0.136	LOC100130899	0.410	MAFA	0.452
INCENP	0.452	KIF20A	0.131	LOC100130938	0.424	MAP3K12	0.475
ING5	0.398	KIF20A	0.146	LOC100132240	0.341	MAP6	0.469
INSR	0.474	KIF20A	0.150	LOC100132984	0.500	MAP6	0.299
INTS10	0.426	KIF20A	0.133	LOC100133263	0.451	MAP6D1	0.374
IPO4	0.438	KIF20A	0.127	LOC100134253	0.472	MAP7D3	0.443
IPO5	0.463	KIF20A	0.124	LOC100287241	0.427	MAP7D3	0.410
IPO5	0.294	KIF20B	0.239	LOC100288418	0.395	MAP7D3	0.443
IPO9	0.376	KIF20B	0.374	LOC100288418	0.487	MAP7D3	0.448
IQGAP3	0.326	KIF22	0.229	LOC100293193	0.361	MAP7D3	0.429
IQSEC1	0.452	KIF22	0.231	LOC120364	0.469	MAP7D3	0.458
IRS1	0.325	KIF23	0.084	LOC151146	0.432	MAP7D3	0.476
IRS1	0.216	KIF23	0.136	LOC151162	0.430	MAP7D3	0.477
IRS2	0.276	KIF24	0.478	LOC153577	0.350	MAP7D3	0.499
IRX2	0.500	KIF2C	0.082	LOC25845	0.440	MAP7D3	0.427
ISL1	0.471	KIF4A	0.158	LOC283378	0.275	MAP7D3	0.464
ISM1	0.247	KIF4A	0.424	LOC285178	0.176	MAP9	0.341
ISYNA1	0.380	KIFC1	0.237	LOC338620	0.499	MAPKAP1	0.467
ISYNA1	0.377	KITLG	0.267	LOC338756	0.367	MAPKAPK3	0.483
ITGA6	0.326	KLHL13	0.331	LOC340335	0.406	MCCC1	0.499
ITGA6	0.315	KLHL24	0.406	LOC389831	0.486	MCEE	0.411
ITGB3BP	0.205	KLK5	0.262	LOC389842	0.485	MCM10	0.345
ITGB3BP	0.208	KLK8	0.390	LOC390282	0.403	MCM2	0.167
ITGB3BP	0.214	KNTC1	0.332	LOC390424	0.345	MCM3	0.198
ITGB3BP	0.223	KNTC1	0.325	LOC390940	0.373	MCM4	0.184
ITGB3BP	0.199	KNTC1	0.331	LOC391359	0.499	MCM5	0.256
ITGB3BP	0.194	KNTC1	0.337	LOC399804	0.421	MCM5	0.258
ITGB3BP	0.209	KNTC1	0.339	LOC400743	0.393	MCM6	0.173
ITGB3BP	0.219	KNTC1	0.330	LOC402360	0.461	MCM7	0.303
ITGB3BP	0.221	KNTC1	0.333	LOC440957	0.455	MCM7	0.150
ITGB3BP	0.219	KNTC1	0.326	LOC441795	0.416	MCM8	0.404
ITM2A	0.420	KNTC1	0.324	LOC541471	0.432	MDC1	0.479
IVNS1ABP	0.435	KNTC1	0.346	LOC642366	0.426	MEGF9	0.443
JAG2	0.284	KPNA2	0.298	LOC642587	0.305	MEST	0.102
JAG2	0.279	KRT13	0.402	LOC643873	0.382	METRN	0.451
JAG2	0.324	KRT15	0.332	LOC646049	0.358	METT10D	0.486
JAG2	0.297	KRT16	0.435	LOC646791	0.491	METTL7A	0.095
JAG2	0.287	KRT31	0.341	LOC646808	0.372	MEX3A	0.442
JAG2	0.278	KRT5	0.401	LOC647086	0.343	MGAT5B	0.386
JAG2	0.291	KRT80	0.428	LOC647302	0.411	MGC16121	0.096
JAG2	0.300	KRTAP19-5	0.481	LOC653113	0.339	MGC27345	0.478
JAG2	0.302	L1TD1	0.408	LOC729595	0.486	MIB1	0.379
JAG2	0.318	LAGE3	0.373	LOC729687	0.325	MINA	0.447
JMJD7	0.334	LAMP2	0.418	LOC729860	0.233	MIPEP	0.393
JMJD7-PLA2G4B	0.456	LAPTM4B	0.301	LOC729983	0.406	MIPEP	0.435
JPH1	0.317	LAPTM4B	0.440	LOC730107	0.361	MIPEP	0.415
KAL1	0.489	LARS	0.468	LOC93622	0.430	MIPEP	0.426
KANK2	0.380	LAS1L	0.424	LONP1	0.479	MIPEP	0.468
KANK4	0.480	LASS6	0.324	LOXL2	0.459	MIPEP	0.459
KANK4	0.455	LCE1B	0.492	LOXL2	0.473	MIPEP	0.432
KAT2A	0.223	LCE1C	0.258	LOXL2	0.450	MIPEP	0.458
KCNMA1	0.400	LCE1E	0.405	LOXL2	0.455	MIPEP	0.428
KCNMA1	0.225	LCLAT1	0.422	LOXL2	0.462	MIPEP	0.454
KCTD12	0.498	LCTL	0.350	LOXL2	0.446	MIPEP	0.440
KDSR	0.313	LDHB	0.320	LOXL2	0.462	MITF	0.427
KIAA0101	0.109	LDHB	0.325	LOXL2	0.453	MITF	0.486

Table 1.1: continued

Poly (I:C) downregulated genes (1661-1992 of 2769)

Gene Name	Fold Change	Gene Name	Fold Change	Gene Name	Fold Change	Gene Name	Fold Change
MKI67	0.202	MYH10	0.408	NUF2	0.130	PDGFA	0.266
MKI67	0.222	MYLIP	0.428	NUP107	0.392	PDGFA	0.258
MKI67	0.309	MYLK	0.202	NUP133	0.435	PDGFA	0.273
MLEC	0.395	MYLK	0.206	NUP35	0.489	PDGFA	0.234
MLF1	0.419	NAALADL2	0.243	NUP35	0.458	PDGFA	0.245
MLF1	0.283	NANOS1	0.232	NUP35	0.477	PDGFA	0.248
MLF1IP	0.157	NAP1L1	0.201	NUP35	0.482	PDGFA	0.240
MLH1	0.477	NARS2	0.402	NUP35	0.491	PDGFA	0.237
MMP3	0.276	NASP	0.471	NUP35	0.488	PDGFA	0.239
MND1	0.128	NAV2	0.410	NUP37	0.371	PDGFA	0.262
MNS1	0.439	NCAPD2	0.179	NUSAP1	0.150	PDGFA	0.256
MOBKL2B	0.298	NCAPD2	0.141	NXPH4	0.432	PDPR	0.498
MOCS2	0.467	NCAPD3	0.386	NXT1	0.486	PDSS1	0.473
MORC4	0.403	NCAPG	0.163	OBSL1	0.227	PDXK	0.284
MORN2	0.370	NCAPG2	0.202	ODC1	0.261	PDXP	0.481
MOSC1	0.375	NCAPH2	0.474	ODF2	0.403	PDZD8	0.452
MPP1	0.408	NCRNA00094	0.444	ODZ2	0.128	PEG10	0.161
MRAP2	0.396	NCRNA00173	0.342	ODZ2	0.056	PFAS	0.453
MRC2	0.440	NCRNA00185	0.460	OIP5	0.080	PFKM	0.318
MRE11A	0.486	NCRNA00188	0.369	OLFML2A	0.059	PFN2	0.458
MRM1	0.491	NDC80	0.069	ORAI2	0.381	PGF	0.384
MRPL12	0.446	NDUFA4L2	0.469	ORC1L	0.325	PGPEP1	0.487
MRPL12	0.491	NEDD4L	0.363	ORC5L	0.475	PHB2	0.499
MRPL19	0.481	NEDD4L	0.372	ORC6L	0.291	PHF19	0.319
MRPL24	0.479	NEFH	0.476	ORC6L	0.286	PHF19	0.326
MRPL3	0.392	NEFL	0.166	ORC6L	0.284	PHGDH	0.248
MRPL30	0.461	NEFM	0.157	ORC6L	0.305	PHKA2	0.456
MRPS27	0.391	NEIL3	0.402	ORC6L	0.321	PHLDB1	0.430
MRTO4	0.470	NEK2	0.409	ORC6L	0.284	PHTF2	0.343
MSH2	0.332	NEK2	0.159	ORC6L	0.317	PHYH	0.467
MSH2	0.346	NEK6	0.343	ORC6L	0.317	PHYH	0.452
MSH2	0.338	NETO2	0.298	ORC6L	0.329	PHYH	0.454
MSH2	0.349	NEURL1B	0.462	ORC6L	0.321	PHYH	0.440
MSH2	0.350	NEXN	0.144	OSBPL1A	0.426	PHYH	0.453
MSH2	0.342	NEXN	0.201	OSCP1	0.423	PHYH	0.480
MSH2	0.354	NFIA	0.331	OSCP1	0.427	PHYH	0.481
MSH2	0.340	NFIB	0.393	OSCP1	0.427	PHYH	0.488
MSH2	0.357	NFIB	0.174	OSCP1	0.437	PHYH	0.479
MSH2	0.340	NFKBIL2	0.384	OSCP1	0.463	PID1	0.240
MSH2	0.339	NFYA	0.325	OSCP1	0.449	PIF1	0.243
MSH5	0.496	NFYB	0.461	OSCP1	0.436	PIGK	0.306
MSH6	0.250	NGFRAP1	0.295	OSCP1	0.443	PIK3C2B	0.206
MSH6	0.235	NHP2	0.491	OSCP1	0.461	PIR	0.381
MSH6	0.234	NHP2L1	0.427	OSCP1	0.456	PITPNM3	0.187
MSH6	0.250	NIF3L1	0.390	OSCP1	0.475	PKD2	0.416
MSH6	0.233	NKRF	0.500	OSGEP	0.493	PKMYT1	0.150
MSH6	0.237	NKRF	0.495	OSGEPL1	0.278	PKNOX1	0.399
MSH6	0.242	NKRF	0.489	PA2G4	0.445	PKP4	0.491
MSH6	0.243	NKRF	0.491	PA2G4	0.439	PKP4	0.415
MSH6	0.239	NKRF	0.494	PAAF1	0.411	PKP4	0.450
MSH6	0.249	NLE1	0.449	PAAF1	0.434	PLA2G12A	0.249
MT1M	0.331	NLE1	0.353	PABPC1	0.445	PLA2G4A	0.417
MT1X	0.480	NME7	0.468	PABPC3	0.441	PLA2G4A	0.427
MTA1	0.447	NMT2	0.409	PABPC4	0.259	PLA2G4A	0.409
MTAP	0.487	NMT2	0.396	PAFAH1B1	0.419	PLA2G4A	0.397
MTBP	0.464	NMU	0.448	PAICS	0.243	PLA2G4A	0.429
MTERFD3	0.434	NOG	0.179	PALLD	0.369	PLA2G4A	0.466
MTHFD1	0.381	NOL8	0.497	PALLD	0.345	PLA2G4A	0.410
MTHFD1	0.373	NOLC1	0.301	PAMR1	0.208	PLA2G4A	0.432
MTHFD1	0.384	NOP16	0.403	PANK1	0.341	PLA2G4A	0.443
MTHFD1	0.383	NOP56	0.425	PARD6G	0.451	PLAC1	0.391
MTHFD1	0.371	NOP56	0.489	PARP2	0.468	PLCB2	0.443
MTHFD1	0.381	NPHP4	0.491	PASK	0.465	PLCD4	0.404
MTHFD1	0.377	NPM1	0.467	PBK	0.071	PLEKHA6	0.353
MTHFD1	0.377	NPM1	0.431	PBX1	0.249	PLIN2	0.374
MTHFD1	0.384	NPM1	0.376	PCCA	0.462	PLIN4	0.477
MTHFD1	0.391	NPM3	0.240	PCM1	0.372	PLK1	0.318
MYBBP1A	0.397	NQO1	0.364	PCNA	0.187	PLK1	0.413
MYBL1	0.219	NR2C2AP	0.473	PCNA	0.177	PLK1S1	0.346
MYBL2	0.334	NR2F2	0.348	PCNA	0.196	PLK4	0.409
MYBPHL	0.383	NRGN	0.355	PCNA	0.187	PMEPA1	0.444
MYC	0.344	NSMCE1	0.453	PCNA	0.184	PMP22	0.344
MYC	0.359	NSMCE1	0.383	PCNA	0.190	PMP22	0.337
MYC	0.355	NT5DC2	0.275	PCNA	0.194	PMP22	0.346
MYC	0.359	NT5DC3	0.479	PCNA	0.194	PMP22	0.339
MYC	0.373	NTHL1	0.438	PCNA	0.190	PMP22	0.350
MYC	0.353	NTN4	0.237	PCNA	0.195	PMP22	0.343
MYC	0.367	NUBPL	0.293	PCNA	0.192	PMP22	0.373
MYC	0.361	NUCKS1	0.457	PCOLCE2	0.333	PMP22	0.372
MYC	0.377	NUDCD2	0.436	PCYOX1	0.361	PMP22	0.370
MYC	0.372	NUDT1	0.449	PCYOX1	0.398	PMP22	0.365
MYCBPAP	0.395	NUDT21	0.366	PDCD4	0.325	PMS1	0.366
MYCL1	0.420	NUDT6	0.412	PDE1C	0.473	PNKD	0.311

Table 1.1: continued

Poly (I:C) downregulated genes (1993-2324 of 2769)

Gene Name	Fold Change	Gene Name	Fold Change	Gene Name	Fold Change	Gene Name	Fold Change
PNMAL1	0.340	PXMP2	0.457	RHOD	0.253	RPS6	0.424
PNPLA3	0.422	PXMP4	0.393	RIN1	0.204	RPS6	0.405
PNPO	0.430	PYCR1	0.374	RNASEH2A	0.376	RPS6	0.417
POLA1	0.305	PYCR2	0.413	RNASEH2C	0.459	RPS6	0.420
POLD1	0.377	PYGL	0.451	RNF141	0.247	RPS6	0.407
POLD2	0.313	PYGO1	0.447	ROM1	0.426	RPS6	0.427
POLD3	0.436	QSER1	0.396	ROM1	0.421	RPS6	0.436
POLE2	0.217	R3HDM1	0.364	ROM1	0.405	RRM1	0.149
POLE3	0.346	RAB11FIP4	0.297	ROM1	0.435	RRM2	0.115
POLH	0.481	RAB22A	0.245	ROM1	0.386	RRP15	0.293
POLQ	0.263	RAB36	0.330	ROM1	0.444	RRP1B	0.364
POLR1C	0.345	RAB40B	0.222	ROM1	0.442	RRS1	0.246
POLR1C	0.492	RAB4A	0.408	ROM1	0.387	RSAD1	0.452
POLR1E	0.342	RAB7B	0.066	ROM1	0.393	RUVBL1	0.427
POLR3H	0.467	RABEPK	0.373	ROM1	0.477	RUVBL2	0.460
POLR3K	0.491	RACGAP1	0.253	ROR1	0.326	RXRA	0.493
POMT2	0.396	RAD18	0.408	ROR1	0.268	S1PR5	0.391
POP5	0.377	RAD18	0.425	ROR1	0.310	S1PR5	0.409
PORCN	0.304	RAD18	0.396	ROR1	0.306	S1PR5	0.425
PPA2	0.421	RAD18	0.413	ROR1	0.315	S1PR5	0.448
PPAP2B	0.353	RAD18	0.407	ROR1	0.282	S1PR5	0.382
PPAPDC1A	0.316	RAD18	0.399	ROR1	0.260	S1PR5	0.401
PPARGC1B	0.284	RAD18	0.415	ROR1	0.313	S1PR5	0.416
PPARGC1B	0.449	RAD18	0.420	ROR1	0.262	S1PR5	0.433
PPAT	0.490	RAD18	0.416	ROR1	0.316	S1PR5	0.419
PPAT	0.417	RAD18	0.429	ROR1	0.314	S1PR5	0.472
PPIA	0.428	RAD51	0.244	RP11-529I10.4	0.261	SAAL1	0.416
PPIH	0.468	RAD51AP1	0.255	RP11-529I10.4	0.211	SAC3D1	0.372
PPP1R14C	0.376	RAD51C	0.230	RPA1	0.326	SACS	0.348
PPP1R3C	0.333	RAD54B	0.368	RPA1	0.431	SALL2	0.296
PPP2R3B	0.428	RAD54B	0.353	RPA3	0.349	SAMD5	0.426
PPT1	0.458	RAD54B	0.345	RPF2	0.421	SAP30	0.408
PRAGMIN	0.096	RAD54B	0.384	RPL15	0.465	SAP30	0.443
PRC1	0.206	RAD54B	0.345	RPL22	0.282	SAP30	0.419
PREPL	0.234	RAD54B	0.354	RPL23	0.477	SAP30	0.436
PREPL	0.383	RAD54B	0.389	RPL27A	0.126	SAP30	0.412
PRICKLE1	0.418	RAD54B	0.349	RPL3	0.376	SAP30	0.421
PRIM1	0.231	RAD54B	0.343	RPL3	0.435	SAP30	0.453
PRIM1	0.223	RAD54B	0.372	RPL39L	0.290	SAP30	0.429
PRIM1	0.230	RAD54L	0.196	RPL4	0.420	SAP30	0.447
PRIM1	0.219	RAMP1	0.278	RPL5	0.386	SAP30	0.451
PRIM1	0.224	RAMP1	0.200	RPL5	0.410	SCAI	0.457
PRIM1	0.217	RANBP1	0.400	RPL5	0.409	SCARB1	0.364
PRIM1	0.222	RARA	0.473	RPL6	0.468	SCARNA13	0.416
PRIM1	0.226	RASA3	0.394	RPL7	0.377	SCD	0.409
PRIM1	0.235	RASA4	0.489	RPL7	0.361	SCEL	0.440
PRIM1	0.228	RASL11B	0.381	RPL7	0.476	SCLY	0.340
PRKCA	0.363	RBBP4	0.273	RPLP0	0.388	SCN2B	0.256
PRKDC	0.331	RBL1	0.437	RPLP0	0.406	SCN4B	0.220
PRKRA	0.478	RBM12	0.491	RPLP0	0.389	SDK2	0.425
PRKX	0.376	RBM12	0.357	RPLP0	0.382	SEH1L	0.479
PRKXP1	0.411	RCC1	0.488	RPLP0	0.372	SEMA5A	0.358
PRMT3	0.429	RCCD1	0.382	RPLP0	0.380	SEPP1	0.430
PRODH	0.408	RCCD1	0.358	RPLP0	0.393	SEPP1	0.440
PROM2	0.383	RCCD1	0.363	RPLP0	0.393	SEPP1	0.487
PROM2	0.336	RCCD1	0.354	RPLP0	0.397	SEPP1	0.490
PRPF19	0.434	RCCD1	0.359	RPLP0	0.396	SEPP1	0.436
PRPS1	0.332	RCCD1	0.387	RPLP0	0.384	SEPP1	0.438
PRPS1	0.406	RCCD1	0.369	RPLP0P3	0.342	SEPP1	0.466
PRPS1L1	0.447	RCCD1	0.363	RPLP0P5	0.351	SEPP1	0.449
PRR11	0.289	RCCD1	0.368	RPP40	0.464	SEPP1	0.425
PRR7	0.238	RCCD1	0.348	RPP40	0.465	SEPP1	0.439
PRTFDC1	0.416	RCL1	0.313	RPP40	0.452	SEPP1	0.445
PSAPL1	0.416	RCL1	0.454	RPP40	0.489	SERBP1	0.358
PSAT1	0.368	RCN2	0.212	RPP40	0.473	SERPINB13	0.283
PSD3	0.257	RDH10	0.415	RPP40	0.455	SERTAD4	0.186
PSIP1	0.372	RECQL4	0.191	RPP40	0.493	SETD6	0.466
PSIP1	0.276	REEP2	0.174	RPP40	0.471	SFRS2B	0.360
PSMC3IP	0.358	REEP4	0.478	RPS2	0.383	SFRS3	0.473
PSMG1	0.462	REEP5	0.437	RPS2	0.453	SFRS6	0.310
PSRC1	0.171	REEP6	0.474	RPS23	0.280	SFXN2	0.407
PTGS1	0.189	REPS2	0.291	RPS2P32	0.359	SFXN4	0.463
PTGS1	0.231	REV3L	0.451	RPS2P32	0.429	SGEF	0.468
PTHLH	0.206	RFC2	0.375	RPS3A	0.340	SGOL1	0.365
PTPLAD1	0.423	RFC3	0.311	RPS3A	0.340	SGOL1	0.418
PTPLAD1	0.460	RFC3	0.208	RPS3A	0.386	SGOL2	0.281
PTPLB	0.467	RFC4	0.153	RPS3A	0.343	SHCBP1	0.111
PTPN3	0.476	RFC5	0.161	RPS3A	0.325	SHMT1	0.400
PTPRS	0.305	RFX2	0.411	RPS4Y1	0.496	SHMT1	0.455
PTTG1	0.195	RGS16	0.460	RPS4Y2	0.473	SHROOM3	0.330
PTTG2	0.142	RHOBTB1	0.467	RPS6	0.432	SIGMAR1	0.422
PTTG3P	0.246	RHOBTB2	0.285	RPS6	0.410	SIPA1L2	0.426
PUS7	0.457	RHOBTB3	0.333	RPS6	0.415	SIVA1	0.421

Table 1.1: continued

Poly (I:C) downregulated genes (2325-2656 of 2769)

Gene Name	Fold Change	Gene Name	Fold Change	Gene Name	Fold Change	Gene Name	Fold Change
SKA1	0.205	SNRPF	0.438	TCTN1	0.392	TP53AIP1	0.283
SKA3	0.150	SNX29	0.340	TCTN3	0.460	TP53TG1	0.403
SKIV2L2	0.467	SNX30	0.276	TDP1	0.373	TP53TG1	0.496
SKIV2L2	0.464	SNX5	0.327	TELO2	0.346	TPCN1	0.320
SKIV2L2	0.467	SORL1	0.177	TEX2	0.496	TPCN1	0.193
SKIV2L2	0.467	SOST	0.262	TFAM	0.346	TPD52L1	0.425
SKIV2L2	0.473	SOST	0.241	TFB2M	0.470	TPM1	0.487
SKIV2L2	0.457	SOST	0.259	TFRC	0.272	TPM2	0.350
SKIV2L2	0.492	SOST	0.275	TFRC	0.287	TPM2	0.372
SKIV2L2	0.500	SOST	0.258	TFRC	0.278	TPX2	0.227
SKP2	0.302	SOST	0.223	TFRC	0.290	TRAIP	0.160
SLC16A5	0.383	SOST	0.251	TFRC	0.280	TRAM2	0.257
SLC16A9	0.403	SOST	0.219	TFRC	0.278	TREM2	0.157
SLC16A9	0.407	SOST	0.239	TFRC	0.284	TRERF1	0.430
SLC16A9	0.377	SOST	0.252	TFRC	0.293	TRERF1	0.454
SLC16A9	0.425	SOX6	0.357	TFRC	0.296	TRIAP1	0.387
SLC16A9	0.435	SOX7	0.441	TFRC	0.284	TRIM2	0.260
SLC16A9	0.410	SP100	0.283	TGFB2	0.362	TRIM45	0.403
SLC16A9	0.377	SPA17	0.383	TGFBI	0.302	TRIM59	0.465
SLC16A9	0.412	SPA17	0.373	TGFBR1	0.417	TRIM6	0.465
SLC16A9	0.415	SPA17	0.382	THAP10	0.472	TRIM65	0.414
SLC16A9	0.435	SPA17	0.374	THAP10	0.463	TRIP13	0.088
SLC19A1	0.380	SPA17	0.367	THAP10	0.445	TRIP13	0.417
SLC1A3	0.458	SPA17	0.365	THAP10	0.495	TRIT1	0.496
SLC20A1	0.344	SPA17	0.382	THAP10	0.462	TRIT1	0.499
SLC22A23	0.478	SPA17	0.363	THAP10	0.499	TRMT5	0.335
SLC23A2	0.377	SPA17	0.387	THAP10	0.480	TROAP	0.162
SLC25A10	0.260	SPA17	0.381	THAP10	0.480	TSC22D1	0.277
SLC25A15	0.451	SPAG16	0.476	THBS2	0.069	TSC22D3	0.455
SLC25A29	0.278	SPAG5	0.104	THEM4	0.379	TSEN2	0.238
SLC25A32	0.448	SPATA7	0.391	THEM4	0.451	TSEN34	0.458
SLC25A5	0.367	SPC25	0.077	THNSL1	0.498	TSGA14	0.458
SLC26A2	0.271	SPHAR	0.358	THOP1	0.489	TSHZ1	0.456
SLC27A1	0.333	SPNS2	0.392	THY1	0.270	TSN	0.441
SLC27A5	0.310	SPON2	0.494	THYN1	0.491	TSPAN5	0.433
SLC29A1	0.397	SPON2	0.492	TIGD2	0.289	TSPAN6	0.419
SLC2A1	0.271	SPON2	0.492	TIMELESS	0.202	TSPAN9	0.479
SLC2A4RG	0.259	SPON2	0.493	TIMM8A	0.413	TTC12	0.347
SLC2A9	0.440	SPON2	0.494	TIMM9	0.409	TTC12	0.280
SLC35B4	0.286	SPON2	0.489	TK1	0.208	TTC19	0.486
SLC35F3	0.307	SPRR1B	0.318	TKT	0.464	TTC39C	0.469
SLC38A1	0.396	SPTLC3	0.247	TLE2	0.436	TTC8	0.281
SLC43A1	0.434	SRXN1	0.395	TM7SF3	0.443	TTK	0.126
SLC47A2	0.203	SSBP4	0.399	TM7SF3	0.295	TTL	0.447
SLC48A1	0.466	SSR1	0.233	TMEM106C	0.397	TTLL12	0.364
SLC6A10P	0.402	SSRP1	0.373	TMEM107	0.272	TUBA4A	0.492
SLC6A6	0.432	SSX2IP	0.458	TMEM117	0.420	TUBB	0.482
SLC6A8	0.434	ST3GAL5	0.303	TMEM120B	0.419	TXNDC17	0.498
SLC6A8	0.403	STAC	0.359	TMEM121	0.400	TYMS	0.123
SLC7A11	0.228	STAR	0.270	TMEM161A	0.410	TYRO3	0.420
SLC7A5	0.474	STEAP3	0.355	TMEM164	0.447	UBASH3B	0.496
SLC7A8	0.385	STK17B	0.440	TMEM177	0.359	UBE2C	0.083
SLCO2A1	0.394	STK32B	0.414	TMEM201	0.455	UBE2S	0.436
SLITRK6	0.111	STMN1	0.212	TMEM30A	0.497	UBE2T	0.212
SMARCD3	0.273	STON1	0.422	TMEM45A	0.375	UBE2T	0.216
SMC1A	0.335	STXBP4	0.483	TMEM48	0.359	UBE2T	0.207
SMC2	0.433	SUB1	0.430	TMEM52	0.344	UBE2T	0.199
SMC4	0.172	SULF2	0.171	TMEM8B	0.495	UBE2T	0.211
SMC4	0.147	SULT1E1	0.474	TMEM9	0.497	UBE2T	0.207
SMO	0.177	SUMF1	0.438	TMEM97	0.366	UBE2T	0.208
SMOC1	0.303	SUV39H1	0.343	TMSB15B	0.387	UBE2T	0.200
SMYD3	0.463	SUV39H2	0.243	TNFRSF10D	0.269	UBE2T	0.207
SNHG1	0.350	SYNGR1	0.370	TNFRSF21	0.374	UBE2T	0.205
SNHG10	0.385	SYT8	0.288	TNFSF4	0.385	UBE4B	0.465
SNHG3	0.498	SYTL1	0.410	TNNI2	0.233	UBR7	0.363
SNHG7	0.366	SYTL1	0.485	TNS4	0.414	UBTF	0.425
SNHG8	0.369	TACC2	0.379	TOMM20	0.489	UBXN8	0.434
SNHG9	0.216	TACC3	0.181	TOMM40	0.489	UGT1A6	0.163
SNORA10	0.348	TAF15	0.389	TOMM40	0.455	UGT1A6	0.111
SNORD123	0.444	TAF9B	0.469	TOP1MT	0.428	UGT1A8	0.126
SNRNP25	0.347	TANC2	0.481	TOP2A	0.071	UHRF1	0.131
SNRNP40	0.497	TBC1D14	0.409	TOP2A	0.073	UHRF1	0.303
SNRPE	0.421	TBCD	0.434	TOP2A	0.078	ULBP1	0.366
SNRPE	0.485	TBL1X	0.489	TOP2A	0.067	UNC119B	0.272
SNRPF	0.446	TBL1X	0.427	TOP2A	0.075	UNC5B	0.228
SNRPF	0.456	TCEB2	0.446	TOP2A	0.070	UNG	0.246
SNRPF	0.460	TCF19	0.448	TOP2A	0.082	URB2	0.401
SNRPF	0.446	TCF3	0.287	TOP2A	0.071	USP1	0.445
SNRPF	0.455	TCFL5	0.443	TOP2A	0.069	USP1	0.463
SNRPF	0.453	TCOF1	0.298	TOP2A	0.076	USP1	0.453
SNRPF	0.457	TCOF1	0.481	TOP2B	0.498	USP1	0.454
SNRPF	0.449	TCOF1	0.493	TOPBP1	0.419	USP1	0.450
SNRPF	0.448	TCTEX1D2	0.261	TOX2	0.445	USP1	0.438

Table 1.1: continued

Poly (I:C) downregulated genes (2657-2769 of 2769)

Gene Name	Fold Change	Gene Name	Fold Change	Gene Name	Fold Change	Gene Name	Fold Change
USP1	0.481	ZDHHC8P	0.492				
USP1	0.464	ZHX3	0.354				
USP1	0.449	ZMAT3	0.473				
USP1	0.471	ZMAT3	0.465				
USP13	0.416	ZMAT3	0.482				
USP7	0.464	ZMAT3	0.475				
UTP15	0.450	ZMAT3	0.451				
UTP20	0.436	ZMAT3	0.454				
VAPB	0.325	ZMAT3	0.449				
VASN	0.197	ZMAT3	0.483				
VAV3	0.208	ZMAT3	0.475				
VDR	0.323	ZMAT3	0.452				
VDR	0.325	ZNF148	0.420				
VDR	0.335	ZNF286B	0.447				
VDR	0.333	ZNF323	0.457				
VDR	0.333	ZNF331	0.406				
VDR	0.345	ZNF362	0.500				
VDR	0.332	ZNF385D	0.479				
VDR	0.336	ZNF385D	0.498				
VDR	0.329	ZNF395	0.284				
VDR	0.344	ZNF573	0.398				
VGLL1	0.303	ZNF584	0.485				
VIPR1	0.450	ZNF658	0.431				
VMA21	0.365	ZNF658	0.445				
VPS37D	0.340	ZNRF1	0.377				
VRK1	0.361	ZNRF3	0.323				
VSNL1	0.189	ZP3	0.459				
WASF3	0.440	ZWILCH	0.289				
WDHD1	0.155	ZWINT	0.135				
WDHD1	0.155	ZWINT	0.183				
WDHD1	0.167						
WDHD1	0.162						
WDHD1	0.172						
WDHD1	0.166						
WDHD1	0.173						
WDHD1	0.168						
WDHD1	0.181						
WDHD1	0.174						
WDR12	0.396						
WDR3	0.317						
WDR34	0.223						
WDR35	0.220						
WDR43	0.383						
WDR5	0.435						
WDR51A	0.156						
WDR54	0.354						
WDR62	0.272						
WDR63	0.288						
WDR66	0.264						
WDR66	0.334						
WDR77	0.493						
WDR77	0.490						
WDR77	0.466						
WDR77	0.464						
WDR77	0.463						
WDR77	0.470						
WDR77	0.484						
WDR77	0.483						
WDR77	0.470						
WDR77	0.487						
WDR90	0.290						
WEE1	0.410						
WFDC5	0.471						
WHSC1	0.355						
WHSC1	0.387						
WNT10A	0.311						
WNT10A	0.286						
WNT10A	0.296						
WNT10A	0.306						
WNT10A	0.276						
WNT10A	0.260						
WNT10A	0.268						
WNT10A	0.280						
WNT10A	0.327						
WNT10A	0.314						
WNT6	0.430						
XG	0.332						
XRCC2	0.462						
XRCC3	0.299						
XRCC6BP1	0.362						
ZAK	0.286						
ZBED3	0.317						
ZC3H14	0.422						

Table 1.2: Poly (I:C)-induced gene expression changes. Data in table represents real-time PCR and microarray fold change data from NHEK treated with 1 μg/ml Poly (I:C) versus control, water-treated NHEK. *P < 0.05,**P < 0.01,***P < 0.001. Student's T-Test. Data are mean of triplicate samples and representative of at least three independent experiments for real-time PCR. Data are mean of triplicate samples and analyzed for significance with SAM (fold change >2, FDR < 0.01%; delta value = 1.397).

Table 1. Poly(I:C)-induced gene expression changes

Gene name	Fold change (real-time PCR)	±SD	*t*-Test	Fold change (microarray)	SAM
ABCA12	22.68	5.551	**	3.74	+
GBA	10.84	1.243	***	2.03	+
SMPD1	9.48	1.143	***	2.05	+
TGM1	30.65	4.231	***	2.40	+
TNF	23.07	0.564	***	5.31	+
IL-6	41.99	2.480	***	27.31	+
TLR3	69.66	9.100	***	14.58	+
MAVS	1.40	0.309	NS	1.70	–
KRT1	1.33	1.727	NS	0.52	–
KRT14	0.74	0.012	***	1.02	–
IVL	0.79	0.064	NS	0.60	–
LOR	1.43	1.216	NS	1.53	–
FLG	0.83	1.224	NS	0.84	–
SPTLC1	1.36	0.071	**	1.19	–
SPTLC2	3.72	0.834	**	0.81	–
UGCG	2.61	0.174	***	0.67	–
ACACA	0.37	0.079	**	0.33	+
FASN	0.48	0.113	*	0.67	–
HMGCR	1.24	0.057	*	1.04	–
HMGCS1	1.07	0.143	NS	1.60	–
FDFT1	0.71	0.096	*	0.85	–

Abbreviations: NS, nonsignificant; Poly(I:C), polyinosinic acid:polycytidylic acid; SAM, Significance Analysis of Microarrays.
*P< 0.05, **P< 0.01, and ***P<0.001. Student's *t*-test.
Data are mean of triplicate samples and representative of at least three independent experiments for real-time PCR. Data are mean of triplicate samples and analyzed for significance with SAM (fold change >2, false discovery rate (FDR) <0.01%; delta value=1.397).
Data in table represent real-time PCR and microarray fold change data from normal human epidermal keratinocyte (NHEKs) treated with 1 μg ml^{-1} Poly(I:C) versus control, water-treated NHEKs.

References

[1] G. K. Menon, K. R. Feingold, and P. M. Elias, “Lamellar body secretory response to barrier disruption.,” *J. Invest. Dermatol.*, vol. 98, no. 3, pp. 279–289, 1992.

[2] M. Akiyama, Y. Sugiyama-Nakagiri, K. Sakai, J. R. McMillan, M. Goto, K. Arita, Y. Tsuji-Abe, N. Tabata, K. Matsuoka, R. Sasaki, D. Sawamura, and H. Shimizu, “Mutations in lipid transporter ABCA12 in harlequin ichthyosis and functional recovery by corrective gene transfer,” *J. Clin. Invest.*, vol. 115, no. 7, pp. 2–9, 2005.

[3] C. Lefévre, S. Audebert, F. Jobard, B. Bouadjar, H. Lakhdar, O. Boughdene-Stambouli, C. Blanchet-Bardon, R. Heilig, M. Foglio, J. Weissenbach, M. Lathrop, J.-F. Prud’homme, and J. Fischer, “Mutations in the transporter ABCA12 are associated with lamellar ichthyosis type 2.,” *Hum. Mol. Genet.*, vol. 12, no. 18, pp. 2369–78, Sep. 2003.

[4] W. M. Holleran, Y. Takagi, G. K. Menon, S. M. Jackson, J. M. Lee, K. R. Feingold, and P. M. Elias, “Permeability barrier requirements regulate epidermal beta-glucocerebrosidase.,” *J. Lipid Res.*, vol. 35, no. 5, pp. 905–12, May 1994.

[5] J. M. Jensen, S. Schütze, M. Förl, M. Krönke, and E. Proksch, “Roles for tumor necrosis factor receptor p55 and sphingomyelinase in repairing the cutaneous permeability barrier.,” *J. Clin. Invest.*, vol. 104, no. 12, pp. 1761–70, Dec. 1999.

[6] G. Menon, K. Feingold, and A. Moser, “De novo sterologenesis in the skin. II. Regulation by cutaneous barrier requirements.,” *J. Lipid Res.*, vol. 26, no. 5, pp. 418–427, 1985.

[7] M. Mao-Qiang, P. M. Elias, and K. R. Feingold, “Fatty acids are required for epidermal permeability barrier function.,” *J. Clin. Invest.*, vol. 92, no. 2, pp. 791–8, Aug. 1993.

[8] K. Ottey and L. Wood, “Cutaneous permeability barrier disruption increases fatty acid synthetic enzyme activity in the epidermis of hairless mice.,” *J. Invest. Dermatol.*, vol. 104, no. 3, pp. 401–404, 1995.

[9] W. M. Holleran, K. R. Feingold, M. Q. Man, W. N. Gao, J. M. Lee, and P. M. Elias, “Regulation of epidermal sphingolipid synthesis by permeability barrier function.,” *J. Lipid Res.*, vol. 32, no. 7, pp. 1151–8, Jul. 1991.

[10] W. M. Holleran, W. N. Gao, K. R. Feingold, and P. M. Elias, “Localization of epidermal sphingolipid synthesis and serine palmitoyl transferase activity: alterations imposed by permeability barrier requirements.,” *Arch. Dermatol. Res.*, vol. 287, no. 3–4, pp. 254–8, Jan. 1995.

[11] S. H. Lee, P. M. Elias, E. Proksch, G. K. Menon, M. Mao-Quiang, and K. R. Feingold, “Calcium and potassium are important regulators of barrier homeostasis in murine epidermis.,” *J. Clin. Invest.*, vol. 89, no. 2, pp. 530–8, Feb. 1992.

[12] G. K. Menon, P. M. Elias, S. H. Lee, and K. R. Feingold, “Localization of calcium in murine epidermis following disruption and repair of the permeability barrier,” *Cell Tissue Res.*, vol. 270, no. 3, pp. 503–512, Dec. 1992.

[13] Y. Lai, A. Di Nardo, T. Nakatsuji, A. Leichtle, Y. Yang, A. L. Cogen, Z.-R. Wu, L. V Hooper, R. R. Schmidt, S. von Aulock, K. a Radek, C.-M. Huang, A. F. Ryan, and R. L. Gallo, “Commensal bacteria regulate Toll-like receptor 3-dependent inflammation after skin injury.,” *Nat. Med.*, vol. 15, no. 12, pp. 1377–82, Dec. 2009.

[14] J. J. Bernard, C. Cowing-Zitron, T. Nakatsuji, B. Muehleisen, J. Muto, A. W. Borkowski, L. Martinez, E. L. Greidinger, B. D. Yu, and R. L. Gallo, “Ultraviolet radiation damages self noncoding RNA and is detected by TLR3.,” *Nat. Med.*, vol. 18, no. 8, pp. 1286–90, Aug. 2012.

[15] F. Dunlevy, N. McElvaney, and C. Greene, “TLR3 Sensing of Viral Infection,” *Open Infect. Dis. J.*, vol. 4, pp. 1–10, 2010.

[16] T. Kawai and S. Akira, “Toll-like receptor and RIG-I-like receptor signaling.,” *Ann. N. Y. Acad. Sci.*, vol. 1143, pp. 1–20, Nov. 2008.

[17] S.-Y. Zhang, E. Jouanguy, S. Ugolini, A. Smahi, G. Elain, P. Romero, D. Segal, V. Sancho-Shimizu, L. Lorenzo, A. Puel, C. Picard, A. Chapgier, S. Plancoulaine, M. Titeux, C. Cognet, H. von Bernuth, C.-L. Ku, A. Casrouge, X.-X. Zhang, L. Barreiro, J. Leonard, C. Hamilton, P. Lebon, B. Héron, L. Vallée, L. Quintana-Murci, A. Hovnanian, F. Rozenberg, E. Vivier, F. Geissmann, M. Tardieu, L. Abel, and J.-L. Casanova, “TLR3 deficiency in patients with herpes simplex encephalitis.,” *Science*, vol. 317, no. 5844, pp. 1522–7, Sep. 2007.

[18] A. Casrouge, S.-Y. Zhang, C. Eidenschenk, E. Jouanguy, A. Puel, K. Yang, A. Alcais, C. Picard, N. Mahfoufi, N. Nicolas, L. Lorenzo, S. Plancoulaine, B. Sénéchal, F. Geissmann, K. Tabeta, K. Hoebe, X. Du, R. L. Miller, B. Héron, C. Mignot, T. B. de Villemeur, P. Lebon, O. Dulac, F. Rozenberg, B. Beutler, M. Tardieu, L. Abel, and J.-L. Casanova, “Herpes simplex virus encephalitis in human UNC-93B deficiency.,” *Science*, vol. 314, no. 5797, pp. 308–12, Oct. 2006.

[19] V. Sancho-Shimizu, R. Perez de Diego, L. Lorenzo, R. Halwani, A. Alangari, E. Israelsson, S. Fabrega, A. Cardon, J. Maluenda, M. Tatematsu, F. Mahvelati, M. Herman, M. Ciancanelli, Y. Guo, Z. AlSum, N. Alhamis, A. S. Al-Makadma, A. Ghadiri, S. Boucherit, S. Plancoulaine, C. Picard, F. Rozenberg, M. Tardieu, P. Lebon, E. Jouanguy, N. Rezaei, T. Seya, M. Matsumoto, D. Chaussabel, A. Puel, S.-Y. Zhang, L. Abel, S. Al-Muhsen, and J.-L. Casanova, “Herpes simplex encephalitis in children with autosomal recessive and dominant TRIF deficiency,” *J. Clin. Invest.*, vol. 121, no. 12, pp. 4890–4902, 2011.

[20] K. A. Cavassani, M. Ishii, H. Wen, M. A. Schaller, P. M. Lincoln, N. W. Lukacs, C. M. Hogaboam, and S. L. Kunkel, “TLR3 is an endogenous sensor of tissue necrosis during acute inflammatory events.,” *J. Exp. Med.*, vol. 205, no. 11, pp. 2609–21, Oct. 2008.

[21] Q. Lin, D. Fang, J. Fang, X. Ren, X. Yang, F. Wen, and S. B. Su, “Impaired wound healing with defective expression of chemokines and recruitment of myeloid cells in TLR3-deficient mice.,” *J. Immunol.*, vol. 186, no. 6, pp. 3710–7, Mar. 2011.

[22] Q. Lin, L. Wang, Y. Lin, X. Liu, X. Ren, S. Wen, X. Du, T. Lu, S. Y. Su, X. Yang, W. Huang, S. Zhou, F. Wen, and S. B. Su, “Toll-like receptor 3 ligand polyinosinic:polycytidylic acid promotes wound healing in human and murine skin.,” *J. Invest. Dermatol.*, vol. 132, no. 8, pp. 2085–92, Aug. 2012.

[23] D. W. Huang, B. T. Sherman, and R. A. Lempicki, “Systematic and integrative analysis of large gene lists using DAVID bioinformatics resources.,” *Nat. Protoc.*, vol. 4, no. 1, pp. 44–57, Jan. 2009.

[24] D. W. Huang, B. T. Sherman, and R. A. Lempicki, “Bioinformatics enrichment tools: paths toward the comprehensive functional analysis of large gene lists.,” *Nucleic Acids Res.*, vol. 37, no. 1, pp. 1–13, Jan. 2009.

[25] Y. Uchida, A. Di Nardo, V. Collins, P. M. Elias, and W. M. Holleran, “De novo ceramide synthesis participates in the ultraviolet B irradiation-induced apoptosis in undifferentiated cultured human keratinocytes.,” *J. Invest. Dermatol.*, vol. 120, no. 4, pp. 662–9, Apr. 2003.

[26] C. L. Simpson, S. Kojima, and S. Getsios, “RNA interference in keratinocytes and an organotypic model of human epidermis.,” *Methods Mol. Biol.*, vol. 585, no. 2, pp. 127–146, 2010.

[27] H. Matsushima, N. Yamada, H. Matsue, and S. Shimada, “TLR3-, TLR7-, and TLR9-Mediated production of proinflammatory cytokines and chemokines from murine connective tissue type skin-derived mast cells but not from bone marrow-derived mast,” *J. Immunol.*, vol. 173, no. 1, pp. 531–541, 2004.

[28] K. R. Feingold and M. Denda, “Regulation of permeability barrier homeostasis.,” *Clin. Dermatol.*, vol. 30, no. 3, pp. 263–8, 2012.

[29] K. R. Feingold, “Thematic review series: skin lipids. The role of epidermal lipids in cutaneous permeability barrier homeostasis.,” *J. Lipid Res.*, vol. 48, no. 12, pp. 2531–46, Dec. 2007.

[30] W. M. Holleran, M. Q. Man, W. N. Gao, G. K. Menon, P. M. Elias, and K. R. Feingold, “Sphingolipids are required for mammalian epidermal barrier function. Inhibition of sphingolipid synthesis delays barrier recovery after acute perturbation.,” *J. Clin. Invest.*, vol. 88, pp. 1338–1345, 1991.

[31] K. R. Feingold, “The regulation and role of epidermal lipid synthesis.,” *Adv. Lipid Res.*, vol. 24, pp. 57–82, 1991.

[32] M. Yu and S. J. Levine, “Toll-like receptor, RIG-I-like receptors and the NLRP3 inflammasome: key modulators of innate immune responses to double-stranded RNA viruses.,” *Cytokine Growth Factor Rev.*, vol. 22, no. 2, pp. 63–72, Apr. 2011.

[33] X.-P. Wang, M. Schunck, K.-J. Kallen, C. Neumann, C. Trautwein, S. Rose-John, and E. Proksch, “The interleukin-6 cytokine system regulates epidermal permeability barrier homeostasis.,” *J. Invest. Dermatol.*, vol. 123, no. 1, pp. 124–31, Jul. 2004.

[34] B. Melnik, J. Hollmann, and G. Plewig, “Decreased stratum corneum ceramides in atopic individuals--a pathobiochemical factor in xerosis?,” *Br. J. Dermatol.*, vol. 119, no. 4, pp. 547–549, 1988.

[35] a Yamamoto, S. Serizawa, M. Ito, and Y. Sato, “Stratum corneum lipid abnormalities in atopic dermatitis.,” *Arch. Dermatol. Res.*, vol. 283, no. 4, pp. 219–23, Jan. 1991.

[36] C. N. a Palmer, A. D. Irvine, A. Terron-Kwiatkowski, Y. Zhao, H. Liao, S. P. Lee, D. R. Goudie, A. Sandilands, L. E. Campbell, F. J. D. Smith, G. M. O’Regan, R. M. Watson, J. E. Cecil, S. J. Bale, J. G. Compton, J. J. DiGiovanna, P. Fleckman, S. Lewis-Jones, G. Arseculeratne, A. Sergeant, C. S. Munro, B. El Houate, K. McElreavey, L. B. Halkjaer, H. Bisgaard, S. Mukhopadhyay, and W. H. I. McLean, “Common loss-of-function variants of the epidermal barrier protein filaggrin are a major predisposing factor for atopic dermatitis.,” *Nat. Genet.*, vol. 38, no. 4, pp. 441–6, Apr. 2006.

[37] I. Jakasa, E. S. Koster, F. Calkoen, W. H. I. McLean, L. E. Campbell, J. D. Bos, M. M. Verberk, and S. Kezic, “Skin barrier function in healthy subjects and patients with atopic dermatitis in relation to filaggrin loss-of-function mutations.,” *J. Invest. Dermatol.*, vol. 131, no. 2, pp. 540–2, Mar. 2011.

[38] J. Ishikawa, H. Narita, N. Kondo, M. Hotta, Y. Takagi, Y. Masukawa, T. Kitahara, Y. Takema, S. Koyano, S. Yamazaki, and A. Hatamochi, “Changes in the ceramide profile of atopic dermatitis patients.,” *J. Invest. Dermatol.*, vol. 130, no. 10, pp. 2511–4, Oct. 2010.

[39] M. Janssens, J. van Smeden, G. S. Gooris, W. Bras, G. Portale, P. J. Caspers, R. J. Vreeken, S. Kezic, A. P. M. Lavrijsen, and J. a Bouwstra, “Lamellar lipid organization and ceramide composition in the stratum corneum of patients with atopic eczema.,” *J. Invest. Dermatol.*, vol. 131, no. 10, pp. 2136–8, Oct. 2011.

CHAPTER 2:

Toll-like receptor 3 activation is required for normal skin barrier repair following UV damage

Abstract

Ultraviolet (UV) damage to the skin leads to the release of noncoding RNA from necrotic keratinocytes that activates toll-like receptor 3. Since this release of RNA has been shown to trigger inflammation in the skin following UV damage and toll-like receptor 3 (TLR3) activation can increase expression of genes associated with barrier repair, we hypothesized that the activation of TLR3 would promote repair of the skin barrier after UVB damage. Herein we demonstrate that damaged keratinocyte products and noncoding, small nuclear RNAs induce barrier repair genes. We observe that the noncoding RNA, U1 RNA induces expression of skin barrier repair genes in a TLR3-dependent manner. Additionally we show that tight junction gene expression and function is also increased in keratinocytes treated with the double-stranded RNA, Poly (I:C). Finally we demonstrate that *Tlr3*$^{-/-}$ mice display a delay in skin barrier repair following UVB damage. These data suggest that TLR3 participates in the program of skin barrier repair.

Introduction

Although ultraviolet (UV) light exposure is important for synthesizing Vitamin D, excessive levels cause damage to the skin resulting in painful sunburn and promote skin cancer. In the year 2000, excessive ultraviolet (UV) exposure was linked to 60,000 deaths worldwide with over 1.5 million disability-adjusted life years [1]. Previous studies have shown that skin barrier repair is dependent on changes in the epidermal calcium gradient [2], [3]. Disruption of this gradient results in changes in gene expression, epidermal lipid metabolism, and lamellar body secretion that help to restore the skin barrier. It has also been seen that disruptions to the skin barrier following UVB exposure result in increases in lipid metabolism and lamellar body dynamics [4], [5]. Although UVB exposure has a number of undesirable outcomes, low doses of UVB can also have beneficial effects on the barrier by inducing epidermal lipid synthesis enzymes and antimicrobial peptides [6]. Overall however, mechanisms that regulate skin barrier repair after UVB exposure have been incompletely described.

Inflammation following sunburn was recently found to be partially dependent on the function of toll-like receptor 3 (TLR3) and detection of endogenous non-coding RNA [7]. These observations are consistent with similar findings that TLR3 can sense damage to mammalian cells [8]–[10] and can influence wound repair [11], [12], but are a departure from the classically known role of this pattern recognition receptor as being responsible for effective responses to viral double stranded RNA (dsRNA) [13], [14]. Furthermore, activation of TLR3 in cultured human keratinocytes induces the expression of genes involved in formation of the skin barrier and increases lamellar bodies and keratohyalin granules in cultured human skin equivalents [15]. Therefore, in this study we hypothesized that the release of endogenous RNA and the subsequent activation of TLR3, is necessary to permit normal restoration of skin barrier function after UVB injury. Given the evidence presented here, we propose that activation of TLR3 by UVB injury

promotes skin barrier repair in addition to the current model for activation by disruption of the epidermal calcium gradient.

Methods

UVB exposure. NHEKs were irradiated with UVB at 15 mJ cm^{-2}, using Spectronics handheld UVB lamps with two 8W bulbs (312 nm) as previously described [10]. Dosimetry was performed using a digital ultraviolet radiometer by Solartech Inc. UVB-irradiated cells were used 24 hours after exposure, and lysates from 600,000 cells were added to 200,000 NHEKs grown to 80% confluence. Sonicated nonirradiated NHEKs treated identically were used as controls. For mouse irradiation, hair was shaved and chemically depilated from the back, and 96 h later, the hairless skin was exposed to UVB (5 kJ m^{-2}).

In vitro transcription of snRNA. snRNA was generated using Ampliscribe™ T7-*Flash*™ Transcription Kit from (Epicentre©, an Illumina© company, Madison, WI). Templates used for reactions were gel purified PCR products from the following primer pairs:

Transepidermal Water Loss. Transepidermal water loss (TEWL) was measured using a TEWAMETER TM300 (C & K, Cologne, Germany). TEWL was measured prior to UVB barrier disruption and every 24 hours for 5 days.

Mice. Sex-matched C57BL/6 wild-type controls, male and female TLR3-deficient mice on a C57BL/6 background were housed at the University Research Center at the University of California, San Diego (UCSD). All animal experiments were approved by the UCSD Institutional Animal Care and Use Committee.

Cell culture and stimuli. NHEKs were obtained from Cascade Biologics/Invitrogen (catalog number: C-001-5C; Portland, OR), and grown in serum-free EpiLife cell culture media (Cascade Biologics/Invitrogen) containing 0.06 mM Ca^{2+} and 1 × EpiLife Defined Growth Supplement (EDGS, Cascade Biologics/Invitrogen) at 37°C under standard tissue culture conditions. All cultures were maintained for up to eight passages in this medium with the addition of 100 U ml^{-1} penicillin, 100 µg ml^{-1} streptomycin, and 250 ng ml^{-1} amphotericin B. Cells at 60–80% confluence were treated with Poly (I:C) (1 µg ml^{-1}; Invivogen, San Diego, CA) in 12-well flat-bottom plates (Corning Incorporated Life Sciences, Lowell, MA) for up to 24 hours. After cell stimulation, RNA was extracted using TRIzol reagent (Invitrogen, Carlsbad, CA). RNA was stored at −80 °C.

Quantitative real-time PCR. Total RNA was extracted from cultured keratinocytes using TRIzol Reagent (Invitrogen) and 1 µg RNA was reverse-transcribed using iScript cDNA Synthesis Kit (Bio-Rad, Hercules, CA). Pre-developed Taqman Gene Expression Assays (Applied Biosystems, Foster City, CA) were used to evaluate mRNA transcript levels of ABCA12, GBA, SMPD1, TGM1, TNF, IL-6, CDSN, TJP1, OCLN, CLDN1, DSG1, DSG3, PKP1, DSP, JUP, DSC1, DSC2, CLDN4, CLDN5, CLDN7, CLDN11, CLDN23, and TLR3. Glyceraldehyde-3-phosphate dehydrogenase mRNA transcript levels were evaluated using a VIC-CATCCATGACAACTTTGGTA-MGB probe with primers 5′-CTTAGCACCCCTGGCCAAG-3′ and 5′-TGGTCATGAGTCCTTCCACG-3′. All analyses were performed in triplicate and were representative of three to five independent cell stimulation experiments that were analyzed in an ABI Prism 7000 Sequence Detection System (Life Technologies, Carlsbad, CA). Fold induction relative to glyceraldehyde-3-phosphate dehydrogenase was calculated using the $\Delta\Delta C_t$ method. Results were considered to be significant if $P<0.05$.

Gene expression profiling. Labeling of cDNA and hybridization to Agilent Unrestricted AMADID Release GE 4x44K 60mer (G4845A) was performed at UCSD's Biomedical Genomics (BIOGEM) Core. Gene expression analysis was performed following multiple loess normalization of the raw data. Significant changes in gene expression were identified using Significance of Microarrays (SAM) 4.0 with the following filters: 1. False Discovery Rate of 0.01% and 2. Average fold change of 2. Gene ontology and pathway term enrichment was performed using DAVID. P-values represent a modified Fisher's exact test (EASE = 1) n = 3. [16], [17].

Transepithelial Electric Resistance (TEER). Primary human keratinocytes (PHK) were isolated from discarded neonatal foreskins. PHK were plated in K-SFM in 24-well *Costar*® *Transwell inserts* (polyester membranes, *0.4*-μm pore size; *Corning Life Sciences, Corning, NY).* After cells were confluent, media were switched to DMEM media allowing PHK differentiation and TJ formation. At the same time, TLR3 ligand, Poly (I:C(*Amersham*/GE Healthcare, Piscataway, NJ) was placed in upper wells for 8 days. Culture media was changed every other day. TEER was measured as previously described [18]. The study was approved by the Research Subject Review Board at the University of Rochester Medical Center and was conducted according to Declaration of Helsinki Principles [19].

Paracellular flux assay. PHK were seeded in Transwell inserts and treated as described above. After 48 h, 0.02% fluorescein sodium (Sigma-Aldrich) in PBS was added to the upper well, while PBS alone was added to the lower well. Samples were collected from the lower well after 30 minutes. The amount of fluorescein sodium that diffused from across the filter was measured with the iQ5 Multicolor real-time PCR detection system (Bio-Rad). Paracellular flux

was presented as follows: Paracellular flux (fold of control)= fluorescein intensity of treatment groups/ fluorescein intensity of control group [18]**.**

siRNA constructs. TLR3 and control siRNA were purchased from Dharmacon (Chicago, IL). One nanomole of each siRNA was electroporated into 3 x 10^6 keratinocytes using Amaxa nucleofection reagents as previously described [15] (VPD-1002) (Lonza AG, Walkersville, MD).

Sequences of in vitro transcribed RNA.

U1 RNA
U1 sequence (164 bp): atacttacct ggcaggggag ataccatgat cacgaaggtg gttttcccag ggcgaggctt atccattgca ctccggatgt gctgacccct gcgatttccc caaatgtggg aaactcgact gcataatttg tggtagtggg ggactgcgtt cgcgctttcc cctg
U1 Forward Primer (*T7*):
*TAATACGACTCACTATAGGG*ATACTTACCTGGCAGGGGAGA
U1 Reverse Primer:
CAGGGGAAAGCGCGA

U2 RNA
U2 Sequence (188 bp): atcgcttctc ggccttttgg ctaagatcaa gtgtagtatc tgttcttatc agtttaatat ctgatacgtc ctctatccga ggacaatata ttaaatggat ttttggagca gggagatgga ataggagctt gctccgtcca ctccacgcat cgacctggta ttgcagtacc tccaggaacg gtgcaccc
U2 Forward Primer (T7):
*TAATACGACTCACTATAGGG*ATCGCTTCTCGGCCTTTT
U2 Reverse Primer:
GGGTGCACCGTTCCTG

U4 RNA
U4 Sequence (144 bp): agctttgcgc agtggcagta tcgtagccaa tgaggtctat ccgaggcgcg attattgcta attgaaaact tttcccaata ccccgccgtg acgacttgca atatagtcgg cactggcaat ttttgacagt ctctacggag actg
U4 Forward Primer (*T7*):
*TAATACGACTCACTATAGGG*AGCTTTGCGCAGTGGC
U4 Reverse Primer:
TCTCCGTAGAGACTGTCAAAAATTG

U6 RNA
U6 Sequence (106 bp): gtgctcgctt cggcagcaca tatactaaaa ttggaacgat acagagaaga ttagcatggc ccctgcgcaa ggatgacacg caaattcgtg aagcgttcca tatttt
U6 Forward Primer (T7):
*TAATACGACTCACTATAGGG*GTGCTCGCTTCGGCAG

U6 Reverse Primer:
AAAAATATGGAACGCTTCACG

U12 RNA
U12 Sequence (149 bp): tgccttaaac ttatgagtaa ggaaaataac gattcggggt gacgcccgaa tcctcactgc taatgtgaga cgaatttttg agcgggtaaa ggtcgccctc aaggtgaccc gcctactttg cgggatgcct gggagttgcg atctgcccg
U12 Forward Primer (T7):
*TAATACGACTCACTATAGGG*TGCCTTAAACTTATGAGTAAGGAAAAT
U12 Reverse Primer:
CGGGCAGATCGCAACT

SCARNA9
SCARNA9 Sequence (353 bp): ctttctgaga tctgctttta gtgaagtgga tcaatgatga aactagccaa atctgagcat cagaagtctt tccagtctac ctgatgcatg atctctacag ttctgagaag caaaactata aaacaatgta aaacaataag ggcatatgtc tggtgtgtgt gtgtgtgtgt gtgtgtgtgt gtgtgtgtac gcacatgtgt ttataaagat aacagctgta ggaatgaatg agattgaggg tgggggggtg cgtatgtatg tctatgaaag cctaatcatt tctgggcaat gatgaaaagg ttttactact gatctttgta actatgatgg tttctacact tgacctgagc tca
SCARNA9 Forward Primer (T7):
*TAATACGACTCACTATAGGG*CTTTCTGAGATCTGCTTTTAGTGAAGT
SCARNA9 Reverse Primer:
TGAGCTCAGGTCAAGTGTAGAAAC

SCARNA18
SCARNA18 Sequence (134 bp): ttgcatgtgg aaatgtctgc ttctcattcc ttgggagcag gaatatgttc ataacatgct acattaacaa aggagttctc agggctgcca accttctagt aaaggttgag tggtagtata tttctccaac ataa
SCARNA18 Forward Primer (T7):
*TAATACGACTCACTATAGGG*TTGCATGTGGAAATGTCTGC
SCARNA18 Reverse Primer:
TTATGTTGGAGAAATATACTACCACTCAAC

Secondary RNA structure generation. In order to depict the secondary structure of the snRNAs in this manuscript, sequences were taken from Pubmed or UCSC genome browser. These sequences were then analyzed for complementary base pairing using RNAfold (http://rna.tbi.univie.ac.at/cgi-bin/RNAfold.cgi). The following filters were selected to obtain the secondary structure information:

(1) minimum free energy (MFE) and partition function

(2) avoid isolated base pairs

The secondary structure and sequence information was then used with the VARNA applet (http://varna.lri.fr/) to generate the secondary structure diagrams [20], [21]

Ultrastructural Analysis. Mouse dorsal skin was excised 24 hours after UVB exposure and then immersed in modified Karnovsky's fixative (2.5% glutaraldehyde and 2% paraformaldehyde in 0.15 M sodium cacodylate buffer, pH 7.4) for at least 4 hours, post fixed in 1% osmium tetroxide in 0.15 M cacodylate buffer for 1 hour and stained en bloc in 3% uranyl acetate for 1 hour. Samples were dehydrated in ethanol, embedded in Durcupan epoxy resin (Sigma-Aldrich), sectioned at 50 to 60 nm on a Leica UCT ultramicrotome, and picked up on Formvar and carbon-coated copper grids. Sections were stained with 3% uranyl acetate for 5 minutes and Sato's lead stain for 1 minute. Grids were viewed using a JEOL 1200EX II (JEOL, Peabody, MA) transmission electron microscope and photographed using a Gatan digital camera (Gatan, Pleasanton, CA), or viewed using a Tecnai G2 Spirit BioTWIN transmission electron microscope equipped with an Eagle 4k HS digital camera (FEI, Hilsboro, OR). Pictures taken at 2000X represent 73 μm^2. Samples were also sectioned and stained with Toluidine Blue.

Bone Marrow Reconstitution. 6 week old mice were administered antibiotics (200 mg Sulfamethoxazole and 40 mg Trimethoprim) (Hi-Tech Pharmacal, Amityville, NY) in the drinking water 1 day prior to lethal irradiation. Mice were placed in a cesium source irradiator (J.L. Shepherd & Associates, San Fernando, CA), and exposed to 10 Gy (1000 Rad) of total body γ-irradiation. The following day, bone marrow was isolated from the femur and tibia of 10 week old mice. $6*10^6$ cells were injected suborbitally into lethally irradiated mice. Mice were allowed to recover 6 weeks before experimentation. Antibiotics were continued for 14 days after reconstitution with cages and water changed every other day during this time.

Cytokine/Chemokine Analysis. 8 mm biopsy punches were taken from the dorsal skin of UVB exposed mice and homogenized in 700 ul RIPA buffer. BCA Assay was performed to normalize protein amounts. 10 ug of total protein was used for analysis using MILLIPLEX MAP Mouse Cytokine/Chemokine Magnetic Bead Panel - Immunology Multiplex Assay (MCYTOMAG-70K, Millipore, Billerica, MA).

Results

UVB damaged keratinocytes stimulate genes important for the skin barrier. To detect whether products of UVB damaged keratinocytes trigger expression of genes involved in skin barrier repair we exposed cultured normal human epidermal keratinocytes (NHEK) to UVB and then transferred these irradiated cells to nonirradiated NHEK cultures. The exposure of NHEK to the products of UVB-damaged keratinocytes caused significant increases in mRNA abundance of ATP-binding cassette sub-family A member 12 (ABCA12), glucocerebrosidase (GBA), acid sphingomyelinase (SMPD1), and transglutaminase 1 (TGM1) (Figure 2.1a). These increases in mRNA were significantly higher than NHEK cultures that were exposed to sonicated, non-irradiated NHEK although significant increases in ABCA12 mRNA were also observed following treatment with sonicated NHEK (Figure 2.1a).

Desmosomes and tight junctions play an important role in barrier function of the skin [22], [23]. To determine whether these components of the skin barrier were influenced by dsRNA or UVB-damaged NHEK products, we measured the transcript abundance of the genes corneodesmosin (CDSN), occludin (OCLN), tight junction protein 1 (TJP1), and claudin 1 (CLDN1) after similar treatments with Poly (I:C), sonicated NHEK, and UVB-damaged NHEK. We observed that Poly (I:C) and UVB-treated NHEK applied to NHEK cultures stimulated significant increases in CDSN, OCLN, TJP1, and CLDN1 mRNA (Figure 2.1b). Sonicated NHEK also significantly increased mRNA levels of CDSN, OCLN, and CLDN1 (Figure 2.1b).

Only CDSN and TJP1 mRNA were induced significantly more in UVB-treated NHEK treatments compared to sonicated NHEK treatments (Figure 2.1b).

In order to assess the global effects of dsRNA on desmosomes and tight junctions in keratinocytes, we analyzed data from a microarray in which NHEK were treated for 24 hours with 1 μg/ml Poly (I:C) [15]. Findings of this microarray analysis showed that CDSN, periplakin 1 (PKP1), desmocolin 2 (DSC2), OCLN, CLDN4, CLDN7, and CLDN23 were all significantly increased (Table 2.1). In order to validate the microarray results, we performed real-time PCR for desmosomal and tight junctional genes. In NHEK treated for 24 hours with 1 μg/ml Poly (I:C), we observed significant increases in desmoglein 1 (DSG1), DSG3, CDSN, plakophilin 1 (PKP1), desmoplakin (DSP), junction plakoglobin (JUP), desmocolin 1 (DSC1), OCLN, TJP1, CLDN1, CLDN 4, CLDN 7, CLDN 11, and CLDN 23 (Table 2.1).

Poly (I:C) increases tight junction function in keratinocytes. As we observed increases in mRNA for genes associated with the tight junction following treatment of NHEK cultures with both Poly (I:C) and UVB-damaged NHEK products, we next evaluated the function of tight junctions in response to dsRNA. In this set of experiments, NHEK were grown to confluence in 24-well inserts and allowed to differentiate as previously described [18], [19]. Differentiated keratinocyte monolayers were then treated with Poly (I:C) and transepithelial electrical resistance (TEER) values were measured using an EVOMX voltohmmeter (World Precision Instruments, Sarasota, FL). We observed that Poly (I:C)-treatment lead to dose-dependent increases in TJ function as seen by increased TEER readings at 24 and 48 hours after treatment (Figure 2.2a and 2.2b). The initial increase in TEER values stimulated by Poly (I:C) diminished over time and was no longer significantly different than control samples by day 4 (Figure. 2.2c).

Another way to assess tight junction function is to measure paracellular flux of fluorescein sodium across a confluent monolayer of cells. In this experiment, keratinocyte monolayers were grown as previously described and Poly (I:C) was added and allowed to incubate for 48 hours. Fluorescein sodium was then added to the upper chamber and measured in the bottom chamber after 15 minutes. We observed that doses of 0.1 and 1 μg/ml Poly (I:C) significantly decreased the paracellular flux of fluorescein sodium (Figure. 2.2d).

TLR3 activation is required for U1 RNA-induced changes in skin barrier gene expression. U1 spliceosomal RNA (U1 RNA), a noncoding, small nuclear RNA (snRNA), has been shown to be altered following exposure of keratinocytes to UVB light. It was also observed that U1 RNA stimulates inflammation in keratinocytes and mouse skin in a TLR3-dependent manner [7]. In order to determine the effects of U1 RNA and TLR3 activation on skin barrier genes, NHEK were treated with 1 μg/ml U1 RNA for 24 hours and compared to NHEK in which TLR3 had been knocked down using small interfering RNA (siRNA). U1 RNA caused significant increases in transcripts of ABCA12, GBA, SMPD1 and TNF in control-treated NHEK, while the induction of these genes was significantly decreased in NHEK treated with TLR3 siRNA (Fig. 2.3).

Additional snRNAs can stimulate skin barrier and inflammatory cytokine gene expression. TLR3 is activated by double stranded RNA, and it was proposed that an increase of double stranded stem loops of U1 RNA after UVB exposure explains how this mammalian RNA can serve to activate a TLR best known for detection of viral dsRNA [7]. In addition to U1, numerous other noncoding snRNAs were also observed to show increases in read frequency after UVB [7]. To determine whether some of these noncoding RNAs could act in a similar manner to U1, we synthesized the spliceosomal RNAs U2, U4, U6, and minor spliceosomal RNA U12 (U2

RNA, U4 RNA, U6 RNA, and U12 RNA), as well as the small Cajol Body-specific RNAs 9 and 18 (scaRNA9 and scaRNA18). All of these snRNAs are predicted to contain double stranded regions using RNAfold software and the VARNA applet (Figure 2.4a) [20], [21] . Treatment of NHEK for 24 hours with these snRNAs resulted in significant increases in mRNA abundance of ABCA12, GBA, SMPD1, TGM1, TNF, and IL-6 (Figure 2.4b).

***Tlr3*$^{-/-}$ mice display a barrier repair defect after UVB-induced barrier disruption.** The capacity of UVB irradiated NHEK, and dsRNAs, to alter the expression of genes involved in barrier repair and increase NHEK tight junction function prompted us to directly test if TLR3 influenced skin barrier function after UVB injury. *Tlr3*$^{-/-}$ mice and controls were exposed to a single 5 kJ/m^2 dose of UVB as previously described [7], and transepidermal water loss (TEWL) was examined to evaluate the kinetics of barrier disruption and repair. This high dose of UVB has been previously described to cause apoptosis and necrosis in cell culture and cause barrier disruption in mice. [4], [10], [24]. Although TEWL levels of WT and *Tlr3*$^{-/-}$ mice were similar over the first 3 days following UVB light exposure, *Tlr3*$^{-/-}$ mice displayed elevated and prolonged high levels of TEWL with a significantly higher TEWL value at Day 4 (Figure 2.5a). WT mice exhibit a 3.3-fold faster recovery between day 3 and 4 ($p = 0.055$) than *Tlr3*$^{-/-}$ mice (Figure 2.5b). Conversely, barrier disruption caused by a chemical depilatory reagent or by tape stripping did not have a significant effect on barrier disruption or repair in *Tlr3*$^{-/-}$ or *Trif*$^{-/-}$ mice, respectively, when compared to WT mice (Figure 2.6). 24 hours after UVB exposure, no gross morphological differences could be observed between WT and *Tlr3*$^{-/-}$ mice in semi-thin Toluidine blue stained sections (Figure 2.5c). However, transmission electron microscopy found that *Tlr3*$^{-/-}$ mice displayed more abundant vacuolization of cells subjacent to the first layer of the stratum granulosum in comparison to WT mice (Figure 2.5d). Interestingly, these *Tlr3*$^{-/-}$ mice failed to

repitheilialize and exhibited chronic non-healing wounds at 8 and 16 weeks following a single acute 5 kJ/m^2 dose of UVB (Figure 2.5e).

As previous results have been described *in vitro* in which only keratinocytes were present, we wanted to determine which cell types contributed to the barrier repair defect observed in *Tlr3*$^{-/-}$ mice. In order to assess relative contributions of Tlr3 from different cell types in the skin on UVB-induced skin barrier disruption and repair, WT and *Tlr3-/-* mice were lethally irradiated and reconstituted with WT or *Tlr3*$^{-/-}$ bone marrow. Control mice (WT → WT and *Tlr3*$^{-/-}$ → *Tlr3*$^{-/-}$) showed similar differences in skin barrier repair after UVB induced barrier disruption as previously shown. When WT bone marrow was injected into *Tlr3*$^{-/-}$ mice (WT → *Tlr3-*$^{-/-}$), the barrier defect was not rescued, and TEWL levels were significantly higher at days 3 and 4 (Figure 2.5f). Conversely when *Tlr3*$^{-/-}$ bone marrow was injected into WT mice (*Tlr3*$^{-/-}$ → WT), TEWL levels were also significantly higher than control at day 3 (Figure 2.5g). In order to explore differences in response to UVB radiation we assessed the levels of 25 common cytokines and chemokines in the skin 24 hours after UVB treatment. It was observed that significantly lower amounts of IL-5, RANTES, IL-15, and GM-CSF were present in *Tlr3*$^{-/-}$ → WT mice skin when compared to control mice. No other significant differences in cytokine/chemokines levels were observed between control (WT → WT) and other groups (Table 2.2).

Discussion

TLR3 activation has classically been described in the context of innate immunity as a mechanism for detecting viruses [13], [14], though recent evidence has revealed its ability to sense endogenous injury [7], [9]–[12]. Herein we describe how injury to keratinocytes in the form of UVB damage activates TLR3 to promote expression of skin barrier repair genes, and that snRNAs or Poly (I:C) can initiate a similar response. Furthermore, mice lacking TLR3 demonstrate a decreased capacity to restore normal levels of TEWL after UVB damage. Though

triggers of skin barrier repair has previously been thought to involve sensing a disturbed calcium gradient in the epidermis [2], [3], the results reported in this study supports the hypothesis that TLR3 also serves as a sensor of skin damage by UVB. Furthermore, as skin barrier disruption is usually delayed 48-72 hours following acute UVB exposure [4], [5], TLR3 activation during this time may serve as a mechanism for accelerating skin barrier repair.

UVB exposure results in many molecular changes, and this damage to keratinocytes causes both apoptotic and necrotic forms of cell death. It has been shown that non-apoptotic forms of cell death trigger greater cytokine release from keratinocytes [10], likely through the release of cellular contents that present as damage associated molecular patterns (DAMPs) to numerous pattern recognition receptors (PRRs) present in or on neighboring cells [25]. More specifically U1 RNA, a single stranded, noncoding RNA is altered and released from necrotic cells following UV damage, and TLR3 detects this mammalian RNA [7]. In the present study, similar products from UVB-damaged keratinocytes that induce cytokine responses also enhanced expression of mRNA for the skin barrier genes ABCA12, GBA, SMPD1, and TGM1, as well as the desmosomal gene CDSN, and tight junction genes OCLN, TJP1, and CLDN1. Similar responses occurred after exposure to the dsRNA, Poly (I:C), and synthetic U1 RNA. All of these stimulated expression of the skin barrier genes ABCA12, GBA, and SMPD1 in a TLR3 dependent manner. Thus, although it is not directly shown that a specific non-coding RNA is responsible for the induction of barrier repair genes by UVB-necrotic cells, these observations support the hypothesis that UV exposure results in mobilization of DAMPs from keratinocytes that act through TLR3.

In order to demonstrate that similar effects on skin barrier genes occur in response to any one of a number of endogenous RNA species and are not limited to U1 RNA, we synthesized a number of noncoding snRNAs including: U2, U4, U6, U12, scaRNA9, and scaRNA18. These noncoding RNAs were chosen because they are upregulated following treatment of NHEK with

UVB after 24 hours [7]. Secondary structures of these snRNAs are predicted to contain a number of double stranded regions, which could potentially activate TLR3. Double stranded RNA at least 21 base pairs in length has been demonstrated to activate TLR3 [26]. The stem-loop structures of the snRNAs that we synthesized satisfy this requirement and were able to activate TLR3. While this response to these non-coding RNAs has not been previously shown, the activation of TLR3 by self RNA has previously been demonstrated. The first known example of TLR3 activation by self RNA occurred when cells were treated with *in vitro* transcribed mRNA [8]. It was also predicted at this time that the considerable secondary structure of mRNA could activate TLR3. Thus, our findings are consistent with previous literature in other cell types. Our work extends the significance of these observations by suggesting that repair of UV injury could be influenced by TLR3.

In order to determine whether TLR3 is in fact important for skin barrier repair, *Tlr3*$^{-/-}$ mice were treated with a single high dose of UVB to induce barrier disruption. The kinetics of barrier disruption were similar in WT and *Tlr3*$^{-/-}$ mice. However, *Tlr3*$^{-/-}$ mice display an elongated elevation in TEWL values in comparison to WT, suggesting that these mice have a defect in barrier repair. Previous experiments in which barrier disruption in mice was achieved by tape stripping or chemical depilation revealed no significant difference in barrier disruption or repair between WT and *Trif*$^{-/-}$ or WT and *Tlr3*$^{-/-}$ mice respectively. This is most likely due to the fact that barrier disruptions of this type instantly disrupt the calcium gradient in the epidermis through removal of outer layers of the cornified envelope without causing much cell death and or release of cellular contents as would be expected during necrosis.

Because Tlr3 is present on infiltrating immune cells that migrate to the skin following UV injury, we wanted to determine whether Tlr3 deficiency in these infiltrating immune cells or alternatively whether Tlr3 deficiency in keratinocytes or other radio-resistant resident skin cells would more significantly affect skin barrier repair after UVB-damage to the skin. To determine

the effect of Tlr3 present on bone marrow derived immunocytes on skin barrier repair, we injected WT bone marrow into *Tlr3*$^{-/-}$ mice prior to administering UV-induced barrier disruption. The skin barrier defect in these *Tlr3*$^{-/-}$ mice was not rescued, and appears to be exacerbated, as significant differences in TEWL values were observed earlier than in traditional *Tlr3*$^{-/-}$ mice. This finding demonstrates that Tlr3 present on keratinocytes or other radio resistant cells is important for skin barrier repair. Conversely, when *Tlr3*$^{-/-}$ bone marrow is injected into WT mice, we also observed a higher TEWL value at day 3. While this later finding was somewhat unexpected, it is not surprising and demonstrates that Tlr3 on bone marrow derived cells is also sensing dsRNA in UVB-damaged skin and mediating skin barrier repair in a yet unknown way. As these mice show deficiencies in certain cytokines (IL-5, RANTES, IL-15, and GM-CSF), this might hold a clue to why these mice show a barrier repair deficit at day 3. These findings demonstrate that Tlr3 present on both keratinocytes, or other resident skin cells, and bone marrow derived cells is important for skin barrier repair. Future studies should focus on the specific contributions of each cell type to skin barrier repair.

We have also found that *Tlr3*$^{-/-}$ mice exhibit chronic non-healing wounds at 8 and 16 weeks after an initial acute 5 kJ/m^2 dose of UVB (Figure. 2.5e). This finding is in agreement of the findings of Lin et al [11], [12] who have demonstrated that TLR3 is important for wound healing. They find that *Tlr3*$^{-/-}$ mice display slower wound closure in a punch biopsy wound healing model than WT mice and also that Poly (I:C)-treatment accelerates wound closure [11], [12]. While it is known that wound healing is delayed in *Tlr3*$^{-/-}$ mice, this is the first time that skin barrier repair, which is localized to the epidermis, has been shown to be affected by TLR3 deficiency. Although the deficiency in skin barrier repair may play a role in the wound healing phenotype that was observed, it is not sufficient to explain this phenotype and future studies will aim to more completely characterize these findings.

Though we previously described that changes in lipids and epidermal organelles are regulated by TLR3 activation, we focused primarily on the lipid component of the skin barrier. Tight junctions and desmosomes also play an important role in maintaining the skin barrier [27], evidenced by the fact that numerous skin diseases result from mutations in adhesional proteins or autoimmunity to components of the desmosome or tight junction [28]. This manuscript reports for the first time to our knowledge that Poly (I:C), a ligand of TLR3, increases tight junction gene expression and function in human keratinocytes. Thus, in addition to influences on genes related to the barrier formed by the outer lipid barrier of the skin, TLR3 also regulates tight junctions. This gives a more complete description of genes that are affected by TLR3 activation following UVB damage and suggests multiple mechanisms may be responsible for the observed delayed repair in *Tlr3*$^{-/-}$ mice.

In recent years, innate immune receptors, such as toll-like receptors have been shown to be responsible for more than just pathogen detection and clearance. Their role in recognizing and responding to DAMPs has become increasingly evident with many diseases being identified as being exacerbated or caused by PRR activation [29]. Deepening our understanding of the pathways downstream of TLRs, may lead to better therapeutics for wound healing or barrier repair. Thus, future work should focus on the downstream signaling pathways of TLR3 that activate genes that promote skin barrier homeostasis and repair as well as the relative contributions of other cell types in the skin that could potentially influence this essential process.

Acknowledgements

We thank J Sprague, G Hardiman, and R Sasik at the UCSD Biomedical Genomics laboratory for performing microarray. We thank Y Jones and T Meerloo at the UCSD EM Core for processing samples and helpful discussion and Dr. Marilyn Farquhar for helpful discussion of EM images.

This work was supported by US National Institutes of Health (NIH) grants R01-AR052728, NIH R01-AI052453 and R01 AI0833358 to R.L.G., the UCSD Training in Immunology Grant 5T32AI060536-05 and UCSD Dermatologist Investigator Training Program Grant 1T32AR062496-01 supporting A.W.B.

Chapter 2, in full, is currently being prepared for publication. A. W. Borkowski, I. Kuo, J. J. Bernard, T.Yoshida, M. R. Williams, N. Hung, B. D. Yu, L. A. Beck, and R. L. Gallo. The dissertation author was the primary investigator and author of this paper.

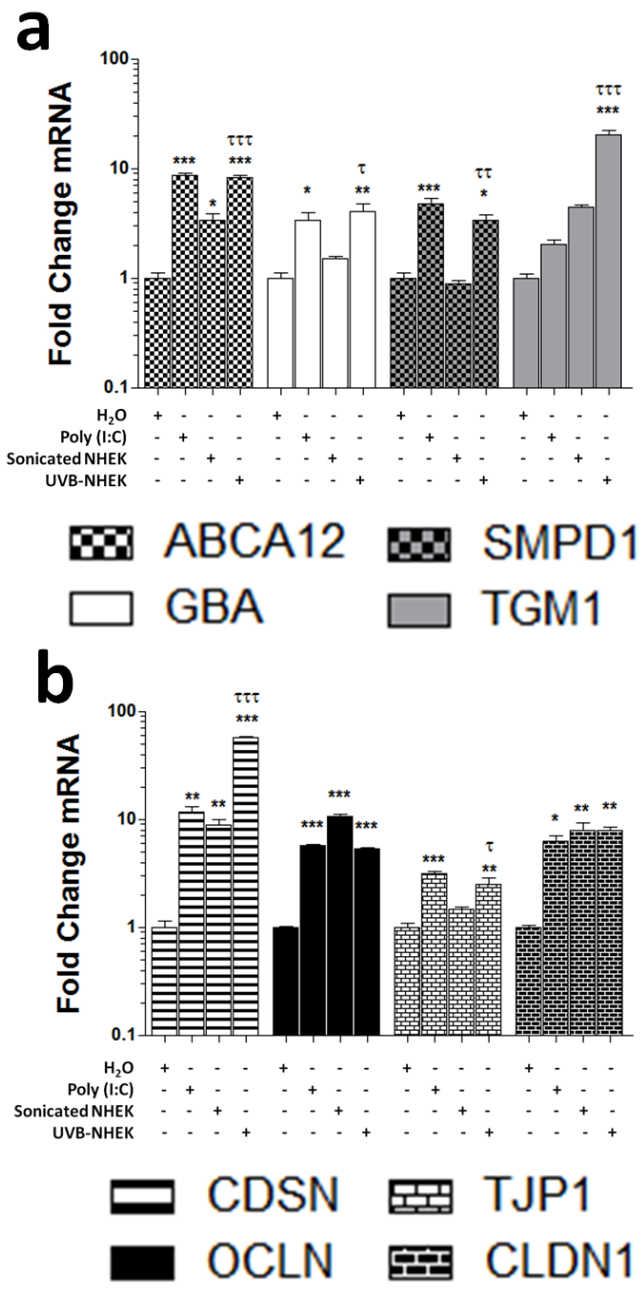

Figure 2.1: UVB-damaged keratinocyte products stimulate genes important for skin barrier. Normal human keratinocytes were treated with either 1 µg/ml Poly (I:C), sonicated keratinocytes, or UVB-treated keratinocytes for 24 hours. Real-time PCR was used to quantify mRNA levels and fold change values are calculated relative and normalized to glyceraldehyde-3-phosphate dehydrogenase (GAPDH) expression for (a) lipid transport (ABCA12), lipid metabolism (GBA and SMPD1), transglutaminase-1 (TGM1) and (b) desmosome (CDSN) and tight junction (OCLN,TJP1, and CLDN1) transcripts. Data are mean +/- SEM, n = 3, and are representative of at least three independent experiments. * = $P < 0.05$, ** = $P < 0.01$, *** = $P < 0.001$ compared to control. τ = $P < 0.05$, τ τ = $P < 0.01$, τ τ τ = $P < 0.001$ comparing sonicated to UVB treated NHEK treatments. One-way ANOVA with Bonferroni post test.

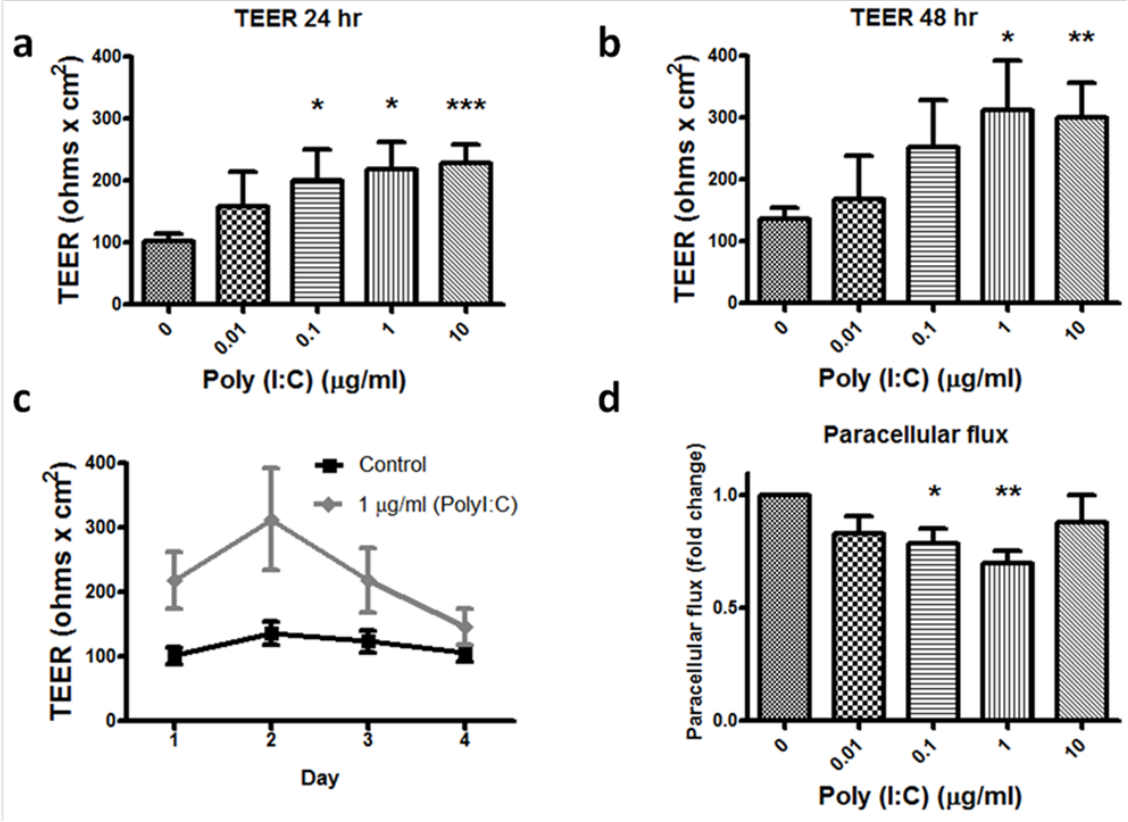

Figure 2.2: Poly (I:C)-treatment increases tight junction function in keratinocyte monolayer. Transepithelial electrical resistance (TEER) was measured in confluent primary human keratinocyte monolayers grown in transwell inserts that were treated with various concentrations of Poly (I:C) for 24 hours (a) and 48 hours (b). (c) Time course data of TEER values. (d) Paracellular flux was measured 30 minutes after addition of fluorescein sodium to NHEK monolayers that were treated with various concentrations of Poly (I:C) for 48 hours. Data are mean +/- SEM, n = 3-8, and are representative of at least three independent experiments. * = $P < 0.05$, ** = $P < 0.01$, *** = $P < 0.001$. One-tailed *t*-test.

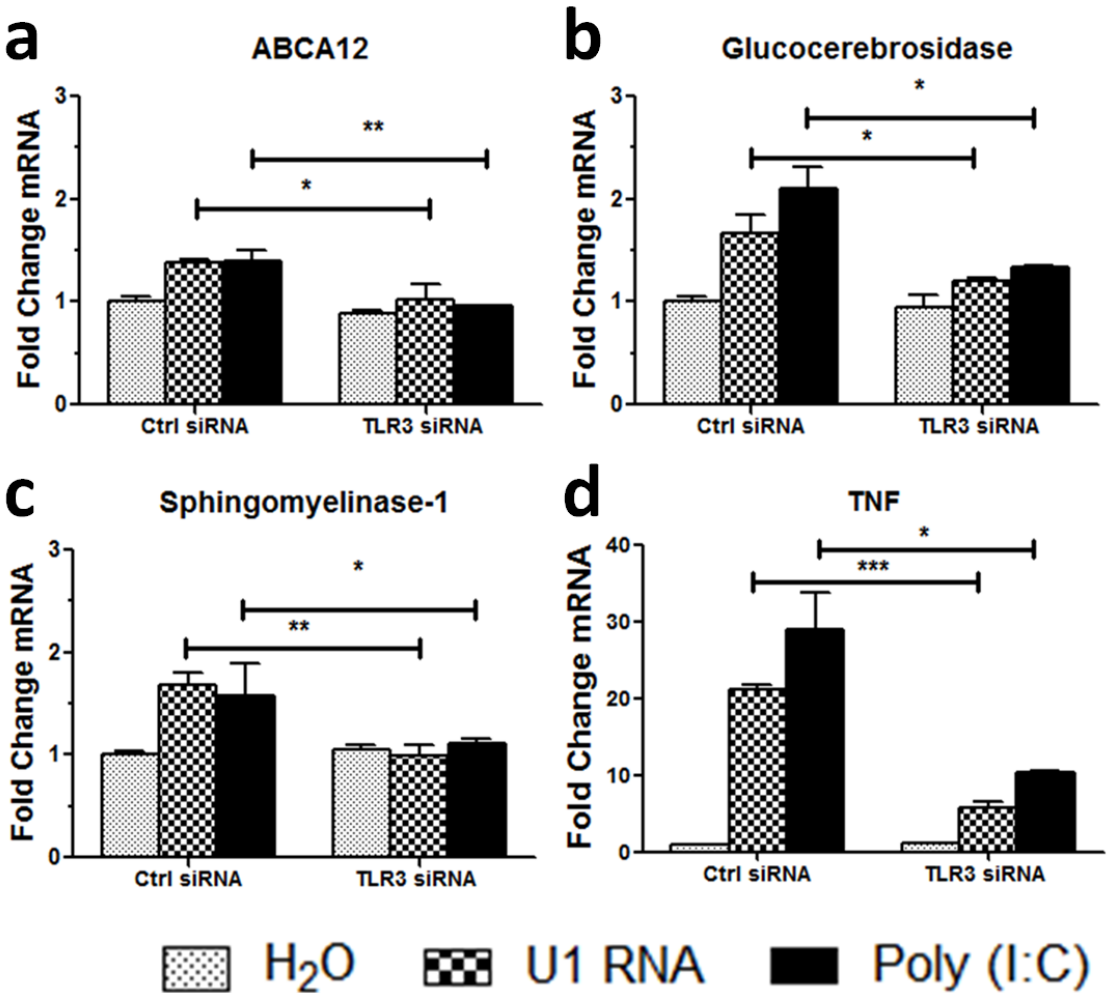

Figure 2.3: U1 RNA stimulates skin barrier genes in a TLR3-dependent manner. TLR3 was silenced in normal human epidermal keratinocytes (NHEKs) for 48 hours before treatment with 1 μg/ml U1 RNA or 1 μg/ml Poly(I:C) for 24 hours. Real-time PCR was used to quantify (a) ABCA12, (b) GBA, (c) SMPD1, and (d) TNF mRNA levels and fold change values are calculated relative to and normalized to glyceraldehyde-3-phosphate dehydrogenase (GAPDH) expression. Data are mean +/- SEM, n = 3, and are representative of at least three independent experiments. * = $P < 0.05$, ** = $P < 0.01$, *** = $P < 0.001$. Two-tailed *t*-test.

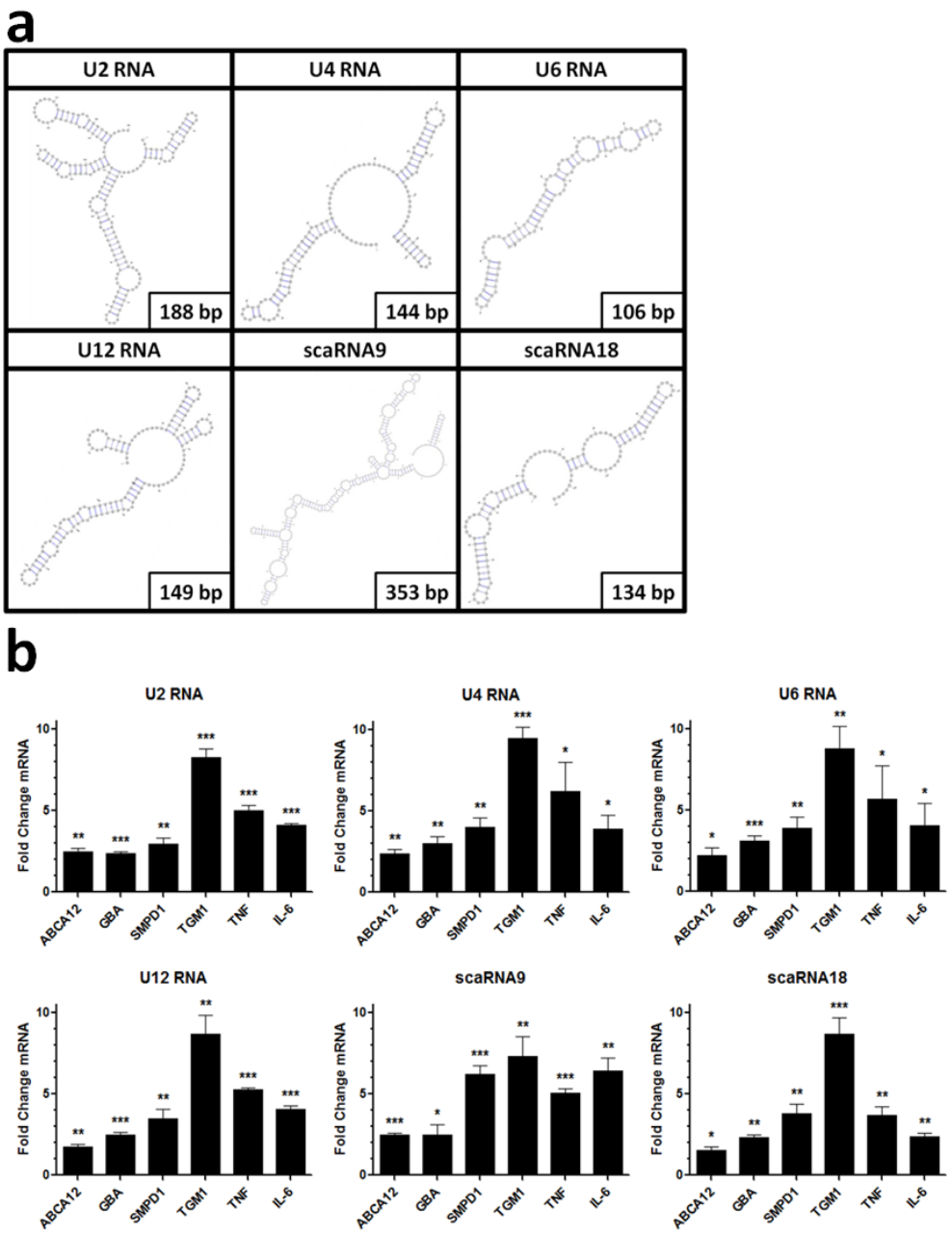

Figure 2.4: small nuclear RNAs stimulate skin barrier genes. (a) Structures of snRNA species generated using RNAfold and VARNA applet. (b) Normal human epidermal keratinocytes were treated with 1 µg/ml *in vitro* transcribed snRNAs for 24 hours in the presence of a transfection reagent. Real-time PCR was used to quantify mRNA levels and fold change values are calculated relative to and normalized to glyceraldehyde-3-phosphate dehydrogenase (GAPDH) expression and then to NHEK that have been treated with a control *in vitro* transcribed RNA. Data are mean +/- SEM, n = 3, and are representative of at least three independent experiments. * = $P < 0.05$, ** = $P < 0.01$, *** = $P < 0.001$. Two-tailed *t*-test.

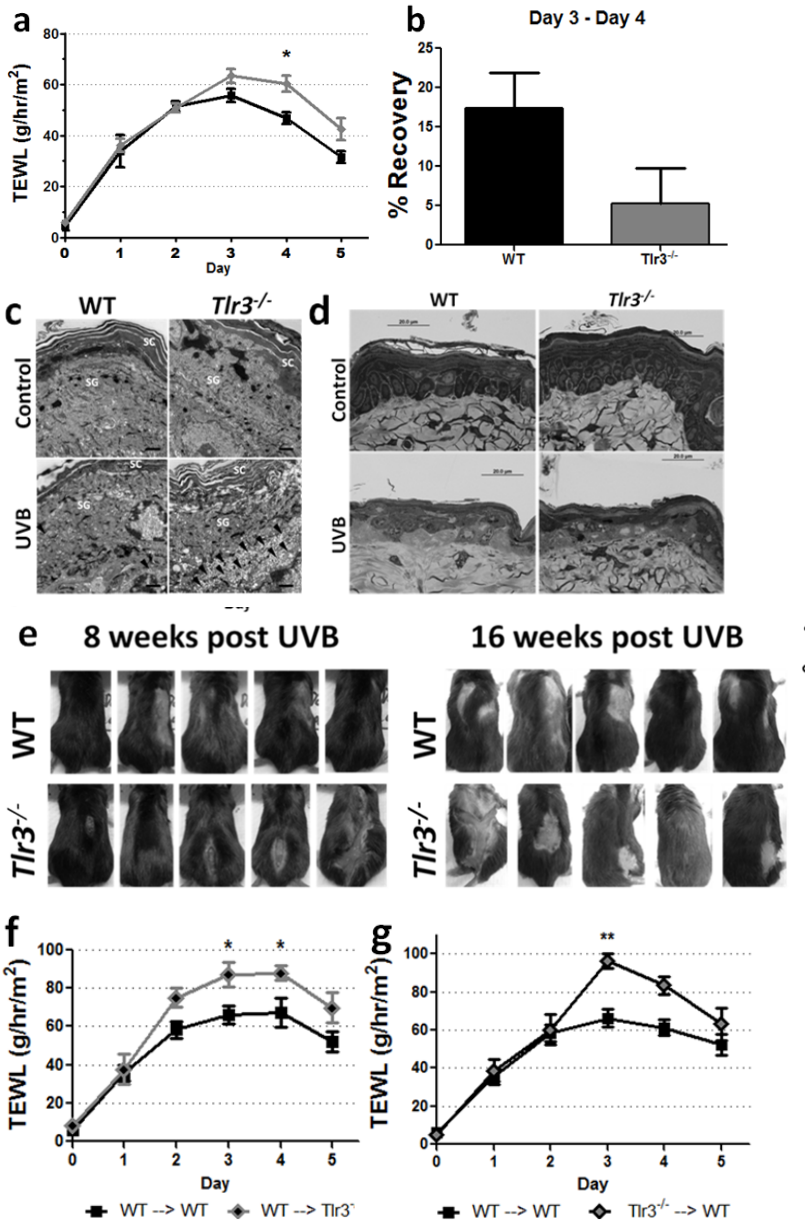

Figure 2.5: *Tlr3*$^{-/-}$ mice exhibit delayed barrier repair following UV-treatment. (a) TEWL values were measured daily for 5 days in WT and *Tlr3*$^{-/-}$ mice exposed to 5 kJ/m^2 UVB. Data are mean +/- SEM, n = 3 WT. n = 5 *Tlr3*$^{-/-}$, and are representative of at least two independent experiments. * = $P < 0.05$, Two-way ANOVA. (b) Barrier recovery between day 3 and 4. One-tailed *t*-test. Skin was harvested from mice 24 hours after treatment with 5 kJ/m^2 UVB. (c) Toluidine blue stained ultrathin sections. Scale bar = 20 µm (d) Transmission electron microscopy images of UVB-treated skin of WT and *Tlr3*$^{-/-}$ mice. Scale bar = 1 µm. (e) Photographs of mice 8 and 16 weeks after 5 kJ/m^2 dose of UVB. Photographs are from two separate experiments. (f+g) Mice were lethally irradiated and subsequently reconstituted with bone marrow 7 weeks prior to UVB irradiation and TEWL measurements. Data are mean +/- SEM, n = 6-8, and are representative of at least two independent experiments. * = $P < 0.05$, ** = $P < 0.01$ Two-way ANOVA.

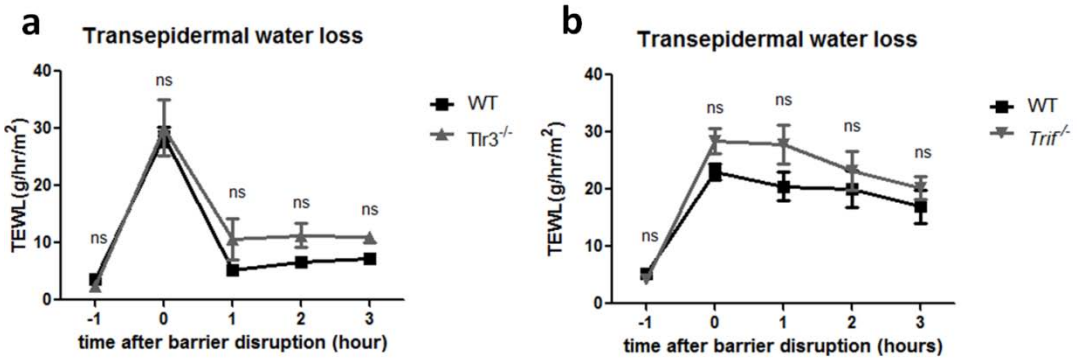

Figure 2.6: *Tlr3*$^{-/-}$ and *Trif*$^{-/-}$ mice show no barrier defect after chemical depilation or tape stripping barrier disruption. TEWL was measured in mice at hourly intervals after barrier disruption using a chemical depilatory reagent (a). n = 3. 2-way ANOVA. TEWL was measured in mice at hourly intervals after barrier disruption by tape stripping (b). n = 6. Two-way ANOVA. Data are mean +/- SEM and are representative of at least three independent experiments. ns = P > 0.05.

Table 2.1: Desmosome and tight junction genes affected by Poly (I:C)-treatment. Data in table represent real-time PCR and microarray fold change data from normal human epidermal keratinocytes (NHEK) treated with 1 µg/ ml Poly (I:C) versus control , water-treated NHEK. * = $P < 0.05$, ** = $P < 0.01$, *** = $P < 0.001$ compared to control. Two-tailed *t*-test. SAM (Significance Analysis of Microarrays) is a statistical technique for finding significant genes in a set of microarray experiments. Significant changes in gene expression were identified using the following filters: 1. False Discovery Rate of 0.01% and 2. Average fold change of ≥ 2.

Gene name	Fold change (real-time PCR)	+/-SD	*t*-test	Fold change (microarray)	SAM
DSG1	4.612094	1.547762	*	0.9260365	-
DSG3	4.777717	0.534666	***	1.0089869	-
CDSN	126.246	10.74039	***	11.963589	+
PKP1	9.261414	0.938554	***	5.4230203	+
DSP	3.214903	0.12011	***	1.4213832	-
JUP	6.283739	0.99608	***	1.9009632	-
DSC1	4.046007	0.414921	**	0.6470588	-
DSC2	2.049086	0.185581	ns	5.139698	+
OCLN	5.675572	0.339136	***	5.7689206	+
TJP1	3.185831	0.237387	***	1.7437945	-
CLDN1	6.255171	1.483514	**	1.5293075	-
CLDN4	9.753152	0.667299	***	11.020382	+
CLDN5	1.125494	0.680026	ns	1.1162791	-
CLDN7	8.111757	1.608655	**	12.165712	+
CLDN11	0.194614	0.027026	**	0.6492942	-
CLDN14	undetectable			71.771586	+
CLDN23	9.001574	2.290738	**	8.4851813	+

Table 2.2: Cytokine levels in mouse skin 24 hours after UVB exposure. Data in table represents presence cytokines/chemokines present in mouse skin 24 hours after exposure to 5 kJ/m^2 UVB. Mean values are pg of analyte/mg of mouse skin. One-Way ANOVA. n = 3-5 mice/group. P values are from One-Way ANOVA in comparison to WT → WT group. Abbreviations: SEM, standard error of the mean; N/A, not applicable. ND, not detectable.

	WT -> WT			WT -> *Tlr3*$^{-/-}$			*Tlr3*$^{-/-}$ -> WT			*Tlr3*$^{-/-}$ -> Tlr3$^{-/-}$		
Cytokine	Mean	SEM	P-value	Mean	SEM	P-value	Mean	SEM	P-value	Mean	SEM	P-value
IL-5	72.08	8.408707	N/A	40.82	9.34030781	> 0.05	25.50	5.757232408	0.006	62.35	11.06	> 0.05
RANTES	6.73	1.782714	N/A	6.46	1.6622434	> 0.05	ND	-	0.014	7.54	0.90	> 0.05
IL-15	278.50	83.72844	N/A	120.48	30.3674194	> 0.05	63.25	10.93201748	0.036	130.23	39.14	> 0.05
GM-CSF	21.30	3.415604	N/A	16.74	1.82875641	> 0.05	11.25	1.117579695	0.039	20.09	3.05	> 0.05
G-CSF	135.15	68.55	N/A	46.60	16.09	> 0.05	129.47	56.93	> 0.05	22.16	7.75	> 0.05
IFN-gamma	2.04	1.283029	N/A	3.71	0.9680328	> 0.05	2.04	1.283028643	> 0.05	6.18	0.77	> 0.05
IL-1a	615.10	209.1771	N/A	459.99	35.5081933	> 0.05	400.23	99.95082342	> 0.05	519.37	29.16	> 0.05
IL-1b	153.55	59.82371	N/A	247.61	42.5125448	> 0.05	222.95	95.60430606	> 0.05	439.99	26.89	> 0.05
IL-2	ND	-	N/A	ND	-	> 0.05	ND	-	> 0.05	ND	-	> 0.05
IL-4	ND	-	N/A	ND	-	> 0.05	ND	-	> 0.05	ND	-	> 0.05
IL-6	149.85	37.15638	N/A	78.78	18.3660223	> 0.05	67.17	15.81535863	> 0.05	68.28	8.68	> 0.05
IL-7	ND	-	N/A	ND	-	> 0.05	1.16	1.155	> 0.05	2.34	2.34	> 0.05
IL-9	453.23	11.01505	N/A	470.46	23.5753537	> 0.05	448.80	21.0788447	> 0.05	442.86	22.47	> 0.05
IL-10	14.59	3.956146	N/A	12.49	6.31328163	> 0.05	8.55	5.064819839	> 0.05	11.71	1.11	> 0.05
IL-12(p40)	19.07	4.014722	N/A	21.42	5.54364698	> 0.05	14.84	6.191444955	> 0.05	30.18	7.63	> 0.05
IL-12(p70)	0.95	0.95	N/A	ND	-	> 0.05	ND	-	> 0.05	ND	-	> 0.05
IL-13	ND	-	N/A	ND	-	> 0.05	ND	-	> 0.05	ND	-	> 0.05
IL-17	ND	-	N/A	ND	-	> 0.05	ND	-	> 0.05	ND	-	> 0.05
IP-10	317.53	65.20764	N/A	354.87	73.5810227	> 0.05	191.12	78.09087969	> 0.05	463.12	110.37	> 0.05
KC	317.53	65.20764	N/A	354.87	73.5810227	> 0.05	191.12	78.09087969	> 0.05	463.12	110.37	> 0.05
MCP-1	254.87	16.79207	N/A	202.96	45.181638	> 0.05	120.94	41.32464428	> 0.05	208.80	23.98	> 0.05
MIP-1a	92.91	45.62654	N/A	59.36	15.5208306	> 0.05	44.27	14.92826158	> 0.05	87.52	23.94	> 0.05
MIP-1b	81.69	33.94318	N/A	46.46	16.0218833	> 0.05	26.65	11.07750282	> 0.05	69.35	36.84	> 0.05
MIP-2	850.93	728.6568	N/A	171.57	73.7736632	> 0.05	267.11	168.6153988	> 0.05	172.70	58.77	> 0.05
TNFa	4.56	1.971684	N/A	1.17	1.165	> 0.05	1.17	1.165	> 0.05	5.83	-	> 0.05

References

[1] R. Lucas, T. McMichael, W. Smith, and B. Armstrong, “Solar ultraviolet radiation: global burden of disease from solar ultraviolet radiation,” in *Environmental Burden of Disease Series, No. 13*, no. 13, A. Prüss-Üstün, H. Zeeb, C. Mathers, and M. Repacholi, Eds. Geneva: WHO Document Production Services, 2006, p. 87 pp.

[2] G. K. Menon, P. M. Elias, S. H. Lee, and K. R. Feingold, “Localization of calcium in murine epidermis following disruption and repair of the permeability barrier,” *Cell Tissue Res.*, vol. 270, no. 3, pp. 503–512, Dec. 1992.

[3] S. H. Lee, P. M. Elias, E. Proksch, G. K. Menon, M. Mao-Quiang, and K. R. Feingold, “Calcium and potassium are important regulators of barrier homeostasis in murine epidermis.,” *J. Clin. Invest.*, vol. 89, no. 2, pp. 530–8, Feb. 1992.

[4] A. Haratake, Y. Uchida, and M. Schmuth, “UVB-induced alterations in permeability barrier function: roles for epidermal hyperproliferation and thymocyte-mediated response,” *J. Invest. Dermatol.*, vol. 108, no. 5, pp. 769–775, 1997.

[5] W. M. Holleran, Y. Uchida, L. Halkier-Sorensen, a Haratake, M. Hara, J. H. Epstein, and P. M. Elias, “Structural and biochemical basis for the UVB-induced alterations in epidermal barrier function.,” *Photodermatol. Photoimmunol. Photomed.*, vol. 13, no. 4, pp. 117–28, Aug. 1997.

[6] S. P. Hong, M. J. Kim, M.-Y. Jung, H. Jeon, J. Goo, S. K. Ahn, S. H. Lee, P. M. Elias, and E. H. Choi, “Biopositive effects of low-dose UVB on epidermis: coordinate upregulation of antimicrobial peptides and permeability barrier reinforcement.,” *J. Invest. Dermatol.*, vol. 128, no. 12, pp. 2880–7, Dec. 2008.

[7] J. J. Bernard, C. Cowing-Zitron, T. Nakatsuji, B. Muehleisen, J. Muto, A. W. Borkowski, L. Martinez, E. L. Greidinger, B. D. Yu, and R. L. Gallo, “Ultraviolet radiation damages self noncoding RNA and is detected by TLR3.,” *Nat. Med.*, vol. 18, no. 8, pp. 1286–90, Aug. 2012.

[8] K. Karikó, H. Ni, J. Capodici, M. Lamphier, and D. Weissman, “mRNA is an endogenous ligand for Toll-like receptor 3.,” *J. Biol. Chem.*, vol. 279, no. 13, pp. 12542–50, Mar. 2004.

[9] K. A. Cavassani, M. Ishii, H. Wen, M. A. Schaller, P. M. Lincoln, N. W. Lukacs, C. M. Hogaboam, and S. L. Kunkel, “TLR3 is an endogenous sensor of tissue necrosis during acute inflammatory events.,” *J. Exp. Med.*, vol. 205, no. 11, pp. 2609–21, Oct. 2008.

[10] Y. Lai, A. Di Nardo, T. Nakatsuji, A. Leichtle, Y. Yang, A. L. Cogen, Z.-R. Wu, L. V Hooper, R. R. Schmidt, S. von Aulock, K. a Radek, C.-M. Huang, A. F. Ryan, and R. L. Gallo, “Commensal bacteria regulate Toll-like receptor 3-dependent inflammation after skin injury.,” *Nat. Med.*, vol. 15, no. 12, pp. 1377–82, Dec. 2009.

[11] Q. Lin, D. Fang, J. Fang, X. Ren, X. Yang, F. Wen, and S. B. Su, “Impaired wound healing with defective expression of chemokines and recruitment of myeloid cells in TLR3-deficient mice.,” *J. Immunol.*, vol. 186, no. 6, pp. 3710–7, Mar. 2011.

[12] Q. Lin, L. Wang, Y. Lin, X. Liu, X. Ren, S. Wen, X. Du, T. Lu, S. Y. Su, X. Yang, W. Huang, S. Zhou, F. Wen, and S. B. Su, “Toll-like receptor 3 ligand polyinosinic:polycytidylic acid promotes wound healing in human and murine skin.,” *J. Invest. Dermatol.*, vol. 132, no. 8, pp. 2085–92, Aug. 2012.

[13] T. Kawai and S. Akira, “Toll-like receptor and RIG-I-like receptor signaling.,” *Ann. N. Y. Acad. Sci.*, vol. 1143, pp. 1–20, Nov. 2008.

[14] F. Dunlevy, N. McElvaney, and C. Greene, “TLR3 Sensing of Viral Infection,” *Open Infect. Dis. J.*, vol. 4, pp. 1–10, 2010.

[15] A. W. Borkowski, K. Park, Y. Uchida, and R. L. Gallo, “Activation of TLR3 in keratinocytes increases expression of genes involved in formation of the epidermis, lipid accumulation, and epidermal organelles.,” *J. Invest. Dermatol.*, vol. 133, no. 8, pp. 2031–40, Aug. 2013.

[16] D. W. Huang, B. T. Sherman, and R. A. Lempicki, “Bioinformatics enrichment tools: paths toward the comprehensive functional analysis of large gene lists.,” *Nucleic Acids Res.*, vol. 37, no. 1, pp. 1–13, Jan. 2009.

[17] D. W. Huang, B. T. Sherman, and R. A. Lempicki, “Systematic and integrative analysis of large gene lists using DAVID bioinformatics resources.,” *Nat. Protoc.*, vol. 4, no. 1, pp. 44–57, Jan. 2009.

[18] I.-H. Kuo, A. Carpenter-Mendini, T. Yoshida, L. Y. McGirt, A. I. Ivanov, K. C. Barnes, R. L. Gallo, A. W. Borkowski, K. Yamasaki, D. Y. Leung, S. N. Georas, A. De Benedetto, and L. a Beck, “Activation of epidermal toll-like receptor 2 enhances tight junction function: implications for atopic dermatitis and skin barrier repair.,” *J. Invest. Dermatol.*, vol. 133, no. 4, pp. 988–98, Apr. 2013.

[19] A. De Benedetto, N. M. Rafaels, L. Y. McGirt, A. I. Ivanov, S. N. Georas, C. Cheadle, A. E. Berger, K. Zhang, S. Vidyasagar, T. Yoshida, M. Boguniewicz, T. Hata, L. C. Schneider, J. M. Hanifin, R. L. Gallo, N. Novak, S. Weidinger, T. H. Beaty, D. Y. M. Leung, K. C. Barnes, and L. a Beck, “Tight junction defects in patients with atopic dermatitis.,” *J. Allergy Clin. Immunol.*, vol. 127, no. 3, pp. 773–86.e1–7, Mar. 2011.

[20] A. R. Gruber, R. Lorenz, S. H. Bernhart, R. Neuböck, and I. L. Hofacker, “The Vienna RNA websuite.,” *Nucleic Acids Res.*, vol. 36, no. Web Server issue, pp. W70–4, Jul. 2008.

[21] G. Blin, A. Denise, S. Dulucq, C. Herrbach, and H. Touzet, “Alignments of RNA structures.,” *IEEE/ACM Trans. Comput. Biol. Bioinform.*, vol. 7, no. 2, pp. 309–22, 2009.

[22] E. a Leclerc, A. Huchenq, N. R. Mattiuzzo, D. Metzger, P. Chambon, N. B. Ghyselinck, G. Serre, N. Jonca, and M. Guerrin, “Corneodesmosin gene ablation induces lethal skin-

barrier disruption and hair-follicle degeneration related to desmosome dysfunction.," *J. Cell Sci.*, vol. 122, no. Pt 15, pp. 2699–709, Aug. 2009.

[23] M. Furuse, M. Hata, K. Furuse, Y. Yoshida, A. Haratake, Y. Sugitani, T. Noda, A. Kubo, and S. Tsukita, "Claudin-based tight junctions are crucial for the mammalian epidermal barrier: a lesson from claudin-1-deficient mice.," *J. Cell Biol.*, vol. 156, no. 6, pp. 1099–111, Mar. 2002.

[24] Y. Uchida, E. Houben, K. Park, S. Douangpanya, Y.-M. Lee, B. X. Wu, Y. a Hannun, N. S. Radin, P. M. Elias, and W. M. Holleran, "Hydrolytic pathway protects against ceramide-induced apoptosis in keratinocytes exposed to UVB.," *J. Invest. Dermatol.*, vol. 130, no. 10, pp. 2472–80, Oct. 2010.

[25] A. Kaczmarek, P. Vandenabeele, and D. V Krysko, "Necroptosis: the release of damage-associated molecular patterns and its physiological relevance.," *Immunity*, vol. 38, no. 2, pp. 209–23, Feb. 2013.

[26] K. Karikó, P. Bhuyan, J. Capodici, H. Ni, J. Lubinski, H. Friedman, and D. Weissman, "Exogenous siRNA mediates sequence-independent gene suppression by signaling through toll-like receptor 3.," *Cells. Tissues. Organs*, vol. 177, no. 3, pp. 132–8, Jan. 2004.

[27] N. Kirschner and J. M. Brandner, "Barriers and more: functions of tight junction proteins in the skin.," *Ann. N. Y. Acad. Sci.*, vol. 1257, pp. 158–66, Jun. 2012.

[28] J. E. Lai-Cheong, K. Arita, and J. a McGrath, "Genetic diseases of junctions.," *J. Invest. Dermatol.*, vol. 127, no. 12, pp. 2713–25, Dec. 2007.

[29] D. L. Rosin and M. D. Okusa, "Dangers within: DAMP responses to damage and cell death in kidney disease.," *J. Am. Soc. Nephrol.*, vol. 22, no. 3, pp. 416–25, Mar. 2011.

CHAPTER 3:

Scavenger receptor ligands stimulate expression of skin barrier repair genes

Abstract

Infection or injury to the epidermis can cause cell lysis or necrosis, both of which release either exogenous viral and/or endogenous host RNA. This RNA serves as a danger signal and is taken up by keratinocytes initiating an immune or barrier repair response. How this RNA is taken up from the extracellular environment by keratinocytes is an unknown process. Recent publications have demonstrated that scavenger receptors can facilitate entry of Poly (I:C) into airway epithelial cells. For this reason we hypothesized that scavenger receptors on keratinocytes allowed uptake of dsRNA into keratinocytes in order to mount proper immune and barrier repair responses. We observe that scavenger receptor ligands block Poly (I:C) induced inflammatory responses in keratinocytes but surprisingly, in addition to Poly (I:C), can stimulate increases in ABCA12, GBA, and SMPD1 mRNA. Additionally knockdown of CD36, MARCO, or OLR1 had no effect on Poly (I:C)-induced gene expression. *Msr1*$^{-/-}$ mice do however display a skin barrier repair defect in response to tape-stripping. These findings demonstrate an important role for scavenger receptors in skin barrier repair.

Introduction

Toll-like receptor 3 (TLR3) activation occurs when double-stranded RNA (dsRNA) binds endosomally localized TLR3 leading to activation of IRF3 and NF-κB signaling resulting in Type 1 interferon and inflammatory cytokine expression [1]–[3]. TLR3 can recognize both exogenous viral sources of dsRNA [4] as well as endogenous dsRNA resulting from mechanical or UVB damage [5]–[8]. While these processes have been well described in numerous cell types, the mechanisms that traffic dsRNA to the endosome, however, have been incompletely defined. Additionally, recent studies have shown that TLR3 activation in keratinocytes induce a program of skin barrier repair characterized by increases in skin barrier repair genes, lipid accumulation and increases in lamellar bodies and organelles [9]. In this study we aimed to characterize the role of scavenger receptors in Poly (I:C)-induced gene expression of skin barrier repair genes in keratinocytes and how barrier repair is affected by mice lacking macrophage scavenger receptor 1 (*Msr1*).

In recent years, a number of studies have shown that scavenger receptors play a role in the uptake of dsRNA from the extracellular environment. Scavenger receptors are a heterogeneous group of cell surface molecules that can bind numerous exogenous and endogenous ligands [10]. While these receptors were initially characterized by their ability to bind modified low density lipoproteins (LDLs) [11] and were observed to contribute to atherosclerosis [12]–[15], they have more recently been shown to have a broad range of functions including ability to recognize microbe associated molecular patterns (MAMPs) to help in pathogen clearance [16], [17], recognize danger associated molecular patterns to help clear apoptotic cells (DAMPs) [18], [19], function in lipid transport [20], [21], and function as chaperones for cellular transport [22]. In keratinocytes, scavenger receptors have only briefly been described. Scavenger receptor class B type I (SR-BI) has been shown to be important for cholesterol homeostasis in keratinocytes [23]. As cholesterol in an important component of the

skin barrier [24], [25], SR-B1 might also be important for skin barrier homeostasis. Also more recently, it was observed that a scavenger receptor known as macrophage receptor with collagenous structure (MARCO) is an important mediator of herpes simplex virus 1 infection of keratinocytes [26].

The epidermis is the site of constant assault from the environment and epidermal keratinocytes are in constant danger of infection and injury. Viral infection can result in cell lysis and viral dsRNA can spill into the extracellular milieu [27]. Necrotic cell death following infection and injury can also cause extracellular release of host dsRNA [28], [29]. While it has been demonstrated that dsRNA is released from necrotic keratinocytes [5], no current research describes the uptake of extracellular dsRNA into keratinocytes. The Macrophage scavenger receptor 1 (MSR1) [30], oxidized low-density lipoprotein receptor 1 (OLR1) [31], and SR-B1 [31] have been observed to bind Poly (I:C), a synthetic dsRNA and facilitate its uptake into bronchial epithelial cells [30], [31]. Herein we demonstrated that scavenger receptor ligands unexpectedly induce skin barrier repair gene expression while blocking Poly (I:C)-induced inflammatory gene expression. We also observe that knockdown of either CD36, MARCO or OLR1 is not sufficient to block Poly (I:C)-induced changes in gene expression. Finally we show that mice deficient in *Msr1* have a skin barrier repair defect. These data demonstrate that scavenger receptors likely play an important role in skin barrier repair.

Methods

Cell Culture and Stimuli. NHEK were obtained from Cascade Biologics/Invitrogen. (catalog number: C-001-5C, Portland, OR), and grown in serum-free EpiLife cell culture media (Cascade Biologics/Invitrogen) containing 0.06 mM Ca^{2+} and 1 × EpiLife Defined Growth Supplement (EDGS, Cascade Biologics/Invitrogen) at 37 °C under standard tissue culture conditions. All cultures were maintained for up to eight passages in this media with the addition

of 100 U ml^{-1} penicillin, 100 μg ml^{-1} streptomycin, and 250 ng ml^{-1} amphotericin B. Cells at 60-80% confluence were treated with Poly (I:C) (Invivogen, San Diego, CA), dextran sulfate (Sigma-Aldrich, St. Louis, MO), fucoidan(Sigma-Aldrich, St. Louis, MO), oxidized LDL (Biomedical Technologies Inc, Stoughton, MA) and acetylated LDL (Biomedical Technologies Inc, Stoughton, MA) in 12-well flat bottom plates (Corning Incorporated Life Sciences, Lowell, MA) for up to 24 hours. After cell stimulation, RNA was extracted using TRIzol reagent (Invitrogen, Carlsbad, CA). RNA was stored at −80°C.

Quantitative real-time PCR. Total RNA was extracted from cultured keratinocytes using TRIzol® Reagent (Invitrogen, Carlsbad, CA) and 1 ug RNA was reverse-transcribed using iScript™ cDNA Synthesis Kit (Bio-Rad, Hercules, CA). Pre-developed Taqman® Gene Expression Assays (Applied Biosystems, Foster City, CA) were used to evaluate mRNA transcript levels of ABCA12, GBA, SMPD1, TNF, TLR3, CD36, MARCO and OLR1. GAPDH mRNA transcript levels were evaluated using a VIC-CATCCATGACAACTTTGGTA-MGB probe with primers 5' CTTAGCACCCCTGGCCAAG-3' and 5'-TGGTCATGAGTCCTTCCACG-3'. All analyses were performed in triplicate and representative of three to five independent cell stimulation experiments that were analyzed in an ABI Prism 7000 Sequence Detection System. Fold induction relative to GAPDH was calculated using the $\Delta\Delta C_t$ method. Results were considered to be significant if $P < 0.05$.

siRNA knockdown. TLR3, CD36, MARCO, OLR1 and control siRNA were purchased from Dharmacon (Chicago, IL). One nanomole of each siRNA was electroporated into 3 x 10^6 keratinocytes using Amaxa nucleofection reagents (VPD-1002) (Lonza AG, Walkersville, MD). Cells were plated after transfection. 24 hours later cells were split into 24-well plates. 48 hours

after transfection, cells were treated with Poly (I:C) for 24 hours longer. RNA was then isolated and mRNA measured as previously mentioned.

Transepidermal Water Loss. Transepidermal water loss (TEWL) was measured using a TEWAMETER TM300 (C & K, Cologne, Germany). TEWL was measured prior to, immediately after and at 1, 2, and 3 hours after tape stripping barrier disruption. Tape stripping was done 3-5 times per mouse in order to see a disruption yielding a TEWL value between 20-30 $g/hr/m^2$.

Results

Scavenger receptor ligands stimulate skin barrier repair genes, while blocking Poly (I:C)-induced inflammatory gene expression. As Poly (I:C) has been shown to be taken up from the extracellular environment of airway epithelial cells by a scavenger receptor dependent mechanism [30], [31], we wanted to test whether this process was involved in Poly (I:C)-induced skin barrier repair gene expression in keratinocytes. Dextran sulfate (DS), a sulfated polysaccharide which has been shown to be a competitive inhibitor of scavenger receptors binding to LDL [32], was added to the media of normal human epidermal keratinocytes (NHEK) 30 minutes prior to addition of Poly (I:C). 24 hours after addition of Poly (I:C), total RNA was harvested and mRNA abundance of ABCA12, GBA, TLR3 and TNF was measured. Addition of DS to NHEK did not block expression of ABCA 12, GBA, or TLR3 (Figure 3.1a). Addition of DS did however inhibit increases in TNF mRNA (Figure 3.1a). Interestingly, addition of DS alone, induced dose dependent increases in ABCA12, GBA, and TLR3 while TNF mRNA levels were unaffected (Figure 3.1a). Fucoidan (Fuc), another sulfated polysaccharide and inhibitor of Poly (I:C) induced scavenger receptor dependent uptake also caused increases in ABCA12, GBA and TLR3 mRNA while TNF levels were unaffected (Figure 3.1b). Fuc treatment blocked Poly

(I:C) induced increases of TNF and TLR3 mRNA levels in a dose dependent manner though had no effect on Poly (I:C) induced increases in ABCA12 or GBA mRNA (Figure 3.1b).

Modified forms of low-density lipoprotein (LDL) are endogenous ligands that can be recognized and taken up into cells by scavenger receptors [10]. To determine if these modified LDLs act similarly to other scavenger receptor ligands, we pretreated NHEK with oxidized LDL (OxLDL) or acetylated LDL (AcLDL) for 30 minutes prior to treatment with Poly (I:C). OxLDL and AcLDL induced dose dependent increases in mRNA for ABCA12 and GBA though did not have significant effects on mRNA for TNF or TLR3 (Figure 3.1c). OxLDL and AcLDL blocked Poly (I:C)-induced increases in TLR3 and TNF mRNA though did not block Poly (I:C)-induced increases in ABCA12 or GBA (Figure 3.1c).

CD36, MARCO, or OLR1 is not required for dsRNA-induced changes in gene expression. CD36, MARCO, and OLR1 are scavenger receptors known to be involved in binding and cellular uptake of modified LDLs [33]–[36] and we hypothesized could be involved in Poly (I:C) uptake into keratinocytes. To determine whether specific scavenger receptors were important for Poly (I:C) uptake and subsequent induced gene expression changes, we used siRNA to knock down mRNA CD36, MARCO or OLR1 prior to Poly (I:C) treatment. There was no significant effects on Poly (I:C)-induced gene expression of ABCA12, GBA, SMPD1, or TNF when either CD36, MARCO, or OLR1 was knocked down (Figure 3.2a). In this experiment, siRNA knockdown of TLR3 (63.8%), CD36 (83.3%), MARCO (64.2%) and OLR1 (82.9%) were all significant (Figure 3.2b). Poly (I:C) caused increases in OLR1 and TLR3 mRNA and decreased CD36 mRNA except for when CD36 was silenced (Figure 3.2c). There was no observed effects of Poly (I:C) on MARCO mRNA levels (Figure 3.2c).

***Msr1*$^{-/-}$ mice display a barrier repair defect after tape stripping.** Because scavenger receptor ligands induce expression of skin barrier repair genes, we wanted to determine whether mice that are deficient in the scavenger receptor *Msr1*, exhibited proper skin barrier repair. WT and *Msr1*$^{-/-}$ were shaven and chemically depilated 96 hours before being tape-stripped to create a barrier disruption. Transepidermal water loss (TEWL) measurements were taken at hourly intervals to assess barrier integrity before and after tape-stripping. *Msr1*$^{-/-}$ mice displayed significantly higher TEWL levels than WT mice at 2 and 3 hours after initial tape-stripping skin barrier disruption (Figure 3.3).

Discussion

Recent findings that TLR3 activation can stimulate a skin barrier repair program in keratinocytes [9] lead to the question of what other cellular mechanisms might play a role in recognizing dsRNA in an extracellular environment and how this dsRNA is trafficked to the endosome. Because it was previously shown that multiple scavenger receptor ligands could block uptake of Poly (I:C) and the resulting inflammatory response [10], [30], [37] and that antibodies specific for MSR1 could also block Poly (I:C)-induced cellular responses [30], we wanted to determine whether scavenger receptor uptake of Poly (I:C) was necessary for Poly (I:C)-induced barrier repair processes in keratinocytes. Herein we show that numerous scavenger receptor ligands including DS, Fuc, as well as the modified LDLs, OxLDL and AcLDL, can stimulate numerous genes involved in skin barrier repair including ABCA12, GBA, and SMPD1. Also very interestingly, these scavenger receptor ligands can block Poly (I:C)-induced increases in TNF and TLR3 mRNA although TLR3 mRNA levels were mildly but significantly increased by treatment with DS and Fuc. This leads us to the belief that some signaling pathways either upstream or independent of TLR3 activation will likely lead to increases in skin barrier repair. It

seems that scavenger receptor ligands block inflammatory signaling while stimulating barrier repair gene expression.

Scavenger receptors have been shown to have numerous types of self ligands including lipoproteins, native proteins, modified proteins, lipids and dead cells or debris as well as microbial ligands such as bacteria, viruses, and fungi [10]. Downstream signaling of scavenger receptors has remained enigmatic, as most lack any identifiable signaling domains in their short cytoplasmic segments[10], though SRC family kinases have been shown to associate with CD36 [10]. It is likely that scavenger receptors form complexes with other signaling molecules and although remain a necessary component of signaling are not sufficient on their own. Future studies should focus on finding which proteins make up these putative signaling complexes.

In order to assess the importance of specific scavenger receptors, we tested whether knockdown of these receptors with siRNA could block Poly (I:C)-induced increases in barrier repair genes. Silencing of CD36, MARCO, or OLR1, all which are expressed on human keratinocytes [26], [38]–[40], had no significant effect on Poly (I:C)-induced increases in ABCA12, GBA, SMPD1, or TNF mRNA. While we still believe that scavenger receptor binding of dsRNA is important for cellular uptake and induction of skin barrier repair genes, it is likely that these specific receptors may be functionally redundant and only by knocking down all surface expression of scavenger receptors will lead to decreases in Poly (I:C)-induced expression of skin barrier repair gene mRNA.

Finally we wanted to determine whether mice deficient in scavenger receptors had any deficit in skin barrier repair. Herein we demonstrate that *Msr1*$^{-/-}$ mice have a clear deficiency in barrier repair, as they exhibit significantly higher transepidermal water loss than WT mice at 2 and 3 hours after tape-stripping barrier disruption. While this result was a bit surprising as knockdown of single scavenger receptors *in vitro* had no effect on Poly (I:C)-induced gene expression, it is possible that different scavenger receptors contribute differently to skin barrier

repair in different species. It remains to be determined which scavenger receptors in humans are essential for dsRNA uptake and skin barrier repair.

The field of keratinocyte scavenger receptor function is underexplored and much research remains to be performed in order to assess the importance of scavenger receptors in keratinocyte homeostasis and skin barrier repair. A majority of the research on scavenger receptors has been done in macrophages and it remains to be seen whether similar signaling pathways are activated in keratinocytes following ligand binding. Some scavenger receptors such as CD36 are only expressed on human keratinocytes during in psoriasis or other dysbiotic conditions suggesting a role for CD36 in maintaining keratinocyte homeostasis [38], [39]. The opposite result however is observed in response to treatment with Poly (I:C), as CD36 levels dropped and no significant changes in MARCO mRNA were observed. OLR1 mRNA was the only scavenger receptor that we measured that showed significant increases after Poly (I:C) treatment. Future studies should focus on the role of OLR1 in skin barrier repair its possible role in immunity.

Acknowledgments

This work was supported by US National Institutes of Health (NIH) grants R01-AR052728, NIH R01-AI052453 and R01 AI0833358 to R.L.G., the UCSD Training in Immunology Grant 5T32AI060536-05 and UCSD Dermatologist Investigator Training Program Grant 1T32AR062496-01 supporting A.W.B.

Chapter 3, in full, is unpublished data. A. W. Borkowski, R. L. Gallo. The dissertation author was the primary investigator and author of this material.

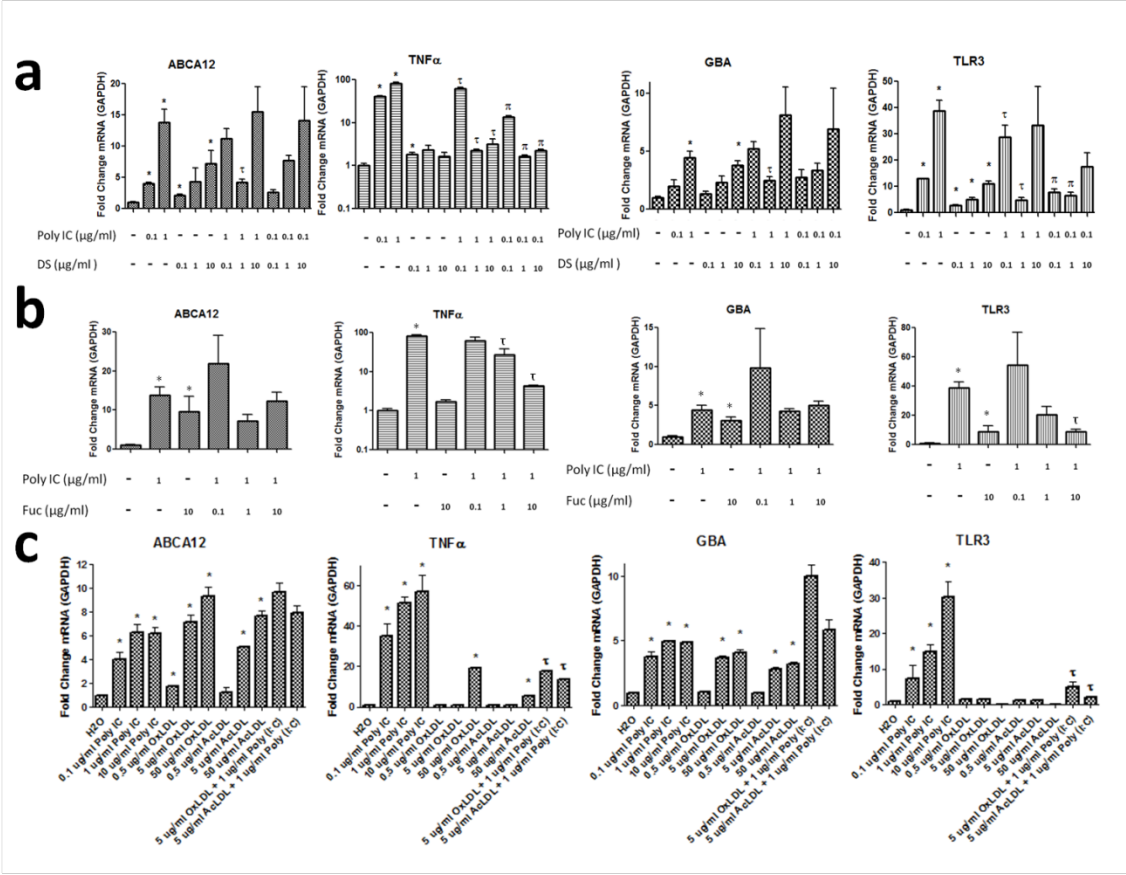

Figure 3.1: Scavenger receptor ligands stimulate skin barrier repair genes, while blocking Poly (I:C)-induced inflammatory gene expression. NHEK were cultured in the presence of either 0, 0.1, 1, or 10 μg/ml DS for 30 minutes before addition of either 0, 0.1 or 1 μg/ml Poly (I:C) for 24 h. Real-time PCR was used to quantify mRNA levels and fold change values are calculated relative and normalized to GAPDH (a). NHEK were cultured in the presence of either 0, 0.1, 1, or 10 μg/ml Fuc for 30 minutes before addition of either 0 or 1 μg/ml Poly (I:C) for 24 h. Real-time PCR was used to quantify mRNA levels and fold change values are calculated relative and normalized to GAPDH (b). NHEK were cultured in the presence of either 0, 0.1, 1, or 10 μg/ml OxLDL or AcLDL for 30 minutes before addition of either 0, 0.1 or 1 μg/ml Poly (I:C) for 24 h. Real-time PCR was used to quantify mRNA levels and fold change values are calculated relative and normalized to GAPDH (c). Data are mean ± SEM, n = 3, and are representative of at least three independent experiments. * = $P < 0.05$ compared to water control. τ = $P < 0.05$ compared to 1 μg/ml Poly (I:C). π = $P < 0.05$ compared to 1 μg/ml Poly (I:C). Two-tailed student's T-test.

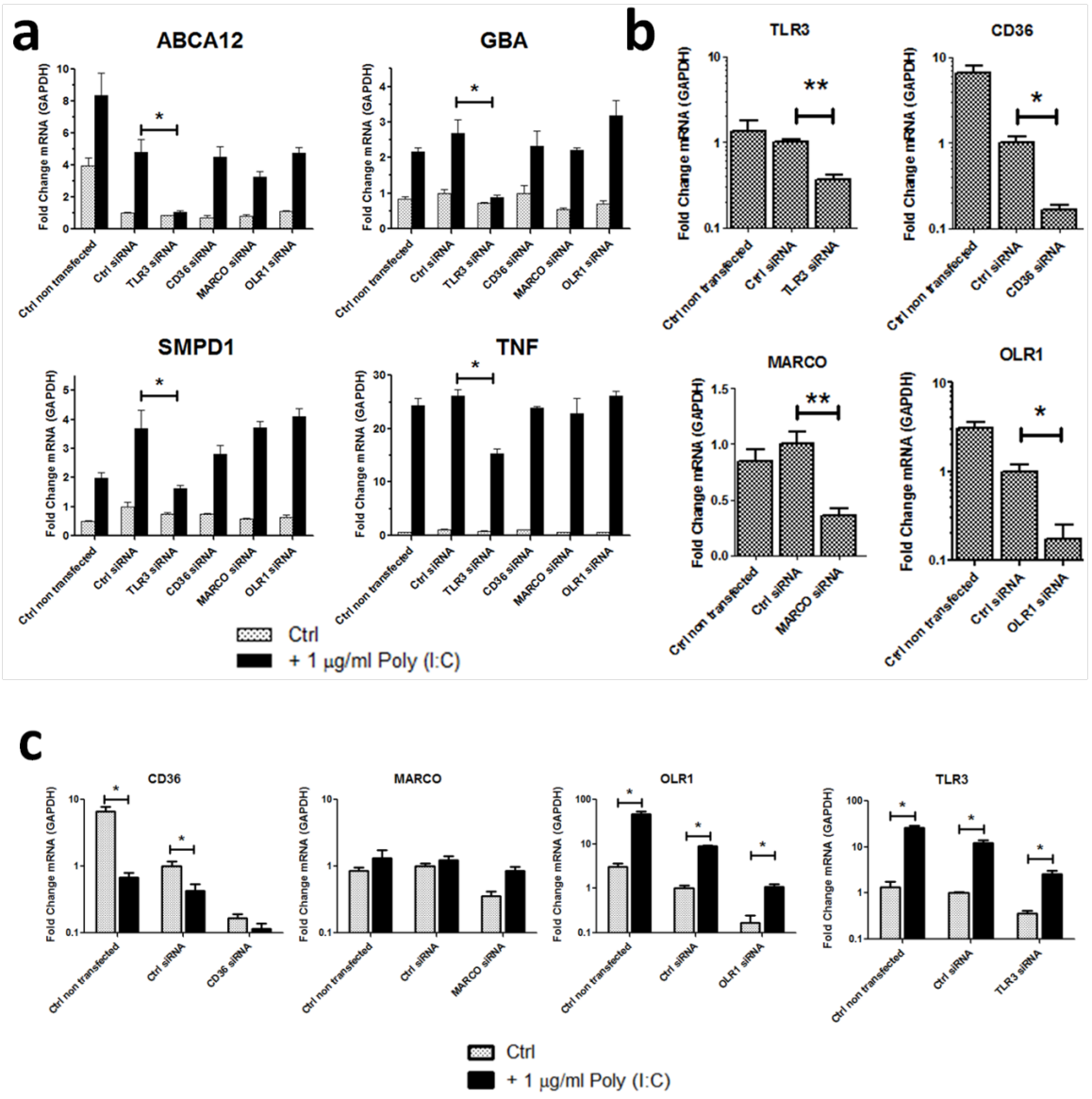

Figure 3.2: CD36, MARCO, or OLR1 is not required for dsRNA-induced changes in gene expression. (a-c) CD36, MARCO, or OLR1 was silenced in NHEK for 48 h before treatment with 1 µg/ml Poly (I:C) for 24 h. Real-time PCR was used to quantify mRNA levels and fold change values are calculated relative and normalized to GAPDH expression. *$P < 0.05$. **$P < 0.01$. Two tailed T-test. Data are mean ± SEM, n = 3, and are representative of at least three independent experiments.

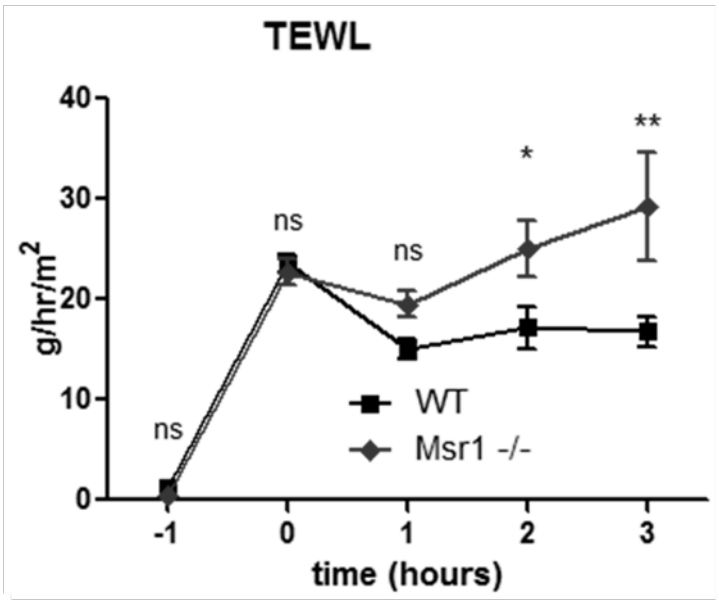

Figure 3.3: *Msr1*$^{-/-}$ mice display a barrier repair defect after tape stripping. TEWL was measured in mice at hourly intervals prior to and after barrier disruption by tape stripping n = 3-4 mice. Two-way ANOVA. ns = P > 0.05. *P < 0.05. **P < 0.01. Data are mean +/- SEM and are representative of at least two independent experiments.

References

[1] L. Alexopoulou, A. C. Holt, R. Medzhitov, and R. A. Flavell, “Recognition of double-stranded RNA and activation of NF-kappaB by Toll-like receptor 3.,” *Nature*, vol. 413, pp. 732–738, 2001.

[2] M. Matsumoto, K. Funami, M. Tanabe, H. Oshiumi, M. Shingai, Y. Seto, A. Yamamoto, and T. Seya, “Subcellular localization of Toll-like receptor 3 in human dendritic cells.,” *J. Immunol.*, vol. 171, pp. 3154–3162, 2003.

[3] T. Kawai and S. Akira, “Toll-like receptor and RIG-I-like receptor signaling.,” *Ann. N. Y. Acad. Sci.*, vol. 1143, pp. 1–20, Nov. 2008.

[4] F. Dunlevy, N. McElvaney, and C. Greene, “TLR3 Sensing of Viral Infection,” *Open Infect. Dis. J.*, vol. 4, pp. 1–10, 2010.

[5] Y. Lai, A. Di Nardo, T. Nakatsuji, A. Leichtle, Y. Yang, A. L. Cogen, Z.-R. Wu, L. V Hooper, R. R. Schmidt, S. von Aulock, K. a Radek, C.-M. Huang, A. F. Ryan, and R. L. Gallo, “Commensal bacteria regulate Toll-like receptor 3-dependent inflammation after skin injury.,” *Nat. Med.*, vol. 15, no. 12, pp. 1377–82, Dec. 2009.

[6] J. J. Bernard, C. Cowing-Zitron, T. Nakatsuji, B. Muehleisen, J. Muto, A. W. Borkowski, L. Martinez, E. L. Greidinger, B. D. Yu, and R. L. Gallo, “Ultraviolet radiation damages self noncoding RNA and is detected by TLR3.,” *Nat. Med.*, vol. 18, no. 8, pp. 1286–90, Aug. 2012.

[7] K. A. Cavassani, M. Ishii, H. Wen, M. A. Schaller, P. M. Lincoln, N. W. Lukacs, C. M. Hogaboam, and S. L. Kunkel, “TLR3 is an endogenous sensor of tissue necrosis during acute inflammatory events.,” *J. Exp. Med.*, vol. 205, no. 11, pp. 2609–21, Oct. 2008.

[8] K. Karikó, H. Ni, J. Capodici, M. Lamphier, and D. Weissman, “mRNA is an endogenous ligand for Toll-like receptor 3.,” *J. Biol. Chem.*, vol. 279, no. 13, pp. 12542–50, Mar. 2004.

[9] A. W. Borkowski, K. Park, Y. Uchida, and R. L. Gallo, “Activation of TLR3 in keratinocytes increases expression of genes involved in formation of the epidermis, lipid accumulation, and epidermal organelles.,” *J. Invest. Dermatol.*, vol. 133, no. 8, pp. 2031–40, Aug. 2013.

[10] J. Canton, D. Neculai, and S. Grinstein, “Scavenger receptors in homeostasis and immunity.,” *Nat. Rev. Immunol.*, vol. 13, pp. 621–34, 2013.

[11] Y. I. Miller, S.-H. Choi, P. Wiesner, L. Fang, R. Harkewicz, K. Hartvigsen, A. Boullier, A. Gonen, C. J. Diehl, X. Que, E. Montano, P. X. Shaw, S. Tsimikas, C. J. Binder, and J. L. Witztum, “Oxidation-specific epitopes are danger-associated molecular patterns recognized by pattern recognition receptors of innate immunity.,” *Circ. Res.*, vol. 108, pp. 235–248, 2011.

[12] J. Kzhyshkowska, C. Neyen, and S. Gordon, “Role of macrophage scavenger receptors in atherosclerosis,” *Immunobiology*, vol. 217, pp. 492–502, 2012.

[13] G. K. Hansson and A. Hermansson, “The immune system in atherosclerosis.,” *Nat. Immunol.*, vol. 12, pp. 204–212, 2011.

[14] H. Suzuki, Y. Kurihara, M. Takeya, N. Kamada, M. Kataoka, K. Jishage, O. Ueda, H. Sakaguchi, T. Higashi, T. Suzuki, Y. Takashima, Y. Kawabe, O. Cynshi, Y. Wada, M. Honda, H. Kurihara, H. Aburatani, T. Doi, A. Matsumoto, S. Azuma, T. Noda, Y. Toyoda, H. Itakura, Y. Yazaki, and T. Kodama, “A role for macrophage scavenger receptors in atherosclerosis and susceptibility to infection.,” *Nature*, vol. 386, pp. 292–296, 1997.

[15] W. J. de Villiers and E. J. Smart, “Macrophage scavenger receptors and foam cell formation.,” *J. Leukoc. Biol.*, vol. 66, pp. 740–746, 1999.

[16] M. Krieger, “The other side of scavenger receptors: pattern recognition for host defense.,” *Curr. Opin. Lipidol.*, vol. 8, pp. 275–280, 1997.

[17] T. Areschoug and S. Gordon, “Scavenger receptors: role in innate immunity and microbial pathogenesis.,” *Cell. Microbiol.*, vol. 11, pp. 1160–1169, 2009.

[18] V. A. Fadok, M. L. Warner, D. L. Bratton, and P. M. Henson, “CD36 is required for phagocytosis of apoptotic cells by human macrophages that use either a phosphatidylserine receptor or the vitronectin receptor (alpha v beta 3).,” *J. Immunol.*, vol. 161, pp. 6250–6257, 1998.

[19] J. C. Todt, B. Hu, and J. L. Curtis, “The scavenger receptor SR-A I/II (CD204) signals via the receptor tyrosine kinase Mertk during apoptotic cell uptake by murine macrophages.,” *J. Leukoc. Biol.*, vol. 84, pp. 510–518, 2008.

[20] X. Gu, R. Lawrence, and M. Krieger, “Dissociation of the high density lipoprotein and low density lipoprotein binding activities of murine scavenger receptor class B type I (mSR-BI) using retrovirus library-based activity dissection.,” *J. Biol. Chem.*, vol. 275, pp. 9120–9130, 2000.

[21] X. Gu, B. Trigatti, S. Xu, S. Acton, J. Babitt, and M. Krieger, “The Efficient Cellular Uptake of High Density Lipoprotein Lipids via Scavenger Receptor Class B Type I Requires Not Only Receptor-mediated Surface Binding but Also Receptor-specific Lipid Transfer Mediated by Its Extracellular Domain The Efficient Cellula,” *J. Biol. Chem.*, vol. 273, no. 41, pp. 26338–26348, 1998.

[22] D. Reczek, M. Schwake, J. Schröder, H. Hughes, J. Blanz, X. Jin, W. Brondyk, S. Van Patten, T. Edmunds, and P. Saftig, “LIMP-2 Is a Receptor for Lysosomal Mannose-6-Phosphate-Independent Targeting of β-Glucocerebrosidase,” *Cell*, vol. 131, pp. 770–783, 2007.

[23] H. Tsuruoka, W. Khovidhunkit, B. E. Brown, J. W. Fluhr, P. M. Elias, and K. R. Feingold, “Scavenger receptor class B type I is expressed in cultured keratinocytes and epidermis.

Regulation in response to changes in cholesterol homeostasis and barrier requirements.," *J. Biol. Chem.*, vol. 277, pp. 2916–2922, 2002.

[24] K. R. Feingold, "Thematic review series: skin lipids. The role of epidermal lipids in cutaneous permeability barrier homeostasis.," *J. Lipid Res.*, vol. 48, no. 12, pp. 2531–46, Dec. 2007.

[25] K. R. Feingold, M. Q. Man, G. K. Menon, S. S. Cho, B. E. Brown, and P. M. Elias, "Cholesterol synthesis is required for cutaneous barrier function in mice.," *J. Clin. Invest.*, vol. 86, pp. 1738–1745, 1990.

[26] D. T. MacLeod, T. Nakatsuji, K. Yamasaki, L. Kobzik, and R. L. Gallo, "HSV-1 exploits the innate immune scavenger receptor MARCO to enhance epithelial adsorption and infection.," *Nat. Commun.*, vol. 4, p. 1963, 2013.

[27] J. A. Majde, N. Guha-Thakurta, Z. Chen, S. Bredow, and J. M. Krueger, "Spontaneous release of stable viral double-stranded RNA into the extracellular medium by influenza virus-infected MDCK epithelial cells: implications for the viral acute phase response.," *Arch. Virol.*, vol. 143, pp. 2371–2380, 1998.

[28] H. Kono and K. L. Rock, "How dying cells alert the immune system to danger.," *Nat. Rev. Immunol.*, vol. 8, no. 4, pp. 279–89, Apr. 2008.

[29] T. V Berghe, N. Vanlangenakker, E. Parthoens, W. Deckers, M. Devos, N. Festjens, C. J. Guerin, U. T. Brunk, W. Declercq, and P. Vandenabeele, "Necroptosis, necrosis and secondary necrosis converge on similar cellular disintegration features.," *Cell Death Differ.*, vol. 17, no. 6, pp. 922–30, Jun. 2010.

[30] G. V Limmon, M. Arredouani, K. L. McCann, R. a Corn Minor, L. Kobzik, and F. Imani, "Scavenger receptor class-A is a novel cell surface receptor for double-stranded RNA.," *FASEB J.*, vol. 22, pp. 159–67, 2008.

[31] A. Dieudonné, D. Torres, S. Blanchard, S. Taront, P. Jeannin, Y. Delneste, M. Pichavant, F. Trottein, and P. Gosset, "Scavenger receptors in human airway epithelial cells: Role in response to double-stranded RNA," *PLoS One*, vol. 7, no. 8, pp. 1–13, 2012.

[32] Y. Tsubamotoa, N. Yamada, Y. Watanabe, T. Inaba, M. Shiomi, H. Shimano, T. Gotoda, K. Harada, M. Shimada, J. I. Ohsuga, M. Kawamura, and Y. Yazaki, "Dextran sulfate, a competitive inhibitor for scavenger receptor, prevents the progression of atherosclerosis in Watanabe heritable hyperlipidemic rabbits," *Atherosclerosis*, vol. 106, pp. 43–50, 1994.

[33] A. C. Nicholson, S. Frieda, A. Pearce, and R. L. Silverstein, "Oxidized LDL binds to CD36 on human monocyte-derived macrophages and transfected cell lines. Evidence implicating the lipid moiety of the lipoprotein as the binding site.," *Arterioscler. Thromb. Vasc. Biol.*, vol. 15, pp. 269–275, 1995.

[34] E. A. Podrez, M. Febbraio, N. Sheibani, D. Schmitt, R. L. Silverstein, D. P. Hajjar, P. A. Cohen, W. A. Frazier, H. F. Hoff, and S. L. Hazen, "Macrophage scavenger receptor

CD36 is the major receptor for LDL modified by monocyte-generated reactive nitrogen species.," *J. Clin. Invest.*, vol. 105, pp. 1095–1108, 2000.

[35] J. R. M. Ojala, T. Pikkarainen, A. Tuuttila, T. Sandalova, and K. Tryggvason, "Crystal structure of the cysteine-rich domain of scavenger receptor MARCO reveals the presence of a basic and an acidic cluster that both contribute to ligand recognition.," *J. Biol. Chem.*, vol. 282, pp. 16654–16666, 2007.

[36] I. Ohki, T. Ishigaki, T. Oyama, S. Matsunaga, Q. Xie, M. Ohnishi-Kameyama, T. Murata, D. Tsuchiya, S. Machida, K. Morikawa, and S. Tate, "Crystal structure of human lectin-like, oxidized low-density lipoprotein receptor 1 ligand binding domain and its ligand recognition mode to OxLDL.," *Structure*, vol. 13, pp. 905–917, 2005.

[37] S. J. DeWitte-Orr, S. E. Collins, C. M. T. Bauer, D. M. Bowdish, and K. L. Mossman, "An accessory to the 'Trinity': SR-As are essential pathogen sensors of extracellular dsRNA, mediating entry and leading to subsequent type I IFN responses," *PLoS Pathog.*, vol. 6, no. 3, pp. 1–15, 2010.

[38] L. Juhlin, "Expression of CD36 (OKM5) antigen on epidermal cells in normal and diseased skin.," *Acta Derm. Venereol.*, vol. 69, pp. 403–406, 1989.

[39] S. Lisby, E. Ralfkiaer, E. R. Hansen, and G. L. Vejlsgaard, "Keratinocyte and epidermal leukocyte expression of CD36 (OKM5) in benign and malignant skin diseases.," *Acta Derm. Venereol.*, vol. 70, pp. 18–22, 1990.

[40] M.-H. Lin and D. Khnykin, "Fatty acid transporters in skin development , function and disease," *Biochim. Biophys. Acta*, vol. 1841, no. 3, pp. 362–8, Mar. 2014.

CHAPTER 4:

Interleukin-1 receptor is important in maintaining skin homeostasis in response to ultraviolet B radiation

Abstract

UVB damage to the skin can lead to the release of interleukin-1 and activation of interleukin-1 receptor dependent pathways that stimulate inflammation and leads to infiltration of myeloid derived inflammatory cells. While this inflammatory cascade is necessary for proper repair to damaged tissue, improper activation of these pathways can lead to different inflammatory diseases or contribute to carcinogenesis. Herein we show that *Il1r*$^{-/-}$ mice develop dermal hair cysts after chronic UVB exposure and that their skin contains significantly fewer macrophages than WT mouse skin. We also demonstrate that IL-1R signaling is required for barrier disruption after UVB exposure in mice, though does not significantly contribute to the upregulation of Poly (I:C)-induced skin barrier repair genes, an *in vitro* model for UVB-induced keratinocyte damage. These observations show that IL-1R signaling maintains homeostasis in skin following UVB exposure.

Introduction

Interleukin-1 receptor (IL-1R) signaling plays in important role in the response to cellular damage and infection in the host [1]. Ultraviolet B (UVB) damage to keratinocytes induces the release of IL-1α [2], [3] as well as activation and release of IL-1β, which is processed from its pro-form following activation of the inflammasome by UVB-induced cellular damage [4]–[6]. Recent studies have shown that TLR3 activation by UVB damage also modulates inflammation in the skin [7], [8] and that barrier repair processes are also stimulated by TLR3 activation [9]. In contrast to these beneficial processes, a number of inflammatory pathways in the skin have been linked to a role in skin carcinogenesis. It has been shown that IL-1R and myeloid differentiation primary response gene 88 (MYD88), a downstream signaling molecule of IL-1R, are required for the appearance of tumors in a DMBA/TPA carcinogenesis model [10]. It has also been shown that IL-10, which is an important factor linked to immunosuppression leading to skin carcinogenesis, is essential for the formation of UVB-induced tumors in a UVB-skin cancer model [11]. In this study we aimed to determine the roles of both TLR3 and IL-1R in UVB-induced skin cancer.

Although our experiments yielded no tumor growth or insight into whether IL-1R or TLR3 are important in UVB-induced carcinogenesis, we found that *Il1r*$^{-/-}$ mice developed dermal hair cysts following 4-6 months of chronic UVB exposure while WT mouse skin was free of these cysts. The role of IL-1R in hair growth remains to be elucidated, though many past studies have shown that IL-1R activation may influence hair growth. It has been shown that both IL-1α [12] and IL-1β [13] can inhibit hair growth *in vitro*. It has also been observed that patients with alopecia areata, a disease characterized by round patches of hair loss on the scalp or other parts of the body [14], have higher levels of IL-1β mRNA [15] and may have mutations in IL-1R antagonist (IL-1RA), a negative regulator of IL-1R signaling [16].

Acute effects of UVB exposure include sunburn which has recently been shown to be mediated by TLR3 signaling [8]. As IL-1R also is stimulated by UVB exposure [6], we investigated the acute effects of UVB on skin homeostasis. Herein we find that UVB-induced skin barrier disruption is delayed and dampened in *Il1r*$^{-/-}$ mice although the transcripts for the inflammatory cytokines Tnf and Il6 were increased. *In vitro* studies showed no significant changes in the skin barrier repair genes transglutaminase 1 or acid sphingomyelinase when keratinocytes were treated with IL-1R ligands. These findings demonstrate that IL-1R signaling plays a key role in maintaining homeostasis in the skin following UVB exposure though may not directly stimulate skin barrier repair.

Methods

Mice. Sex-matched C57BL/6 wild-type controls, male and female TLR3-deficient mice on a C57BL/6 background, and IL-1R-deficient mice on a C57BL/6 background were housed at the University Research Center at the University of California, San Diego (UCSD). All animal experiments were approved by the UCSD Institutional Animal Care and Use Committee.

UVB induced carcinogenesis/cyst formation. 12 week old WT, *Tlr3*$^{-/-}$, and *Il1r*$^{-/-}$ mice were dorsal hair was shaven and further removed using a chemical depilatory reagent. 96 hours later mice were exposed to 2 kJ/m^2 narrowband UVB (312 nm). This exposure was continued 3 times per week for four weeks. After 4 weeks the dose was increased to 5 kJ/m^2 for the remaining 5-6 months of the experiment. Mice were checked 3 times a week for growths. At conclusion of experiment, mice were sacrificed and skin samples were fixed in 4% paraformaldehyde prior to histological analysis.

Immunohistochemistry and Histology. Skin samples were paraffinized and cut in 5 μm

sections. Hematoxylin and eosin staining was performed following deparaffinization using xylenes and graded ethanol washes. Immunostaining was performed using antibodies recognizing keratin-10 (Thermo Scientific; MS-611-P0; 1:50 dil, mouse), trichohyalin (Santa Cruz; sc80607; 1:50 dil, mouse), pan-cytokeratin (Santa Cruz; sc57012; 1:100 dil, mouse), p63 (Thermo Scientific; MS-1084-P0; 1:100; mouse), keratin 14 (Thermo Scientific; PA1-38001;1:100, rabbit), and Sox-9 (Millipore; AB5335; 1:100; rabbit) were performed following deparaffinization, antigen retrieval and blocking. Antigen retrieval was performed in 1 mm EDTA (pH 8.0) for 20 minutes at 95°C in a water bath. M.O.M. Immunodetection kit (Vector) was used according to manufacturer's protocol to block detection of endogenous mouse IgG. Endogenous Biotin blocking kit (Life Technologies) was also used per manufacturer's instructions. Sections were then incubated for 30 minutes in primary antibodies. After washing biotinylated anti-mouse IgG (or anti-rabbit IgG) were added per manufacturer's instructions (Vector). Avidin-Alexa Fluor® 488 conjugate (Life Technologies; A-21370; 1:1000) was used to detect primary/secondary antibody complex.

Fontana-Masson staining was performed according to manufacturer's instructions (American MasterTech). Slides were cleared in xylene and mounted in DPX mounting medium. For immunohistochemistry (IHC), sections were deparaffinized using xylene and rehydrated using graded alcohols. Antigen retrieval was performed in a 95°C-100°C bath for 20 minutes with pH 6.0 citrate buffer. All sections were then washed three times with 0.05% PBS-Tween (PBST), and blocked with 10% normal goat serum in PBST for 30 minutes to block nonspecific antibody binding. Sections were then incubated overnight with primary antibody at 4°C (αRXRα, Santa Cruz, 1:50 dil., rabbit; αMAC1; or αTYRP1, NIH (kindly provided by V. Hearing), 1:1000 dil., rabbit). Primary antibody incubation was followed by three washes with PBS-Tween before addition of either biotin or fluorophore-conjugated secondary antibodies, which were incubated on the sections for 2 hours at room temperature. For fluorescent IHC, nuclei were counterstained

with DAPI (200 ng/mL) for 10 minutes at room temperature. For chromogenic IHC, sections were incubated with streptavidin-horseradish peroxidase (Vector Laboratories) for 30 minutes at room temperature, signal developed with DAB peroxidase substrate kit (Vector Laboratories), and counterstained with hematoxylin (1:1 in H20) for 15 minutes at room temperature. Finally, sections were rinsed with PBST (fluorescent IHC) or running tap water (chromogenic IHC), dehydrated through sequential alcohol washes and then cleared in xylene. Slides were mounted with DPX mounting medium. Sections stained without primary antibody was used as negative controls, and all experiments were performed in triplicates.

Imaging and Quantitation of Histological and IHC Experiments. Bright field images were captured with a Leica DME light microscope using the Leica Application Suite software, version 3.3.1. Fluorescent images were captured using a Zeiss AXIO Imager.Z1 with a digital AxioCam HRm and processed using AxioVision 4.8 and Adobe Photoshop. Quantifications of cell labeling were performed by randomly choosing multiple fields imaged from several replicate animals in each group and counting cells using ImageJ software (NIH). All slides were analyzed independently in a double-blinded manner by two investigators and significance was determined using a Student's two-tailed t-test as calculated by GraphPad Prism software.

UVB induced barrier disruption. 12 week old WT and *Il1r*$^{-/-}$ mice were shaven and dorsal hair was chemically depilated. 96 hours later, mice were exposed to 0.5 kJ/m^2 narrowband UVB (312 nm). Transepidermal water loss (TEWL) was measured using a TEWAMETER TM300 (C & K, Cologne, Germany) to assess skin barrier disruption. TEWL was measured prior to UVB barrier disruption and every 24 hours for 7 days. For mice treated with

cyclophosphamide, animals were given 300mg/kg of cyclophosphamide 48 hours prior to UVB exposure. Cyclophosphamide was injected into the peritoneum.

Cell culture and stimuli. NHEKs were obtained from Cascade Biologics/Invitrogen (catalog number: C-001-5C; Portland, OR), and grown in serum-free EpiLife cell culture media (Cascade Biologics/Invitrogen) containing 0.06 mM Ca^{2+} and 1 × EpiLife Defined Growth Supplement (EDGS, Cascade Biologics/Invitrogen) at 37 °C under standard tissue culture conditions. All cultures were maintained for up to eight passages in this medium with the addition of 100 U ml^{-1} penicillin, 100 μg ml^{-1} streptomycin, and 250 ng ml^{-1} amphotericin B. Cells at 60–80% confluence were treated with either Poly (I:C) (1 μg ml^{-1}; Invivogen, San Diego, CA), recombinant human IL-1α (2.5 ng/ml or 25 ng/ml; R&D, Minneapolis), or IL-1β (2.5 ng/ml or 25 ng/ml; R&D, Minneapolis) in 12-well flat-bottom plates (Corning Incorporated Life Sciences, Lowell, MA) for up to 24 hours. After cell stimulation, RNA was extracted using TRIzol reagent (Invitrogen, Carlsbad, CA). RNA was stored at −80 °C.

Quantitative real-time PCR. Total RNA was extracted from cultured keratinocytes using TRIzol Reagent (Invitrogen) and 1 μg RNA was reverse-transcribed using iScript cDNA Synthesis Kit (Bio-Rad, Hercules, CA). Pre-developed Taqman Gene Expression Assays (Applied Biosystems, Foster City, CA) were used to evaluate mRNA transcript levels of human SMPD1, TGM1, TNF, IL-6, IL-1R, TLR3 and mouse Abca12, Tgm1, Gba, Tnf, Il6, Edn1, Hgf, Mc5r, Egf, Egfr, Kit, Kitl and Gapdh. Glyceraldehyde-3-phosphate dehydrogenase mRNA transcript levels were evaluated using a VIC-CATCCATGACAACTTTGGTA-MGB probe with primers 5′-CTTAGCACCCCTGGCCAAG-3′ and 5′-TGGTCATGAGTCCTTCCACG-3′. All analyses were performed in triplicate and were representative of two to three independent cell

stimulation experiments that were analyzed in an ABI Prism 7000 Sequence Detection System (Life Technologies, Carlsbad, CA). Fold induction relative to glyceraldehyde-3-phosphate dehydrogenase was calculated using the $\Delta\Delta C_t$ method. Results were considered to be significant if $P<0.05$.

siRNA knockdown. TLR3, IL-1R, and control siRNA were purchased from Dharmacon (Chicago, IL). One nanomole of each siRNA was electroporated into 3 x 10^6 keratinocytes using Amaxa nucleofection reagents as previously described [9] (VPD-1002) (Lonza AG, Walkersville, MD).

Results

Chronic UVB exposure induces dermal cysts in *Il1r*$^{-/-}$ mice. It has been observed that inflammation involved with Myd88-dependent signaling pathways are important for cutaneous carcinogenesis [10]. It has also been observed that IL-10, an important mediator of UV-induced immunosupression, is required in the skin for UVB-induced carcinogenesis [11]. As TLR3 activation has been shown to be an important source of inflammation in the skin following UVB exposure [7], [8], we hypothesized that TLR3 activation was important to UVB-induced carcinogenesis in the skin. As IL-1α is also released in the skin following UVB exposure [17], [18], we wanted to confirm the results of previous cutaneous carcinogenesis studies to determine if IL-1R is important to UVB-induced carcinogenesis as previous studies demonstrated its necessity a 2-stage chemical carcinogenesis model. As TLR3 and IL-1R signaling are both proinflammatory pathways and it has been shown that a proinflammatory stimulus is needed for cutaneous carcinogenesis [10], we hypothesized that both *Tlr3*$^{-/-}$ and *Il1r*$^{-/-}$ mice would develop fewer tumors than WT mice. In order to test our hypothesis, we exposed back skin of WT, *Tlr3*$^{-/-}$ and *Il1r*$^{-/-}$ mice to 2 kJ/m^2 narrowband UVB (312 nm), 3 times a week for 4 weeks, followed by 5

kJ/m^2 for another 5-6 months. After 184 days, 77% (10 out of 13) of *Il1r*$^{-/-}$ mice had palpable skin growths while only 6% of WT mice had palpable skin growths (Figure 4.1a). Beginning at 126 days after UVB exposure, *Il1r*$^{-/-}$ mice had significantly more palpable growths per mouse than WT mice (Figure 4.1b) and this amount increased until termination of the study. *Tlr3*$^{-/-}$ mice however, did not show any difference in appearance of palpable growths (10%; 1 out of 10) than WT mice (12.5%; 2 out of 16) (Figure 4.1c) and did not have a significant difference in number of palpable growths per mouse than WT mice (Figure 4.1d).

Histological examination by a dermatopathologist of the growths of these mice showed that none of the growths were in fact cancerous tumors. Some hyperplasia of the epidermis was revealed though the majority of the growths were characterized as dermal cysts (Figure 4.2a) in the *Il1r*$^{-/-}$ mice. As these cysts appeared to possibly be of hair follicle in origin, we stained for the hair markers, trichohyalin and pan-cytokeratin. These cysts stained positive for both trichohyalin (Figure 4.2c) and pan-cytokeratin (Figure 4.d). In WT mice hair follicles can be seen to stain positive for both trichohyalin (Figure 4.2c) and pan-cytokeratin (Figure 4.d). The epithelial cells surrounding the cysts also stained positive for the keratinocyte differentiation marker keratin-10 (Figure 4.2b). To test the hypothesis that outer root sheath progenitor cells may be failing to die after UVB damage, we stained for marker of the outer root sheath in these dermal cysts. Cysts from *Il1r*$^{-/-}$ mice stain positive for p63 (Figure 4.3b), keratin-14 (Figure 4.3c), and Sox-9 (Figure 4.3d).

***Il1r*$^{-/-}$ mice have fewer cutaneous macrophages following chronic UVB exposure.** The Indra Lab has previously shown a similar phenotype in RXRα-deficient mice following chronic UVB treatments (unpublished data not shown). They report the appearance of dark colored epidermal cysts in RXRα-deficient mice following chronic UVB. To test whether these pathways might be connected, we stained for levels of RXRα in WT and *Il1r*$^{-/-}$ mice. Similar

staining was observed in dorsal skin of WT and *Il1r*$^{-/-}$ mice that were chronically exposed to UVB (Figure 4.4). Because a majority of these cysts were darkly pigmented, we wanted to determine whether there were differences in melanocytes in the skin of these mice. Staining for tyrosinase-related protein 1 (TYRP1), a marker for melanocytes, revealed no significant differences of either epidermal, dermal, or total melanocytes (Figure 4.5a and 4.5b). Staining for melanin, a marker of differentiated melanocytes also revealed no significant differences between WT and *Il1r*$^{-/-}$ mice (Figure 4.5c and 4.5d). Staining for macrophage-1 antigen (MAC1), revealed that *Il1r*$^{-/-}$ mice had significantly fewer macrophages present in the skin after chronic UVB exposure (Figure 4.6).

***Il1r*$^{-/-}$ mice have fewer cutaneous macrophages following chronic UVB exposure than WT mice.** Because chronic doses of UVB had a significant effect on *Il1r*$^{-/-}$ mice, we wanted to determine if acute effects of UVB exposure could also be measured in these mice. We exposed WT and *Il1r*$^{-/-}$ mice to an acute low dose of UVB (0.5 kJ/m^2) and measured transepidermal water loss over 7 days to assess barrier disruption and repair processes. We observed that barrier disruption in *Il1r*$^{-/-}$ mice was significantly lower than WT mice at 2 and 3 days after initial exposure (Figure 4.7a). A similar result is observed when WT mice are first injected with 300mg/kg cyclophosphamide, a chemotherapy reagent that kills myeloid derived inflammatory cells, 48 hours before exposure to UVB (Figure 4.7b). We next looked at gene expression of a number of skin barrier, inflammatory, and growth factor genes to determine whether transcriptional differences are present after acute UVB exposure. No significant changes were seen in Abca12 or Tgm1 transcript levels between up to three days after UVB exposure (Figure 4.8a+b), although Gba levels were elevated at day 3 in *Il1r*$^{-/-}$ mice (Figure 4.8c). Both Tnf and Il6 transcript levels were significantly higher in *Il1r*$^{-/-}$ mice at day 3 after UVB exposure (Figure 4.8d+e). Endothelin 1(Edn1), hepatocyte growth factor (Hgf), melanocortin 5 receptor (Mc5r), epidermal growth factor (Egf), and epidermal growth factor receptor (Efgr) transcript

levels were not significantly different between WT and *Il1r*$^{-/-}$ mice (figure 4.8g-j). Transcript levels of both stem cell growth factor receptor (Kit) or stem cell factor (Kitl) were both significantly higher in *Il1r*$^{-/-}$ mice at day 3 (Figure 4.8k+l).

IL-1R is not required for induction of Poly (I:C)-induced skin barrier gene expression. As IL-1R activation looks to be in important factor in UVB-induced skin barrier disruption and is also activated following UV exposure to keratinocytes [1], [6], we wanted to investigate whether it played a role in skin barrier repair. We first tested whether ligands for IL-1R signaling could induce expression of skin barrier repair genes. NHEK were treated for 24 hours with either IL-1α or IL-1β and expression of inflammatory and skin barrier repair genes was examined by real time PCR. IL-1α had no significant effect on SMPD1, TGM1, TLR3, TNF, IL-6 or IL-1R transcript levels (Figure 4.9a-f). IL-1β caused significant increases in TGM1 at the 25 ng/ml dose and caused small but insignificant increases in SMPD1, TNF, IL-6, and IL-1R (Figure 4.9a-f). We then wanted to determine whether knockdown of IL-1R had any effect on Poly (I:C)-induced skin barrier gene expression. While TLR3 knockdown caused significant decreases in SMPD1, TGM1, TLR3, TNF, IL-6 and IL-1R transcripts after Poly (I:C) treatment (Figure 4.10a-f), IL-1R knockdown had no effect on Poly (I:C)-induced changes in SMPD1, TGM1, TLR3, TNF, and IL-6(Figure 4.10a-e). Poly (I:C)-induced increases in IL-1R were significantly lower when IL-1R was knocked down (Figure 4.10f).

Discussion

IL-1R plays a critical role in inflammation in the skin following damage or UVB exposure [19]–[21]. In this study we demonstrate that IL-1R signaling may play an important role in regulating hair growth following chronic UVB exposure, as dermal cysts that stain positive for hair follicle markers appear in chronic UVB treated skin of *Il1r*$^{-/-}$ mice. While IL-1R

signaling may not contribute to skin barrier repair, it appears that it plays an important role in skin barrier disruption following UVB exposure. IL-1α fails to increase skin barrier repair genes, while IL-1β may have an effect on skin barrier repair genes. Poly (I:C)- or UVB-induced increases in skin barrier repair genes are not dependent on IL-1R activation by evidence of siRNA knockdown and genetic deletion of IL-1R, respectively. The observed lack of macrophage infiltration into the UVB-treated skin of *Il1r*$^{-/-}$ mice may serve as a clue as to why hair cysts develop in *Il1r*$^{-/-}$ mice or why barrier disruption fails to occur to the level we observe in WT mice.

A number of studies in the early 1990s showed that IL-1R signaling had inhibitory effects on hair growth [12], [13], [22], [23]. It was observed that both IL-1α [12] and IL-1β [13] had inhibitory effects on *in vitro* hair follicle growth. It has also been observed that elevated IL-1β mRNA levels are present in patients with alopecia areata [15], [23], a disease associated with hair loss to the scalp and body with an unknown etiology though an autoimmune mechanism related to improper activation of T lymphocytes has been proposed [14]. Interestingly, it has also been shown that a polymorphism in interleukin-1 receptor antagonist (IL-1RA), a negative regulator of IL-1R signaling, is associated with disease severity in patients with alopecia areata [16]. Additionally, although UV treatments are common for a number of dermatological conditions, both UVA- [24] and UVB-treatments [25] fail to stimulate hair growth in patients with alopecia areata. IL-1R is also present in distinct compartments of hair follicles during different stages of hair growth and is used to distinguish these different stages [26]. Based on this evidence and what we have observed in these studies, IL-1R likely plays an important role in hair growth following UVB damage. If excessive IL-1R signaling may be causing loss of hair in patients with alopecia areata by some type of negative regulatory mechanism on hair follicle growth, it is possible that a lack of IL-1R may cause improperly regulated signals that lead to the appearance of the dermal hair cysts that we observe in chronic UVB-treated *Il1r*$^{-/-}$ mice. Future

research should focus on the specific parts of the hair growth cycles that are regulated by IL-1R signaling and how this is affected by UVB exposure.

IL-1R signaling provides an important stimulus to recruit neutrophils and macrophages to the site of injury [5], [27]. As we observe a lack of macrophages in chronic UVB-treated skin of *Il1r*$^{-/-}$ mice, it is possible that macrophages play a role in controlling hair growth. Future studies should examine whether other inflammatory cells types such as neutrophils or T cells are present in UVB-treated skin of *Il1r*$^{-/-}$ mice. Bone marrow reconstitution studies with WT and *Il1r*$^{-/-}$ mice would better elucidate the mechanism behind the appearance of these dermal hair cysts. Examination of the skin of *Il1r*$^{-/-}$ mice that had been treated with an acute low dose of UVB ($0.5kJ/m^2$) showed elevated levels of the inflammatory cytokines Il6 and Tnf, as well as increases in Kit and Kitl. It remains to be tested whether these increases in these mRNA transcripts have an effect on the growth of dermal hair cysts.

While IL-1R may play in important role in recruitment of myeloid derived inflammatory cells to the skin after UVB exposure, this appears to have a detrimental effect on barrier disruption. As we observe little increase in TEWL levels in *Il1r*$^{-/-}$ mice after acute UVB exposure, it appears that IL-1R activation provides an important signal that causes skin barrier disruption. A similar phenotype is seen in mice that have been treated with cyclophosphamide, a chemotherapy drug that has also been used heavily as an immunosuppressive agent as it is able to kill rapidly dividing cells such as bone marrow derived immunocytes [28]. Previous studies of UVB-induced barrier disruption demonstrated that T cells were essential for UVB-induced barrier disruption, as athymic mice did not show increases in TEWL after UVB-exposure [29]. They also observed that by treating mice with cyclosporine A, an anti-inflammatory reagent that blocks T cell and keratinocyte derived cytokine production [30], [31] including IL-1α, one could block UVB-induced increases in TEWL [29]. It appears as though IL-1R signaling is important for UVB-induced barrier disruption, though may not have a significant effect on barrier repair, as IL-

1R ligands do not significantly increase skin barrier repair gene expression at levels found in the body. We also demonstrate that Poly (I:C)-induced skin barrier repair gene expression increases, which models keratinocytes responses following release of endogenous RNA following cellular damage, are not dependent on IL-1R signaling.

Inflammatory signaling is an essential to proper resolution of infection and injury. Although excessive inflammation can exacerbate a number of dermatological conditions as well as promote carcinogenesis, it is required to properly heal. Future studies must focus on specific inflammatory responses to different stimuli as well as which cell type in the skin, whether it be keratinocytes, or any of the other minority cell types that reside in or are recruited to the skin following specific inflammatory signals. A deeper understanding of these processes will likely lead to better treatments for dermatological conditions and decrease the morbidity and mortalities associated with excessive UV exposure and inflammation in the skin.

Acknowledgements

We thank Robert Lee, MD, PhD, Associate Clinical Professor and Director of Dermatopathology at UCSD for help with characterizing the dermal cysts in chronic UVB-treated mouse skin.

We thank Benjamin D. Yu, MD, PhD, Associate Professor at UCSD for helpful discussion in characterizing the dermal cysts.

We thank Arup K. Indra and Daniel J. Coleman for their helpful discussion and for performing immunostaining of TYRP1, MAC1, melanocytes, and RXRα and quantifications in chronic UVB treated mouse skin.

This work was supported by US National Institutes of Health (NIH) grants R01-AR052728, NIH R01-AI052453 and R01 AI0833358 to R.L.G., the UCSD Training in

Immunology Grant 5T32AI060536-05 and UCSD Dermatologist Investigator Training Program Grant 1T32AR062496-01 supporting A.W.B.

Chapter 4, in full, is unpublished data. A. W. Borkowski, D. J. Coleman, A. K. Indra, R. L. Gallo. The dissertation author was the primary investigator and author of this material.

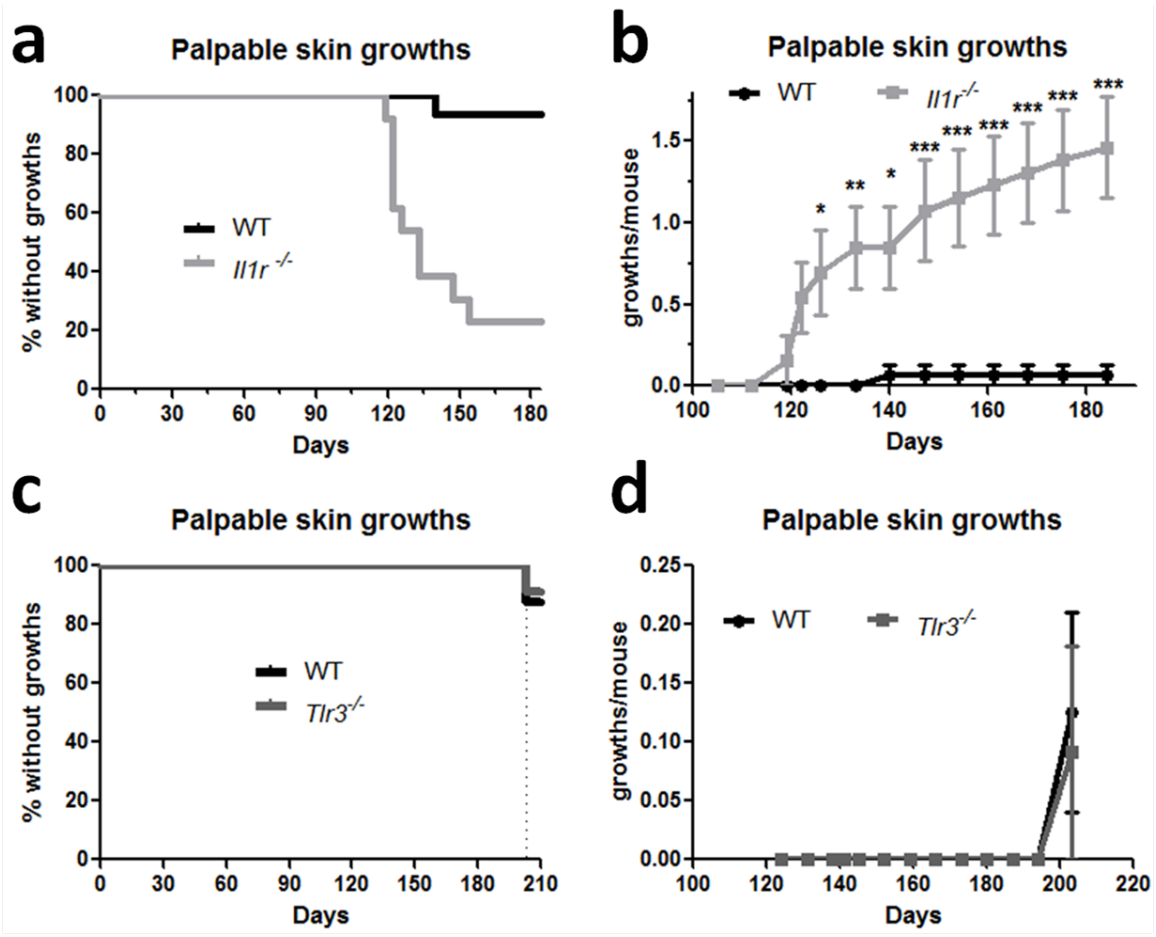

Figure 4.1: Chronic UVB induces cutaneous growths in *Il1r*$^{-/-}$ mice. (a-d) WT, *Il1r*$^{-/-}$ and *Tlr3*$^{-/-}$ mice were exposed to 2 kJ/m^2 UVB 3X/week for 4 weeks and then 5 kJ/m^2 UVB 3X/week for the remainder of the experiment. Mice were checked for palpable skin growths twice a week.

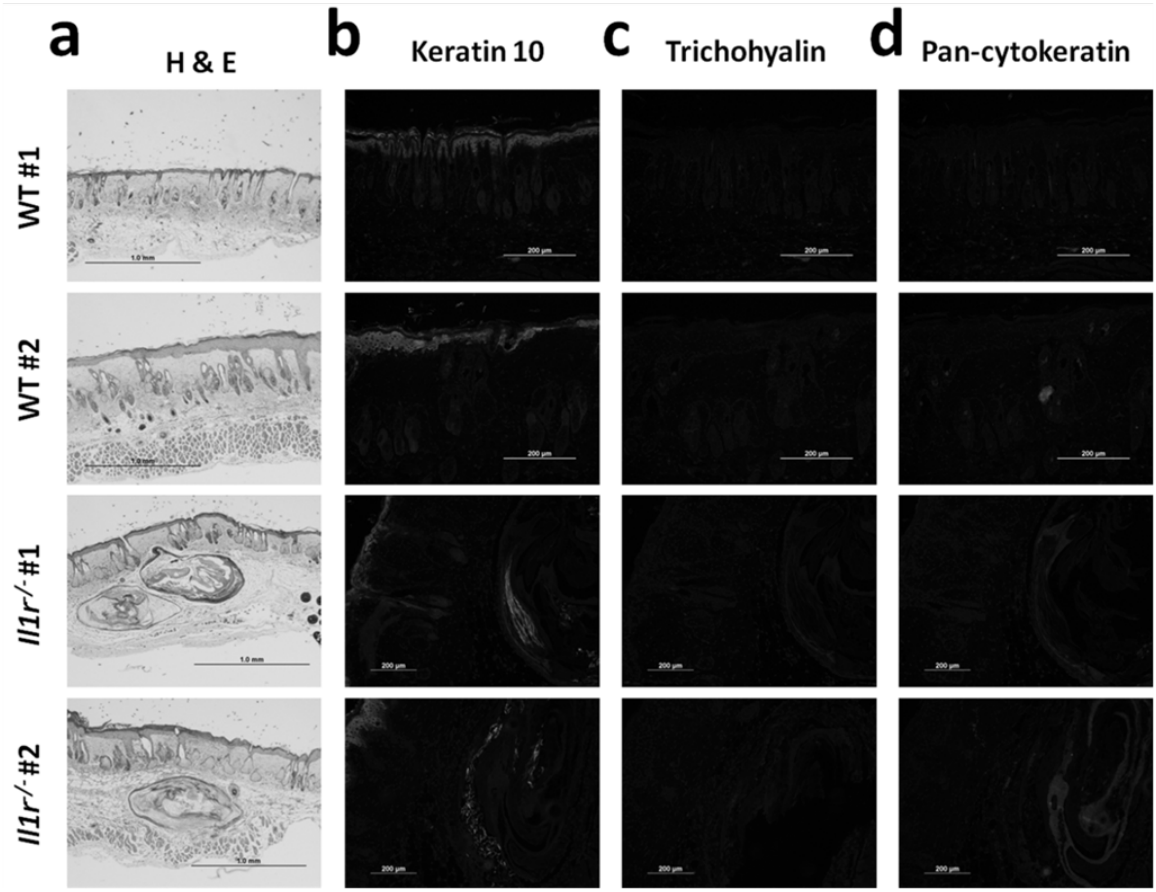

Figure 4.2: Cutaneous growths in chronic UVB-treated in *Il1r*$^{-/-}$ mice are dermal cysts that stain positive for epidermal and hair markers. Growths or dorsal back skin was taken from WT and *Il1r*$^{-/-}$ mice at conclusion of experiment and stained with (a) hematoxylin and eosin or immunostained for either (b) keratin 10, (c) trichohyalin, or (d) pan-cytokeratin. Bright staining represents antibody of interest. Samples were counterstained with DAPI.

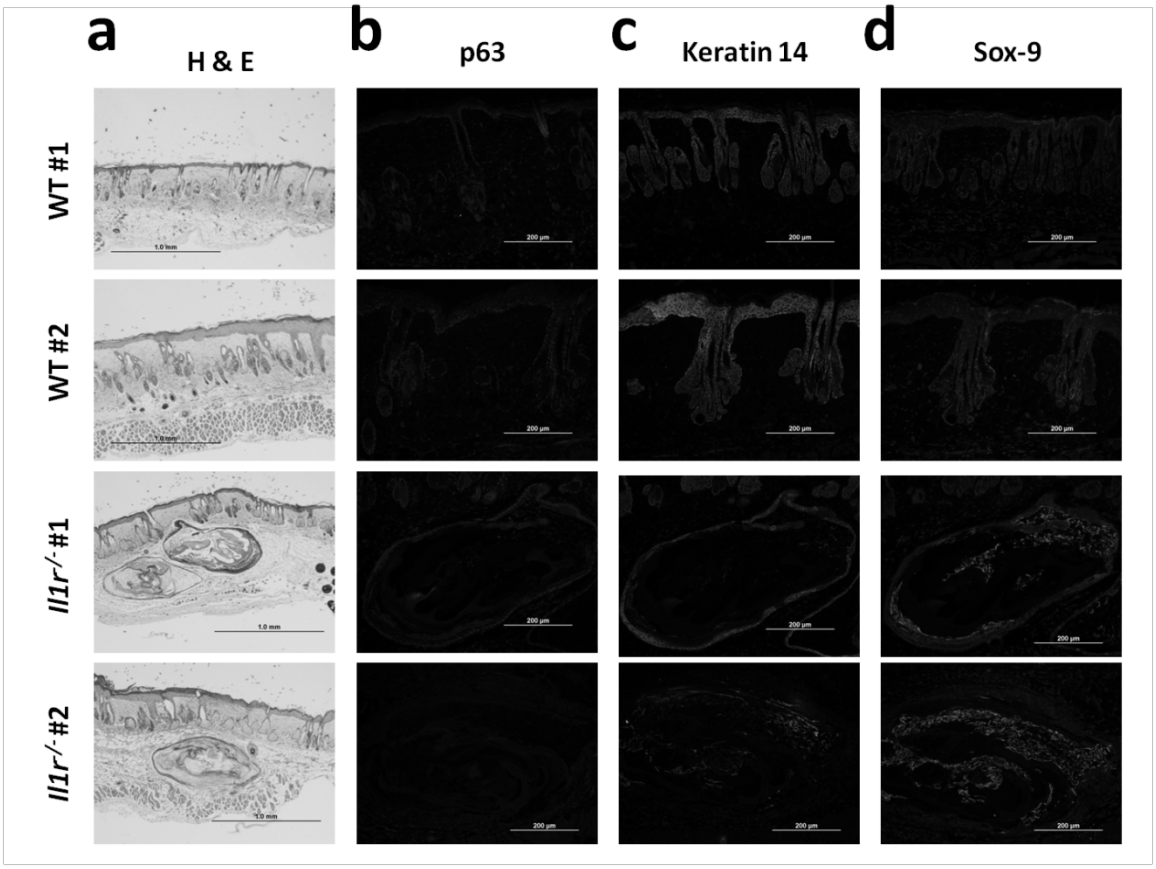

Figure 4.3: Cutaneous growths in chronic UVB-treated in *Il1r*$^{-/-}$ mice are dermal cysts that stain positive for outer root sheath markers. Growths or dorsal back skin was taken from WT and *Il1r*$^{-/-}$ mice at conclusion of experiment and stained with (a) hematoxylin and eosin or immunostained for either (b) p63 10, (c) keratin 14, or (d) sox-9. Bright staining represents antibody of interest. Samples were counterstained with DAPI.

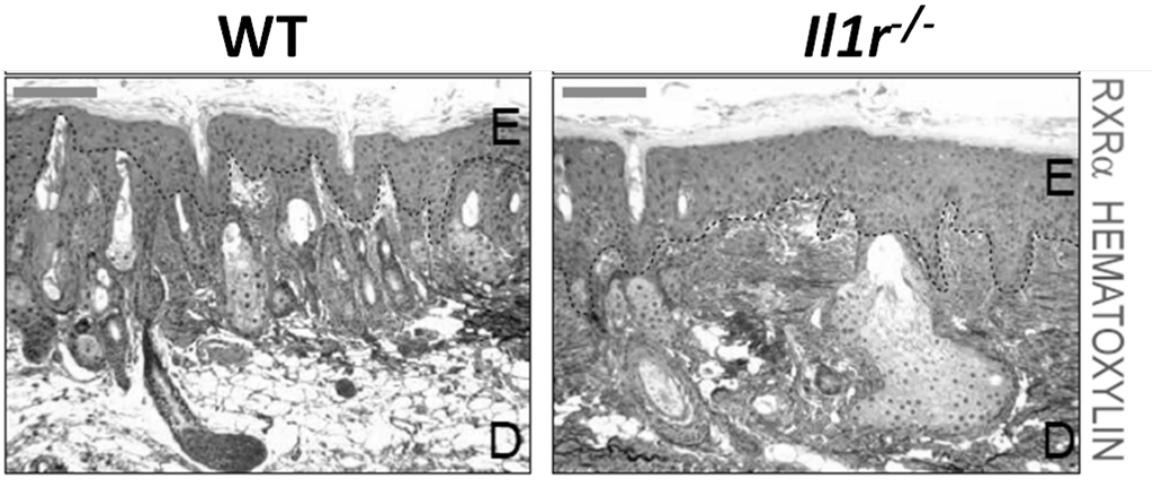

Figure 4.4: No differences in RXRα staining in chronic UVB treated WT and *Il1r*$^{-/-}$ mice. Dorsal skin of WT and *Il1r*$^{-/-}$ mice was stained for RXRα. Samples were counterstained with hematoxylin. Scale bar = 100 μm. E, epidermis; D, dermis. Dotted line represents dermal/epidermal border.

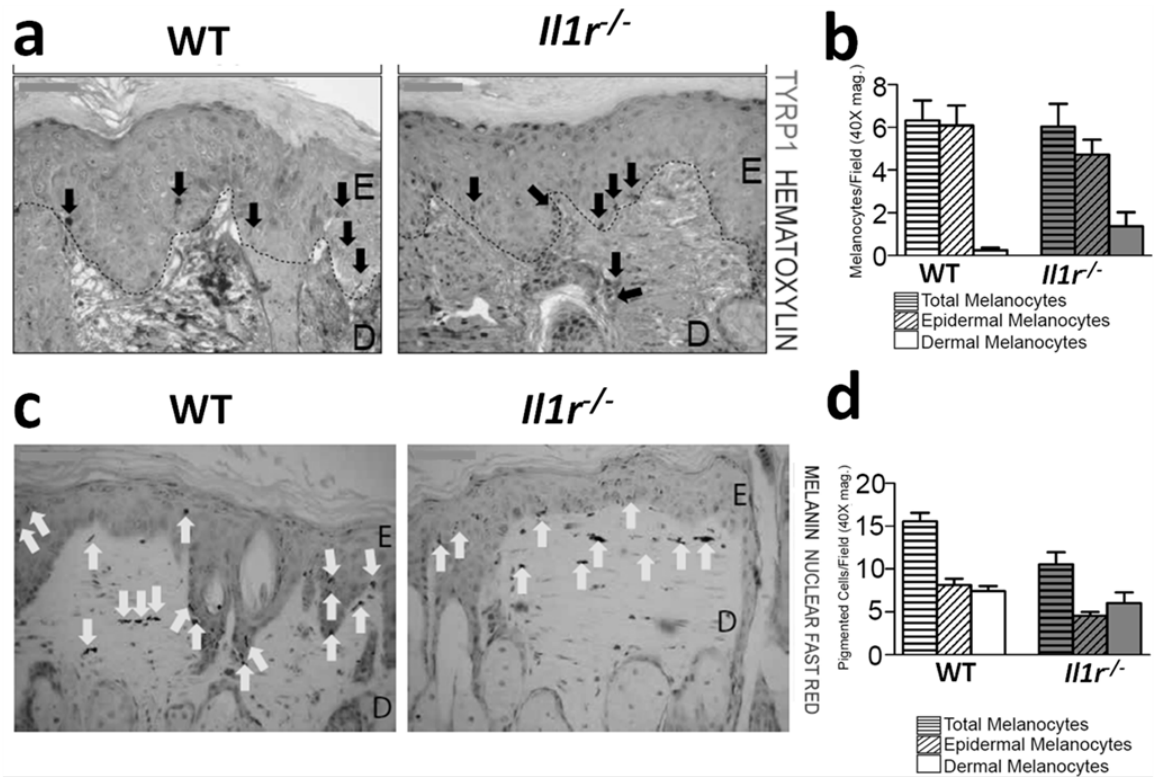

Figure 4.5: No differences in melanocytes in chronic UVB treated WT and *Il1r*$^{-/-}$ mice. Dorsal skin of WT and *Il1r*$^{-/-}$ mice was stained for (a) TYRP1 or (c) melanin. Melanocytes were quantitated using imageJ software (b,d). Samples were counterstained with hematoxylin. Scale bar = 50 µm. E, epidermis; D, dermis. Dotted line represents dermal/epidermal border. Student's t-test.

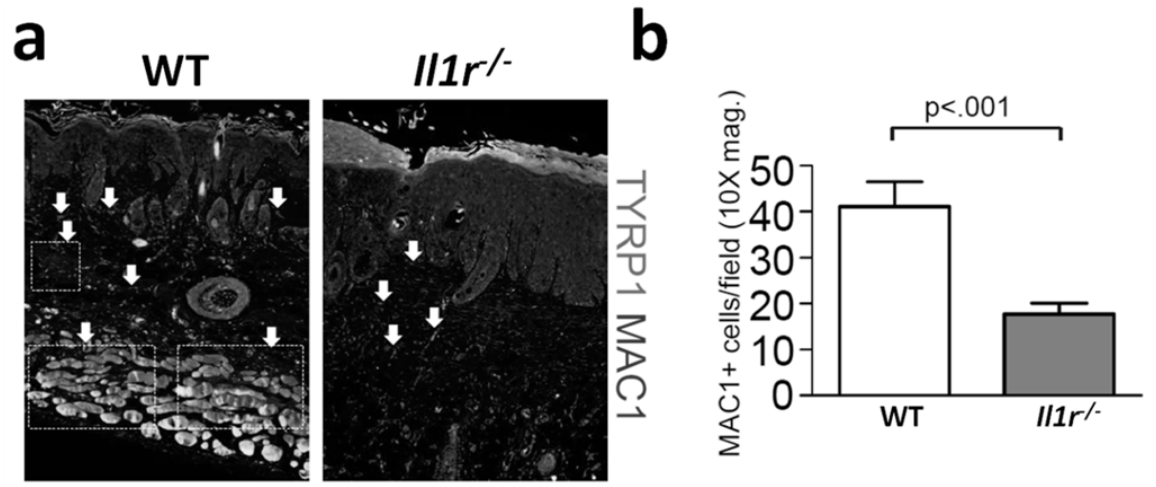

Figure 4.6: *Il1r*$^{-/-}$ mice have fewer cutaneous macrophages following chronic UVB exposure. Dorsal skin of WT and *Il1r*$^{-/-}$ mice was stained for (a) MAC1 and TYRP1 and then (b) quantitated using imageJ software. Samples were counterstained with DAPI. Student's t-test.

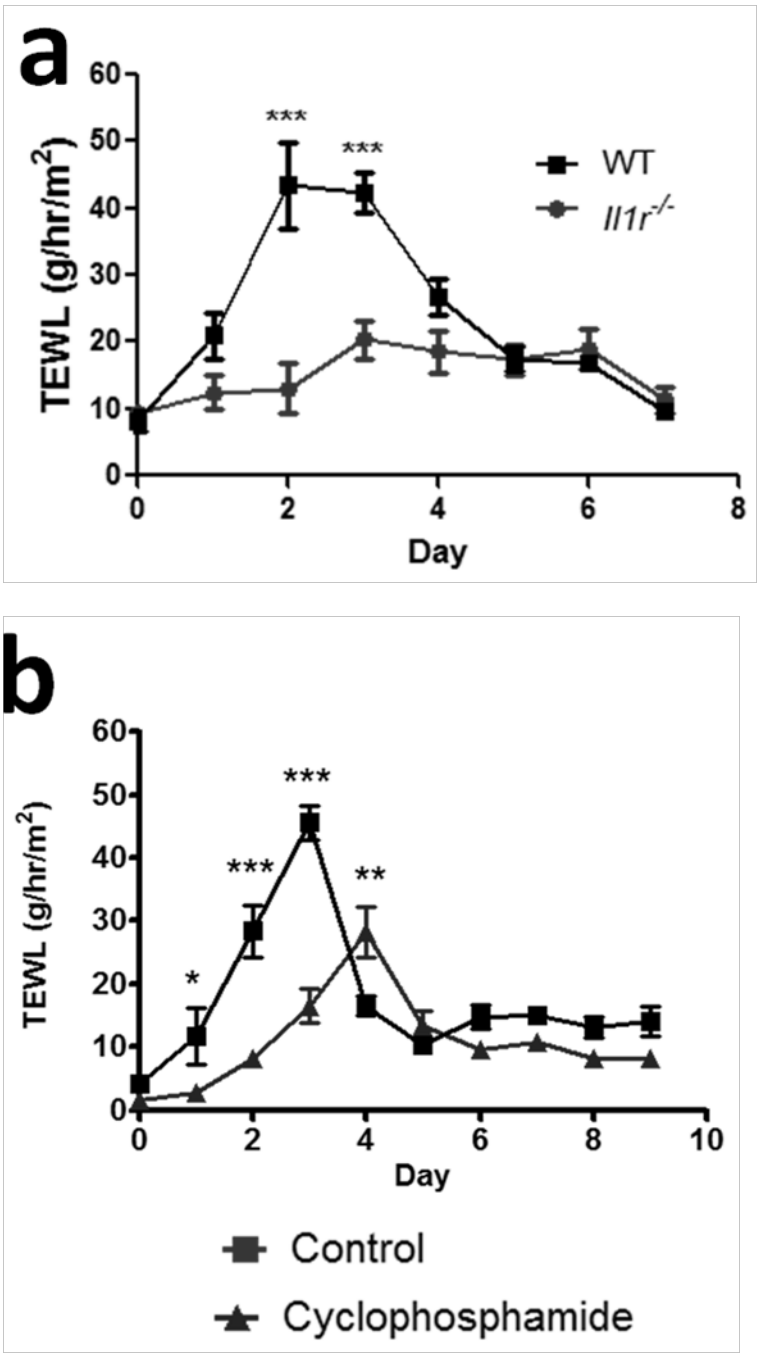

Figure 4.7: *Il1r*$^{-/-}$ mice show display less barrier disruption after acute UVB exposure than WT mice. (a) Mice were exposed to single dose of 0.5 kJ/m^2 UVB and TEWL was measured every 24 hours for 7 days. n = 5-6. (b) Mice were injected with cyclophosphamide prior to being exposed to a 0.5 kJ/m^2 dose of UVB and TEWL was measured every day for 9 days. n= 10. *** = P < 0.001. 2-way ANOVA.

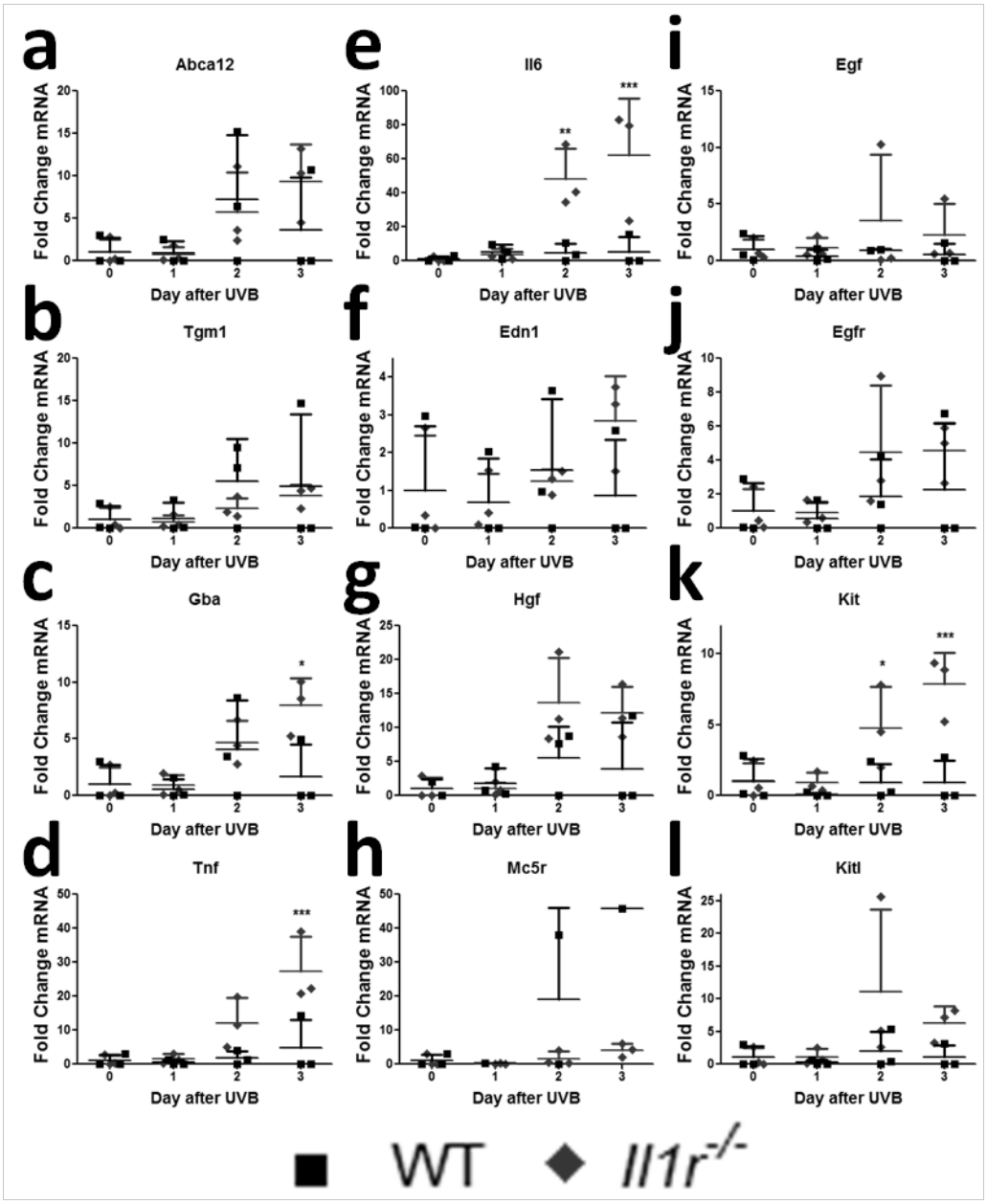

Figure 4.8: Differences in gene expression in acute UVB-treated WT and *Il1r*$^{-/-}$ mice. Dorsal skin of WT and *Il1r*$^{-/-}$ mice was exposed to 0.5 kJ/m^2 narrowband UVB (312 nm). Full thickness biopsies were taken at 0,1,2, and 3 days after UVB exposure and real time PCR was used to quantify mRNA levels and fold change values are calculated relative and normalized to Gapdh. * = P < 0.05. ** = P < 0.01. *** = P < 0.001. 2-way ANOVA. n = 3.

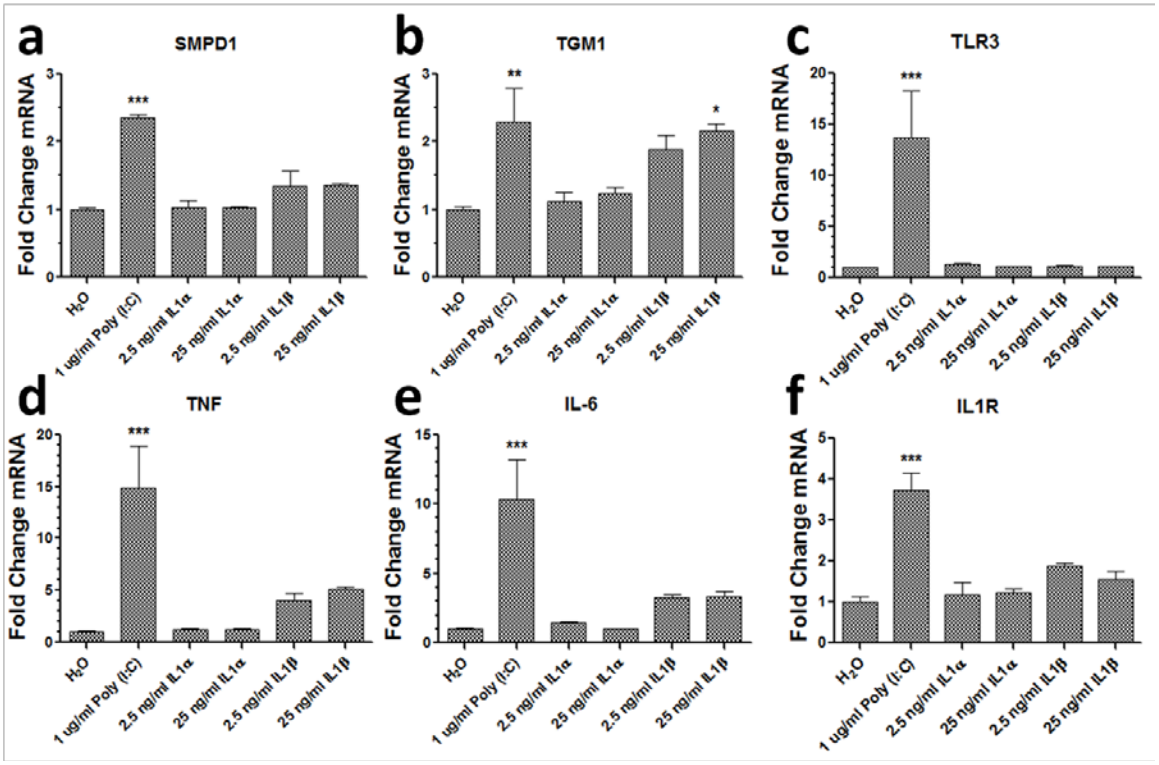

Figure 4.9: IL1R ligands have little to no significant effect on skin barrier genes. NHEK were cultured for 24 hour in the presence of either Poly (I:C), IL-1α, or IL-1β for 24 hours. Real-time PCR was used to quantify mRNA levels and fold change values are calculated relative and normalized to GAPDH. **P* < 0.01. ***P* < 0.01. ****P* < 0.001. One-way ANOVA. Data are mean ± SEM, n = 3, and are representative of at least three independent experiments.

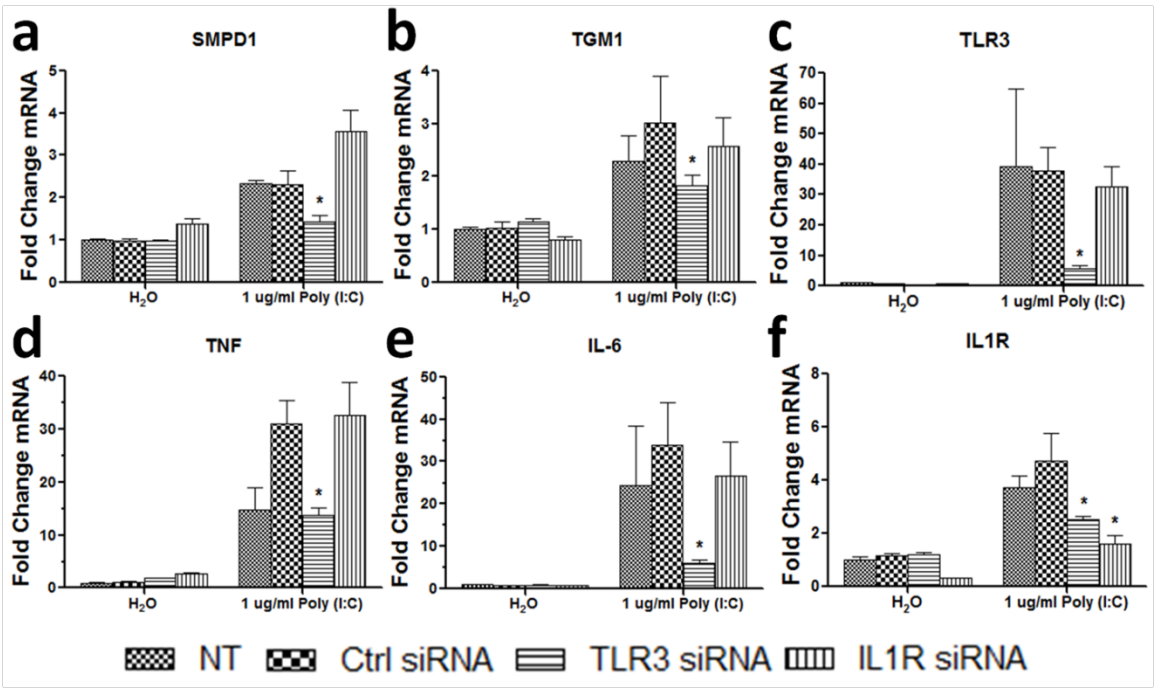

Figure 4.10: IL1R knockdown has no effect on skin barrier repair gene expression. IL1R or TLR3 was silenced in NHEK for 48 h before treatment with 1 µg/ml Poly (I:C) for 24 h. Real-time PCR was used to quantify mRNA levels and fold change values are calculated relative and normalized to GAPDH expression. **P* < 0.05. One-tailed T-test. Data are mean ± SEM, n = 3, and are representative of at least three independent experiments.

References

[1] J. E. Sims and D. E. Smith, “The IL-1 family: regulators of immunity.,” *Nat. Rev. Immunol.*, vol. 10, pp. 89–102, 2010.

[2] T. S. Kupper, D. W. Ballard, A. O. Chua, J. S. McGuire, P. M. Flood, M. C. Horowitz, R. Langdon, L. Lightfoot, and U. Gubler, “Human keratinocytes contain mRNA indistinguishable from monocyte interleukin 1 alpha and beta mRNA. Keratinocyte epidermal cell-derived thymocyte-activating factor is identical to interleukin 1.,” *J. Exp. Med.*, vol. 164, pp. 2095–2100, 1986.

[3] A. V Marionnet, Y. Chardonnet, J. Viac, and D. Schmitt, “Differences in responses of interleukin-1 and tumor necrosis factor alpha production and secretion to cyclosporin-A and ultraviolet B-irradiation by normal and transformed keratinocyte cultures.,” *Exp. Dermatol.*, vol. 6, pp. 22–28, 1997.

[4] T. H. Nasti and L. Timares, “Inflammasome activation of IL-1 family mediators in response to cutaneous photodamage.,” *Photochem. Photobiol.*, vol. 88, no. 5, pp. 1111–25, 2012.

[5] C.-J. Chen, H. Kono, D. Golenbock, G. Reed, S. Akira, and K. L. Rock, “Identification of a key pathway required for the sterile inflammatory response triggered by dying cells.,” *Nat. Med.*, vol. 13, pp. 851–856, 2007.

[6] L. Feldmeyer, M. Keller, G. Niklaus, D. Hohl, S. Werner, and H.-D. Beer, “The inflammasome mediates UVB-induced activation and secretion of interleukin-1beta by keratinocytes.,” *Curr. Biol.*, vol. 17, no. 13, pp. 1140–5, Jul. 2007.

[7] Y. Lai, A. Di Nardo, T. Nakatsuji, A. Leichtle, Y. Yang, A. L. Cogen, Z.-R. Wu, L. V Hooper, R. R. Schmidt, S. von Aulock, K. a Radek, C.-M. Huang, A. F. Ryan, and R. L. Gallo, “Commensal bacteria regulate Toll-like receptor 3-dependent inflammation after skin injury.,” *Nat. Med.*, vol. 15, no. 12, pp. 1377–82, Dec. 2009.

[8] J. J. Bernard, C. Cowing-Zitron, T. Nakatsuji, B. Muehleisen, J. Muto, A. W. Borkowski, L. Martinez, E. L. Greidinger, B. D. Yu, and R. L. Gallo, “Ultraviolet radiation damages self noncoding RNA and is detected by TLR3.,” *Nat. Med.*, vol. 18, no. 8, pp. 1286–90, Aug. 2012.

[9] A. W. Borkowski, K. Park, Y. Uchida, and R. L. Gallo, “Activation of TLR3 in keratinocytes increases expression of genes involved in formation of the epidermis, lipid accumulation, and epidermal organelles.,” *J. Invest. Dermatol.*, vol. 133, no. 8, pp. 2031–40, Aug. 2013.

[10] C. Cataisson, R. Salcedo, S. Hakim, B. A. Moffitt, L. Wright, M. Yi, R. Stephens, R.-M. Dai, L. Lyakh, D. Schenten, H. S. Yuspa, and G. Trinchieri, “IL-1R-MyD88 signaling in keratinocyte transformation and carcinogenesis.,” *J. Exp. Med.*, vol. 209, no. 9, pp. 1689–702, Aug. 2012.

[11] K. Loser, J. Apelt, M. Voskort, M. Mohaupt, S. Balkow, T. Schwarz, S. Grabbe, and S. Beissert, “IL-10 controls ultraviolet-induced carcinogenesis in mice.,” *J. Immunol.*, vol. 179, no. 1, pp. 365–71, Jul. 2007.

[12] C. S. Harmon and T. D. Nevins, “IL-1 alpha inhibits human hair follicle growth and hair fiber production in whole-organ cultures.,” *Lymphokine Cytokine Res.*, vol. 12, pp. 197–203, 1993.

[13] R. Hoffmann, W. Eicheler, E. Wenzel, and R. Happle, “Interleukin-1beta-induced inhibition of hair growth in vitro is mediated by cyclic AMP.,” *J. Invest. Dermatol.*, vol. 108, pp. 40–42, 1997.

[14] A. J. Papadopoulos, R. A. Schwartz, and C. K. Janniger, “Alopecia areata. Pathogenesis, diagnosis, and therapy.,” *Am. J. Clin. Dermatol.*, vol. 1, no. 2, pp. 101–5.

[15] R. Hoffmann, E. Wenzel, A. Huth, P. van der Steen, M. Schäufele, H. P. Henninger, and R. Happle, “Cytokine mRNA levels in Alopecia areata before and after treatment with the contact allergen diphenylcyclopropenone.,” *J. Invest. Dermatol.*, vol. 103, no. 4, pp. 530–3, Oct. 1994.

[16] J. K. Tarlow, F. E. Clay, M. J. Cork, A. I. Blakemore, A. J. McDonagh, A. G. Messenger, and G. W. Duff, “Severity of alopecia areata is associated with a polymorphism in the interleukin-1 receptor antagonist gene.,” *J. Invest. Dermatol.*, vol. 103, pp. 387–390, 1994.

[17] L. C. Wood, P. M. Elias, C. Calhoun, J. C. Tsai, C. Grunfeld, and K. R. Feingold, “Barrier disruption stimulates interleukin-1 alpha expression and release from a pre-formed pool in murine epidermis.,” *J. Invest. Dermatol.*, vol. 106, pp. 397–403, 1996.

[18] E. Corsini, N. Sangha, and S. R. Feldman, “Epidermal stratification reduces the effects of UVB (but not UVA) on keratinocyte cytokine production and cytotoxicity.,” *Photodermatol. Photoimmunol. Photomed.*, vol. 13, pp. 147–152, 1997.

[19] L. E. Jensen, “Targeting the IL-1 family members in skin inflammation.,” *Curr. Opin. Investig. Drugs*, vol. 11, pp. 1211–1220, 2010.

[20] D. E. Griswold, J. R. Connor, B. J. Dalton, J. C. Lee, P. Simon, L. Hillegass, D. J. Sieg, and N. Hanna, “Activation of the IL-1 gene in UV-irradiated mouse skin: association with inflammatory sequelae and pharmacologic intervention.,” *J. Invest. Dermatol.*, vol. 97, pp. 1019–1023, 1991.

[21] C. L. Kutsch, D. A. Norris, and W. P. Arend, “Tumor necrosis factor-alpha induces interleukin-1 alpha and interleukin-1 receptor antagonist production by cultured human keratinocytes.,” *J. Invest. Dermatol.*, vol. 101, pp. 79–85, 1993.

[22] R. HOFFMANN, R. HAPPLE, and R. PAUS, “Elements of the interleukin-1 signaling system show hair cycle-dependent gene expression in murine skin,” *Eur. J. Dermatology*, vol. 8, no. 7, pp. 475–7, Oct. 1998.

[23] R. Hoffmann, W. Eicheler, a Huth, E. Wenzel, and R. Happle, “Cytokines and growth factors influence hair growth in vitro. Possible implications for the pathogenesis and treatment of alopecia areata.,” *Arch. Dermatol. Res.*, vol. 288, pp. 153–6, 1996.

[24] E. Healy and S. Rogers, “PUVA treatment for alopecia areata--does it work? A retrospective review of 102 cases.,” *Br. J. Dermatol.*, vol. 129, pp. 42–44, 1993.

[25] D. Bayramgürler, E. O. Demirsoy, A. Ş. Aktürk, and R. Kıran, “Narrowband ultraviolet B phototherapy for alopecia areata.,” *Photodermatol. Photoimmunol. Photomed.*, vol. 27, pp. 325–7, 2011.

[26] S. Müller-Röver, B. Handjiski, C. van der Veen, S. Eichmüller, K. Foitzik, I. A. McKay, K. S. Stenn, and R. Paus, “A comprehensive guide for the accurate classification of murine hair follicles in distinct hair cycle stages.,” *J. Invest. Dermatol.*, vol. 117, pp. 3–15, 2001.

[27] P. Rider, Y. Carmi, O. Guttman, A. Braiman, I. Cohen, E. Voronov, M. R. White, C. a Dinarello, and R. N. Apte, “IL-1α and IL-1β recruit different myeloid cells and promote different stages of sterile inflammation.,” *J. Immunol.*, vol. 187, pp. 4835–43, 2011.

[28] A. Emadi, R. J. Jones, and R. A. Brodsky, “Cyclophosphamide and cancer: golden anniversary.,” *Nat. Rev. Clin. Oncol.*, vol. 6, pp. 638–647, 2009.

[29] A. Haratake, Y. Uchida, and M. Schmuth, “UVB-induced alterations in permeability barrier function: roles for epidermal hyperproliferation and thymocyte-mediated response,” *J. Invest. Dermatol.*, vol. 108, no. 5, pp. 769–775, 1997.

[30] T. Kono, S. Kondo, T. J. Venner, D. N. Sauder, and R. C. McKenzie, “Inhibition of cytokine gene expression in mouse skin by subcutaneous injection of cyclosporine.,” *Skin Pharmacol.*, vol. 8, pp. 149–155, 1995.

[31] Y. H. Won, D. N. Sauder, and R. C. McKenzie, “Cyclosporin A inhibits keratinocyte cytokine gene expression.,” *Br. J. Dermatol.*, vol. 130, pp. 312–319, 1994.

CONCLUSION

The skin serves as the body's first line of defense against the environment. It withstands a constant assault by pathogenic microbes, ultraviolet radiation, desiccating atmospheric conditions, and physical damage to prevent bodily harm. In addition to serving as a protective barrier, it also serves as an environment for commensal bacteria that in turn contribute to the protective capacity of the skin, both producing antimicrobial molecules and occupying niches that prevent colonization by pathogenic bacteria. Damage to the skin, originating from infection or injury, stimulates common pathways that lead to both an immune response as well as a skin barrier repair response. Though past manuscripts have described the dual immunological and permeability barriers of the skin as originating from distinct pathways, more recent research has shown that these pathways are linked and that common stimuli promote both an immunological as well as a permeability barrier repair response.

The aim of the research conducted and presented in this thesis was to determine whether pattern recognition receptors contributed to skin permeability barrier homeostasis. The canonical function of pattern recognition receptors had previously been described a means of recognizing infectious microbes and mounting an immune response. We had initially hypothesized that due to the skin's proximity to numerous commensal and possibly pathogenic microbes, that recognition of these microbes by pattern recognition receptors in the epidermis could stimulate keratinocyte differentiation. Though we determined that TLR stimulation didn't affect epidermal differentiation, we discovered that TLR3 activation in keratinocytes promotes skin barrier repair. We observe that numerous genes essential for skin barrier repair are upregulated in keratinocytes following treatment with dsRNA. We also observe increases in epidermal lipids, lamellar bodies, and keratohyalin granules following treatment with dsRNA. We also determined that endogenous sources of dsRNA can activate TLR3-dependent skin barrier repair pathways in the epidermis. This can occur when UVB-damage to keratinocytes causes necrosis, which results in

release of endogenous RNA, and can serve as an activator of TLR3. These noncoding, endogenous ssRNAs form double-stranded regions which are then able to activate TLR3. Most importantly, we demonstrate that skin barrier repair following UVB exposure in *Tlr3*$^{-/-}$ mice is delayed and that TLR3 on both epithelial and myeloid derived cells are essential for proper skin barrier repair. The work contained in this thesis describes how TLR3, long described as a pattern recognition receptor recognizing viral dsRNA, can recognize RNA from damaged cells and promote skin barrier repair.

In Chapter 1, we describe how activation of TLR3 in keratinocytes can promote a program of skin barrier repair. We had initially tested numerous TLR ligands to assess their ability to activate differentiation markers, though showed that only Poly (I:C), a ligand of TLR3, could stimulate ABCA12, a lipid transporter important for proper skin barrier formation and permeability barrier repair. We initially also measured transcripts of structural components of the epidermis including keratin 10, involucrin and filaggrin, though saw that these genes which are markers of epidermal differentiation did not change following treatment with Poly (I:C). As ABCA12 had been shown to be important for trafficking epidermal lipids during keratinocyte differentiation and skin barrier repair, we hypothesized that Poly (I:C) might affect lipid metabolism in keratinocytes. To determine whether other genes in lipid metabolism pathways were affected in keratinocytes after exposure to dsRNA, we performed a microarray analysis, exploring global changes in gene expression. As we had hypothesized, the microarray analysis identified pathways in epidermal lipid metabolism including glycosphingolipid biosynthesis, sphingolipid metabolism, glycerophospholipid metabolism, ABC transporters, biosynthesis of unsaturated fatty acids, fatty acid metabolism, glycerolipid metabolism, and lineoleic acid metabolism as being important after dsRNA treatment of keratinocytes.

While a number of these lipid metabolism pathways are important during keratinocyte differentiation, they are highly upregulated following skin barrier disruption. Skin barrier

disruption research was a very active field of study during the 1990s though the mechanisms that regulated skin barrier repair had been identified as being dependent on calcium gradients that exist within the epidermis. Disruption of this gradient stimulated skin barrier repair, which is characterized by rapid trafficking of lamellar bodies to the stratum corneum where specialized epidermal lipids and other components important for skin barrier repair were released in order to restore permeability barrier function. These rapid changes were accompanies by increased lipid synthesis during the following days in order to replenish the contents of lamellar bodies. Disruption of the calcium gradient by means that did not disrupt the permeability barrier mimicked the results of barrier disruption. Additionally, barrier disruption followed by application of an occluding membrane to the skin, as to prevent water loss and thus maintain the calcium gradient, blocked the traditionally observed barrier repair response.

For this reason, we proposed that TLR3 activation may present an alternative mechanism to stimulate skin barrier repair in the absence of or in addition to calcium gradient disruption. We went on to demonstrate that treatment of keratinocytes or skin equivalents with dsRNA caused increased staining of lipids and that analysis of specific lipids by high performance thin layer chromatography showed that specific lipid content was altered by dsRNA treatment. We then demonstrated that skin barrier repair gene expression changes were dependent on TLR3 activation. We also showed that changes in sphingomyelin were dependent on TLR3 activation though other measured lipids did not show dependence on TLR3 activation. Future studies of lipid dynamics should explore the time dependent changes in the populations of different lipids in keratinocytes and skin after TLR3 activation as previous studies have shown delays of up to 48 hours in ceramide synthesis after barrier disruption. Looking at time dependent effects of dsRNA on lipid content may reveal other significant changes in specific epidermal lipids. Finally we were able to demonstrate TLR3-dependent changes in both lamellar bodies and keratohyalin granules in skin equivalents that had been exposed to dsRNA. In summary we show that dsRNA

treatment of keratinocytes mimics the response of keratinocytes to barrier disruption in that gene expression, lipid content, and epidermal organelles are affected during both processes.

In Chapter 2, we describe a physiological relevance of TLR3 activation on skin barrier repair processes in keratinocytes and identify addtional genes affected by TLR3 activation. While viral infection has historically been believed to the the source of ligands for TLR3 activation, a number of studies in the past decade have demonstrated that TLR3 can be activated by endogenous sources of RNA. As host sources of RNA exist as either coding or noncoding RNA, they all have the ability to complimentary base pair to itself forming double stranded stem loop regions. These double stranded stem loops can activate TLR3. In normal circumstances, RNA is compartmentalized away from TLR3 which signals from the endosome, and this interaction should not take place in homeostatic conditions. However in times of cell death, especially necrotic cell death, cells lose their membrane integrity and cellular contents are spilled into extracellular spaces. In this way, host RNA can be taken up by neighboring cells, trafficked to the endosome where it will encounter TLR3 and stimulate its activation.

In this skin, UVB radiation can cause damage to keratinocytes. Only the necrotic fraction of UV-damaged keratinocytes has been shown to stimulate TLR3 dependent inflammation. For this reason we decided to measure the effects of UVB-damaged keratinocytes on skin barrier repair gene expression. Like Poly (I:C), UVB-damaged keratinocyte products caused increased in skin barrier repair genes. Additionally, we observed that both Poly (I:C) and UVB-damaged keratinocytes stimulated tight junction and desmosome gene expression and that Poly(I:C) increased tight junction function in keratinocytes, which is another important component of the skin barrier. Recent studies had also shown that bacterial products can stimulate tight junction function through TLR2 signaling in keratinocytes but this was the first time that a TLR3 ligand was shown to stimulate keratinocyte tight junction function.

Recent studies in our lab have shown that U1 RNA, a single-stranded, noncoding RNA, increases in keratinocytes following UVB exposure and can stimulate TLR3-dependent inflammation in the skin due to the double stranded stem loop regions in its RNA structure. For this reason we wanted to determine whether U1 RNA, an endogenous RNA, could cause similar changes in skin barrier repair gene expression. As we had expected, U1 RNA caused TLR3-dependent changes in skin barrier repair gene expression almost identically to those caused by Poly (I:C). We were also able to demonstrate that other noncoding RNAs (U2, U4, U6, U12, scaRNA9, scaRNA18) showed similar changes in skin barrier repair and inflammatory gene expression. Similarly to U1 RNA, these noncoding RNAs can form double stranded stem loops.

We next hypothesized that because TLR3 activation was important for skin barrier repair processes in keratinocytes, *Tlr3*$^{-/-}$ mice would have a defect in skin barrier repair. Initial experiments however showed no difference in skin barrier repair phenotypes between wild type and *Tlr3*$^{-/-}$ mice by observing transepidermal water loss. In these experiments, we used tape-stripping or application of a keratolytic depilatory reagent to induce skin barrier disruption. As no differences were seen between wild type and mutant mice following these experiments, we then hypothesized that these models of barrier disruption might be too superficial of gentle to cause cell death that would release RNA that could activate TLR3. It was also probable that even in *Tlr3*$^{-/-}$ mice, changes in calcium gradient caused by these forms of barrier disruption would stimulate barrier repair and that any changes dependent on TLR3 activation would be masked by calcium gradient-dependent skin barrier repair. We then decided to use UVB exposure as a means of skin barrier disruption. It had been published that UVB exposure caused dose dependent increases in skin barrier disruption, and recent studies from our lab showed that UVB had significant effects on TLR3-dependent inflammation. UVB-barrier disruption proved to be an ideal model, as *Tlr3*$^{-/-}$ mice showed a barrier repair defect following this form of barrier disruption. We were also able to demonstrate that TLR3 present on both resident epithelial cells

and myeloid cells contribute to proper skin barrier repair. Future research in this area will explore cell type specific contributions to skin barrier repair following UVB damage to the skin.

In Chapter 3, we describe how scavenger receptors on keratinocytes likely play an important role in recognizing damaged cellular products such as RNA and also stimulate skin barrier repair independent of TLR3 activation. This finding was quite interesting as we attempted to block uptake of dsRNA into keratinocytes by pretreatment with scavenger receptor ligands only to discover that scavenger receptors were able to stimulate skin barrier repair genes without Poly (I:C) present. We next attempted to determine whether specific scavenger receptors were necessary for Poly (I:C)-induced skin barrier repair gene expression by knockdown of CD36, MARCO, or OLR1. Single knockdown of these receptors had no effect on Poly (I:C)-induced skin barrier repair gene expression. It is likely though that specific scavenger receptors in keratinocytes serve a redundant role and that knockdown of a single receptor may not prevent uptake of Poly (I:C) or scavenger receptor dependent changes in skin barrier repair genes. Interestingly, mice deficient in *Msr1* show a skin barrier repair defect following tape-stripping skin barrier disruption. Though an interesting finding, more studies need to be done as to why this receptor is important to skin barrier repair in mice. It is likely that this process does not depend on TLR3 and is probably recognizing a yet unknown ligand that could activate skin barrier repair processes. As tape-stripping disturbs the epidermal calcium gradient, it would be interesting to determine whether *Msr1* somehow recognizes ligands associated with this change in the epidermis following barrier disruption.

In Chapter 4, we present data that shows the importance of IL-1R in chronically UVB exposed skin. In these studies we had initially wanted to test whether TLR3 or IL-1R contributed to UVB-induced carcinogenesis as it had been previously shown that other inflammatory pathways contribute to cutaneous carcinogenesis, including IL-1R. Interestingly we observed the appearance of dermal hair cysts in *Il1r*$^{-/-}$ mice that had been chronically treated with UVB

radiation. Though the effects of UVB on hair growth are relatively unknown, a few studies have shown that IL-1R signaling may prevent hair growth and be involved in patient with alopecia areata. Future studies should determine how UVB exposure may influence hair growth and how IL-1R signaling is involved in hair growth. Additionally in this chapter we provide evidence that IL-1R signaling does not stimulate Poly (I:C)-induced skin barrier repair, though is important for UVB-induced skin barrier disruption.

In summary, TLR3 activation in the skin is an important process that is essential for proper skin barrier repair in response to UVB damage and may also be important during other types of damage to the skin. As TLR3 activation alters lipid composition and trafficking in the skin, this pathway should be explored in the context of atopic dermatitis. A number of recent studies have shown correlation between lipid chain length and severity of atopic dermatitis phenotypes. It has yet to be investigated whether TLR3 activation in atopic dermatitis patients is altered. While changes in gene expression, lipids, and epidermal organelles have only been explored at 24 to 72 hours after TLR3 activation, future studies should aim to define the time dependent changes in lipid content in the skin and how organelle trafficking changes during the skin barrier repair process. Future studies should also aim to identify cellular mediators that are downstream of TLR3 signaling that have direct effects on skin barrier repair. We have shown in preliminary studies that cultured supernatants of keratinocytes treated with Poly (I:C) have more robust effects on skin barrier repair gene expression so it is likely that there are soluble factors released by keratinocytes that promote skin barrier repair. While excessive TLR3 signaling can be detrimental, it is clear that certain components of downstream signaling are beneficial to tissue repair. A better understanding of these processes will help future researchers and physicians to design better therapeutics for excessive inflammatory diseases that might involve excessive TLR3 signaling. As TLR3 continues to be implicated in non infectious processes in various cell types, research on this important receptor should remain a focal point for years to come.

APPENDIX A:

The coordinated response of the physical and antimicrobial peptide barriers of the skin

Abstract

Antimicrobial peptides (AMPs) are an essential and multifunctional element for immune defense of the skin during infection and injury. In this issue, Ahrens *et al.* characterize the response of β-defensins, a class of AMPs, following acute and chronic challenges to the permeability barrier of the skin. Their findings suggest that the antimicrobial and permeability barriers of the skin are closely linked.

Introduction

The multiple defensive functions of the skin depend on its ability to detect danger from a broad range of physical, chemical and microbiological challenges and are interconnected in a way to minimize damage. These defensive functions are often thought of as acting through two simultaneously acting barriers, the immune antimicrobial barrier and the physical permeability barrier. Following physical injury to the skin a cascade of events occurs to restore the breached skin barrier and reestablish homeostasis. In contrast, during infection, microbes encounter both the complex lipid and protein structures of the stratum corneum and an array of antimicrobial molecules that are present or may be triggered by a set of pattern recognition receptors. In combination, these barriers typically act to facilitate the elimination of the pathogen. In recent years, it has been shown that the pathways that generate and regulate the antimicrobial barrier of the skin are closely tied to pathways that modulate permeability barrier function [1]–[4]. In this issue, Ahrens *et al*. report that both acute and chronic skin barrier disruption lead to increased expression of murine β-defensins (mBDs)-1, -3, and -14 and that this increase in expression is diminished when the barrier is artificially restored [5]. Their data contribute to the concept that the antimicrobial and permeability barriers of the skin are closely linked.

Antimicrobial nature of the skin

The integrity of the skin barrier is essential for it to properly serve its purpose as a shield from the environment. Keratinocytes are at the forefront of this defense as they are the cell type that makes up a majority of the epidermis and are in constant contact with the outside world. Keratinocytes are responsible for producing the stratum corneum, the terminally differentiated outer layer of the epidermis comprised of rigid anucleate corneocytes cemented by hydrophobic lipid-rich lamellar bilayers that functions to impede water loss and protect from pathogenic organisms [6]. While keratinocytes serve as a physical barrier, they also express a vast array of

molecules that contribute to the antimicrobial properties of the skin [7]. The skin possesses a wide arsenal of weapons to combat possible invaders. Constant desquamation of the skin makes it difficult for organisms to establish a permanent residence. The surface of the skin is an acidic environment (pH ~5.5) that makes it uninhabitable to many microorganisms. Additionally, it has been suggested that the microflora that normally inhabit our skin can contribute to barrier defenses by competing for nutrients and niches that more pathogenic organisms desire, by expressing antimicrobial molecules that kill or inhibit the growth of pathogenic microbes [8], [9], and by modulating the inflammatory response [10].

Over the past decade it has become increasingly apparent that keratinocytes and other cells resident to the skin produce a number of antimicrobial molecules that are important to maintaining immunological homeostasis [11]. A large number of studies of antimicrobial peptides (AMPs) in many organ systems have shown them to possess a wide range of activities including direct microbial killing, chemotaxis, modification of inflammatory responses, as well as angiogenesis and wound healing [10]. Over 1200 AMPs have thus far been identified or predicted. They are generally small in size (12-50aa), positively charged and have an amphipathic structure. They contain common secondary structures that vary from alpha helical to beta-sheets, and their unifying characteristic is the ability to kill microbes or inhibit them from growing. Cathelicidins and defensins are two classes of AMPs that have been well characterized and studied in the skin. The cathelicidin protein hCAP18 as well as the human β-defensins (hBD)-1, -2, and -3 are directly produced in keratinocytes and packaged in lamellar bodies prior to extrusion to the stratum corneum [12]. hBD2 and hBD3 are induced following activation with bacteria or cytokines [13], [14]. hCAP18 can be induced by vitamin D, and is proteolytically activated to several peptide forms, the most commonly studied being LL-37, a form that is predominantly produced by neutrophils. Though these two groups of AMPs dominate the AMP literature, over 20 other AMPs have been identified in the skin. In addition to their antimicrobial

activity, some AMPs possess protease/enzyme activity, chemotactic activity and neuropeptide activity [15]. Other skin resident cells such as sebocytes, eccrine glands and mast cells also produce AMPs while neutrophils and natural killer cells can be recruited to the skin and deposit additional AMPs following wounding or infection [1]. The elucidation of the multifunctional roles of AMPs in the skin has made the regulation of their expression a focus of research in recent years.

AMPs have a wide range of functions, some still yet to be understood. First and foremost AMPs exert direct antimicrobial activity. This effect is achieved by binding of the cationically charged AMP to negatively charged phospholipid head groups present in many bacteria in the form of lipopolysaccharide, teichoic acids, lipoteichoic acids and lysylphosphatidylglycerol [10]. This binding results in membrane destabilization and produces a physical disruption of the membrane or cell wall of the microbe leading to decreased growth or death. AMPs also play an important role in modulating the host immune response following infection or injury. They can recruit leukocytes directly or stimulate cells to release IL-8, MCP-1, and IFN-α, thereby indirectly recruiting other effector cells including: neutrophils, macrophages, monocytes, immature dendritic cells and T cells to the site of injury/infection. These functions can also influence wound healing where some AMPs have been shown to stimulate migration, proliferation, and tube formation of endothelial cells, cell proliferation, and have been implicated in reepithelialization of the skin [16].

Interdependence of the antimicrobial and permeability barriers

Because AMPs play such a wide range of roles in the skin, it is not hard to imagine that they would also impact the permeability barrier of the skin. Several papers that have studied the expression of the endogenous AMPs in keratinocytes have suggested that their expression coincides with a number of epidermal structural components (involucrin, loricrin, keratin-1, -10,

transglutaminase-1, -3, specialized lipids, and other processing enzymes) and may become part of the permeability barrier. Importantly, prior studies by Aberg *et al.*, 2007 and Aberg *et al.*, 2008 have shown that the murine cathelin-related antimicrobial peptide CRAMP (the murine ortholog of LL37), and mBD-3 (the murine ortholog of hBD-2), are essential for permeability barrier homeostasis. This work also demonstrated that acute and chronic disruption of the physical barrier leads to induction of CRAMP and mBD-3.

In this issue, Ahrens *et al*. further characterize the response of AMP expression to barrier disruption. They show that mBD-1, -3, and -14 (orthologs of hBD-1, -2, -3) are all upregulated following barrier disruption. In their experiments they use acute barrier disruption methods including tape stripping and acetone treatment as well as a metabolically induced chronic barrier disruption achieved by maintaining mice on an essential fatty acid deficient (EFAD) diet. These methods of barrier disruption all lead to increased levels of mBD mRNA and protein. Artificial restoration of the barrier by occlusion moderately inhibited the increases in mBD expression following acute barrier disruption or drastically inhibited it following chronic barrier disruption. They also showed that the growth factor TGF-α modulates the mBD-14 response and that TNF-α modulates the mBD-3 response. These studies highlight the importance of AMPs to the permeability barrier of the skin, and provide further evidence of a dynamic interplay between the physical barrier and the chemical shield provided by AMPs against infection (Figure A.1).

This field remains wide-open to discovery and promises to continue to advance our understanding of many aspects of skin biology. AMP dysfunction has been implicated in a number of skin diseases including psoriasis, rosacea and atopic dermatitis (AD). In psoriasis, AMPs including LL37, hBD-2 and hBD-3 are all upregulated and are believed to contribute to inflammation and the etiology of the disease [17], [18]. In rosacea, LL37 is also highly upregulated and contributes to the progression of the disease [19]. On the other hand, in AD, LL37, hBD-2 and hBD-3 are all downregulated and this dearth of AMPs in AD patients leaves

them more susceptible to infection [20]. Based on the current studies it is intriguing to speculate that the decrease in AMPs after injury could also be a reason that they show increased levels of transepidermal water loss in both lesional and nonlesional skin [21]. By gaining a better understanding of the processes that regulate AMP expression, and their interactions with the barrier properties of the epidermis, it may be possible to develop novel and more effective therapeutics for diseases associated with disruption of the physical and immunological homeostatic mechanisms of the skin.

Clinical Implications:

- Antimicrobial peptides play a multifunctional role in the body; protecting from infection, modulating immune responses, and contributing to wound repair.
- Control of the antimicrobial and permeability barriers of the skin occurs simultaneously following disruption of the skin barrier, strengthening the concept that they are closely linked.
- Antimicrobial peptide expression is dysregulated in a number of inflammatory skin diseases including psoriasis, rosacea and atopic dermatitis.

Acknowledgement:

Appendix A, in full, is a reprint of the material as it appears in The Journal of Investigative Dermatology 2011. A. W. Borkowski, R. L. Gallo. The coordinated response of the physical and antimicrobial peptide barriers of the skin. *J Invest Dermatol*. 2011, 131(2): 285-287. The dissertation author was the primary investigator and author of this paper.

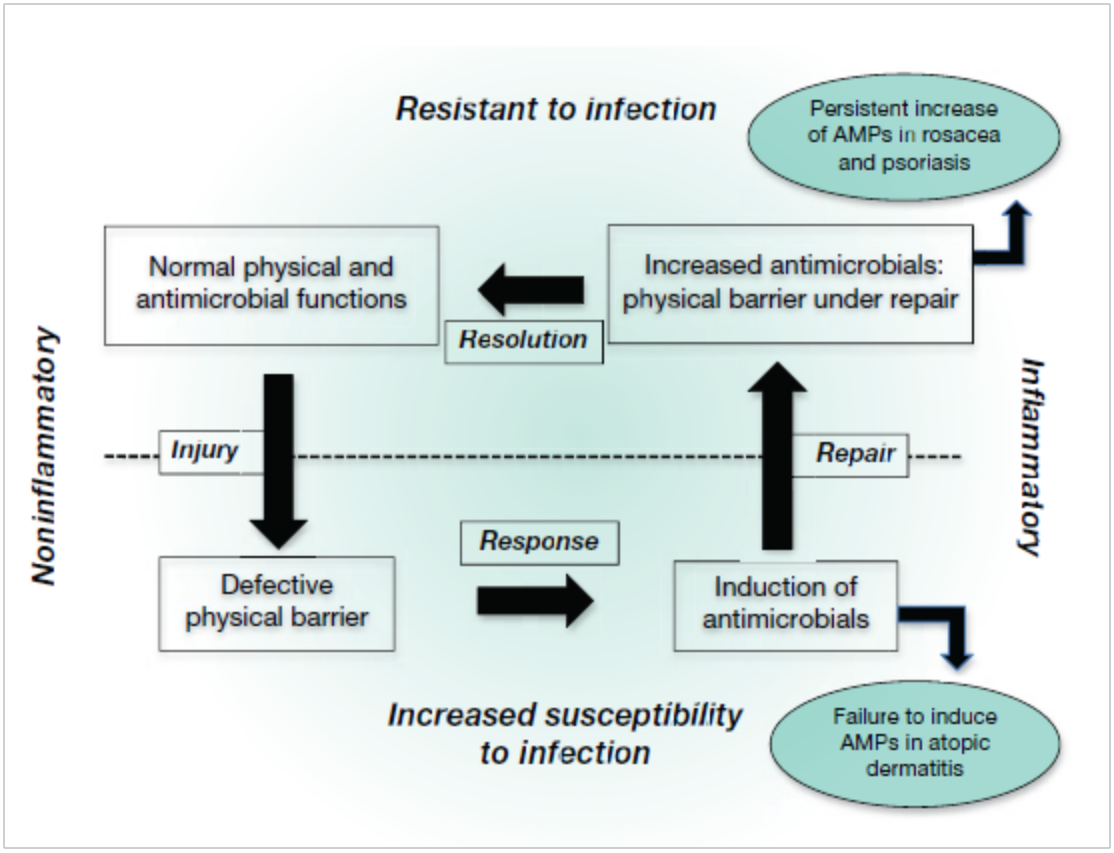

Figure A.1: Homeostasis of the physical and antimicrobial barrier of the skin. Counterclockwise upper left: Under resting conditions the multiple elements of the physical permeability barrier and the antimicrobial defense shield combine for resistance to microbial invasion in the absence of inflammation. Following injury, a defect in barrier function triggers a response that includes induction of antimicrobial peptide production. The increase in antimicrobials is deficient in patients with atopic dermatitis. Under normal conditions the repair process results in increased antimicrobial expression in a setting of a decreased barrier, thus restoring resistance to microbial invasion. Patients with rosacea and psoriasis have persistent elevated expression of antimicrobials that perpetuates inflammation. Upon resolution of the repair process the physical and antimicrobial barriers regain a state of homeostasis. AMP, antimicrobial peptide.

References:

[1] R. A. Dorschner, V. K. Pestonjamasp, S. Tamakuwala, T. Ohtake, J. Rudisill, V. Nizet, B. Agerberth, G. H. Gudmundsson, and R. L. Gallo, "Cutaneous injury induces the release of cathelicidin anti-microbial peptides active against group A Streptococcus.," *J. Invest. Dermatol.*, vol. 117, pp. 91–97, 2001.

[2] J. Schauber, R. A. Dorschner, A. B. Coda, A. S. Büchau, P. T. Liu, D. Kiken, Y. R. Helfrich, S. Kang, H. Z. Elalieh, A. Steinmeyer, U. Zügel, D. D. Bikle, R. L. Modlin, and R. L. Gallo, "Injury enhances TLR2 function and antimicrobial peptide expression through a vitamin D-dependent mechanism.," *J. Clin. Invest.*, vol. 117, pp. 803–811, 2007.

[3] K. M. Aberg, K. A. Radek, E.-H. Choi, D.-K. Kim, M. Demerjian, M. Hupe, J. Kerbleski, R. L. Gallo, T. Ganz, T. Mauro, K. R. Feingold, and P. M. Elias, "Psychological stress downregulates epidermal antimicrobial peptide expression and increases severity of cutaneous infections in mice.," *J. Clin. Invest.*, vol. 117, pp. 3339–3349, 2007.

[4] K. M. Aberg, M.-Q. Man, R. L. Gallo, T. Ganz, D. Crumrine, B. E. Brown, E.-H. Choi, D.-K. Kim, J. M. Schröder, K. R. Feingold, and P. M. Elias, "Co-regulation and interdependence of the mammalian epidermal permeability and antimicrobial barriers.," *J. Invest. Dermatol.*, vol. 128, pp. 917–925, 2008.

[5] K. Ahrens, M. Schunck, G.-F. Podda, J. Meingassner, A. Stuetz, J.-M. Schröder, J. Harder, and E. Proksch, "Mechanical and metabolic injury to the skin barrier leads to increased expression of murine β-defensin-1, -3, and -14.," *J. Invest. Dermatol.*, vol. 131, pp. 443–452, 2011.

[6] E. Candi, R. Schmidt, and G. Melino, "The cornified envelope: a model of cell death in the skin.," *Nat. Rev. Mol. Cell Biol.*, vol. 6, no. 4, pp. 328–40, Apr. 2005.

[7] P. M. Elias, "The skin barrier as an innate immune element.," *Semin. Immunopathol.*, vol. 29, pp. 3–14, 2007.

[8] A. L. Cogen, K. Yamasaki, K. M. Sanchez, R. A. Dorschner, Y. Lai, D. T. MacLeod, J. W. Torpey, M. Otto, V. Nizet, J. E. Kim, and R. L. Gallo, "Selective antimicrobial action is provided by phenol-soluble modulins derived from Staphylococcus epidermidis, a normal resident of the skin.," *J. Invest. Dermatol.*, vol. 130, pp. 192–200, 2010.

[9] T. Nakatsuji, M. C. Kao, L. Zhang, C. C. Zouboulis, R. L. Gallo, and C.-M. Huang, "Sebum free fatty acids enhance the innate immune defense of human sebocytes by upregulating beta-defensin-2 expression.," *J. Invest. Dermatol.*, vol. 130, pp. 985–994, 2010.

[10] Y. Lai and R. L. Gallo, "AMPed up immunity: how antimicrobial peptides have multiple roles in immune defense," *Trends in Immunology*, vol. 30. pp. 131–141, 2009.

[11] R. L. Gallo and K. M. Huttner, “Antimicrobial peptides: an emerging concept in cutaneous biology.,” *J. Invest. Dermatol.*, vol. 111, pp. 739–743, 1998.

[12] M. H. Braff, A. Di Nardo, and R. L. Gallo, “Keratinocytes store the antimicrobial peptide cathelicidin in lamellar bodies.,” *J. Invest. Dermatol.*, vol. 124, pp. 394–400, 2005.

[13] A. Y. Liu, D. Destoumieux, A. V Wong, C. H. Park, E. V Valore, L. Liu, and T. Ganz, “Human beta-defensin-2 production in keratinocytes is regulated by interleukin-1, bacteria, and the state of differentiation.,” *J. Invest. Dermatol.*, vol. 118, pp. 275–281, 2002.

[14] Y. Lai, A. L. Cogen, K. A. Radek, H. J. Park, D. T. Macleod, A. Leichtle, A. F. Ryan, A. Di Nardo, and R. L. Gallo, “Activation of TLR2 by a small molecule produced by Staphylococcus epidermidis increases antimicrobial defense against bacterial skin infections.,” *J. Invest. Dermatol.*, vol. 130, pp. 2211–2221, 2010.

[15] M. H. Braff and R. L. Gallo, “Antimicrobial peptides: an essential component of the skin defensive barrier.,” *Curr. Top. Microbiol. Immunol.*, vol. 306, pp. 91–110, 2006.

[16] J. D. Heilborn, M. F. Nilsson, G. Kratz, G. Weber, O. Sørensen, N. Borregaard, and M. Ståhle-Bäckdahl, “The cathelicidin anti-microbial peptide LL-37 is involved in re-epithelialization of human skin wounds and is lacking in chronic ulcer epithelium.,” *J. Invest. Dermatol.*, vol. 120, pp. 379–389, 2003.

[17] M. Gilliet and R. Lande, “Antimicrobial peptides and self-DNA in autoimmune skin inflammation,” *Current Opinion in Immunology*, vol. 20. pp. 401–407, 2008.

[18] R. Lande, J. Gregorio, V. Facchinetti, B. Chatterjee, Y.-H. Wang, B. Homey, W. Cao, Y.-H. Wang, B. Su, F. O. Nestle, T. Zal, I. Mellman, J.-M. Schröder, Y.-J. Liu, and M. Gilliet, “Plasmacytoid dendritic cells sense self-DNA coupled with antimicrobial peptide.,” *Nature*, vol. 449, pp. 564–569, 2007.

[19] K. Yamasaki, A. Di Nardo, A. Bardan, M. Murakami, T. Ohtake, A. Coda, R. A. Dorschner, C. Bonnart, P. Descargues, A. Hovnanian, V. B. Morhenn, and R. L. Gallo, “Increased serine protease activity and cathelicidin promotes skin inflammation in rosacea.,” *Nat. Med.*, vol. 13, pp. 975–980, 2007.

[20] P. Y. Ong, T. Ohtake, C. Brandt, I. Strickland, M. Boguniewicz, T. Ganz, R. L. Gallo, and D. Y. M. Leung, “Endogenous antimicrobial peptides and skin infections in atopic dermatitis.,” *N. Engl. J. Med.*, vol. 347, pp. 1151–1160, 2002.

[21] Y. Werner and M. Lindberg, “Transepidermal water loss in dry and clinically normal skin in patients with atopic dermatitis.,” *Acta Derm. Venereol.*, vol. 65, pp. 102–105, 1985.

APPENDIX B:

Ultraviolet B radiation illuminates the role of TLR3 in the epidermis

Abstract:

UV radiation poses a significant risk to human health. The mechanisms that help repair UV-damaged cells have recently been more clearly defined with the observation that Toll-like receptor 3 can sense self RNA released from necrotic keratinocytes following UV damage. TLR3 activation in the skin induces inflammation and increases expression of genes involved in skin barrier repair. Activation of TLR2 in the skin by commensal microbial products prevents excessive inflammation by blocking downstream TLR3 signaling. This review highlights how UV damage induced inflammation in the skin is propagated by host products and regulated by host inhabitants.

Introduction

Excessive exposure to ultraviolet (UV) radiation is dangerous and has significant negative effects on human health. In the year 2000, excessive exposure to UV light led to 60,000 deaths worldwide with 1.5 million disability-adjusted life years (DALYs) also lost [1]. A majority of the reported morbidity and mortalities were linked to skin cancer; including melanoma, basal cell carcinoma, and squamous cell carcinoma, though sunburn also had a significant contribution to the 1.5 million DALYs lost. Furthermore, the economic and psychological impact of solar aging remains unquantified.

Despite the great impact on human health, relatively little research has been dedicated towards understanding the biological events associated with this common process. Much more work has been applied to understanding the benefits of solar exposure. UV light is needed to synthesize Vitamin D, which is necessary for human health [2], [3]. Complete sun avoidance would result in diseases related to Vitamin D deficiency and it is predicted that these diseases would lead to 3,304 million DALYs to be lost [1]. In addition to generation of Vitamin D, low levels of UV radiation also enhance permeability barrier function of the skin. Skin exposed to either UVA or UVB radiation prior to chemical irritant application is more resistant to damage as measured by transepidermal water loss (alkali resistance test, dimethylsulfoxide test and sodium lauryl sulfate test) [4]. Barrier repair is also accelerated in skin that has been previously exposed to sub-erythemal broadband UVB radiation prior to tape-stripping barrier disruption. In these studies, it was also observed that antimicrobial peptide production is increased following low level broadband UVB exposure [5]. Furthermore, UVB radiation can provide therapeutic benefit to patients with certain dermatological conditions. Patients with Psoriasis are commonly treated with narrow band UVB [6] and atopic dermatitis patients with either narrow, broad, or combination UVA/UVB [7], [8] exposure as the beneficial effects typically outweigh the apparent long term negative effects. UVB damage to the skin results in inflammation

characterized by increased NF-κB activation, increased inflammatory cytokines including TNF and IL-6, increases in cis-urocanic acid, prostaglandins, reactive oxygen species, and DNA damage [9], [10]. As is the case for the negative effects of UV on the skin, the mechanisms behind the beneficial effects of UVB are still unclear. However, new insights into the functions of the innate immune system have opened a window of opportunity to better understand these important interactions.

Innate immune receptors recognize products of cell death

It has been historically described that the primary function of the innate immune system is to detect pathogens and to rid them from the body. These microbes have unique physical characteristics termed microbe associated molecular patterns (MAMPs) that allow them to be recognized as foreign by the host's array of pattern recognition receptors (PRRs) that are present on various immune cells as well as epithelial cells including keratinocytes [11]. At the most fundamental level, it is appropriate to recognize that activation of these PRRs causes an immune response that induces inflammation and eliminates the microbe from the host. However, these same innate immune receptors have the capability to recognize many different chemical structures in addition to those found on microbes. An important class of such non-microbial compounds is made up of certain endogenous molecules made by the host but normally separated from PRR by nature of their compartmentalization. During times of cell death, when compartmentalization of intracellular environments is disturbed, many of these host components are released into an extracellular environment, and this can illicit an immune response. These endogenous molecules that can activate an immune response in a sterile environment, absent of infection, are termed damage associated molecular patterns (DAMPs) and similarly to MAMPs, they activate PRRs resulting in inflammation and recruitment of leukocytes [12].

Regulated cell death in the skin is an ongoing process as keratinocytes terminally differentiate and undergo the process of cornification in order to produce the stratum corneum [13]. UV damage however, can cause unintended damage to keratinocytes and subsequent cell death in the skin, often observable in histological sections as “sunburn cells”, which are accepted to be keratinocytes undergoing apoptosis [14]. High doses of UV radiation cause formation of cyclobutane pyrimidine dimers and (6-4) photoproducts in DNA which leads to mutations that can eventually result in skin cancer [9] when nucleotide excision repair fails [15]. For this reason, it is essential for the health of an individual to dispose of these mutated cells by way of apoptosis. It has been shown that mice lacking p53, an important factor for apoptotic signaling, accumulate significantly more skin tumors than wild-type mice after chronic exposure to broadband UVB [16]. Apoptosis serves an essential role in response to sunburn, though is generally shown to be an anti-inflammatory or immunosuppressive event [17], [18].

While UVB-induced apoptosis has been extensively described as occurring in the skin after UVB damage, much less is known about the extent of necrosis that occurs following UVB damage to keratinocytes *in vivo*. *In vitro* studies have shown that exposing keratinocytes to narrowband UVB radiation produces fractions of immunostimulatory, necrotic cells (Annexin V –, PI+) in addition to non-immunostimulatory apoptotic cells (Annexin V+, PI-)[19]. While *in vivo* studies have not explicitly shown necrosis occurring in the epidermis, it has also been described that apoptotic cells can progress to secondary necrosis if they are not properly cleared by phagocytic cells [12], [20], [21]. Many mediators of both apoptosis and necrosis, including TNF, are known to be stimulated following UVB exposure [19], [22], [23]. In this context, it could be speculated that sunburn leads to necrosis in the skin. Interestingly it has recently been shown that HMGB1, a danger signal released from necrotic cells [24], is released from both cultured keratinocytes as well as keratinocytes present in murine skin following UVB exposure [25]. While this DAMP has also been shown to be actively secreted from monocytes and

macrophages, [26], [27], its immunostimulatory potential has been well described following necrosis [12], [24], [28]. HMGB1 has also been shown to be released during pyroptosis, a specialized form of proinflammatory cell death [29]. Whether HMGB1 release from keratinocytes exposed to UVB is an active or passive process remains to be determined.

As necrosis has classically been described as an unregulated form of cell death in which membrane integrity is lost, it has only been observed *in vitro* in keratinocytes in which membrane permeability can be measured or where morphology of a rupturing cell membrane could be observed. This has made observing necrosis *in vivo* difficult. In more recent years however, necrotic cell death has been shown to be dependent on the activation of RIPK1 and/or RIPK3 and has earned the name necroptosis when dependence on these kinases is demonstrated [30], [31]. Additionally, another specialized type of proinflammatory cell death known as pyroptosis, which is dependent on caspase-1 activation, may also be occurring after UVB damage to keratinocytes. It has been demonstrated that UVB radiation can stimulate inflammasome dependent IL-1β activation and secretion in keratinocytes [32]. This process is dependent on caspase-1 and can be induced by either inflammasome or pyroptosome formation [33], which can lead to pyroptosis [22], [34]. To what extent levels of apoptosis and necrosis or other forms of cell death are mediated after UVB exposure or whether one pathway is more prevalent at different UV doses is yet to be determined. It has been demonstrated however, that increasing UVC and broadband UVB exposure causes dose-dependent increases in apoptosis [35], [36]. It has also been shown that higher doses of broadband UVB can induce necrosis in keratinocytes [36], [37]. As not all cells in the epidermis visably undergo apoptosis, though theoretically receive the same amount of energy from UV radiation, it is possible that nonapoptotic forms of cell death are occurring in the epidermis after UV damage.

Once membrane integrity is lost during necrosis, cellular components from these damaged cells spill into extracellular spaces [21]. These intracellular components are ‘foreign’ to

an extracellular environment, and thus are treated so by the immune system. A number of cellular products have been observed to stimulate PRRs, especially during necrosis, including HMGB1 [24], S100 proteins [38], heat shock proteins [39], ATP [40], uric acid [41], hyaluronan [42], [43], chromatin [44] and RNA [19], [23], [45], [46]. These molecules, some of which are normally confined to the interior of a cell, gain the ability to activate certain PRRs including Toll-like receptors (TLRs). It has been demonstrated that the PRRs TLR2, TLR3, TLR4, and TLR9 can recognize certain DAMPs and induce an immune response.

TLR3 senses cellular damage following sunburn

TLR3 is a PRR that binds double-stranded RNA (dsRNA) [47]. Though it has traditionally been accepted that dsRNA is a marker of viral infection or replication [48], more recent evidence demonstrates that endogenous sources of RNA can also activate TLR3. In 2004 Kariko et al., showed that TLR3 on dendritic cells could be activated by RNA associated with necrotic cells and also by *in vitro* transcribed mRNA [45]. In this study, when necrotic cells or mRNA was treated with benzonase, a nuclease that degrades all DNA and RNA, the necrotic cells no longer showed the ability to activate inflammatory pathways. In 2008, Cavassani et al., confirmed these findings *in vivo* demonstrating that less inflammation was present in sterile gut injury models in *Tlr3*$^{-/-}$ mice. They also showed that macrophages treated with necrotic cells needed functional Tlr3 to produce chemokines. Additionally, they demonstrated that macrophages treated with apoptotic cells produced significantly less cytokines than when treated with necrotic cells [46]. This study demonstrates that if RNA is confined to intracellular compartments, as in apoptotic cells, it is unable to activate Tlr3. Only when RNA leaves the confines of the cell membrane, does it become immunostimulatory.

In 2009, Lai et al. demonstrated that in a sterile wound model in the skin, TNF and IL-6 production was diminished in *Tlr3*$^{-/-}$ mice [19]. This publication also demonstrated that

narrowband UVB-damaged keratinocytes, when added to keratinocyte cultures, could stimulate the inflammatory cytokines TNF and IL-6, through activation of TLR3. When the UVB-damaged normal human epidermal keratinocytes were treated with RNase, they no longer induced inflammatory cytokines [19]. In 2011, Lin et al. demonstrated that Tlr3 activation was also important for wound healing in the skin. They showed that *Tlr3*$^{-/-}$ mice displayed a delay in wound healing, showing deficiencies of infiltrating neutrophils and macrophages [49]. They also were able to demonstrate that by applying the TLR3 ligand Poly (I:C), a dsRNA mimetic, to the wounds of mice as well as humans, wound healing was accelerated [50]. These studies suggest that RNA released from damaged keratinocytes induces TLR3-dependent inflammation that promotes tissue repair. It has also been observed that activation of TLR3 in keratinocytes leads to increases in epidermal lipid transport and lipid metabolism gene expression, lipid accumulation and increased lamellar bodies [51]. Because epidermal lipids are essential for proper barrier function and must be regenerated following injury to the epidermis, it can be speculated that activation of TLR3 in the skin helps to restore proper barrier function following UV injury.

Although the phenomenon that necrotic cells could stimulate TLR3 had been published multiple times in multiple cell types, it wasn't until 2012, that an endogenous ligand for TLR3 was discovered. Bernard et al. demonstrated that narrowband UVB damage to keratinocytes released U1 RNA, a noncoding small nuclear RNA (snRNA), and component of the spliceosome, that could act as a DAMP and activate TLR3 to induce the inflammatory cytokines TNF and IL-6. Bernard and colleagues used RNA sequencing to determine that U1 RNA was significantly increased in keratinocytes 24 hours after narrowband UVB exposure. It was also discovered that in addition to U1 RNA, numerous additional noncoding RNAs were increased in keratinocytes after narrowband UVB exposure [23]. Although these studies focused on the effects of U1 RNA, it is possible that any of these noncoding RNAs could act as DAMPs.

dsRNA is the required ligand for TLR3 activation [47]. Therefore, for an endogenous single-stranded RNA to be recognized by TLR3, it must form double-stranded regions. U1 RNA has a secondary structure comprised of four double-stranded stem-loop regions. These double-stranded regions serve to activate TLR3. The addition of U1 RNA or only a single stem-loop region of U1 RNA to keratinocytes was sufficient to induce TNF. Also, U1 RNA injected into ears of mice only induced inflammation when functional Tlr3 was present [23]. It is believed that UVB damage to keratinocytes causes necrosis and that RNA released from necrotic keratinocytes can signal in a paracrine manner to induce inflammation in the skin through TLR3 on neighboring cells (Figure B.1).

TLR3 is not the only TLR that has been implicated in the host response to UVB damage. While it is believed that dsRNA released from necrotic keratinocytes plays a role in this response, it is possible that other cells types in the skin can also undergo necrosis and contribute to this phenotype. It has been demonstrated that TLR3 and TLR4 activation can cause necrosis in macrophages that are treated with pan-caspase inhibitors [52] TLR4 which can be activated by numerous DAMPs including hyaluronan [42], [43], [53], HMGB1, uric acid, heat shock proteins, defensins as well as the bacterial ligand LPS [12], has also been shown to play a role in UVB induced immune suppression, as *Tlr4*$^{-/-}$ mice fail to exhibit UVB-induced immunosuppression in a contact hypersensitivity model [54]. The same phenotype is seen in *Tlr3*$^{-/-}$ mice, which also fail to show immunosuppression to DNFB contact hypersensitivity when first exposed to narrowband UVB radiation [23]. There is also evidence that TLR4 may play a detrimental role in the response to UVB as *Tlr4*$^{-/-}$ mice show increased nucleotide excision repair in skin [55] after UVB exposure and higher rates of survival in *Tlr4*$^{-/-}$ macrophages exposed to UVB [56]. The role of TLR4 in UVB-induced cutaneous carcinogenesis remains to be tested and it would be interesting to see whether *Tlr4*$^{-/-}$ mice had a different incidence of tumor formation. It has been shown however, that chemically induced cutaneous carcinogenesis is in part dependent on Tlr4- [57] and

downstream MyD88-signaling [58]. No studies to date have investigated the role of TLR3 on UVB-induced skin cancer.

Regulation of inflammation in the skin after UVB injury

If damage to the epidermis is constantly occurring either by UVB-exposure or mechanical injury, one might pose the question as to why the epidermis is not in a constant inflammatory state. It has been shown that TLR2 activation by commensal microbial ligands can dampen TLR3-induced inflammation [19]. In these studies, Lai et al. demonstrated that lipoteichoic acid (LTA) from *Staphylococcus epidermidis*, a major component of the human skin microbiome, can dampen TLR3 signaling in keratinocytes and mouse skin. In these studies, TLR2 activation with LTA increased levels of the signaling molecule TRAF1, which is proteolytically processed by caspase-8 to its active form (N-TRAF1). N-TRAF1 can then bind TRIF to negatively regulate TLR3-TRIF- signaling pathways. The suppressive effects of LTA on TLR3-dependent inflammation were not seen in *Tlr2*$^{-/-}$ and *Traf1*$^{-/-}$ mice, showing that TLR2 is essential for mediating TLR3-induced inflammation in the skin. Interestingly, Traf1 levels in skin were significantly lower in germ-free mice than conventionally raised mice [19]. In this regard, commensal microbes such as *S. epidermidis* have the potential to suppress excessive inflammation in the skin following UVB damage or mechanical injury and the presence of specific microbes may keep excessive inflammation in check.

Inflammation in the skin serves an important purpose. Inflammation following infection or injury helps to sterilize the wound and promotes wound healing by attracting leukocytes that attack microbes or clear apoptotic and necrotic debris [59]. On the other hand it has been demonstrated that certain innate immune pathways, those dependent on MyD88 signaling can promote chemically induced skin carcinogenesis [58]. It has also been demonstrated that *Il-10*$^{-/-}$ mice are resistant to broadband UVB-induced tumorigenesis [60]. IL-10, which has been shown

to be an important immune suppressor, induced following UVB irradiation, has been shown to contribute to UVB-induced skin cancer. While inflammation may help clear infections and resolve wounds in the short term, its role in skin carcinogenesis must be further elucidated as mice deficient in both pro- and anti-inflammatory machinery develop fewer tumors in different models of carcinogenesis. Study of inflammatory pathways should continue to be an important field of research as a balance of short term and long term health effects of UVB are further elucidated.

Conclusions:

Because skin serves as the interface of our bodies to the outside world, it constantly comes in contact with microbes and is at highest risk for injury. It is not unfathomable that common receptors exist to deal with distinctly different threats to our well being. As TLR3 has been demonstrated to be important for inflammation in the skin following injury, the downstream pathways of TLR3 signaling must be further elucidated in order to develop therapeutics that take advantage of the beneficial effects without the adverse effects of excessive inflammation. As TLRs continue to be investigated, they are found to be implicated in a growing number of cellular processes. Recently, TLR3 has been linked to itch [61] as well as cardiac dysfunction following polymicrobial sepsis [62] and will likely continue to be implicated in more disorders in the future. Identifying additional mechanisms of TLR3 activation and further elucidating downstream signaling will give us a better understanding of this pathway and lead to better therapeutics. TLRs and elucidating their expanding roles in various tissues should remain a focal point of future research.

Acknowledgements:

Appendix B, in full, is a reprint of material that is submitted for publication and will appear in The Journal of Investigative Dermatology 2014. A. W. Borkowski, R. L. Gallo. The dissertation author was the primary investigator and author of this paper.

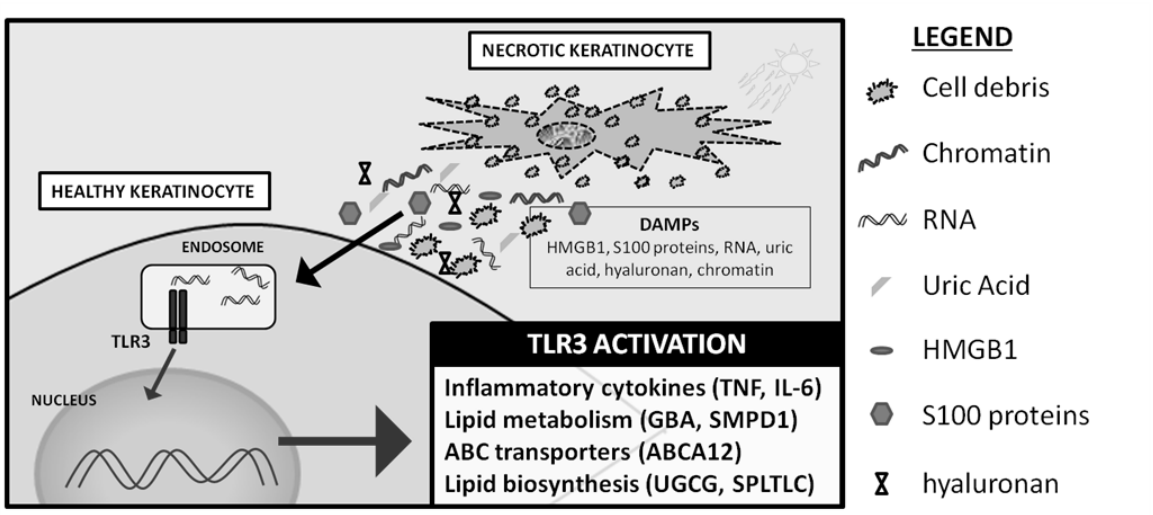

Figure B.1: dsRNA from UV-damaged keratinocytes activates TLR3. Excessive UV exposure causes necrosis in a population of keratinocytes in the epidermis. Loss of membrane integrity in these necrotic keratinocytes causes cellular contents to be spilled into extracellular space. DAMPs released by necrotic keratinocytes are then taken up by neighboring, healthy keratinocytes. dsRNA from necrotic keratinocytes is trafficked to the endosome where it activates TLR3. Downstream signaling leads to inflammation and increases in lipid biosynthesis, metabolism, and transport.

References:

[1] R. Lucas, T. McMichael, W. Smith, and B. Armstrong, “Solar ultraviolet radiation: global burden of disease from solar ultraviolet radiation,” in *Environmental Burden of Disease Series, No. 13*, no. 13, A. Prüss-Üstün, H. Zeeb, C. Mathers, and M. Repacholi, Eds. Geneva: WHO Document Production Services, 2006, p. 87 pp.

[2] Institute of Medicine, “Dietary reference intakes for calcium and vitamin D,” *Natl. Acadamies Press Washingt. DC*, p. , 1116 pp., 2011.

[3] A. C. Ross, J. E. Manson, S. A. Abrams, J. F. Aloia, P. M. Brannon, S. K. Clinton, R. A. Durazo-Arvizu, J. C. Gallagher, R. L. Gallo, G. Jones, C. S. Kovacs, S. T. Mayne, C. J. Rosen, and S. A. Shapses, “The 2011 report on dietary reference intakes for calcium and vitamin D from the Institute of Medicine: what clinicians need to know.,” *J. Clin. Endocrinol. Metab.*, vol. 96, no. 1, pp. 53–8, Jan. 2011.

[4] P. Lehmann, E. Hölzle, B. Melnik, and G. Plewig, “Effects of ultraviolet A and B on the skin barrier: a functional, electron microscopic and lipid biochemical study.,” *Photodermatol. Photoimmunol. Photomed.*, vol. 8, no. 3, pp. 129–134, 1991.

[5] S. P. Hong, M. J. Kim, M.-Y. Jung, H. Jeon, J. Goo, S. K. Ahn, S. H. Lee, P. M. Elias, and E. H. Choi, “Biopositive effects of low-dose UVB on epidermis: coordinate upregulation of antimicrobial peptides and permeability barrier reinforcement.,” *J. Invest. Dermatol.*, vol. 128, no. 12, pp. 2880–7, Dec. 2008.

[6] E. Picot, L. Meunier, M. C. Picot-Debeze, J. L. Peyron, and J. Meynadier, “Treatment of psoriasis with a 311-nm UVB lamp.,” *Br. J. Dermatol.*, vol. 127, no. 5, pp. 509–12, Nov. 1992.

[7] J. Jekler and O. Larkö, “UVB phototherapy of atopic dermatitis,” *Br. J. Dermatol.*, pp. 697–705, 1988.

[8] S. A. Grundmann and S. Beissert, “Modern aspects of phototherapy for atopic dermatitis.,” *J. Allergy*, vol. 2012, pp. 1–8, Jan. 2012.

[9] M. Ichihashi, M. Ueda, a. Budiyanto, T. Bito, M. Oka, M. Fukunaga, K. Tsuru, and T. Horikawa, “UV-induced skin damage,” *Toxicology*, vol. 189, no. 1–2, pp. 21–39, Jul. 2003.

[10] A. T. Black, J. P. Gray, M. P. Shakarjian, V. Mishin, D. L. Laskin, D. E. Heck, and J. D. Laskin, “UVB light upregulates prostaglandin synthases and prostaglandin receptors in mouse keratinocytes.,” *Toxicol. Appl. Pharmacol.*, vol. 232, no. 1, pp. 14–24, Oct. 2008.

[11] M. C. Lebre, A. M. G. van der Aar, L. van Baarsen, T. M. M. van Capel, J. H. N. Schuitemaker, M. L. Kapsenberg, and E. C. de Jong, “Human keratinocytes express functional Toll-like receptor 3, 4, 5, and 9.,” *J. Invest. Dermatol.*, vol. 127, no. 2, pp. 331–41, Feb. 2007.

[12] H. Kono and K. L. Rock, “How dying cells alert the immune system to danger.,” *Nat. Rev. Immunol.*, vol. 8, no. 4, pp. 279–89, Apr. 2008.

[13] E. Candi, R. Schmidt, and G. Melino, “The cornified envelope: a model of cell death in the skin.,” *Nat. Rev. Mol. Cell Biol.*, vol. 6, no. 4, pp. 328–40, Apr. 2005.

[14] A. R. Young, “The sunburn cell.,” *Photodermatol.*, vol. 4, no. 3, pp. 127–34, Jun. 1987.

[15] K. Rass and J. Reichrath, “UV damage and DNA repair in malignant melanoma and nonmelanoma skin cancer.,” *Adv. Exp. Med. Biol.*, vol. 624, pp. 162–78, Jan. 2008.

[16] G. Li, V. Tron, and V. Ho, “Induction of squamous cell carcinoma in p53-deficient mice after ultraviolet irradiation.,” *J. Invest. Dermatol.*, pp. 72–75, 1998.

[17] R. Voll, M. Herrmann, E. Roth, and C. Stach, “Immunosuppressive effects of apoptotic cells,” *Nature*, vol. 534, no. 1988, pp. 350–351, 1997.

[18] C. G. Freire-de-Lima, Y. Q. Xiao, S. J. Gardai, D. L. Bratton, W. P. Schiemann, and P. M. Henson, “Apoptotic cells, through transforming growth factor-beta, coordinately induce anti-inflammatory and suppress pro-inflammatory eicosanoid and NO synthesis in murine macrophages.,” *J. Biol. Chem.*, vol. 281, no. 50, pp. 38376–84, Dec. 2006.

[19] Y. Lai, A. Di Nardo, T. Nakatsuji, A. Leichtle, Y. Yang, A. L. Cogen, Z.-R. Wu, L. V Hooper, R. R. Schmidt, S. von Aulock, K. a Radek, C.-M. Huang, A. F. Ryan, and R. L. Gallo, “Commensal bacteria regulate Toll-like receptor 3-dependent inflammation after skin injury.,” *Nat. Med.*, vol. 15, no. 12, pp. 1377–82, Dec. 2009.

[20] I. Tabas, “Macrophage death and defective inflammation resolution in atherosclerosis.,” *Nat. Rev. Immunol.*, vol. 10, no. 1, pp. 36–46, Jan. 2010.

[21] T. V Berghe, N. Vanlangenakker, E. Parthoens, W. Deckers, M. Devos, N. Festjens, C. J. Guerin, U. T. Brunk, W. Declercq, and P. Vandenabeele, “Necroptosis, necrosis and secondary necrosis converge on similar cellular disintegration features.,” *Cell Death Differ.*, vol. 17, no. 6, pp. 922–30, Jun. 2010.

[22] L. Galluzzi, I. Vitale, J. M. Abrams, E. S. Alnemri, E. H. Baehrecke, M. V Blagosklonny, T. M. Dawson, V. L. Dawson, W. S. El-Deiry, S. Fulda, E. Gottlieb, D. R. Green, M. O. Hengartner, O. Kepp, R. a Knight, S. Kumar, S. a Lipton, X. Lu, F. Madeo, W. Malorni, P. Mehlen, G. Nuñez, M. E. Peter, M. Piacentini, D. C. Rubinsztein, Y. Shi, H.-U. Simon, P. Vandenabeele, E. White, J. Yuan, B. Zhivotovsky, G. Melino, and G. Kroemer, “Molecular definitions of cell death subroutines: recommendations of the Nomenclature Committee on Cell Death 2012.,” *Cell Death Differ.*, vol. 19, no. 1, pp. 107–20, Jan. 2012.

[23] J. J. Bernard, C. Cowing-Zitron, T. Nakatsuji, B. Muehleisen, J. Muto, A. W. Borkowski, L. Martinez, E. L. Greidinger, B. D. Yu, and R. L. Gallo, “Ultraviolet radiation damages self noncoding RNA and is detected by TLR3.,” *Nat. Med.*, vol. 18, no. 8, pp. 1286–90, Aug. 2012.

[24] P. Scaffidi, T. Misteli, and M. E. Bianchi, “Release of chromatin protein HMGB1 by necrotic cells triggers inflammation.,” *Nature*, vol. 418, no. 6894, pp. 191–5, Jul. 2002.

[25] K. E. Johnson, B. C. Wulff, T. M. Oberyszyn, and T. a Wilgus, “Ultraviolet light exposure stimulates HMGB1 release by keratinocytes.,” *Arch. Dermatol. Res.*, vol. 305, no. 9, pp. 805–15, Nov. 2013.

[26] H. Wang, O. Bloom, M. Zhang, J. M. Vishnubhakat, M. Ombrellino, J. Che, A. Frazier, H. Yang, S. Ivanova, L. Borovikova, K. R. Manogue, E. Faist, E. Abraham, J. Andersson, U. Andersson, P. E. Molina, N. N. Abumrad, A. Sama, and K. J. Tracey, “HMG-1 as a Late Mediator of Endotoxin Lethality in Mice,” *Science (80-.).*, vol. 285, no. 5425, pp. 248–251, Jul. 1999.

[27] C. Semino, G. Angelini, A. Poggi, and A. Rubartelli, “NK/iDC interaction results in IL-18 secretion by DCs at the synaptic cleft followed by NK cell activation and release of the DC maturation factor HMGB1.,” *Blood*, vol. 106, no. 2, pp. 609–16, Jul. 2005.

[28] D. V Krysko, T. Vanden Berghe, K. D’Herde, and P. Vandenabeele, “Apoptosis and necrosis: detection, discrimination and phagocytosis.,” *Methods*, vol. 44, no. 3, pp. 205–21, Mar. 2008.

[29] B. Lu, T. Nakamura, K. Inouye, J. Li, Y. Tang, P. Lundbäck, S. I. Valdes-Ferrer, P. S. Olofsson, T. Kalb, J. Roth, Y. Zou, H. Erlandsson-Harris, H. Yang, J. P.-Y. Ting, H. Wang, U. Andersson, D. J. Antoine, S. S. Chavan, G. S. Hotamisligil, and K. J. Tracey, “Novel role of PKR in inflammasome activation and HMGB1 release.,” *Nature*, vol. 488, no. 7413, pp. 670–4, Aug. 2012.

[30] Y. S. Cho, S. Challa, D. Moquin, R. Genga, T. D. Ray, M. Guildford, and F. K.-M. Chan, “Phosphorylation-driven assembly of the RIP1-RIP3 complex regulates programmed necrosis and virus-induced inflammation.,” *Cell*, vol. 137, no. 6, pp. 1112–23, Jun. 2009.

[31] A. Kaczmarek, P. Vandenabeele, and D. V Krysko, “Necroptosis: the release of damage-associated molecular patterns and its physiological relevance.,” *Immunity*, vol. 38, no. 2, pp. 209–23, Feb. 2013.

[32] L. Feldmeyer, M. Keller, G. Niklaus, D. Hohl, S. Werner, and H.-D. Beer, “The inflammasome mediates UVB-induced activation and secretion of interleukin-1beta by keratinocytes.,” *Curr. Biol.*, vol. 17, no. 13, pp. 1140–5, Jul. 2007.

[33] T. Fernandes-Alnemri, J. Wu, J.-W. Yu, P. Datta, B. Miller, W. Jankowski, S. Rosenberg, J. Zhang, and E. S. Alnemri, “The pyroptosome: a supramolecular assembly of ASC dimers mediating inflammatory cell death via caspase-1 activation.,” *Cell Death Differ.*, vol. 14, no. 9, pp. 1590–604, Sep. 2007.

[34] L.-H. Lian, K. a Milora, K. K. Manupipatpong, and L. E. Jensen, “The double-stranded RNA analogue polyinosinic-polycytidylic acid induces keratinocyte pyroptosis and release of IL-36γ.,” *J. Invest. Dermatol.*, vol. 132, no. 5, pp. 1346–53, May 2012.

[35] A. Rehemtulla and C. Hamilton, “Ultraviolet radiation-induced apoptosis is mediated by activation of CD-95 (Fas/APO-1),” *J. Biol. Chem.*, vol. 272, no. 41, pp. 25783–25786, 1997.

[36] T. Mammone, D. Gan, D. Collins, R. a Lockshin, K. Marenus, and D. Maes, “Successful separation of apoptosis and necrosis pathways in HaCaT keratinocyte cells induced by UVB irradiation.,” *Cell Biol. Toxicol.*, vol. 16, no. 5, pp. 293–302, Jan. 2000.

[37] R. Caricchio, L. McPhie, and P. L. Cohen, “Ultraviolet B radiation-induced cell death: critical role of ultraviolet dose in inflammation and lupus autoantigen redistribution.,” *J. Immunol.*, vol. 171, no. 11, pp. 5778–86, Dec. 2003.

[38] C. Ryckman, K. Vandal, P. Rouleau, M. Talbot, and P. a Tessier, “Proinflammatory activities of S100: proteins S100A8, S100A9, and S100A8/A9 induce neutrophil chemotaxis and adhesion.,” *J. Immunol.*, vol. 170, no. 6, pp. 3233–42, Mar. 2003.

[39] S. Basu, R. J. Binder, R. Suto, K. M. Anderson, and P. K. Srivastava, “Necrotic but not apoptotic cell death releases heat shock proteins, which deliver a partial maturation signal to dendritic cells and activate the NF-kappa B pathway.,” *Int. Immunol.*, vol. 12, no. 11, pp. 1539–46, Nov. 2000.

[40] M. J. L. Bours, E. L. R. Swennen, F. Di Virgilio, B. N. Cronstein, and P. C. Dagnelie, “Adenosine 5’-triphosphate and adenosine as endogenous signaling molecules in immunity and inflammation.,” *Pharmacol. Ther.*, vol. 112, no. 2, pp. 358–404, Nov. 2006.

[41] Y. Shi, J. E. Evans, and K. L. Rock, “Molecular identification of a danger signal that alerts the immune system to dying cells,” *Nature*, vol. 425, no. October, pp. 516–521, 2003.

[42] K. R. Taylor, J. M. Trowbridge, J. a Rudisill, C. C. Termeer, J. C. Simon, and R. L. Gallo, “Hyaluronan fragments stimulate endothelial recognition of injury through TLR4.,” *J. Biol. Chem.*, vol. 279, no. 17, pp. 17079–84, Apr. 2004.

[43] K. a Scheibner, M. a Lutz, S. Boodoo, M. J. Fenton, J. D. Powell, and M. R. Horton, “Hyaluronan fragments act as an endogenous danger signal by engaging TLR2.,” *J. Immunol.*, vol. 177, no. 2, pp. 1272–81, Jul. 2006.

[44] K. J. Ishii, K. Suzuki, C. Coban, F. Takeshita, Y. Itoh, H. Matoba, L. D. Kohn, and D. M. Klinman, “Genomic DNA released by dying cells induces the maturation of APCs.,” *J. Immunol.*, vol. 167, no. 5, pp. 2602–7, Sep. 2001.

[45] K. Karikó, H. Ni, J. Capodici, M. Lamphier, and D. Weissman, “mRNA is an endogenous ligand for Toll-like receptor 3.,” *J. Biol. Chem.*, vol. 279, no. 13, pp. 12542–50, Mar. 2004.

[46] K. A. Cavassani, M. Ishii, H. Wen, M. A. Schaller, P. M. Lincoln, N. W. Lukacs, C. M. Hogaboam, and S. L. Kunkel, “TLR3 is an endogenous sensor of tissue necrosis during acute inflammatory events.,” *J. Exp. Med.*, vol. 205, no. 11, pp. 2609–21, Oct. 2008.

[47] L. Liu, I. Botos, Y. Wang, J. N. Leonard, J. Shiloach, D. M. Segal, and D. R. Davies, “Structural basis of toll-like receptor 3 signaling with double-stranded RNA.,” *Science*, vol. 320, no. 5874, pp. 379–81, Apr. 2008.

[48] F. Weber, V. Wagner, S. B. Rasmussen, R. Hartmann, and S. R. Paludan, “Double-Stranded RNA Is Produced by Positive-Strand RNA Viruses and DNA Viruses but Not in Detectable Amounts by Negative-Strand RNA Viruses,” *J. Virol.*, vol. 80, no. 10, pp. 5059–5064, 2006.

[49] Q. Lin, D. Fang, J. Fang, X. Ren, X. Yang, F. Wen, and S. B. Su, “Impaired wound healing with defective expression of chemokines and recruitment of myeloid cells in TLR3-deficient mice.,” *J. Immunol.*, vol. 186, no. 6, pp. 3710–7, Mar. 2011.

[50] Q. Lin, L. Wang, Y. Lin, X. Liu, X. Ren, S. Wen, X. Du, T. Lu, S. Y. Su, X. Yang, W. Huang, S. Zhou, F. Wen, and S. B. Su, “Toll-like receptor 3 ligand polyinosinic:polycytidylic acid promotes wound healing in human and murine skin.,” *J. Invest. Dermatol.*, vol. 132, no. 8, pp. 2085–92, Aug. 2012.

[51] A. W. Borkowski, K. Park, Y. Uchida, and R. L. Gallo, “Activation of TLR3 in keratinocytes increases expression of genes involved in formation of the epidermis, lipid accumulation, and epidermal organelles.,” *J. Invest. Dermatol.*, vol. 133, no. 8, pp. 2031–40, Aug. 2013.

[52] S. He, Y. Liang, F. Shao, and X. Wang, “Toll-like receptors activate programmed necrosis in macrophages through a receptor-interacting kinase-3–mediated pathway,” *Proc. Natl. Acadamy Sci.*, vol. 108, no. 50, pp. 20054–20059, 2011.

[53] J. Muto, Y. Morioka, and K. Yamasaki, “Hyaluronan digestion controls DC migration from the skin,” *J. Clin. Invest.*, vol. 124, no. 3, pp. 1309–1319, 2014.

[54] W. Lewis, E. Simanyi, H. Li, C. a Thompson, T. H. Nasti, T. Jaleel, H. Xu, and N. Yusuf, “Regulation of ultraviolet radiation induced cutaneous photoimmunosuppression by toll-like receptor-4.,” *Arch. Biochem. Biophys.*, vol. 508, no. 2, pp. 171–7, Apr. 2011.

[55] I. Ahmad, E. Simanyi, P. Guroji, I. a Tamimi, H. J. Delarosa, A. Nagar, P. Nagar, S. K. Katiyar, C. a Elmets, and N. Yusuf, “Toll-Like Receptor-4 Deficiency Enhances Repair of UVR-Induced Cutaneous DNA Damage by Nucleotide Excision Repair Mechanism.,” *J. Invest. Dermatol.*, pp. 1–8, Dec. 2013.

[56] E. Harberts, R. Fishelevich, J. Liu, S. P. Atamas, and A. a Gaspari, “MyD88 mediates the decision to die by apoptosis or necroptosis after UV irradiation.,” *Innate Immun.*, pp. 1–11, Sep. 2013.

[57] D. Mittal, F. Saccheri, E. Vénéreau, T. Pusterla, M. E. Bianchi, and M. Rescigno, “TLR4-mediated skin carcinogenesis is dependent on immune and radioresistant cells.,” *EMBO J.*, vol. 29, no. 13, pp. 2242–52, Jul. 2010.

[58] C. Cataisson, R. Salcedo, S. Hakim, B. A. Moffitt, L. Wright, M. Yi, R. Stephens, R.-M. Dai, L. Lyakh, D. Schenten, H. S. Yuspa, and G. Trinchieri, “IL-1R-MyD88 signaling in keratinocyte transformation and carcinogenesis.,” *J. Exp. Med.*, vol. 209, no. 9, pp. 1689–702, Aug. 2012.

[59] P. Martin and S. J. Leibovich, “Inflammatory cells during wound repair: the good, the bad and the ugly.,” *Trends Cell Biol.*, vol. 15, no. 11, pp. 599–607, Nov. 2005.

[60] K. Loser, J. Apelt, M. Voskort, M. Mohaupt, S. Balkow, T. Schwarz, S. Grabbe, and S. Beissert, “IL-10 controls ultraviolet-induced carcinogenesis in mice.,” *J. Immunol.*, vol. 179, no. 1, pp. 365–71, Jul. 2007.

[61] J. V Gruber and R. Holtz, “Examining communication between ultraviolet (UV)-damaged cutaneous nerve cells and epidermal keratinocytes in vitro.,” *Toxicol. Ind. Health*, vol. 25, no. 4–5, pp. 225–30, 2013.

[62] M. Gao, T. Ha, X. Zhang, L. Liu, X. Wang, J. Kelley, K. Singh, R. Kao, X. Gao, D. Williams, and C. Li, “Toll-like receptor 3 plays a central role in cardiac dysfunction during polymicrobial sepsis.,” *Crit. Care Med.*, vol. 40, no. 8, pp. 2390–9, Aug. 2012.